B Cells in Chronic Antibody Mediated Rejection of Renal Transplants

McLaughlin, Laura Bridget

Awarding institution:
King's College London

B Cells in Chronic Antibody Mediated Rejection of Renal Transplants

Laura McLaughlin

Thesis submitted for the degree of Doctor of Philosophy at the Faculty of Life Sciences and Medicine, King's College London

Division of Transplantation Immunology and Mucosal Biology

MRC Centre for Transplantation

Guy's Hospital

King's College London

April 2016

Acknowledgements

I would like to thank Professor Anthony Dorling for providing me with the opportunity to register as a PhD student and being a supportive, kind and enthusiastic supervisor. Professor Jo Spencer for being an excellent source of information on B cells and her kindness and support throughout. I would also like to thank her Postdoc, Verena Hehle, for performing the BCR sequencing on the CMV gB binding B cells. Kin Yee Shiu for investing the time to train me on the IFNγ ELISpot assay when I first started and providing ongoing support over email thereafter. Dr Robert Vaughan for answering all questions HLA related and Chloe Martin for gathering all of the Luminex data from the patients at Guy's. Louise Lines for helping with the biotinylation process. Professor Robert Higgins and Dr Sunil Daga for donating the Pure HLA A2 and DR4 proteins and Maria Hernandez Fuentes for donating the bank of surrogate donor membrane proteins. I'm very grateful to Elli Tham and Vikki Semik for keeping the lab running and processing my blood samples when I didn't have time, and to all of the fellow PhD students and Postdocs from the DTIMB and DIIID divisions at KCL that I have befriended along the way.

The work was carried out in the MRC centre for Transplantation at King's College London and was principally funded by Kidney Research UK. All of the flow cytometry was carried out in the Biomedical Research Centre flow cytometry core at Guy's Hospital.

Finally I would like to thank my family, particularly my mum and sister, who have kept me going through my PhD ups and downs.

Abstract

Immune mediated injury is a major cause of late kidney graft loss. Donor specific HLA antibodies are widely believed to cause chronic rejection because their presence correlates strongly with worse graft outcome. However, some renal transplant recipients have circulating DSA for many years whilst maintaining stable graft function. This dichotomy has led to the hypothesis that the cause of the immune mediated damage observed in chronic rejection is likely to be multi-factorial.

It has previously been demonstrated that donor specific CD4+ T cell activation can be observed in patients with chronic antibody mediated rejection using an IFNγ ELISpot assay. In some samples, this cellular activation was dependent on the presence of B cells, and in others the cellular activation appeared to be regulated by the presence of B cells.

In this thesis, the same patterns of reactivity were observed in renal transplant recipients with chronic antibody mediated rejection recruited onto the RituxiCAN C4 clinical trial. HLA binding B cells were detected flow cytometrically and associations between their phenotype and the different patterns of reactivity were analysed. The majority of HLA binding B cells were found to be IgM+ and were underrepresented in the class switched memory B cell population (CD27+IgM-/CD45RBmem55+IgM-) relative to the global B cell population. B cell dependent IFNγ production in response to donor specific HLA was associated with a higher ratio of IgM+ memory to IgM+ naïve B cells in the HLA binding B cell population.

CMV gB was used as a model protein to investigate the individual contribution that memory (CD27+) and naïve (CD27-) B cells make to antigen specific IFNγ production. The results suggest that memory B cells support IFNγ production and naïve B cells may be suppressing IFNγ production.

Collectively the results in this thesis support a role for a cell-mediated component in chronic antibody mediated rejection. In order to develop more effective treatments for chronic rejection, further investigation into the contribution that T and B cells make to this process is warranted.

Contents

1 Introduction 16
1.1 Transplantation Immunology 16
1.1.1 Human Leukocyte antigen 16
1.1.2 Pathways of allorecognition 17
1.1.3 Types of kidney transplant rejection 22
1.2 B cells 24
1.2.1 B cells develop in the bone marrow 24
1.2.2 Transitional B cells differentiate into different B cell subsets 26
1.2.3 Transitional B cells 29
1.2.4 The T dependent response 30
1.2.5 The T independent response: IgM+ memory and Marginal Zone B cells 35
1.2.6 Origin of IgM+ memory B cells 36
1.2.7 B cell functions: beyond antibody production 40
1.2.8 B cells as regulatory cells 44
1.2.9 The role of B cells in human disease: lessons learned from Rituximab 49
1.3 Rationale for this thesis 52
1.3.1 Chronic antibody mediated rejection: are antibodies really the cause? 52
1.3.2 Evidence for a cellular component in chronic antibody mediated rejection. 55
1.4 Aims 57
1.5 Hypotheses 58
2 Materials and Methods 59
2.1 RituxiCAN C4 trial: Patient recruitment and study overview 59
2.2 Blood Sample acquisition and processing 61
2.2.1 Serum collection 61
2.2.2 PBMC isolation 61

2.2.3 Freezing of PBMC 62
2.2.4 Thawing of PBMC 62
2.3 Detection of IFNγ production in response to donor membrane proteins 63
2.3.1 Donor membrane protein preparation 63
2.3.2 BCA assay 64
2.3.3 Analysis of HLA antibodies 64
2.3.4 Choosing a surrogate donor 65
2.3.5 Indirect IFNγ ELISPOT assay 65
2.3.6 Blocking IL-10 in the IFNγ ELISPOT assay 70
2.4 Flow cytometry 71
2.4.1 General flow cytometry method 71
2.4.2 Intracellular cytokine staining 74
2.4.3 Acquisition on flow cytometer 74
2.5 Detection of antigen binding B cells 75
2.5.1 Biotinylating the CMV gB protein 75
2.5.2 Determining the efficiency of the biotinylation process 75
2.5.3 Phenotyping antigen binding B cells by flow cytometry 79
2.6 Determining if the antigen binding is specific. 80
2.6.1 Cold inhibition assay 80
2.6.2 Blocking the BCR 80
2.6.3 Blocking the FcγRIIB receptor 80
2.6.4 Single cell sorting for downstream sequencing and cloning of CMV gB binding B cells 80
2.7 Isolation of B cells and B cell subsets 83
2.7.1 Isolating B cells from PBMC 83
2.7.2 Isolating CMV gB B cells from isolated B cells 83
2.7.3 Isolating CD27+ and CD27- B cells from isolated B cells 83
2.8 Statistical analysis 86

3 Results part 1 87
3.1 Introduction 87
3.2 Results 88
3.2.1 IFNγ production can be detected in response to donor membrane proteins 88
3.2.2 IFNγ production in response to donor membrane proteins is dependent on B cells 90
3.2.3 Depleting CD25+ cells reveals IFNγ production in response to donor membrane proteins in a subset of samples. 91
3.2.4 Depleting CD19+ and CD25+ cells increases the frequency of samples that can be defined as reactive towards donor membrane proteins. 92
3.2.5 Similar patterns of reactivity observed in the response to donor membrane proteins are also observed in the response to a viral cocktail 96
3.2.6 B cell phenotype does not correlate with pattern of reactivity in the indirect IFNγ ELISpot 99
3.2.7 T cell phenotype does not correlate with patterns of reactivity in the indirect IFNγ ELISpot. 105
3.2.8 Patients who produced IFNγ in response to donor membrane proteins at enrolment did not pass phase I. 108
3.2.9 B cell phenotype at enrolment does not correlate with clinical outcome at the end of phase I 112
3.2.10 Patients who did not pass phase I have a lower frequency of CD4+CD25+ T cells than those who passed phase I..... 116
3.2.11 Correlating B cell phenotype in patients enrolled on the RituxiCAN C4 trial with Leukocyte cones 118
3.2.12 B cell phenotypes post Rituximab 122
3.3 Key points in chapter 3..... 125
3.4 Discussion..... 126
3.4.1 The patterns of reactivity to donor membrane proteins detected in the RituxiCAN C4 cohort broadly replicates those reported in Shiu et al and highlight the complex and dynamic nature of the alloresponse..... 127

3.4.2 Evidence of donor specific reactivity at enrolment was mainly detected in patients who did not stabilise their graft function during phase I 128

3.4.3 Rituximab treatment leads to prolonged depletion of B cells from peripheral blood 129

3.4.4 CD4+ T cell phenotype does not correlate with pattern of reactivity in the IFNγ ELISpot in RituxiCAN C4 patients 130

3.4.5 Global phenotype of B cells at enrolment does not correlate with pattern of reactivity in IFNγ ELISpot or clinical outcome 131

3.4.6 Technical limitations of the IFNγ ELISpot and potential improvements 132

3.4.7 Technical limitations of membrane proteins and potential alternatives 132

3.4.8 Limitations to the interpretation of the data 133

4 Results part 2 135

4.1 Introduction 135

4.1.1 Detection of antigen specific B cells by flow cytometry 135

4.2 Results 138

4.2.1 Developing a method to detect and phenotype CMV gB binding B cells 138

4.2.2 Applying the CMV gB binding assay to a renal transplant patient setting 161

4.2.3 HLA binding B cells can be detected in renal transplant recipients and leukocyte cones 167

4.2.3.3 HLA A2 and HLA DR4 binding B cells are predominantly IgM+ and either predominantly IgM+ memory, or IgM+ naive 177

4.2.3.7 Do Pure HLA proteins elicit an IFNγ response in individuals who do not have an allograft that contains a mismatch for that Pure™ protein? 195

4.3 Key points in chapter 4 200

4.4 Discussion 201

4.4.1 Antigen binding B cells can be detected flow cytometrically using biotinylated recombinant proteins 201

4.4.2 CMV binding B cells are predominantly IgM+ and overrepresented in the IgMhi populations when compared to the global B cell phenotype 202

4.4.3 HLA binding B cells detected using Pure™ HLA proteins are found at a much lower frequency in the peripheral blood than reported using other methods of detection 204

4.4.4 HLA binding B cells are predominantly IgM+ and are either IgM+ naïve or IgM+ memory B cells 207

4.4.5 The ratio of IgM+ memory to IgM+ naïve B cells in the HLA binding B cell population may impact the IFNγ to Pure™ HLA proteins 208

5 Results part 3 210

5.1 Introduction 210

5.2 Results 211

5.2.1 B cell depletion leads to both B dependent and B regulated phenotypes in leukocyte cones when stimulated with CMV gB in the IFNγ ELISpot 211

5.2.2 CMV gB binding B cell phenotype does not correlate with the pattern of reactivity in the IFNγ ELISpot 213

5.2.3 Using an experimental approach to dissect the role that B cells play in producing different patterns of reactivity in the IFNγ ELISpot. 217

5.2.4 HLA DR and CD86 are expressed more brightly on CMV gB binding B cells compared to the overall B cell population 225

5.2.5 BAFFr is not differentially expressed on different B cell subsets 233

5.3 Key points in Chapter 5 236

5.4 Discussion 237

6 Final discussion and future directions 241

6.1.1 Summary 241

6.1.2 Future directions 242

6.1.3 Conclusion 244

7 Appendix 245

8 Bibliography 246

Table of figures

Figure 1.1 Three major pathways of allorecognition 21
Figure 1.2 B cell development in the bone marrow 25
Figure 1.3 Peripheral B cell differentiation in humans (from previous page). 28
Figure 1.4 The germinal centre reaction 32
Figure 1.5 The four stages of CAMR 54
Figure 2.1 Schematic of the RituxiCAN C4 trial 60
Figure 2.2 Representative dot plots to illustrate depletion of different lymphocyte subsets using the Dynabead® system. 67
Figure 2.3 Determining the biotinylation efficiency 77
Figure 2.4 Gating strategy for single cell sorting with dot plots pre and post sort 82
Figure 2.5 Example dot plots of cells pre and post B cell isolation 85
Figure 2.6 Dot plots of CMV gB binding B cell isolation using MACS beads. 85
Figure 2.7 Example dot plots of CD27+/CD27- separation 85
Figure 3.1 Response to donor membrane proteins of all samples tested in the indirect IFNγ ELISpot. 89
Figure 3.2 Impact of CD19+ depletion on IFNγ production 90
Figure 3.3 Impact of CD25+ cell depletion on IFNγ production 91
Figure 3.4 IFNγ response to donor membrane proteins 93
Figure 3.5 IFNγ production in response to a viral protein cocktail 98
Figure 3.6 General gating strategy for phenotyping T and B cells. 100
Figure 3.7 Gating strategy for B cell phenotyping 101
Figure 3.8 Correlation of B cell frequencies and phenotypes with reactivity in the IFNγ ELISpot at enrolment 102
Figure 3.9 Correlation of CD27+ and CD27- B cell subset frequencies with reactivity in the IFNγ ELISpot at enrolment 103
Figure 3.10 Correlation of CD5+, CD1d+ and CD10+ cell frequencies with reactivity in the IFNγ ELISpot at enrolment 104
Figure 3.11 Gating strategy for T cell phenotyping 106
Figure 3.12 Comparison of frequency of T cell subsets between samples grouped according to their pattern of reactivity in IFNγ production upon CD25+ depletion. . 107
Figure 3.13 Estimated glomerular filtration rates over time of patients enrolled on the RituxiCAN C4 trial. 109
Figure 3.14 Correlating ELISpot reactivity at enrolment with clinical outcome 111

Figure 3.15 Comparison of the frequency of B cell subsets at enrolment with clinical outcome at the end of phase I 113
Figure 3.16 Comparison of CD27+ and CD27- B cell frequencies at enrolment with clinical outcome at the end of phase I..... 114
Figure 3.17 Comparison of the frequency of CD5+ cells, CD1d+ cells and CD10+ cells within the naive, intermediate and transitional B cell subsets at enrolment with clinical outcome at end of phase I 115
Figure 3.18 Comparison of frequency of CD4+ T cells and CD4+ T cell subsets at enrolment with clinical outcome at end of phase I 117
Figure 3.19 Comparison of CD19+ lymphocyte frequency between leukocyte cones and enrolment samples from patients enrolled on the RituxiCAN C4 trial 119
Figure 3.20 Comparison of B cell subset frequencies between leukocyte cones and enrolment samples from patients enrolled on the RituxiCAN C4 trial 120
Figure 3.21 Comparison of CD5+, CD1d+ and CD10+ cell frequencies within the naive, intermediate and transitional subsets between leukocyte cones and enrolment samples from patients enrolled on the RituxiCAN C4 trial..... 121
Figure 3.22 Frequency of CD19+ lymphocytes and CD27+ and CD27- B cell subsets pre and post Rituximab in four patients randomised in phase II..... 124
Figure 4.1 Patterns of reactivity in response to three viral proteins in the IFNγ ELISpot 139
Figure 4.2 Example dot plots of CMV gB binding B cells 141
Figure 4.3 Detecting CMV gB binding B cells 142
Figure 4.4 B cells do not bind streptavidin or biotin..... 144
Figure 4.5 Blocking FCγRIIB does not reduce the frequency of CMV gB binding B cells detected 145
Figure 4.6 CMV gB binds the B cell receptor 146
Figure 4.7 Gating strategy for phenotyping CMV gB binding B cells 148
Figure 4.8 Dot plots to illustrate the gating strategy for phenotyping the CMV gB binding B cells 149
Figure 4.9 Frequency of non-transitional and transitional B cells in the overall B cell population compared to the CMV gB binding B cell population..... 150
Figure 4.10 Frequency of different B cell subsets in the overall B cell population compared to the CMV gB+ B cell population 151
Figure 4.11 Frequency of IgM+ memory and naive subsets in the gB+ B cell population compared to the overall B cell population 152

Figure 4.12 CD45RB MEM 55 expression on CD27+ and CD27- B cell populations. 154
Figure 4.13 Dot plots to illustrate the gating strategy for IgM memory and naïve B cell populations based on CD45RB expression. 156
Figure 4.14 Frequency of IgM+ memory and naïve populations in the CMV gB binding B cell population compared to the overall B cell population according to CD45RB expression. 157
Figure 4.15 Binding of biotinylated CMV gB to B cells can be partially inhibited by non-biotinylated CMV gB 159
Figure 4.16 Titrating the Pure™ HLA A1 to determine the optimal concentration to induce antigen specific IFNγ in the indirect ELISpot assay 163
Figure 4.17 Example of ELISpot wells 164
Figure 4.18 Titrating Pure HLA A1 into the indirect ELISpot assay to assess reactivity status of a non-transplant individual 165
Figure 4.19 Reactivity to viral antigen cocktail in patient G002 compared to Cone 23 166
Figure 4.20 Dot plots to illustrate HLA A1 binding B cells in an HLA A1 mismatched kidney transplant patient 168
Figure 4.21 Detecting HLA A1 binding B cells in a renal transplant recipient 169
Figure 4.22 Dot plots to illustrate HLA A1 binding B cells in a leukocyte cone 170
Figure 4.23 Detecting HLA binding B cells in a leukocyte cone 171
Figure 4.24 Using FMO controls to determine spectral overlap post compensation for each fluorochrome used in phenotyping the B cells 173
Figure 4.25 Example of gating strategy for detecting HLA binding B cells 174
Figure 4.26 Example dot plots of the phenotype of HLA A1 binding B cells 176
Figure 4.27 Example dot plots of A2 and DR4 binding B cells 178
Figure 4.28 Example dot plots to show phenotype of HLA A2 binding B cells 180
Figure 4.29 Example dot plot to show phenotype of HLA DR4 binding B cells 182
Figure 4.30 Phenotype of HLA binding B cells compared to the overall B cell population. 184
Figure 4.31 Frequency of HLA binding B cells in all sample groups tested. 194
Figure 5.1 Impact of B cell depletion on 15 leukocyte cones when stimulated with CMV gB in the IFNγ ELISpot 212
Figure 5.2 Correlating the phenotype of CMV gB binding B cells with the pattern of reactivity in the IFNγ ELISpot. 214

Figure 5.3 Correlating the phenotype of the global B cell population with the pattern of reactivity in the IFNγ ELISpot. 215
Figure 5.4 Correlating the ratio of memory to naïve or IgM+ memory to naïve B cells with the pattern of reactivity in IFNγ ELISpot 216
Figure 5.5 Blocking IL-10 in the IFNγ ELISpot 218
Figure 5.6 Example dot plots post CD27+ and CD27- B cell enrichment in the ELISpot wells 222
Figure 5.7 CD27+ B cells support IFNγ production in response to CMV gB..... 224
Figure 5.8 Representative dot plots of HLA DR (a) and CD86 (b) expression on B cells and CMV gB binding B cells. 226
Figure 5.9 Expression of HLA DR on B cells and CMV gB binding B cells..... 227
Figure 5.10 Comparison of HLA DR expression on B cell subsets within the whole B cell population and the CMV gB binding population 228
Figure 5.11 Expression of CD86 on B cells and CMV gB binding B cells..... 230
Figure 5.12 Comparison of CD86+ B cell subsets within the whole B cell population and the CMV gB binding population. 231
Figure 5.13 Comparison of CD86 expression on B cell subsets within the whole B cell population and the CMV gB binding population 232
Figure 5.14 Representative dot plots of TACI and BAFFr expression on B cells and CMV gB binding B cells. 234
Figure 5.15 Expression of BAFFr on B cells and CMV gB binding B cells 235
Figure 7.1 Table for no antigen control from section 4.2.3.3 245

Table of tables

Table 1.1 Use of Rituximab to treat CAMR in a renal transplant setting..... 51
Table 2.1 Recipe for lysis buffer required for preparing donor membrane proteins.. 63
Table 2.2 Dilution volumes for standards in BCA assay 64
Table 2.3 List of flow cytometry antibodies used throughout thesis 72
Table 2.4 Recipe for 10x SDS PAGE running buffer..... 78
Table 2.5 Recipe for fixing solution for Coomassie blue staining 78
Table 2.6 Recipe for Coomassie blue stock solution 78
Table 2.7 Recipe for de-staining solution for Coomassie blue staining 78
Table 3.1a Summary of all samples from West London Renal centre tested in the IFNγ ELISpot 94
Table 3.2 B cell numbers over time in patients randomised in phase II..... 123
Table 4.1 Summary of each sample tested for the presence of HLA binding B cells, presence of DSA and the response to Pure™ HLA proteins in the IFNγ ELISpot before and after CD19+ cell depletion. 187
Table 4.2 Summary of all samples analysed for their HLA phenotype detailing their pattern of reactivity I the IFNγ ELISpot and the ratio of memory:naïve B cells, in the HLA binding B cell population and the overall B cell population..... 190
Table 4.3 Summary of all samples analysed for their HLA phenotype detailing their pattern of reactivity in the IFNγ ELISpot to pure HLA proteins and the ratio of IgM+memory to IgM+naïve cells in the HLA binding B cell population and the overall B cell population. 192
Table 4.4 Patients with A2 or DR4 mismatched kidney transplants tested for reactivity to HLA A1 Pure™ protein and presence of A1 binding B cells..... 196
Table 4.5 Leukocyte cones tested for reactivity to A1 Pure protein and the presence of A1 binding B cells..... 198
Table 4.6 Phenotype of HLA A1 binding B cells compared to the overall B cell population in leukocyte cones. 199
Table 5.1 IFNγ production in response to CMV gB measured by intracellular staining. 220
Table 5.2 IL-10 production in response to CMV gB measured by intracellular staining. 220

List of abbreviations

AID Activation induced cytidine deaminase

ANCA Antineutrophil cytoplasmic antibody

APC Allopycocyanin

APRIL A proliferation inducing ligand

BAFF B cell Activating Factor

Bdep B dependent

Breg Regulatory B cell or ‘B regulated’

BCA Bichinchoninic Acid

BCIP/NBT 5-bromo-4-chloro-3-indolyl-phosphate/nitro blue tetrazolium

BSA Bovine Serum Albumin

BV421 Brilliant Violet 421

CAD Chronic allograft damage

CAN Chronic allograft nephropathy

CAMR Chronic Antibody Mediated Rejection

CD Cluster of Differentiation

CMV gB Cytomegalovirus glycoprotein B

CVID Combined Variable Immunodeficiency Disorder

DNA Deoxyribonucleic acid

EAE Experimental autoimmune encephalomyelitis

EGFR Epidermal Growth Factor Receptor

ELISpot Enzyme Linked Immunospot

FACS Fluorescence Activated Cell Sorting

FCS Foetal Calf Serum

FDA Food and drug administration

FITC Fluorescein Isothiocyanate

FMO Fluorescence Minus One

FSC Forward scatter

HIGM Hyper IgM Syndrome

HLA Human Leukocyte Antigen

IFNγ Interferon Gamma

IL Interleukin

Ig Immunoglobulin

IVIg Intravenous immunoglublin

MHC Major Histocompatibility Complex

MMF Mycophenolate mofetil

MOG Myelin oligodendrocyte glycoprotein

MS Multiple Sclerosis

MZ Marginal zone

PBMC Peripheral Blood Mononuclear Cell

PBS Phosphate Buffered Saline

PCR Polymerase chain reaction

PDGFR Platelet Derived Growth Factor Receptor

PE Phycoerythrin

PMS Pathogen Mediated Selection

RA Rheumatoid arthritis

RNA Ribonucleic acid

RPMI Roswell Park Memorial Institute

SLE Systemic lupus erythematosus

SSC Side scatter

TAC Tacrolimus

Tfh T follicular helper cell

TG Transplant glomerulopathy

Treg Regulatory T Cell or ‘T regulated’

TACI Transmembrane Activator and CAML Interactor

VZV gE Varicella Zoster Virus glycoprotein E

1 Introduction

1.1 Transplantation Immunology

1.1.1 Human Leukocyte antigen

Human leukocyte antigen molecules (HLA) are encoded for by the major histocompatibility complex (MHC) genes, located on chromosome 6 (consortium, 1999). Proteins of both endogenous and foreign origin are broken down into peptides and loaded onto HLA molecules which are then transported to the cell surface and presented to both CD8+ and CD4+ T cells as an HLA:peptide complex by antigen presenting cells (APC). Cognate T cells, i.e. T cells that have a receptor specific for that particular HLA:peptide complex, will be activated upon binding, provided the other necessary signals for activation such as co-stimulation and cytokine binding occur. This is one of the fundamental immunological process that underpins adaptive immune responses.

The MHC is the most polymorphic set of genes expressed in humans so there is a high variation between individuals. In a conventional disease setting such as infection, this has an evolutionary advantage as it creates a population of individuals who have HLA molecules that can present a wide range of pathogenic peptides to T cells. It is widely believed that the polymorphic nature of the MHC has arisen due to pathogen mediated selection (PMS). Several hypotheses have been generated to explain the evolutionary mechanisms behind PMS, however designing experiments to test these hypotheses empirically has proved challenging (Spurgin and Richardson, 2010). The general principles behind these hypotheses are based on an evolutionary interplay between host and pathogen where pressure from different pathogens at different points in time has led to the selection of HLA molecules that confer resistance to that pathogen. In addition, it is thought that being heterozygous for an HLA allele is advantageous, because in theory, this would enable the presentation of a greater variety of pathogen derived peptides (Spurgin and Richardson, 2010). In a transplant setting, the polymorphic nature of the MHC presents a major challenge to successful transplantation as the recipient's immune system recognises any allelic variants of HLA molecules expressed on the donor tissue as foreign and mounts a potent immune response termed an alloresponse. The mechanisms by which the immune system recognises foreign HLA (allorecognition) are described in section 1.1.2.

There are two major types of HLA molecule that are considered important in transplantation: class I and class II. HLA class I molecules are expressed on all nucleated cells and consist of three alpha subunits and a β2 microglobulin molecule. Subtypes of class I molecules considered important in transplantation are HLA-A, HLA-B and HLA-C molecules. HLA class I molecules present mainly intracellular peptides, such as virus-derived peptides, to cognate CD8+ cytotoxic T cells, thus sending a signal to the CD8+ T cell that the cell is infected and needs to be killed. HLA class II molecules are expressed on antigen presenting cells such as dendritic cells, macrophages and B cells, and some other cell types once activated. They consist of two alpha subunits and two beta subunits. There are three subtypes of class II molecules considered important in transplantation: HLA-DR, HLA-DP and HLA-DQ. HLA class II molecules present mostly extracellular peptides, which the cell has taken up and processed, to cognate CD4+ helper T cells. The CD4+ T cell is activated to produce the T cell survival factor IL-2 and other pathogen-appropriate cytokines in order to provide 'help' for the CD8+ T cell (Bennett et al., 1998).

1.1.2 Pathways of allorecognition

In transplantation, there are three pathways of allorecognition that have been described in the literature; the direct, indirect and semi-direct pathways (Figure 1.1).

1.1.2.1 The direct pathway

The direct pathway, which is the dominant pathway early on post-transplant, is unique to the alloresponse (Hornick et al., 1998, Braun et al., 1993, Baker et al., 2001, Benichou et al., 1999). In the direct pathway, recipient T cells recognise in-tact foreign HLA molecules on the surface of the donor's APCs (Lechler and Batchelor, 1982). These APCs, which reside in the graft, are termed passenger leukocytes and once the graft has been re-perfused, they migrate to nearby lymph nodes where they come into contact with alloreactive T cells. The direct pathway leads to a very vigorous immune response due to the high frequency of direct alloreactive T cells which are estimated to represent 1:100-1:1000 T cells (Suchin et al., 2001, Lindahl and Wilson, 1977). Such high frequencies of direct alloreactive T cells are likely to be a result of the inherent capability of a TCR to bind MHC molecules, combined with the fact that some T cells are able to recognise and bind more than one peptide (Zerrahn et al., 1997, Felix et al., 2007, Scott-Browne et al., 2011). It has been demonstrated that T cells are able to cross-react with non-self HLA molecules either by molecular mimicry or by using a different binding strategy (Colf et al., 2007). There are two well-established models

used to explain why so many T cells are activated by foreign HLA molecules: the multiple binary complex and the high determinant density models of allorecognition.

The multiple binary complex is a model in which the peptide that is presented in the donor MHC molecule plays a role in activating the recipient T cell. The source of this antigenic peptide may be a protein of recipient origin, but it is likely that the peptide presented in the donor MHC molecule will be different from the peptide presented by the recipient MHC molecule, due to the requirement that it has to be able to fit into the peptide binding groove of the donor MHC molecule. The recipient T cell in this instance is therefore recognising a foreign peptide presented in the context of foreign MHC (Afzali et al., 2008, Lakkis and Lechler, 2013). In some cases, allelic variants of HLA molecules do not differ greatly in structure and the region that comes into contact with the TCR may remain unchanged or only differ by one or two amino acids – this is known as molecular mimicry and the result is that a recipient's TCR is able to bind a donor MHC molecule with high affinity (Lombardi et al., 1989). Due to differences in the peptide binding groove between the donor and recipient HLA molecules, a large number of donor derived peptides being presented in the donor HLA molecule will appear novel and foreign to the recipients T cell so a high frequency of T cells will be activated. Further to this, it has been shown that a number of alloreactive T cells with direct specificity are memory cells and do not require co-stimulation (Flynn and Mullbacher, 1996).

The high determinant density pattern of allorecognition is a second model based on the principle that the recipient T cell recognises foreign determinants on the HLA molecule itself and activation of the T cell is not dependent on any peptide presented by the molecule. The high density of HLA molecules expressed on the donor cell results in many receptor- ligand interactions, so any T cell specific for the HLA molecule is able to be activated even if it has a TCR with relatively low affinity (Afzali et al., 2008). The result of this is that large numbers of T cells are able to react to antigen. Experimental evidence to support this model comes from two papers published by Elliott and Eisen between 1988 and 1990 where they were able to show that an HLA A2 molecule that had been denatured and then reconstituted to its native form, was able to activate CD8+ cytotoxic T cells (CTL) independently of peptide (Elliott and Eisen, 1990, Smith et al., 1997, Elliott and Eisen, 1988). In addition, Smith et al showed that peptide was not required for alloreactive CTL specific for the murine class I MHC molecule H-2K^{b} to kill the cell line T2 (which is defective at antigen processing and therefore does not express MHC molecules on its surface) that were transfected

with the H-2K^b molecule. These H-2K^b specific CTL also caused rejection of a skin graft when injected into a T cell deficient mouse that had been given an H-2K^b incompatible graft (Smith et al., 1997).

1.1.2.2 The indirect pathway of allorecognition

The indirect pathway of allorecognition is more akin to a conventional immune response whereby HLA antigens from the graft are processed and presented by APC to alloreactive CD4+ T cells. The indirect pathway has been shown to be the dominant pathway of allorecognition long-term post-transplant but can also play a role in driving acute graft rejection early on post-transplant (Baker et al., 2001, Brennan et al., 2009, Benichou et al., 1999, Liu et al., 1996, Ali et al., 2013). Functional consequences of activation of indirect CD4+ T cells include a delayed type hypersensitivity response, the production of alloantibody and enhancement of a cytotoxic CD8+ T cell response (Vella et al., 1997b, Lovegrove et al., 2001, Conlon et al., 2012, Steele et al., 1996, Taylor et al., 2007).

Animal models have been used to show proof of principle that indirect CD4+ T cells are an important component of the alloresponse and can drive rejection independently of the direct response. For example, Fangman et al showed in a skin transplant model that rats immunised with donor derived class I peptides pre-transplant rejected the skin graft quicker than rats who were not immunised (Fangmann et al., 1992). Auchincloss et al showed that indirect CD4+ T cells were required for the rejection of skin grafts in mice by using class II deficient donors and CD8+ T cell depleted recipients to eliminate the effect of the direct pathway (Auchincloss et al., 1993). Valujskikh et al provided evidence for a role of the indirect alloresponse in chronic rejection processes by showing that the adoptive transfer of an indirect allospecific CD4+ T cell clone with a Th1 phenotype into BALB/c SCID mice who had received a skin-graft caused rejection with evidence of mononuclear cell infiltration, necrosis and fibrosis in the graft (Valujskikh et al., 1998). More recently, Ali et al demonstrated that the indirect response to class II antigens was short-lived but the response to class I alloantigens was strong and persistent in a bm12.Kd.IE to C57BL/6 murine transplant model. The authors showed that this was due to decreasing availability of donor derived class II expressing haematopoietic cells post-transplant, whereas donor parenchyma cells provided a constant source of class I alloantigen (Ali et al., 2015).

In humans, there is evidence to show that indirect allospecific T cells are associated with episodes of acute rejection, but may also persist long term post-transplant and

contribute to chronic rejection in heart, lung and kidney transplant settings (Suciu-Foca et al., 1998a, Vella et al., 1997a, Baker et al., 2001, SivaSai et al., 1999, Liu et al., 1996). As chronic stimulation can lead to anergy or apoptosis of T cell clones, it has been hypothesised that the persistence of the indirect alloresponse may be due to epitope spreading (Suciu-Foca et al., 1998b, Ciubotariu et al., 1998). Interestingly, it has been shown that renal transplant recipients with chronic rejection have higher frequencies of indirect CD4+ T cells specific for non-polymorphic regions of class I HLA molecules compared to healthy controls, which highlights the complexity of the alloresponse (Smith et al., 2011).

1.1.2.3 The semi direct pathway of allorecognition

The semi-direct pathway is the most recently described pathway of allorecognition and has provided a potential mechanism for the provision of CD4+ T cell help to a direct alloreactive cytotoxic T cell (Ridge et al., 1998, Bennett et al., 1998, Harper et al., 2015). It has been demonstrated that immune cells are able to exchange many different intact cell surface proteins between each other (Davis, 2007). Included in these proteins are HLA molecules (Montecalvo et al., 2008, Herrera et al., 2004, Smyth et al., 2012). There is evidence to show that an APC can present processed allopeptides to an indirect CD4+ T cell whilst presenting an intact version of the same HLA molecule to a direct CD8+ T cell (Sivaganesh et al., 2013, Harper et al., 2015, Brown et al., 2011) Thus the CD4+ T cell can provide linked help via the APC to the CD8+ T cell (Ridge et al., 1998, Bennett et al., 1998, Schoenberger et al., 1998). There are therefore major implications of these findings to how the alloresponse is measured, as the semi-direct pathway has the potential to contribute to allograft rejection throughout the life of a transplant.

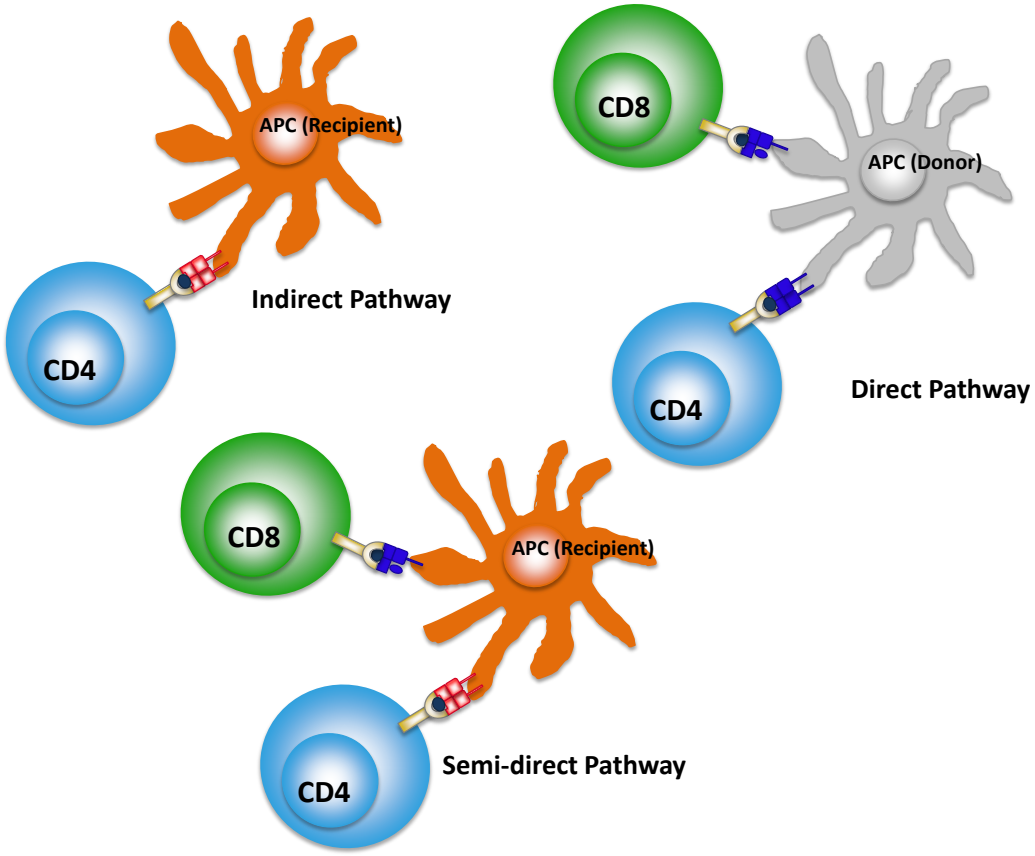

Figure 1.1 Three major pathways of allorecognition
The direct response involves the recognition of in-tact HLA molecules on donor derived APC by recipient T cells. The indirect pathway involves the processing and presentation of donor derived HLA antigens to recipient T cells by recipient APCs, and the semi-direct pathway involves the transfer of intact donor HLA molecules to recipient APCs.

1.1.3 Types of kidney transplant rejection

Both humoral and cellular mechanisms are involved in the rejection process, which can broadly be defined according to three main clinical presentations relating to the timing of rejection after transplantation: hyperacute rejection, acute rejection and chronic rejection.

1.1.3.1 Hyperacute rejection

Hyperacute rejection is rejection occurring within 24 hours of transplantation. It can occur at the time of transplantation, or within minutes of the reperfusion of the graft. This is due to the presence of donor specific HLA antibodies (DSA) circulating in the recipient's blood stream before the transplant. These antibodies are present in individuals who are pre-sensitised to HLA antigens due to a previous sensitisation event such as a previous transplant, pregnancy or a blood transfusion. The DSA bind HLA molecules on the endothelium of blood vessels in the graft and activate the classical pathway of the complement cascade. This results in a swift destruction of the graft (Knechtle et al., 1987, Riella et al., 2014, Kissmeyer-Nielsen et al., 1966, Terasaki, 2003, Dorling, 2012).

1.1.3.2 Acute rejection

Acute rejection often occurs within weeks to months after the transplant but can happen at any point during the life of the transplant. It is characterised by an acute loss of graft function and can be caused by either humoral or cellular mechanisms. Acute humoral rejection is often accompanied by the detection of circulating DSA, neutrophil and macrophage infiltration of the peritubular capillaries and glomeruli, and evidence of complement activation in the form of positive C4d staining (Colvin, 2007). Detection of both CD4+ and CD8+ T cells and macrophages in the parenchyma or blood vessels of the graft is indicative of acute T cell mediated rejection (Sentís et al., 2015, Afzali et al., 2007).

1.1.3.3 Chronic rejection

In recent years, improvements have been made to graft survival rates within the first year post-transplant. This is largely to do with improvements in preservation of the donated organ once it has been extracted from the donor, better surgical techniques, and more effective immunosuppression regimens. However, little improvements have been made in the long term outcomes of graft survival. This was demonstrated in a renal transplant setting in a study of USA graft survival by Lamb et al. It is evident in this study that there is very little change to the slope of the graft survival curve between patients transplanted in 1989 compared to those transplanted 10 years later, and thus

the data can be extrapolated to illustrate that 30-40% of renal transplant patients will lose their graft within 10 years post-transplantation (Lamb et al., 2011). This study highlights the need for improvements to be made in the long-term management of renal transplant patients in order to prolong the life of a transplanted kidney. Chronic rejection in a renal transplant setting is characterised by a slow progressive decline in kidney function, or a 'creeping creatinine', with evidence of interstitial fibrosis and tubular atrophy upon biopsy (Dudley et al., 2005, Li and Zhuang, 2014). As immune mediated injury has been shown to be the major cause of long-term allograft loss in renal transplant patients, there is a need to address the effectiveness of current immunosuppression regimens and to better understand the underlying mechanisms that are driving the chronic rejection process (Einecke et al., 2009).

1.2 B cells

1.2.1 B cells develop in the bone marrow

B cells are lymphocytes that are derived from common lymphoid progenitor cells in the bone marrow. Adherent stromal cell niches provide a suitable micro-environment that promote B cell survival and development from the pro-B cell stage through to when an immature B cell is ready to leave the bone marrow and enter the periphery. (Nagasawa, 2006, Herzog et al., 2009).

Figure 1.2 illustrates the major stages of B cell development from the common lymphoid progenitor cell to an immature B cell that is ready to migrate out of the bone marrow and into the periphery. The Recombination of the Variable, Diversity and Joining (V(D)J) segments of the first allele of the heavy chain locus of the B cell receptor (BCR) begins at the pro-B cell stage and is mediated by the recombination enzymes RAG-1 and RAG-2. The process of allelic exclusion prevents the expression of two BCRs by down-regulating the recombination of the second heavy chain locus. A surrogate light chain, which consists of the germline encoded segments VpreB and λ5, joins the recombined heavy chain (Igμ) to allow the stable expression of the pre-BCR on the surface of the pre-B cell. Signalling through the BCR is essential for the next stages of B cell development and results in an enrichment of this B cell clone by a round of proliferation and progression to the next stage of development, the recombination of the VJ segments of the light chain (Reth M, 1987). Signalling through the pre-BCR is a tightly regulated process in order to avoid the development of mutated B cells that could potentially cause malignant disease (Rickert, 2013).

Once recombination of the light chain has resulted in the stable expression of a BCR, each developing B cell is exposed to autoantigens to judge whether it is suitable for entry into the periphery. Ligation of the BCR with an autoantigen deems that particular cell to be autoreactive and it will either a) undergo clonal deletion and become an apoptotic cell, b) be rendered anergic so it cannot be activated in the periphery, or c) commence receptor editing where recombination of the light chain produces a BCR that is non-autoreactive (Nemazee, 2006, Levesque and St Clair, 2008).

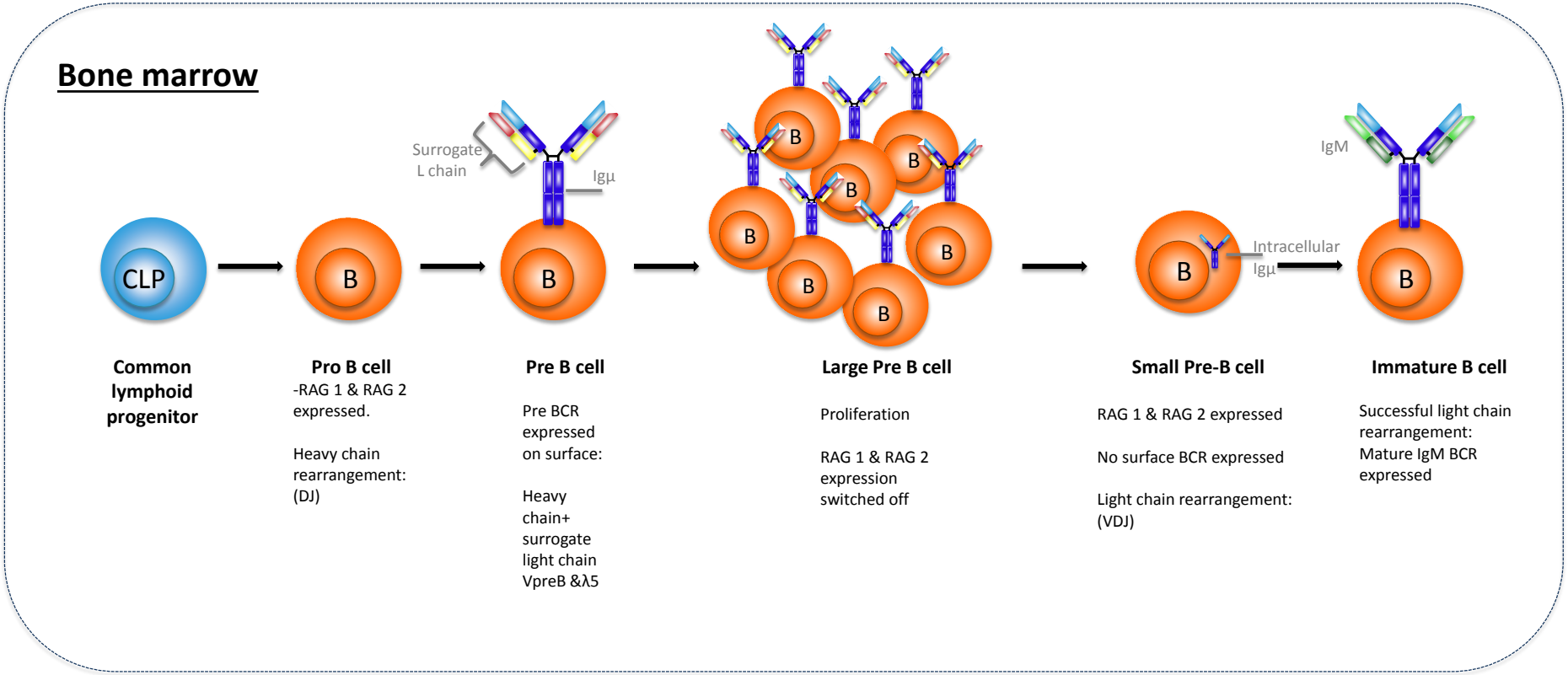

Figure 1.2 B cell development in the bone marrow

1.2.2 Transitional B cells differentiate into different B cell subsets

According to dogma, B cells can be broadly divided into T dependent and T independent subsets. T dependent B cells require close cell-cell contact with T cells to differentiate into high affinity, class switched memory B cells or antibody secreting plasma cells. T independent B cells, as the name suggests, do not require such interactions with T cells to mount an effective humoral response but are more restricted in the type of infection that they are able to clear.

Recent literature suggests that there may be more overlap between these two subsets of B cells than originally thought and a multiple layering of B cell memory has been described (Dogan et al., 2009, Good-Jacobson and Tarlinton, 2012). Dissecting the complexities of the B cell response is a particularly challenging area of immunology because murine and human B cell development do not appear to always follow the same paths. Yet the experiments required to investigate this topic in depth are impossible to implement in a human, so much of the data reported in murine studies must be extrapolated to fit a human setting. Figure 1.3 illustrates a model of human B cell differentiation based on the literature reviewed in the rest of this section.

Periphery

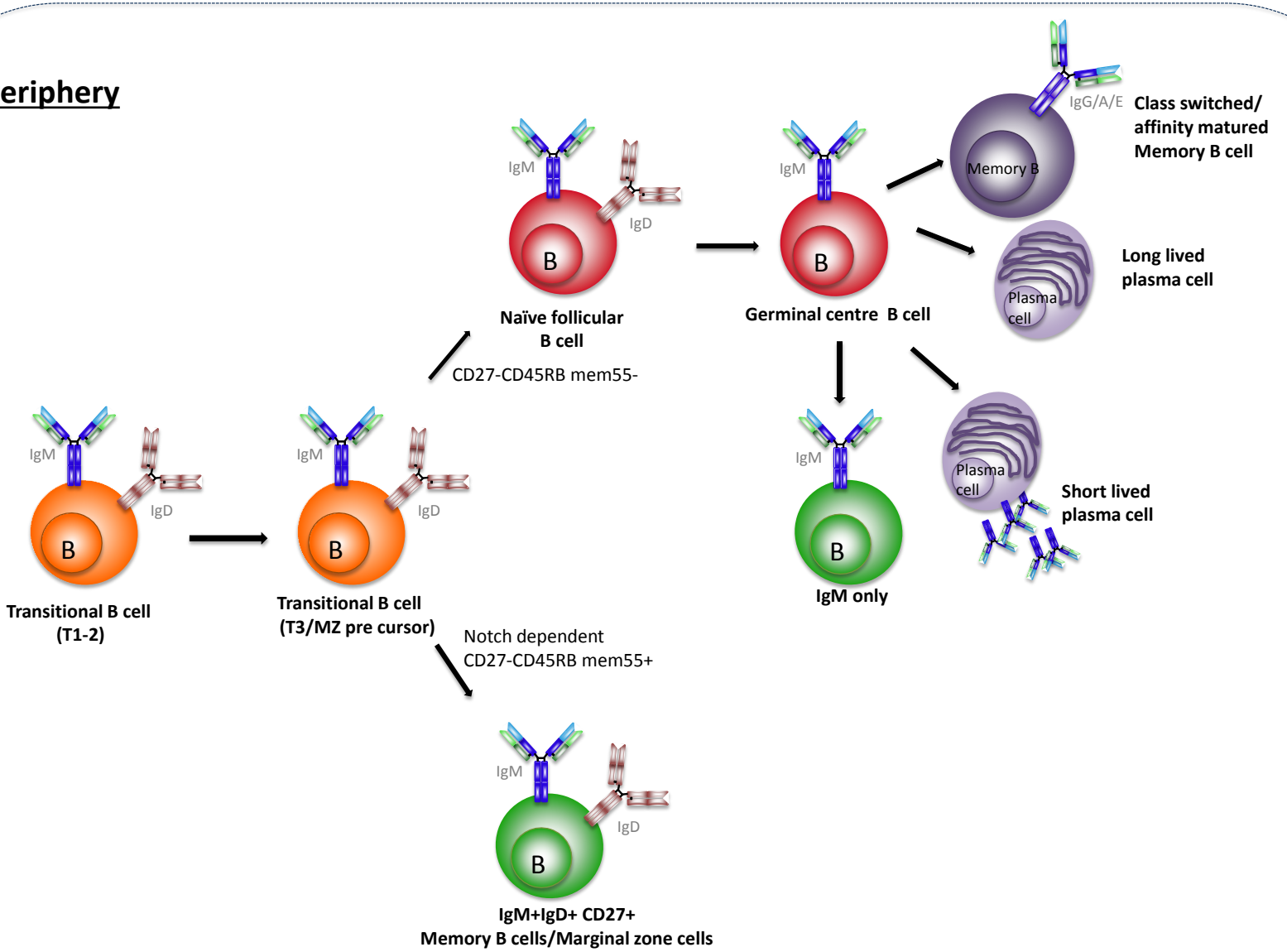
IgM
IgD
B
Transitional B cell
(T1-2)
Transitional B cell
(T3/MZ pre cursor)
Naïve follicular
B cell
CD27-CD45RB mem55-
Notch dependent
CD27-CD45RB mem55+
IgM+IgD+ CD27+
Memory B cells/Marginal zone cells
Germinal centre B cell
IgG/A/E
Memory B
Class switched/
affinity matured
Memory B cell
Plasma
cell
Long lived
plasma cell
IgM only
Short lived
plasma cell

Figure 1.3 Peripheral B cell differentiation in humans (from previous page).

Transitional B cells take one of two differentiation pathways once they reach the T3 stage. T3 cells that are CD27-CD45RBmem55+ differentiate into IgM+ memory B cells or human marginal zone B cells – a process that is dependent on signalling through the Notch receptor. T3 B cells that are CD27-CD45RBmem55- differentiate into naïve follicular B cells and take part in T dependent immune responses

1.2.3 Transitional B cells

Successful formation of a non-autoreactive BCR marks the transition from pre-B cell to immature B cell and the cell can now migrate out of the bone marrow. At present, it is thought that the immature B cell goes through transitional phases T1-T3, which can be detected in human peripheral blood as it matures into a naïve B cell. There are several markers that have emerged over the last decade that have led to more refined subset definitions, however as this is a fast moving area of immunology, discrepancies in these definitions are often encountered when the literature is reviewed as a whole. Broadly speaking, Transitional B cells can be identified by their positive expression of IgD, and high levels of CD24, CD38 and IgM. In addition, they are CD27-, CD5+, and CD9+ (Lee et al., 2009). T1 cells express higher levels of CD10 and lower levels of CD21 than T2 cells, which are often described as having intermediate levels of CD24 and CD38 (Sims et al., 2005). T3 and naïve B cells have even lower levels of CD24, CD38 and CD10 but they can be distinguished from each other by their differential expression of CD5 and the ATP binding cassette transporter-1 (ABCB1): CD5 is expressed more brightly on T3 cells than Naïve cells, and Naïve B cells possess a greater ability to extrude rhodamine dye using the ABCB1 transporter (Wirths and Lanzavecchia, 2005, Lee et al., 2009, Palanichamy et al., 2009). As the transitional cell moves along this development continuum, it takes on some of the functional characteristics of a naïve cell. Upon engagement with CD40 and the BCR, T3 cells are able to differentiate into naïve cells and antibody secreting cells, but remain more sensitive to spontaneous apoptosis than naïve B cells under these stimulation conditions. T3 cells also display a reduced capacity to proliferate compared to naïve B cells (Lee et al., 2009). More recently, it has been shown that T3 cells can be subdivided into two populations based on the expression of IgM and a specific isoform of CD45RB. The specific antibody clone that recognises this epitope on the CD45RB molecule is MEM55, which binds to a glycosylation dependent form of the spliced CD45RB exon (Koethe et al., 2011). CD27-IgMhiCD45RBmem55+ B cells are present in higher proportions in the blood of children and patients who have undergone haematopoietic stem cell transplant indicating that these are a maturing subset of B cells (Bemark et al., 2013). Based on this differential expression of CD45RBmem55, it has been hypothesised that at the T3 stage, the transitional cells diverge into two distinct B cell populations illustrated in Figure 1.3. The CD45RBmem55- subset carry on to become naïve follicular B cells and the CD45RBmem55+ subset differentiate into

the human equivalent of marginal zone B cells or IgM+ memory B cells (Bemark, 2015, Descatoire et al., 2014).

1.2.4 The T dependent response

The majority of surviving transitional B cells become naïve follicular B cells, which express their BCR as a low affinity IgM form. The naïve B cell re-circulates through the lymphatics and the blood system surveying for antigen. B cells are capable of binding antigen in its soluble form but most often, the antigen is picked up by monocytes and dendritic cells at the site of infection and delivered to the draining lymph node that is rich in naive B cells and naïve T cells (Batista et al., 2001, Batista and Harwood, 2009). Within the lymph node, an oligoclonal response is observed, where B cells that are specific for the same antigen but their BCR's are of different affinities are activated (O'Connor et al., 2006). The affinity of the interaction between the BCR and the antigen at this point influences whether the B cell enters a germinal centre reaction, or alternatively by-passes the germinal centre reaction and differentiates into a short lived plasma cell. The divergence of the humoral immune response at this point functions to a) control the spread of the infection by the secretion of low to moderate affinity antibodies by short lived plasma cells and b) provide long lasting immunity by the production of high affinity, class switched memory B cells and long lived plasma cells (O'Connor et al., 2006, Paus et al., 2006, Good et al., 2009). The fate of the B cell is based on the relative affinities of the other B cells in the antigen specific B cell pool at the time of antigen encounter: B cells with high affinity receptors are selected to differentiate into short lived plasma cells, and those with lower affinities are deemed more suitable for a germinal centre reaction, where they can undergo affinity maturation and class switch hypermutation (O'Connor et al., 2006). In order for a successful germinal centre reaction to occur, the B cell must collaborate closely with cognate antigen specific CD4+T cells (Garside et al., 1998).

1.2.4.1 The germinal centre reaction

A germinal centre is a structure located in the B cell follicle of the secondary lymph node that contains a high concentration of activated, antigen specific B cells that are undergoing proliferation, somatic hypermutation and class switch recombination. The aim of the germinal centre reaction is to select for those B cell clones that have the highest affinity for the target antigen and are therefore the most suitable candidates to differentiate into memory B cells and long lived plasma cells. In addition, the germinal centre environment provides the B cell with the appropriate signals to class switch into an isotype that is most suitable for the immune response required. The germinal centre

reaction is highly dynamic and involves the positive selection of the B cell clones that are selected for further differentiation as well as a great deal of cell death. The germinal centre reaction is summarised in Figure 1.4.

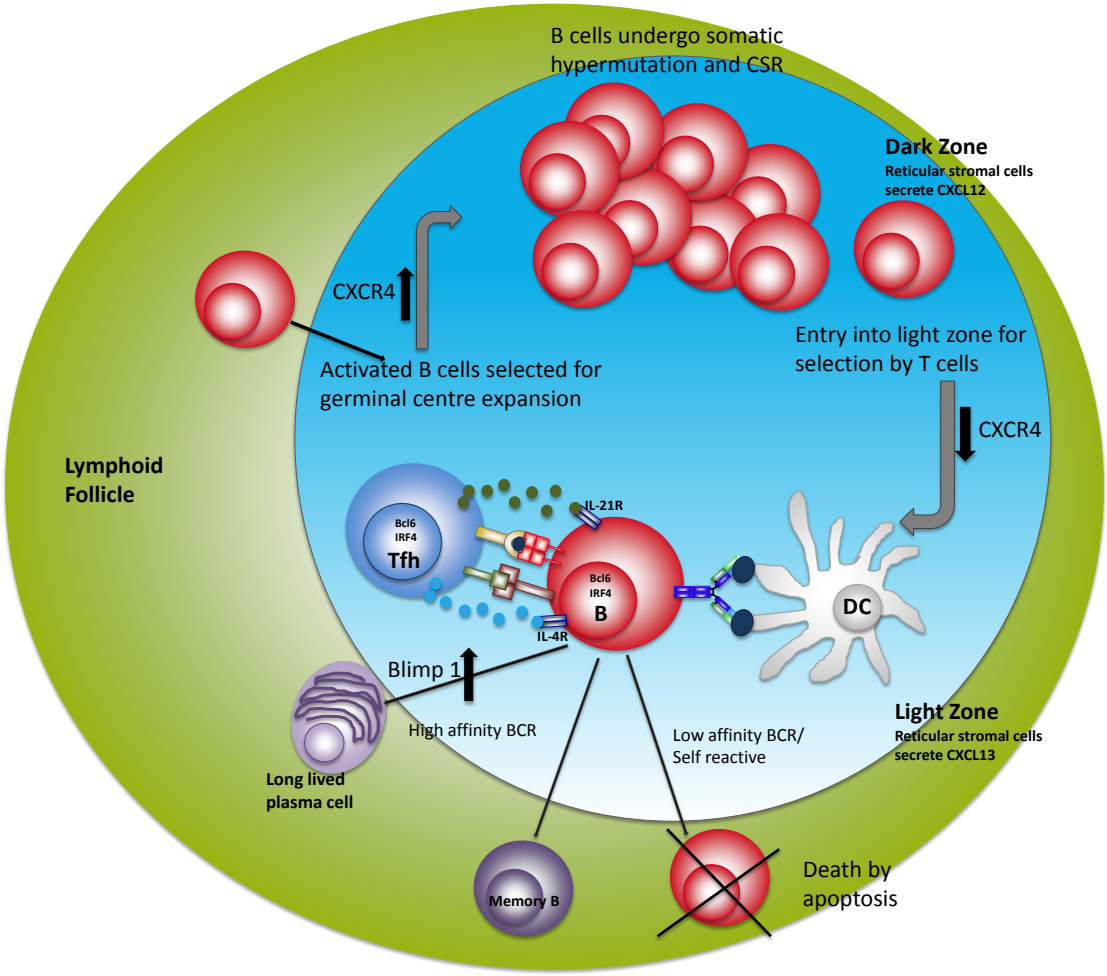

Figure 1.4 The germinal centre reaction

Selection for entry into the germinal centre begins with cognate interactions between T and B cells at the T-B cell border. If the expression of the orphan G-protein-coupled receptor, Epstein Barr virus induced molecule-2 (EBI2) on the B cell is maintained post activation, the B cell will stay in the outer follicle region where it is likely to differentiate into a short lived plasma cell. Down-regulation of EBI2 enables the localisation of the activated B cell into the inner follicle region where it can partake in the formation of a germinal centre (Pereira et al., 2009, Kelly et al., 2011, Gatto et al., 2011).

The full kinetics of the germinal centre reaction are yet to be elucidated, but studies in recent years using photo-imaging have enabled a much more detailed model of the germinal centre reaction to be created. The germinal centre structure is organised into two distinct zones: the dark zone and the light zone. Germinal centre B cells cycle between the two zones during the germinal centre reaction (Victora et al., 2010, Allen et al., 2007, Bannard et al., 2013). The dark zone contains mainly proliferating B cells and its dark appearance is due to the dense mass of nucleated cells. The light zone contains a mixture of cells that includes B cells, CD4+ Follicular helper T cells (Tfh) macrophages and follicular dendritic cells (Victora et al., 2010). Historically, B cells have been divided into centrocytes and centroblasts according to their location within the germinal centre. Centrocytes are found in the light zone and are CXCR4lo, CD83hi and CD86hi. Centroblasts are located in the dark zone and are characterised as CXCR4hi CD83lo and CD86lo (Allen et al., 2004). In addition to the different leukocyte subsets that reside in the germinal centre, a network of reticular stromal cells can also be detected. One function of these stromal cells is to secrete different chemokines in order to retain the appropriate cell types in the relevant zones in the germinal centre. In the dark zone, the stromal cells secrete CXCL12, the ligand for CXCR4 which is expressed more highly on centroblasts than centrocytes. In contrast, the stromal cells in the Light zone have a differentially higher expression of CXCL13 which is the ligand for CXCR5, a chemokine receptor that is expressed highly on Tfh cells (Allen et al., 2004).

The B cell is provided with signals from the Tfh cell to undergo class switching and somatic hypermutation of its B cell receptor. IL-21 derived from the Tfh is essential for the initiation and maintenance of the germinal centre B cells (Zotos et al., 2010, Bryant et al., 2007). IL-21 has been shown to maintain the expression of Bcl6 in the germinal centre B cells. Bcl6 is a transcription factor that is required for successful somatic hypermutation of the variable region and class switching of the Fc portion of the BCR (Dent et al., 1997). The expression of Bcl6 also acts to repress/suppress the

expression of Blimp-1, the master regulator of Plasma cells, so the germinal centre B cells do not prematurely differentiate into plasma cells before they are ready (Tunyaplin et al., 2004).

Once selected, the B cell will either become a long lived plasma cell or a memory B cell. The upregulation of BLIMP-1 signals the germinal centre B cell to become a plasma cell (Angelin-Duclos et al., 2000). IL-4 regulates IL-21 induced class switching in humans and the transcription factor IRF4 is required for both class switch recombination and plasma cell differentiation and is important for regulating the differentiation of germinal centre B cells into plasma cells (Ochiai et al., 2013, Klein et al., 2006, Avery et al., 2008).

The B cell will process and present the antigen via MHC class II molecules to the CD4+ T cell, and an immune synapse will be formed. An important co-stimulatory signal that is sent is via ligation of CD40 on the B cell with CD40ligand (CD40L or CD154) on the T cell (Garside et al., 1998). CD40-CD40L interactions have been shown to be a requirement for a successful germinal centre reaction as patients with Hyper IgM syndrome due to mutations in *CD40L* or *CD40* genes are unable to form germinal centres (Ferrari et al., 2001, Korthauer et al., 1993, Fuleihan et al., 1993). Signalling through CD40 on the B cell induces proliferation and up-regulation of cytokine receptors (Lederman et al., 1992, Elgueta et al., 2009). However, CD40-CD40L interactions are complex and bi-directional, and in order for germinal centre formation to be initiated and maintained, the T cell must receive signals through CD40L (Cayabyab et al., 1994, Gray et al., 1997).

1.2.5 The T independent response: IgM+ memory and Marginal Zone B cells

1.2.5.1 Phenotype of IgM+ memory B cells

The existence of a non-class switched IgM+ memory B cell population in humans was first demonstrated in two studies by Klein et al where they showed that an IgM+ population of B cells with somatically hypermutated V kappa regions could be detected in peripheral blood. These cells did not express CD38, CD23 or CD77 and so were therefore distinct from naïve and germinal centre B cells. They shared characteristics with isotype switched IgM-IgD- populations, such as the ability to quickly differentiate into antibody secreting cells upon stimulation in vitro, and the expression of CD27, the ligand for the co-stimulatory molecule CD70 expressed on T cells. These studies highlighted that within the IgM+CD27+ population, two subsets could be found: IgM+IgD- (IgM only) and IgM+IgD+ (Klein et al., 1998, Klein et al., 1997).

Other studies using a combination of surface phenotype (Kruetzmann et al., 2003) and sequencing of their BCR post immunisation with a pneumococcal vaccine (Weller et al., 2004) have since confirmed their existence in the peripheral blood and have shown that they are directly related to IgM+ memory B cell populations found in the spleen. It has therefore been speculated that human IgM+ memory B cells are a re-circulating equivalent of murine marginal zone cells in the human (Weller et al., 2004, Maglione et al., 2014). Additionally, studies by Berkowska et al and Bagnara et al have shown that the IgM only subset has a higher frequency of mutations in their CDR-H3 region than the IgM+IgD+ subset and are clonally related to CD27+ class switched B cells. It is therefore likely that the IgM only subset represent B cells that have been involved in primary germinal centre reactions and are distinct from the IgM+IgD+ memory subset (Berkowska et al., 2011, Bagnara et al., 2015).

1.2.5.2 Function of IgM+ memory B cells

IgM+ memory B cells are widely considered to be important for the neutralisation of polysaccharide-encapsulated bacteria such as *Streptococcus pneumoniae, Neisseria meningitides or Haemophilus influenzae* (Snapper, 2012, Carsetti et al., 2005, Cameron et al., 2011). These B cells act shortly after pathogen entry into the body by secreting low-affinity, broadly specific IgM antibodies. The immune response is therefore less specific than the response from a class-switched memory B cell, but the pentamer structure of IgM antibodies and the speed at which this response is mounted mean that a variety of microorganisms can be bound by these antibodies to provide effective opsonisation for the destruction of the bacteria by neutrophils and macrophages (Bjornson and Detmers, 1995). Because of their frontline role in the

clearance of bacterial infections, and their lower level of somatic hypermutation compared to isotype switched B cells, IgM+ memory B cells have also been termed natural effector memory B cells (Capolunghi et al., 2013).

1.2.6 Origin of IgM+ memory B cells

The origin of IgM+ memory B cells is still a matter for debate. It was originally hypothesised by Ralf Kuppers and colleagues that IgM+ memory B cells were early products of a germinal centre reaction (Klein et al., 1997, Klein et al., 1998). Since the publication of these papers, many more studies have been conducted in an attempt to elucidate the origins of IgM+ memory B cells and the resultant data provides both arguments for and against this original hypothesis. There is a rather compelling body of data to suggest that the differentiation pathway of IgM+ memory B cells is distinct from class switched memory B cells, where germinal centre formation is not required and somatic hypermutation occurs independently of antigen exposure.

1.2.6.1 IgM+ memory B cells are germinal centre independent but rely on the spleen for their development and signalling through TLRs for their maintenance

The observation that neonates, asplenic/splenectomised individuals or a subset of individuals with combined variable immunodeficiency disorder (CVID) have reduced frequencies of IgM+ memory B cells and often suffer from re-current infections of encapsulated bacteria, provides evidence to support the necessary role that these cells play in the clearance of bacterial infections, but also that the spleen is required for the development and/or maintenance of these cells (Kruetzmann et al., 2003, Weller et al., 2004, Carsetti et al., 2005). Interestingly, Cameron et al showed that adults who have been splenectomised do not suffer from recurrent infections and that a lower IgM+ memory B cell frequency did not correlate with a higher infection rate in these patients. This suggests that by adulthood, a healthy individual will have sufficient levels of IgM and IgG antibodies to neutralise any infection (Cameron et al., 2011).

The differentiation of IgM+ memory B cells is thought to be T-independent as individuals with hyper IgM syndrome caused by mutations in *CD40L* or *CD40* genes (HIGM1 and HIGM3 respectively) are unable to form germinal centres and have reduced levels of isotype switched memory B cells and serum IgG levels, but have a normal IgM+ memory B cell compartment (Ferrari et al., 2001, Korthauer et al., 1993, Fuleihan et al., 1993, Agematsu et al., 1998, Weller et al., 2001). Interestingly, other individuals who have hyper IgM syndrome caused by a mutation in *AICDA*, which encodes for AID expression (HIGM2), differ in the fact that they are able to form

germinal centres, albeit with abnormal pathology, but have higher levels of the IgM only subset of IgM+ memory B cells, presumably because the lack of AID halts their differentiation at the isotype switching stage so the product of any germinal centre reaction is always IgM+ (Revy et al., 2000, Muramatsu et al., 2000, Weller et al., 2004).

Asplenic individuals have markedly reduced IgM+ memory B cell frequencies but maintain a normal class switched memory B cell compartment. Likewise, those who have undergone a splenectomy experience a permanent decrease in their IgM+ memory B cell pool with only a transient reduction in their class switched memory B cell pool. Thus indicating that the origins of IgM+ memory B cells are different from class switched memory B cells (Kruetzmann et al., 2003, Cameron et al., 2011).

Based on their findings that the IgM+ memory B cell subset in infants under 2 years of age have a broad repertoire of antigen receptors, therefore indicating that clonal expansion of antigen specific B cells has not occurred, along with evidence of somatic hypermutation and AID expression that is only detected in this subset early on in life, Weller et al 2008 hypothesised that IgM+ memory B cells may develop in the first two years of life and that whilst somatic mutation is occurring, they remain non-functional and refractory to both TI and TD antigenic stimulus. This hypothesis could explain why infants do not mount immune responses to pneumococcal vaccines under the age of 2 years (Weller et al., 2008). This study was unable to provide evidence of what was inducing the somatic hypermutation in this subset, but subsequent studies have hypothesised that bacterial DNA, perhaps from the microbiota that colonises a neonate could be responsible. Stimulation with hypomethylated DNA cytosine-phosphate-guanine (CpG) for 5 days *in vitro* has been shown to induce a small proportion of cord blood transitional B cells to acquire the same phenotype as IgM+ memory cells (Capolunghi et al., 2008). These cells up-regulate AID expression and have evidence of mutated CDR3 regions (Aranburu et al., 2010). In addition, if these cells are incubated for a further 2-4 days, they down-regulate AID expression whilst up-regulating BLIMP-1 and differentiate into antibody secreting cells of both IgM and IgG isotypes (Aranburu et al., 2010, Capolunghi et al., 2008). Moreover, a small proportion of the IgM antibodies detected after this stimulus are specific for the *S. pneum*oniae antigen PnPS (Capolunghi et al., 2008).

These two studies heavily implicate the involvement of TLR ligation, particularly TLR9, in the differentiation of IgM+ memory B cells. This is supported by the findings that individuals deficient in IRAK-4, MyD88 and TIRAP, which are signalling molecules

downstream of TLR9 and many other TLRs, have markedly reduced frequencies of IgM+IgD+CD27+ B cells, but normal frequencies of switched B cells and suffer from recurrent infections caused by pyogenic bacteria such as *S.pneumoniae* and *S.aureus* (Weller et al., 2012, Maglione et al., 2014, Picard et al., 2010). As these patients have a similar level of mutations in the VH3 of their CDR3 regions as healthy controls, the authors thought that signalling through TLRs is more likely to play a role in the maintenance and activation of these cells as opposed to their development and differentiation. Maglione et al recently showed that patients deficient in IRAK-4 and MyD88 differ from healthy controls as they have reduced serum levels of IgM antibodies specific for a number of pneumococcal antigens. In addition, circulating CD27+ B cells from these patients do not produce IgM antibodies specific for the pneumococcal antigen PC in response to stimulation with TLR9 or TLR7 agonists. Furthermore, proliferation of circulating IgM+IgD+CD27+ B cells in response to TLR9 and TLR7 agonists was observed in healthy controls but not in these patients (Maglione et al., 2014). The response to TLR7 and TLR9 agonists in patients deficient in TIRAP was not included in this study. Interestingly, Weller et al found that the frequency of IgM+IgD+CD27+ B cells in patients deficient in UNC-93B was comparable to healthy controls (Weller et al., 2012). This suggests that TLR7 and TLR9 may not play an essential role in the maintenance of IgM memory B cells as UNC-93B is essential for signalling through TLR7 and TLR9 (Casrouge et al., 2006, Brinkmann et al., 2007). UNC-93B does not play a role in TLR10 signalling however, but TIRAP is downstream of MyD88 in this signalling pathway. Based on this fact and the observations that TLR10 is expressed at higher levels on IgM+IgD+CD27+ B cells than class switched or naïve B cells, and that TIRAP deficient patients had the most marked reduction in their IgM+IgD+CD27+ B cells, the authors proposed that TLR10 may play an essential role in IgM+ memory B cell maintenance (Hasan et al., 2005, Weller et al., 2012). At present this hypothesis cannot be reconciled with the in vitro effects observed on this B cell subset in the presence of TLR7 and TLR9 agonists as the ligand for TLR10 is still not known (Lee et al., 2014, Oosting et al., 2014).

1.2.6.2 IgM+ memory B cells are the pre-cursors of class switched memory B cells and are a product of germinal centres

An alternative hypothesis for the origin of IgM+ memory B cells is that they are early products of a germinal centre reaction and have left the germinal centre before class switching has occurred. This hypothesis is supported by three papers published by Ralf Kuppers and colleagues who believe that the IgM only B cell subset

(IgM+CD27+IgD-) remains in the germinal centre for longer than the IgM+CD27+IgD+ subset, and therefore IgD is down-regulated, but it leaves the germinal centre before class switching has occurred. In the first paper they show how a ‘molecular footprint’ of germinal centre involvement can be detected in the form of mutations in *Bcl6*, the master transcriptional regulator of germinal centre B cells that is highly expressed in germinal centre B cells. By sequencing the CDR3 regions of the IgM+CD27+IgD+ B cell subset, they also provided evidence for a clonal relationship between IgM+ memory B cells and class switched IgG+ B cells in a small number of clones (Seifert and Küppers, 2009). The second paper provided some evidence to suggest that IgM+ memory B cells possess a greater homing capacity to the follicle border than naïve or IgG class switched subsets and that this may indicate that they may participate in secondary germinal centre reactions (Seifert et al., 2015). In the third paper, the group used next generation sequencing to show that the IGHV region of IgM only B cells (IgM+CD27+IgD-) carries an intermediate number of mutations compared to IgM+CD27+IgD+ cells which have the lowest, and IgG+CD27+IgD- which have the highest. They found that there was a substantial number of clones amongst the different subsets that were related to one another. Interestingly, the larger the number of members a clone had, the more likely it was that it would be detected in all three subsets. However, they did also show that not all clones had members shared across the three different subsets and some were exclusively found only in the IgM+CD27+IgD+ subset (Budeus et al., 2015).

1.2.7 B cell functions: beyond antibody production

During the last decade studies focusing on B cells have established that they are much more than just pre-cursors to antibody producing plasma cells. The B cell itself is now regarded as having a whole range of functions that contribute to the pathogenesis of disease but also to the regulation of an immune response. It has emerged that the contribution of B cells in disease pathogenesis is highly complex and an individual's B cells may behave quite differently in two people with the same disease.

1.2.7.1 B cells as antigen presenting cells

Dendritic cells are widely viewed as highly efficient antigen presenting cells and are often termed "professional APC," as they are believed to be the APC that prime naïve antigen specific CD4+ T cells and induce an adaptive immune response. Only once these T cells are primed, can they go on to activate B cells. The influence that these activated B cells have on the immune response is not to be dismissed however, as they provide a source of antigen specific APC that can efficiently take up protein antigen at much lower concentrations than required for DCs, clonally expand and present many different epitopes of the antigen to cognate T cells, thus diversifying the original immune response induced by the dendritic cell (Constant, 1999, Constant et al., 1995b, Constant et al., 1995a, Mamula and Janeway, 1993, Wilson et al., 2012, Rivera et al., 2001). B cells are much more than just pre-cursors to antibody secreting cells and several studies using B cell deficient mice have demonstrated that they are essential for the formation of diverse and effective primary and secondary immune responses.

Linton et al. showed that B cells were required for optimal priming of a T cell response as the expansion of antigen specific CD4+ T cells post immunisation with KLH was reduced in µMT mice, which are B cell deficient, compared to wild type. Interestingly, they found that when they used multiple boosters in an attempt to overcome the lack of B cells and allow DC only priming, this did not have an effect on antigen specific CD4+ T cell numbers. They also showed that this reduced expansion of CD4+ effector cells had a knock on effect on the development of an optimal memory T cell compartment as there were reduced antigen specific memory T cells in µMT mice. By enriching µMT mice with antigen specific B cells, the antigen specific memory T cell compartment could be restored (Linton et al., 2000). Some studies using B cell deficient mice reported that B cells were not required for priming an effective T cell response, so Rivera and colleagues sought to reconcile any differences in the literature with regards to the effect that B cell deficiency had on T cell priming. They used µMT

mice on different genetic backgrounds to show that T cell priming is consistently reduced in the absence of B cells in BALBc, SFL or BALBc/B6 F1 mice, but results were more variable when C57BL/6 (B6) were used. By using bone marrow chimeras where the immune system had been able to develop in the presence of B cells, but was then subsequently depleted of them, they showed that the reduced priming of the T cell response was not due to impaired development of the immune system (Rivera et al., 2001).

B cells may also play a role in skewing the type of T cell response depending on the antigen. For example, Wilson et al described that B cells specific for aggrecan, an antigen important in the induction of proteoglycan-induced arthritis in mice, were as efficient as DCs, and more efficient than macrophages, at stimulating antigen specific CD4+ T cell IFNγ production and differentiation of Th1 cells (Wilson et al., 2012). However, Linton et al found that in OT-II transgenic mice, B cells were required for the production of Th2 cytokines IL-4 and IL-13 and that in their absence the immune response was skewed towards a Th1 phenotype upon antigen challenge with OVA peptide (Linton et al., 2003).

Several studies in mice have demonstrated that the initiation of autoimmune disease is dependent on the presence of B cells (Molnarfi et al., 2013, Noorchashm et al., 1997, Shlomchik et al., 1994). For example, Falcone et al. demonstrated that in NOD mice, B cells were required for an optimal T cell response to Type I Diabetes antigen GAD65 (Falcone et al., 1998). To complement this finding, Serreze et al showed that B cell deficient NOD.Igμ^{null} mice did not develop diabetic disease. Moreover, reconstitution of these mice with immunoglobulin did not render them susceptible to disease. Interestingly, they found that although other APC could propagate T cell responses to GAD, they were less adequate than B cells at inducing these responses in the first place (Serreze et al., 1998). A series of papers published by Shlomchik and colleagues demonstrated that B cells were required for the pathogenesis of murine lupus. In a spontaneous model of murine lupus (MLR *lpr/lpr),* mice who lacked B cells had greater frequencies of CD8+ and CD4+ naïve T cells and therefore reduced frequencies of activated and memory T cells than their B- intact counterparts (Chan and J. Shlomchik, 1998). When this model was genetically modified to have an intact *fas* gene (MR/+) and therefore more representative of a human, the absence of B cells abrogated the development of lupus nephritis (Chan et al., 1999b). By creating a transgenic Ig MLR *lpr/lpr* mouse model so immunoglobulin could not be secreted, Chan et al demonstrated that B cells exerted their pathogenic effect in an antibody independent

manner, most likely mediated by antigen presentation to the T cells, or secretion of pro-inflammatory cytokines (Chan et al., 1999a).

In support of a role for B cells as essential antigen presenting cells, Lund et al. used bone marrow chimeras to specifically knock out MHC Class II expression on B cells in a mouse model of *Pneumocystis carinii*. They showed that formation of effective T cell effector and memory responses as well as clearance of the pathogen was dependent on the presence of B cells that had intact MHC class II expression (Lund et al., 2006, Opata et al., 2015). This study was supported by data from Crawford et al who reported that both primary and secondary responses to a peptide from Moloney murine leukaemia virus were reduced in the MHC class II bone marrow chimeras (Crawford et al., 2006) and Molnarfi et al who more recently demonstrated that B cell MHC class II expression is required for the induction of disease in a rhMOG immunised model of EAE (Molnarfi et al., 2013).

Finally, there is evidence for B cells as antigen presenting cells in murine models of transplantation. The most convincing study was published by Zeng et al. They used a combination of μMT and AID/μS knockout mice (the latter cannot secrete antibodies) to show that B cells in the absence of antibodies are sufficient to mediate chronic allograft vasculopathy in a heterotopic cardiac transplant model. Moreover, they showed that CD4+ and CD8+ T cell cytokine responses and graft infiltration were both reduced in the absence of B cells. The effects observed in the μMT mice were thought to be partially mediated by B cell antigen presentation to T cells and partially by disruption of the lymphoid architecture (Zeng et al., 2014). Noorchasm et al showed that mice deficient in MHC class II expressing B cells reject a vascularised heart transplant at a slower rate than wild type mice and had delayed production of antigen specific antibody. This model did however rapidly reject a skin transplant (Noorchashm et al., 2006). A similar result was observed in a skin transplant using a B cell deficient μMT mouse model, however the authors of this study reported that B cells promoted the differentiation of effector CD8+ and CD4+ T cells into memory T cells (Ng et al., 2010). Recently, Tse et al showed that infiltrating B cells could be detected in tertiary lymphoid structures within a murine renal graft with chronic allograft damage (CAD). These B cells secreted CCL1, CCL5 and CXCL10, which are known chemoattractants of neutrophils, macrophages and T cells, and pro-inflammatory cytokines IL-16, IL-18 and TNFα. When B cells were depleted using an anti-CD20 antibody, the extent of the CAD was reduced along with a reduction in tertiary lymphoid structures (Tse et al., 2015). There is therefore potentially a role for B cells in promoting the alloresponse

long-term and contributing to chronic rejection. As skin is the most immunogenic tissue to transplant, it is possible that any effect of the B cells as APCs is largely overshadowed by resident dendritic cells, but the results from the other studies suggest that B cells may play a more significant role in the rejection of other organs such as the heart or kidney.

1.2.8 B cells as regulatory cells

The capacity for a B cell to provide a regulatory role in an immune response is currently of great interest to many immunologists. Unearthing the mechanism of action and phenotype of so-called Breg cells could potentially lead to novel and effective therapies that could be used in the control of allograft rejection and a number of autoimmune diseases.

1.2.8.1 Evidence for regulatory B cells in mice

Studies have been published in a number of mouse models that suggest an essential role for B cells in the effective regulation of the immune response. Tedder and colleagues have identified a subset of murine IL-10 producing B cells that have been termed B10 cells. B10 cells are found in the spleen and are predominantly CD1dhighCD5+ (Yanaba et al., 2009, Yanaba et al., 2008). In vitro, this subset of cells can be induced to produce IL-10 after stimulation with TLR4 agonist LPS, in combination with mitogens PMA and ionomycin. In vivo, they have been shown to increase in numbers and prolong survival in a NZB/W mouse lupus model (Watanabe et al., 2010). Interestingly, the importance of B10 cells to the regulation of the immune response in this model was emphasised when it was found that reduced regulatory T cell numbers could be restored in CD19-/- NZB/W mice upon adoptive transfer of CD1dhighCD5+ cells from CD19+/+ mice.

B cell deficient mice (μMT) develop more severe disease than wild type mice when injected with MOG antigen known to induce an experimental model of multiple sclerosis (experimental autoimmune encephalitis (EAE)). IL-10 production by B cells, and subsequently its protective effect in this model, was shown to be dependent on stimulation of antigen specific B cells in combination with CD40 ligation (Fillatreau et al., 2002). Interestingly, the protective effect of IL-10+ B cells was only seen after a number of days when disease symptoms in the wild type mice were alleviated compared to the μMT mice. This suggests that the B cells with regulatory function in this model need to undergo a maturation process before they can exert their inhibitory effects. This line of thinking is supported by the fact that when the same mice were knocked out for CD40, only an IgM response was mounted which did not result in the production of IL-10, suggesting that in this model, the B cells may require germinal centre reactions and class switching in order to develop regulatory capacity (Fillatreau et al., 2002).IL-10 producing B cells have been shown to positively impact regulatory T cell numbers in a mouse model of collagen induced arthritis. The specific depletion of IL10+ B cells from mice resulted in exacerbated arthritis disease and a significant

decrease in numbers of FoxP3+ T cells, coupled with an increase of Th1 and Th17 cells. In this model, the marginal zone transitional 2 B cells were deemed the necessary cell population required to restore the Treg/Th1/Th17 cell balance and not B10 cells (Carter et al., 2012).

1.2.8.2 Evidence for regulatory B cells in humans

In humans, B cells have the potential to secrete IL-10 and have been shown to have the ability to expand regulatory T cells, suppress T cell proliferation, inhibit the differentiation of naïve T cells into pro-inflammatory Th1 cells and suppress pro-inflammatory cytokine secretion by monocytes (Blair et al., 2010, Chesneau et al., 2015, Iwata et al., 2011, van de Veen et al., 2013, Chen et al., 2009).

1.2.8.3 Phenotype of regulatory B cells

As the study of regulatory B cells (Bregs) in humans is still in its infancy, work is ongoing to establish whether there is a common origin for all Bregs and if a unique phenotype can be assigned to this population. The potential to produce IL-10 is one of the most common features used to define a Breg. In humans, phenotypes using cell surface markers of circulating B cells are variable and include that of transitional B cells, CD38hiCD24hi (Blair et al., 2010, Flores-Borja et al., 2013, Das et al., 2012a), memory B cells CD24hiCD27+ (Iwata et al., 2011), activated B cells; large CD25+ B cells and CD25+CD71+CD73- (Tretter et al., 2008, van de Veen et al., 2013) and CD24hiCD27int plasmablasts (Matsumoto et al., 2014). Additional markers that have also been used to describe a Breg include CD1d, CD5, CD10 and TIM-1 (Ma et al., 2014, Blair et al., 2010). These varied results suggest that regulatory properties are not exclusive to one subset of B cells, a hypothesis that is supported by the findings of Cherukuri et al which showed that all B cell subsets (transitional, naïve and memory) were able to produce IL-10, but it was the balance between anti-inflammatory IL-10 and pro-inflammatory TNF-a produced by each B cell subset that equipped them with the ability to suppress a Th1 response (Cherukuri et al., 2014).

1.2.8.4 Regulatory B cells suppress the inflammatory T cell response

Maximum inhibition of the production of Th1 cytokines TNFα and IFNγ by CD4+CD25- T cells has been shown to be directly mediated by IL-10 derived from CD40L+CpG stimulated transitional B cells, in combination with the ligation of co-stimulatory molecules CD80 and CD86, indicating that regulatory B cells exert their functions by both soluble factors and direct cell-cell contact (Blair et al., 2010). In addition, this subset of B cells has been shown to inhibit the differentiation of naive T cells into either

IFNγ+T-bet+ (Th1) or RORC2+ (Th17) cells in either Th1 or Th17 cell polarising conditions, but the authors did not investigate whether this was IL-10 dependent (Flores-Borja et al., 2013).

1.2.8.5 Regulatory B cells support the Regulatory T cell response

Flores-Borja et al demonstrated that CD24hiCD38hi B cells were able to convert CD4+CD25- T cells into CD4+CD25+CD127- regulatory T cells that were able to suppress the proliferation of autologous CD4+CD25-CD127+ T cells. This process was partially dependent on IL-10 secretion by the B cells (Flores-Borja et al., 2013).

1.2.8.6 Regulatory B cells Inhibit T cell proliferation

A study by Chesneau et al suggests that one of the mechanisms that B cells use to regulate a T cell response is by inducing apoptosis in the T effector cell. By co-culturing CD40L+CpG activated B cells with activated CD4+CD25- T cells, they showed that the inhibition of T cell proliferation was dependent on B cell derived Granzyme B production and cell-cell contact. In addition, they found that a higher proportion of CD4+CD25- T cells expressed Annexin 5 upon co-culture with activated B cells (Chesneau et al., 2015). Apoptosis was also shown to be the mechanism by which large CD25+ B cells inhibited CD4+ T cell proliferation in a study by Tretter et al where the B cells were polyclonally stimulated with anti IgM/IgG or Cowan I antigen of *S. aureus* (SAC) prior to co-culture with the CD4+ T cells (Tretter et al., 2008).

Bouaziz et al showed that B cells activated with CpG and anti-Ig were able to inhibit proliferation of CD4+CD25- T cells in a partially IL-10 dependent manner (Bouaziz et al., 2010). They did not investigate T cell apoptosis in these experiments but the findings of Chesneau et al may reconcile why IL-10 did not completely inhibit T cell proliferation.

1.2.8.7 Regulatory B cells in disease

Regulatory B cells have been studied in a variety of disease settings. Reduced Breg frequencies are associated with increased disease activity in patients with rheumatoid arthritis (Ma et al., 2014) and the ability of B cells to produce IL-10 upon polyclonal stimulation is reduced in both RA and SLE (Blair et al., 2010, Flores-Borja et al., 2013). In addition, B cell infiltrates have been detected in solid epithelial tumours and are hypothesised to suppress anti-tumour immunity by inhibiting T cell proliferation in a granzyme B dependent manner (Lindner et al., 2013). It has also been hypothesised that regulatory B cells contribute to the control of chronic viral infection through IL-10 production. Serum IL-10 levels and increased frequencies of regulatory B cells

correlate with periods of decreased viral load and disease flares in patients infected with Hepatitis B (Das et al., 2012a).

At present, studies on regulatory B cells suggest that more than one subset of B cells can exhibit a regulatory function if exposed to the correct combination of stimuli. In addition, the mechanism of regulation, and the regulatory or suppressive effect of these B cells differs according to experimental design and disease setting. Most studies that investigate regulatory B cells in humans involve polyclonal methods of B cell stimulation such as LPS, CpG and CD40L, so the importance of BCR ligation and antigen specificity to the differentiation or activation of regulatory B cells remains unclear. Whether the differentiation and activation of regulatory B cells is dependent on specific antigenic stimulation or just the right inflammatory environment requires further investigation.

1.2.8.8 Regulatory B cells in transplantation and transplant tolerance

A patient is defined as operationally tolerant to their transplant if they have stable graft function in the absence of immunosuppression for at least one year (Brouard et al., 2012). These patients are a rare phenomenon in a renal transplant setting, but when such patients are identified, they become a valuable resource for studying potential mechanisms by which the immune system becomes tolerant to a transplant (Brouard et al., 2012).

Interest around the contribution that B cells make to allograft tolerance has gained momentum since it was reported that tolerance could only be induced in a mouse model of cardiac transplantation when B cells were present, and that direct interaction between T and B cells via costimulatory molecules CD40 and CD80/86 was essential for this process (Deng et al., 2007). Since then, there have been several studies published that point towards B cell involvement in the induction or maintenance of operational tolerance in a kidney transplant setting. Several studies have proposed a B cell signature of tolerance as tolerant patients were found to have a differential gene expression from patients who had stable graft function and were on immunosuppression. Many of the differentially expressed genes were associated with B cell differentiation, proliferation, immunoglobulin receptor editing and apoptosis (Newell et al., 2010, Sagoo et al., 2010, Chesneau et al., 2015, Pallier et al., 2010). There is however discordance between these studies with regards to what B cell related genes are differentially expressed, a fact which makes it difficult to know where to focus future studies in terms of functionally assessing the immune-mediated

mechanisms behind these gene expression profiles. Nevertheless, attempts have been made to correlate in vitro findings in these patients with clinical outcomes and their respective gene expression profiles. One of the most consistent findings that has been reported across the studies is that tolerant patients have both higher numbers and frequencies of B cells in their peripheral blood compared to the stable patients on immunosuppression (Sagoo et al., 2010, Newell et al., 2010, Louis et al., 2006, Pallier et al., 2010). It has also been reported that tolerant patients have a higher frequency of transitional B cells than stable patients and thus potentially have a higher frequency of regulatory B cells, as for now, these B cell subsets have an indistinguishable phenotype (Pallier et al., 2010, Chesneau et al., 2015, Newell et al., 2010). Interestingly, one study has reported that tolerant patients produce more IL-10 after polyclonal stimulation than stable patients (Newell et al., 2010) and other studies have reported that there was no difference in the B cell IL-10 profile of the two groups (Chesneau et al., 2015, Pallier et al., 2010, Silva et al., 2012, Sagoo et al., 2012). In addition to these IL-10 related findings, tolerant patients have also been found to express more granzyme B than stable patients (Chesneau et al., 2015), have a skewed phenotype towards increased TGF-β production (Sagoo et al., 2012, Sagoo et al., 2010), express a lower ratio of activating to inhibitory FC receptors (FcgRIIa:FcgRIIb) and have a higher proportion of memory B cells that express co-stimulatory molecules CD80/86 and CD40 (Pallier et al., 2010). It is important to stress that in many of the parameters measured in the studies mentioned above, the tolerant patients were remarkably similar to the healthy controls. This finding was confirmed in a study by Silva et al where they concluded that tolerance was indicated by an intact immune system, particularly with regards to its regulatory capacity (Silva et al., 2012).

In support of a regulatory role for B cells in controlling the alloimmune response, lower frequencies of transitional B cells have been reported in patients who are rejecting their grafts (Cherukuri et al., 2014, Nouel et al., 2014, Shabir et al., 2015). In addition, Cherukuri and colleagues found that the transitional B cells of those patients that were rejecting their grafts expressed a lower ratio of IL-10:TNFα and that this lower ratio of IL10:TNFα correlated with poorer graft outcome on 3 year follow up (Cherukuri et al., 2014).

1.2.9 The role of B cells in human disease: lessons learned from Rituximab

Determining the role that B cells play in human disease requires extrapolation from data reported on patients with the primary immunodeficiency disease x-linked aggamglobulinaemia and the use of the B cell depleting agent Rituximab. Rituximab is a chimeric human/mouse IgG1 anti-human CD20 monoclonal antibody that was first approved in 1997 by the Food and Drug Administration (FDA) for use in the treatment of the B cell malignancy Non-Hodgkins lymphoma (Plosker and Figgitt, 2003, Harrison et al., 2014). CD20 is exclusively expressed on the surface of B cells from the immature bone marrow stage, right up until differentiation into a plasma cell. Rituximab is therefore effective at targeting B cells but not plasma cells. It's mechanism of action remains unclear but it is hypothesised that it could be killing both malignant and healthy B cell populations through 2 different mechanisms. Firstly, by antibody mediated cytotoxicity (ADCC), where Rituximab forms a complex between the B cell via the CD20 specific fab region, and an NK cell or monocyte via CD16, the FCγRIIIA receptor. This interaction would lead to activation of the NK cell and subsequent killing of the B cell. The second proposed mechanism is by complement dependent cytotoxicity (CDC) where the Fc portion of Rituximab binds the classical complement pathway c1q and initiates the cascade of events that leads to the membrane attack complex being formed on the B cell.

1.2.9.1 Rituximab in autoimmune disease

Autoimmune disease is caused by the breakdown of tolerance mechanisms which normally prevent the immune system from recognising self-antigens as foreign. B cells are thought to play a role in the pathogenesis of several autoimmune diseases including rheumatoid arthritis (RA), systemic lupus erythematosus (SLE), multiple sclerosis (MS), pemphigus vulgaris and ANCA-associated vasculitis. In many of these diseases, class switched antibodies against self-antigens, such as rheumatoid factor in RA, anti-dsDNA antibodies in SLE or anti-neutrophil cytoplasmic antibodies in ANCA associated vasculitis, are detected in the blood stream or at the sites of inflammation (Jones, 2014, De and Barnes, 2014, Hoffmann and Meinl, 2014, Bugatti et al., 2014). The presence of these antibodies is an indication that B cells have been activated and are engaged in interactions with cognate T cells. These B cells are therefore potentially contributing to disease pathogenesis not only through antibody-mediated mechanisms, but also through antigen presentation and cytokine secretion as discussed above. This hypothesis has led to the use of Rituximab in the treatment of several autoimmune diseases with varying levels of success. In RA and SLE,

Rituximab use has been reported to be effective at reducing disease activity in patients refractory to traditional lines of treatment (Lu et al., 2009, Edwards et al., 2004, Edwards and Cambridge, 2001, Leandro et al., 2006, Roccatello et al., 2011, Moore et al., 2004) and has been successfully used in combination with mycophenolate mofetil (MMF) and methylprednisolone, but in the absence of oral steroids, to reduce symptoms of lupus nephritis (Condon et al., 2013). A meta-analysis of studies of pemphigus patients concluded that those treated with Rituximab achieve complete remission quicker than those receiving conventional therapy only (Wang et al., 2015), and in multiple sclerosis patients, Rituximab has proved successful in improving disease symptoms in patients with relapsing remitting MS, but less so in those with primary progressive MS (Castillo-Trivino et al., 2013). Dissecting out the role that the B cells are playing as antigen presenting cells and cytokine secretors in these diseases is difficult, as a reduction in autoantibodies is often observed in patients that have improved clinically after receiving Rituximab (Lu et al., 2009, Edwards and Cambridge, 2001, Cambridge et al., 2006). However, Leandro et al reported that relapse in their RA patients was associated with higher frequencies of memory B cells re-populating the B cell compartment post Rituximab treatment (Leandro et al., 2006, Edwards and Cambridge, 2001). Thus, results from studies using Rituximab in humans, combined with data from the animal studies using μMT mice described above, can be extrapolated to hypothesise that depleting B cells affects autoimmune disease pathogenesis in multiple ways, and is not exclusively due to reducing the deleterious effects of autoantibodies.

Rituximab has also informed us of the role that B cells may play in regulating autoimmunity, as in some cases, treatment with Rituximab has led to the exacerbation of existing disease or the onset of new inflammatory diseases (Dass et al., 2007, Mielke et al., 2008, Fassi et al., 2008, Goetz et al., 2007).

Although licensed for use for treating Non–Hodgkins lymphoma, the use of Rituximab for autoimmune disease remains largely off-label due to varying reports of efficacy from clinical trials that have used the drug (Beckwith and Lightstone, 2014).

1.2.9.2 Rituximab and chronic antibody mediated rejection

Off-label use of Rituximab in a transplant setting is becoming more common and its effectiveness at controlling both acute and chronic allograft rejection is being studied in several clinical trials. Table 1.1 provides a summary of studies and clinical trials that have used Rituximab to treat chronic rejection in a kidney transplant setting.

Condition	Treatment Regimen	Outcome	Reference
Transplant glomerulopathy in CAMR. Adults	RTX 2x 375mg/m^2/wk IVIg 1g/kg/wk	Graft survival rates no different to control patients. Treatment associated with higher frequency of adverse events.	(Bachelet et al., 2015)
CAMR. Adults	RTX 1x 375mg/m^2 IVIg 0.4g/kg for four days	Stabilisation of graft function was associated with RTX treatment. Higher graft survival rates at 3 year follow up were associated with RTX treatment and low proteinuria.	(Chung et al., 2014)
CAMR. Paediatrics According to Banff '05 criteria	IVIg 4x 1g/kg/wk RTX 1x 375mg/m^2	Improvement or stabilisation of glomerular filtration rate at 6 months post intervention in 70% patients studied. 100% patients without TG responded, compared to only 45% who had TG. A greater degree of TG was associated with non-responsiveness. Class I and II DSA became undetectable in 7/20 patients 12 months post intervention.	(Billing et al., 2012)
CAMR. Adults	RTX 1x 375mg/m^2 (day 1) IVIg 0.4g/kg/day (days 2-5)	Improvement of graft function seen in 4/4 patients for first 6 months post treatment. Reduction of DSA observed in 2/4 patients.	(Fehr et al., 2009)
Transplant glomerulopathy. Adults	RTX 2-4x 375mg/m^2/wk	Stabilisation of kidney function and reduction in albuminuria observed in 7/14 (50%) of patients given Rituximab when patients monitored for 30 month period post Rituximab administration.	(Rostaing et al., 2009)
CAMR. Paediatrics.	IVIg 4x 1g/kg/wk RTX 1x 375mg/m^2	Improvement or stabilisation of glomerular filtration rate in 4/6 patients studied. Non-responsiveness to therapy associated with a greater degree of TG at intervention.	(Billing et al., 2008)
CAMR. Adults	RTX 2x1g: day 0 and day 14.	N/A	RituxiCAN C4 trial Clinicaltrials.gov.uk no: NCT00476164. Trial still ongoing.

Table 1.1 Use of Rituximab to treat CAMR in a renal transplant setting

1.3 Rationale for this thesis

1.3.1 Chronic antibody mediated rejection: are antibodies really the cause?

The presence of circulating anti-donor antibody pre-transplant is a well-established contraindication to transplantation as it can result in hyperacute rejection. Many studies have reported that kidney transplant patients can generate de novo donor specific HLA antibodies (DSA) within months to years post-transplant, but the importance of these antibodies in terms of mediating rejection remains poorly understood (Wiebe et al., 2012). Despite this lack of mechanistic insight, the term 'chronic antibody mediated rejection' (CAMR) is routinely used as a diagnosis, due to the well-established correlation between the presence of circulating DSA post-transplant and worse long term graft survival (Lachmann et al., 2009, Campos et al., 2006, Worthington et al., 2003, Pelletier et al., 2002, Lee et al., 2002). In support of the hypothesis that antibodies are the cause of the pathology observed in chronic rejection, several studies have found that C4d deposition in the endothelium of renal grafts also correlates with graft deterioration (Böhmig et al., 2002, Feucht et al., 1993, Lederer et al., 2001, Gaston et al., 2010, Mauiyyedi et al., 2001). When an antibody binds graft endothelium, it activates the classical complement cascade. C4d is a stable by-product of the classical complement cascade as it covalently binds to the graft endothelium and hence can be detected long after the antibody first binds and is no longer detectable itself. C4d deposition has therefore become a surrogate marker for antibody mediated complement activation that is routinely used in the diagnosis of antibody mediated rejection (Mauiyyedi et al., 2001). From these associations between poor graft outcome, DSA and C4d deposition, a model to describe the pathogenesis of CAMR was devised by Robert Colvin and colleagues and is frequently referenced by transplant clinicians and scientists throughout the world (Wiebe et al., 2012, Colvin and Smith, 2005, Smith et al., 2008, Colvin, 2007, Djamali et al., 2014). The model is illustrated in Figure 1.5.

Despite these strong associations, it has become apparent that there are some anomalies that require addressing before a definitive mechanistic cause of antibody mediated rejection can really be concluded. Primarily, these are: 1) The observation that some individuals maintain good graft function for many years after the development of donor specific antibody (Bartel et al., 2008, Hayde et al., 2014, Banasik et al., 2013, Campos et al., 2006, Lee et al., 2002). 2) Some individuals meet the histological or clinical criteria for CAMR but do not have evidence of circulating DSA

or C4d deposition (Akalin et al., 2007, Worthington et al., 2003, Campos et al., 2006, Wiebe et al., 2012, Haas et al., 2014, Sis et al., 2009, Rostaing et al., 2009). 3) The length of time between development of DSA and graft dysfunction can be many years. This highlights the question, why do the antibodies in a chronic setting mediate rejection at a much slower rate than in hyperacute or acute AMR? 4) To date, there is no published evidence in humans to demonstrate directly that antibodies are causing the damage observed in CAMR.

In addition, there is evidence to suggest that low concentrations of antibody may play a protective role by promoting accommodation of the graft (Salama et al., 2001, Dorling, 2012).

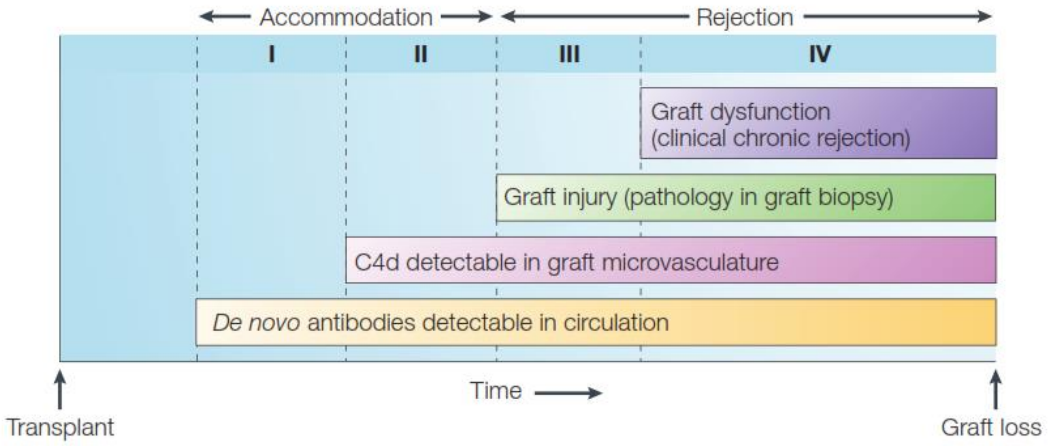

Figure 1.5 The four stages of CAMR

The first three stages of CAMR are sub-clinical, where graft function is yet to deteriorate. The onset of this slow progression to graft deterioration begins with formation and subsequent detection of DSA in the circulation (I). These antibodies then bind the donor HLA molecules on the graft endothelium and activate the classical complement pathway, which is detected by positive C4d staining on the endothelium (II). Once enough complement activation has occurred to cause substantial damage to the architecture of the endothelium, this can be detected on biopsy in the form of interstitial fibrosis and tubular atrophy (III). Eventually, this damage becomes extensive enough to cause a decline in graft function which can be detected clinically by rising creatinine levels, decreasing glomerular filtration rates (eGFR) and proteinuria (IV). Figure taken from (Colvin and Smith, 2005).

1.3.2 Evidence for a cellular component in chronic antibody mediated rejection.

Given the data presented in section 1.2, it is important to keep an open mind when investigating the cause of chronic rejection and long term graft failure. The presence of class switched DSA in the circulation provides evidence that cellular activation of the immune system has occurred and that there has been cognate interactions between T and B cells. It is possible that DSA are merely a biomarker of this cellular activity and potentially non-pathogenic. An observational study carried out in the supervisors lab has provided evidence to suggest that in some individuals, there may be a cellular component involved in driving chronic rejection (Shiu et al., 2015). In this study, an indirect IFNγ ELISpot assay was used to investigate the contribution that B cells and regulatory T cells make to CD4+ T cell IFNγ production in response to donor membrane proteins. The data revealed that cellular responses to donor membrane proteins in kidney transplant patients with CAMR are both complex and heterogeneous. In a subset of samples, in vitro depletion of CD19+ cells revealed B cell dependent IFNγ production. When B cell activation was inhibited by adding Btk/Syk inhibitors to the cultures of these samples, IFNγ production was diminished. In addition, IFNγ production was also diminished in these samples when the antigen processing and presentation pathway was targeted by adding leupeptin/pepstatin A/E64-d or an anti-class II antibody to the cultures. Together, these experiments provide evidence to suggest that B cells may be processing and presenting donor antigens to pro-inflammatory CD4+T cells. Conversely, a potential regulatory role for B cells was revealed in some samples, as IFNγ production in response to donor membrane proteins increased post CD19+ cells depletion (Shiu et al., 2015).

The results from this study also provided evidence to suggest that chronic rejection is not necessarily simply due to a dysregulated alloimmune response as IFNγ production in response to donor membrane proteins was only revealed in some samples when CD25+ cells were depleted from the cultures. To add to the complexity, B cell dependent IFNγ production was only revealed in some samples upon depletion of both CD25+ and CD19+ cells, suggesting that in these samples, CD4+ T cell IFNγ production was mediated by B cell antigen presentation but was suppressed in the presence of CD25+ cells (Shiu et al., 2015).

Finally, the patterns of reactivity in response to donor membrane proteins changed over time suggesting that the cellular alloimmune response in these patients is highly dynamic (personal communication with K Y Shiu and A Dorling). The results from this study have formed a working model on which this thesis is based (Figure 1.6).

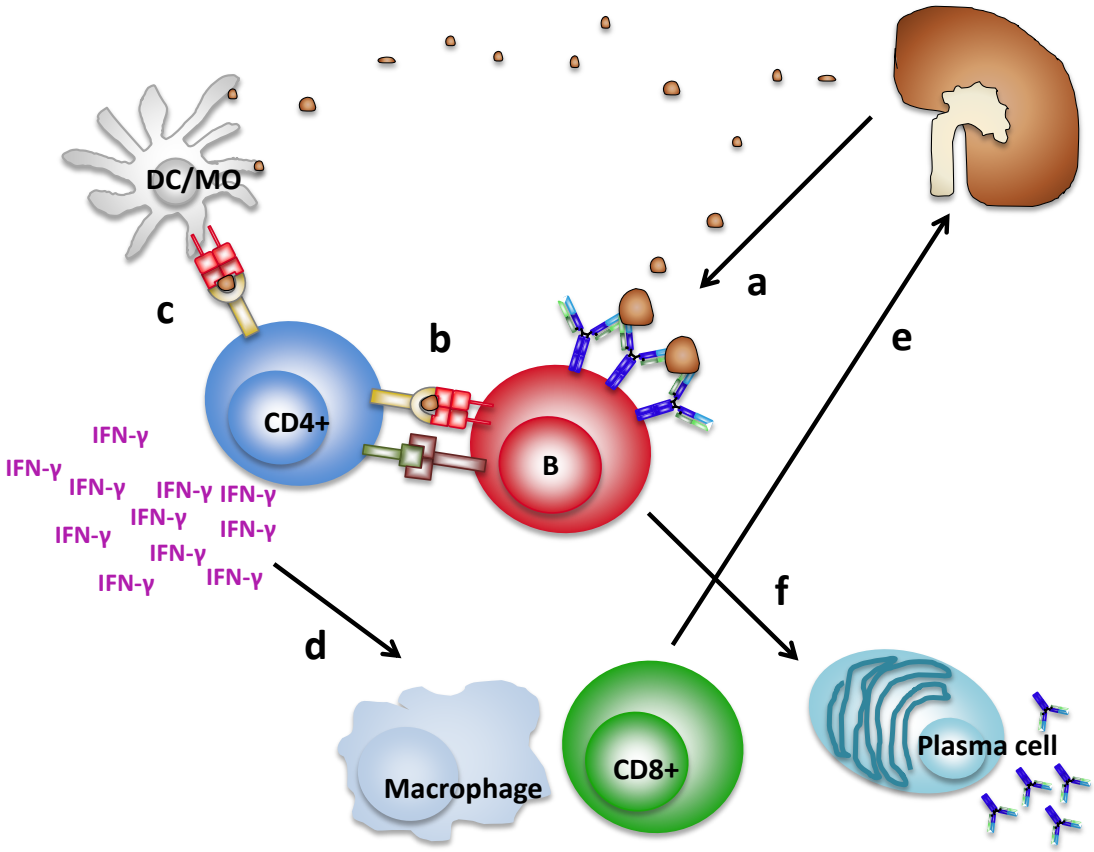

Figure 1.6 A working model for the contribution of B cells to cellular mediated rejection via the indirect pathway of allorecognition.
(a) When HLA antigens are shed from the graft they bind B cells that possess antigen specific B cell receptors on their surface. **(b)** The antigen-BCR complex is internalised and the antigen is processed and presented as peptides to helper CD4+ T cells. These T cells may or may not have been previously primed by other antigen presenting cells **(c)**. **(d)** The CD4+ T cells are activated to produce pro-inflammatory cytokines such as IFNγ which in turn activates effector CD8+ T cells and macrophages which home to the graft and cause damage **(e)**. **(f)** The interaction between the B cell and the CD4+ T cell is reciprocal. The CD4+ T cell provides signals for the B cell to differentiate into a plasma cell which secretes donor specific antibodies that are easily detected in the blood.

1.4 Aims

Based on the results described in Shiu et al, and the working model described in Figure 1.6, the major aims of this thesis were:

1. To replicate the different patterns of reactivity found in the IFNγ ELISpot reported by Shiu et al. in a different cohort of renal transplant patients with chronic antibody mediated rejection who have been enrolled in the RituxiCAN C4 clinical trial.

2. To investigate whether these patterns of reactivity correlate with clinical outcomes.

3. To investigate the phenotype of B cells as they re-populate the periphery in a subset of patients enrolled in the RituxiCAN C4 trial who received Rituximab treatment.

4. To detect and phenotype HLA specific B cells in the circulation of patients enrolled in the RituxiCAN C4 trial.

5. To correlate the phenotype of HLA specific B cells with the pattern of reactivity found in the IFNγ ELISpot.

1.5 Hypotheses

Based on the literature reviewed above, the following hypotheses were made:

1. The patterns of reactivity in the IFNγ ELISpot reported in Shiu et al will be broadly replicated in the patients enrolled in the RituxiCAN C4 trial.

2. The phenotype of HLA specific B cells will be predominantly a class switched memory phenotype.

3. The phenotype of the HLA specific B cells will correlate with the pattern of reactivity in the IFNγ ELISpot:

    a) Individuals who produce IFNγ in response to HLA proteins in a B dependent manner, will have an HLA specific B cell phenotype that is skewed towards a memory phenotype.

    b) Individuals who have a B regulated pattern of reactivity in response to HLA proteins will have an HLA specific B cells that are skewed towards a transitional phenotype.

2 Materials and Methods

2.1 RituxiCAN C4 trial: Patient recruitment and study overview

All patient blood samples used in this thesis were taken from patients enrolled onto the RituxiCAN C4 trial. Ethical approval for this study was obtained from the Hammersmith and Queen Charlotte's ethics committee, the research ethics approval (REC) number for the study is 06/Q0406/119. The clinicaltrials.gov identification number for the trial is NCT00476164. Figure 2.1 provides an overview of the study protocol. Patients enrolled onto the trial must have been given a diagnosis of CAMR with positive C4d staining and an estimated glomerular filtration rate (eGFR) of ≥20 mls/min and have evidence of graft dysfunction, with either a creeping creatinine (Dudley et al., 2005) and/or significant proteinuria (defined as a urine protein:creatinine ratio of >50). A baseline blood sample was taken upon enrolment and processed as described in section 2.2. From a patient's perspective, the trial was split up into three phases. Phase I 'run-in' lasted 3-5 months, and all patients received optimised doses of Tacrolimus and Mycophenolate Mofetil (MMF). There were three potential outcomes at the end of phase I: a) Graft function stabilised (or proteinuria settled), and the patient transitioned into phase III, where they were then followed for three years and peripheral blood mononuclear cell (PBMC) samples were taken every 3 months (Fig. 2.1 (a)); b) Graft function did not stabilise, or proteinuria did not settle, and the patient was consented to be randomised into phase II, where they either received Rituximab in addition to optimised Tacrolimus and MMF or continued with just optimised Tacrolimus and MMF (Fig. 2.1 (b)); c) graft function deteriorated such that eGFR fell to <20mls/min or the graft function was lost altogether during phase I and the patient was withdrawn from the trial or transitioned straight to phase III. Those patients who received Rituximab were given a 1g dose of Rituximab on day 0 followed by a further 1g dose on day 14, with the first dose given within a month of randomisation. The primary endpoint of the trial was reached 3-5 months post randomisation and another PBMC sample was taken. The patient then transitioned into phase III.

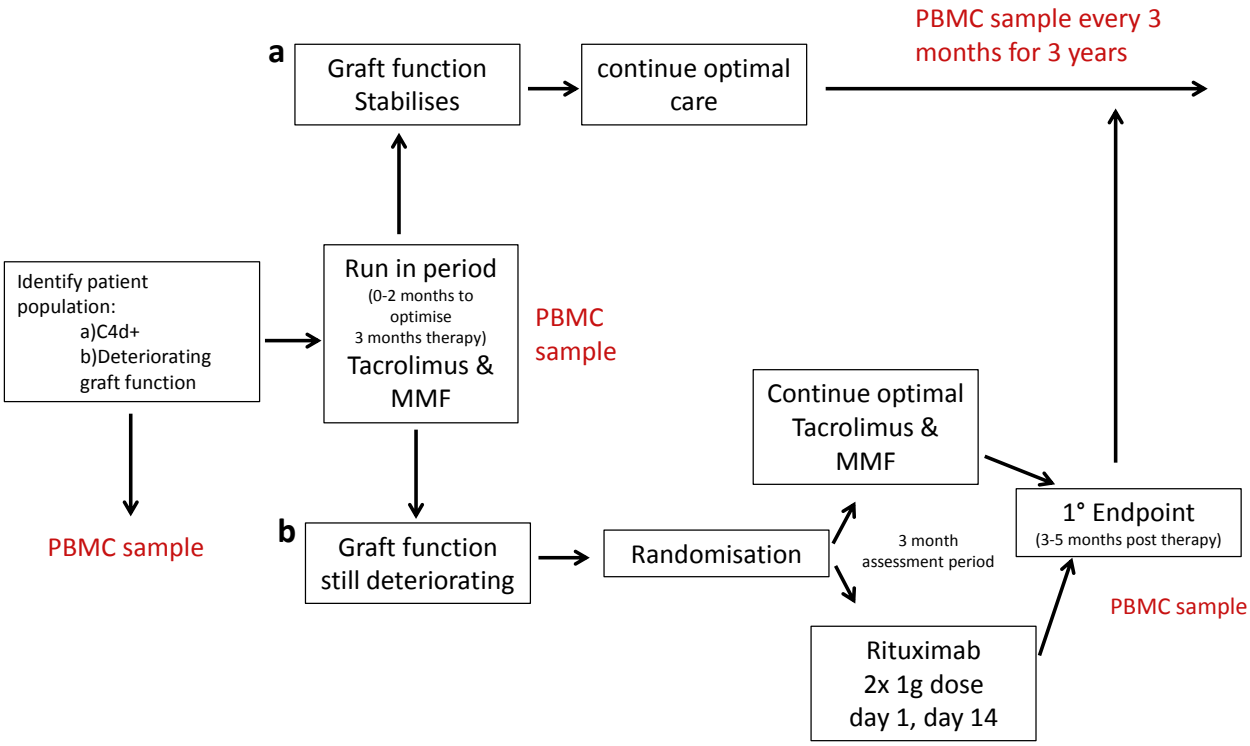

Figure 2.1 Schematic of the RituxiCAN C4 trial

2.2 Blood Sample acquisition and processing

Approximately 60ml of blood was collected in EDTA K2 vacutainers and approximately 20ml of blood was collected in red top vacutainers (BD Bioscience, Oxford, UK) at every time-point in the trial. Blood samples from Guy's Hospital, London and The Hammersmith Hospital, London, were processed on the same day as blood draw. All other samples were shipped overnight at ambient temperature and processed the next morning. External sites that had patients enrolled on the trial were at St. James's University Hospital, Leeds; University Hospital of Wales, Cardiff; Queen Elizabeth Hospital Birmingham; and Glasgow Royal Infirmary, Glasgow. When available, up to 60ml of blood was collected in EDTA K2 vacutainers from live donors to be used for making membrane proteins as detailed in section 2.3.1.

Blood from healthy volunteers was obtained in the form of concentrated leukocytes provided by the blood transfusion service as a by-product of the blood donation process. These samples will be referred to as Leukocyte cones throughout this thesis. The Leukocyte cones were delivered the day after the blood was drawn and processed immediately.

2.2.1 Serum collection

Blood samples were left to clot in the red top vacutainers for two hours and then centrifuged at 500g for 10 minutes. The Serum was aspirated and aliquoted in 2ml volumes and stored at -80°C.

2.2.2 PBMC isolation

Blood was diluted 1:2 with Dulbecco's Phosphate Buffered Saline (PBS) (Sigma-Aldrich, Dorset, UK) and layered onto 15ml of Lymphoprep™ (Alere, Cheshire, UK) in 50ml tubes. The blood was then centrifuged at 800g for 30 minutes at 20°C. The layer of peripheral blood mononuclear cells (PBMC) was removed with a Pasteur pipette and diluted at least 1:3 with PBS. Diluted PBMC were centrifuged at 500g for 10 minutes, the supernatant was poured off and PBMC were pooled and re-suspended in 50ml RPMI medium (SIGMA-ALDRICH). PBMC were then centrifuged at 300g for 7 minutes, and re-suspended in 15ml RPMI ready for counting. To count, the PBMC were inverted to mix and a 10µl aliquot was removed and mixed with 10µl Trypan blue solution (SIGMA-ALDRICH). 10µl PBMC-Trypan blue solution was loaded onto a haemocytometer and PBMC in three large squares on the haemocytometer grid were counted. A live mononuclear cell was defined as bright and round. Red blood cells were identified as smaller, very round cells and were not included in the PBMC count. Cells that were blue in colour were deemed non-viable and excluded from the count.

2.2.3 Freezing of PBMC

Once counted, 1 x10^6 cells were removed for RNA isolation; the cells were centrifuged for 5 minutes at 13000rpm and re-suspended in 800µl TRIzol® solution (Life Technologies, Paisley, UK) for two minutes before being frozen at -80° C. The remaining PBMC were centrifuged at 500g for 5 minutes and re-suspended at a concentration of 40x10^6 cells/ml in human AB serum (Life Technologies). An equal volume of human AB serum+20% DMSO was then added dropwise to make the final concentration 20x10^6 cells/ml and the PBMC were aliquoted in 1ml volumes into cryovials and placed into a Mr Frosty™ (Thermo Scientific, UK) for controlled freezing in the -80° C freezer. PBMC were transferred to Liquid Nitrogen (LN_2) storage the day after.

2.2.4 Thawing of PBMC

All assays in this thesis were carried out using frozen PBMC. All PBMC were thawed using the following method: PBMC were removed from Liquid nitrogen storage and 500µl of warm AIMV media (Life Technologies) plus 10% Human AB serum (from here on in abbreviated to AIMV10) plus 1% Bovine pancreas DNase (Merck Chemicals Ltd, Nottingham, UK) was added to the cryovial before thawing at 37°C in a water bath. The cryovial was removed from the water bath just before the aliquot had completely thawed and transferred into 10ml AIMV10 plus 1% DNase media. Cells were spun at 500g for 5 minutes and re-suspended in 10ml AIMV10 plus 1% DNase. Cells were then rested for 20 minutes at 37° C, 5% $C0_2$.

After the resting period, the cells were passed through a 70µm strainer (BD Bioscience) to remove any clumps and then counted using a haemocytometer as described in section 2.2.2. Cells were centrifuged at 500g for 5 minutes and re-suspended in the appropriate volume of media for the assay that they were to be used in.

2.3 Detection of IFNγ production in response to donor membrane proteins

2.3.1 Donor membrane protein preparation

If a live donor was available, their PBMC was used as a source of donor HLA proteins. Donor PBMCs were thawed in the same way as described in section 2.2.4. Cells were then re-suspended in 50ml cold PBS and washed twice at 500g for 5 minutes. Cells were re-suspended in 1ml of lysis buffer (detailed in Table 2.1) and transferred into a 1.5ml tube. Cells were spun at 13000rpm, 4°C, for 2 minutes and re-suspended in 1ml of lysis buffer. The cells were then subjected to 3x freeze thaw cycles in order to lyse the cells. This involved immersing the cells in LN_2 for 5 minutes, then thawing them in a water bath set to 37°C whilst intermittently shaking and vortexing them to help break up the cells. After the third freeze thaw cycle, the cells were spun at 2000g, 4°C for 2 minutes. The supernatant containing the membrane proteins was transferred into a fresh 1.5ml tube and spun at 3000g, 4°C for 2 minutes. The supernatant was aspirated and transferred into a 10.4ml sterile autoclaved ultracentrifuge bottle (Beckman Coulter, High Wycombe, UK) and topped up with lysis buffer so the bottle was full. The membrane proteins were placed in a cold fixed bucket T1270 rotor and spun in an ultracentrifuge (Thermo Scientific) at 33100rpm for 1 hour. The supernatant was carefully aspirated to leave a small pellet of membrane protein which was dissolved in solubilising solution and frozen in 5µl aliquots at -80°C for long term storage. The concentration of the membrane protein was determined using the BCA assay described in section 2.3.2

Table 2.1 Recipe for lysis buffer required for preparing donor membrane proteins

Reagent	Concentration	Volume	Manufacturer
ddH_2O	NA	17.65ml	NA
Tris (pH 7.5)	0.5M	2.00ml	SIGMA ALDRICH
EDTA (pH 7.5)	0.3M	20µl	SIGMA ALDRICH
Soybean trypsin inhibitor	1mg/ml	10µl	SIGMA ALDRICH
PMSF	0.1M	2µl	SIGMA FLUKA
Protease inhibitor cocktail	NA – mixture of different inhibitors	2.5µl	SIGMA ALDRICH
Nonidet P 40*	NA	2.5µl	SIGMA FLUKA

*Nonidet P 40 only to be added after cells have been washed once in lysis buffer.

2.3.2 BCA assay

The concentration of donor membrane proteins was determined using a bichinchoninic acid (BCA) assay kit (Thermo Scientific). Standards were made up using Bovine serum albumin (BSA) provided in the kit. The dilutions used to make the standard curve are detailed in table 2.2.

Table 2.2 Dilution volumes for standards in BCA assay

Vial	Volume of PBS diluent (µl)	Volume BSA (µl)	Final BSA concentration (µg/ml)
A	0	300 of stock	2000
B	125	375 of stock	1500
C	325	325 of stock	1000
D	175	175 of vial B	750
E	325	325 of vial C	500
F	325	325 of vial E	250
G	325	325 of vial F	125
H	400	100 of Vial G	25
I	400	0	0

Working reagent was made by mixing 50 parts of BCA reagent A with 1 part of BCA reagent B. 100µl of working reagent was mixed with duplicate wells of a flat bottom 96 well plate containing 10µl of either the standards, PBS + solubilising solution control, or the donor membrane protein solution. The plate was wrapped in aluminium foil to prevent evaporation and incubated at 37°C for 30 minutes.

The plate was left to cool to room temperature then read at 562nm to measure the optical density of each well. The mean of each duplicate was calculated and a standard curve was used to calculate the concentration of donor membrane proteins. The value calculated in the PBS only wells was subtracted as background from the wells containing the donor membrane protein.

2.3.3 Analysis of HLA antibodies

As part of their routine patient monitoring, circulating HLA specific antibodies in the patient's serum were detected using a Luminex® assay carried out by the clinical laboratories at each of the sites where patients were recruited onto the RituxiCAN trial. The Luminex® assay uses a matrix of polystyrene beads that are impregnated with different concentrations of fluorescent dye to create a gradient of fluorescence intensity along which each bead can be recognized when acquired. Each different bead is coated with a different HLA antigen. The patient's serum is incubated with the HLA antigen coated beads and antibodies that are specific for that HLA antigen will bind the

bead. A detection anti-IgG antibody conjugated to a different fluorochrome from the polystyrene beads is then added to enable detection of serum antibodies that have bound the beads.

Where available, the raw data read outs of mean fluorescence intensity (MFI) from this assay were obtained from the clinical laboratories and analysed to enable a full analysis of all of the HLA specific antibodies that were present in the patient's serum. Each antibody that gave a positive result was categorized into MFI of 100+, 200+, 300+, 400+, 500+ and 1000+. This method enabled the detection of HLA antibodies that may be relevant for choosing a surrogate donor as described in section 2.3.4. Where the raw data was not available, final analysis conducted by the clinical laboratory was obtained. This included both donor specific and non-donor specific HLA antibodies. However, MFIs of below 500-1000 were not reported in these analyses.

2.3.4 Choosing a surrogate donor

In circumstances where the transplanted kidney was from a deceased donor, membrane proteins were sourced from a bank of surrogate donors that had known HLA genotypes.

When choosing a suitable surrogate donor the HLA type of the recipient, the donor, and any previous donors needed to be considered, along with the HLA antibody profile that each patient had. The following rules were applied when choosing the surrogate donor:

1. The surrogate donor must possess HLA alleles that the donor has and that the recipient has a circulating antibody against.
2. Any HLA alleles that the surrogate donor has, but the real donor does not have, must match those of the recipient where possible.
3. A surrogate donor must not be used if it has an HLA allele that is the same as a previous transplant and not shared with the current donor.
4. A surrogate donor must not be used if it has an HLA allele that is not the same as the donor's but the recipient has circulating antibodies against it.

2.3.5 Indirect IFNγ ELISPOT assay

2.3.5.1 Depleting leukocyte subsets from PBMC

PBMC were thawed as described in 2.2.4 counted and re-suspended at $4x10^6$ cells/ml. As this was an indirect IFNγ ELISpot to assess the antigen presentation capabilities of B cells, magnetically labelled beads were used to deplete all PBMC of CD8+ cells, to eliminate any potential for the direct alloimmune response to cause IFNγ production.

Cells were then depleted of either B cells with CD19+ beads, Treg cells with CD25+ cells or both B cells and Tregs combined. All beads used were Dynabeads® and washed prior to use in PBS + 2mM EDTA+ 0.1% FCS (Dynabead® buffer) according to the manufacturer's instructions. 100µl of beads was applied for every 1ml of cell suspension and the cell-bead mixture was incubated on a roller at 4°C for 30 minutes. The 15ml tube containing the cell-bead suspension was then placed in a magnet (Life Technologies) so any positive cells that had bound to the labelled magnetic beads were removed from suspension and the depleted cells were aliquoted into a fresh 15ml tube. 150µl of cell suspension was removed for staining for flow cytometry to check the efficiency of the depletions. PBMC suspensions were counted post depletion to use in the analysis of the ELISpot as described in section 2.3.5.6.

Figure 2.2 shows example plots of before and after each depletion. The average efficiency of depletion for each condition was 92% for CD8+ cells, 92% for CD19+ cells and 54% for CD25hi cells.

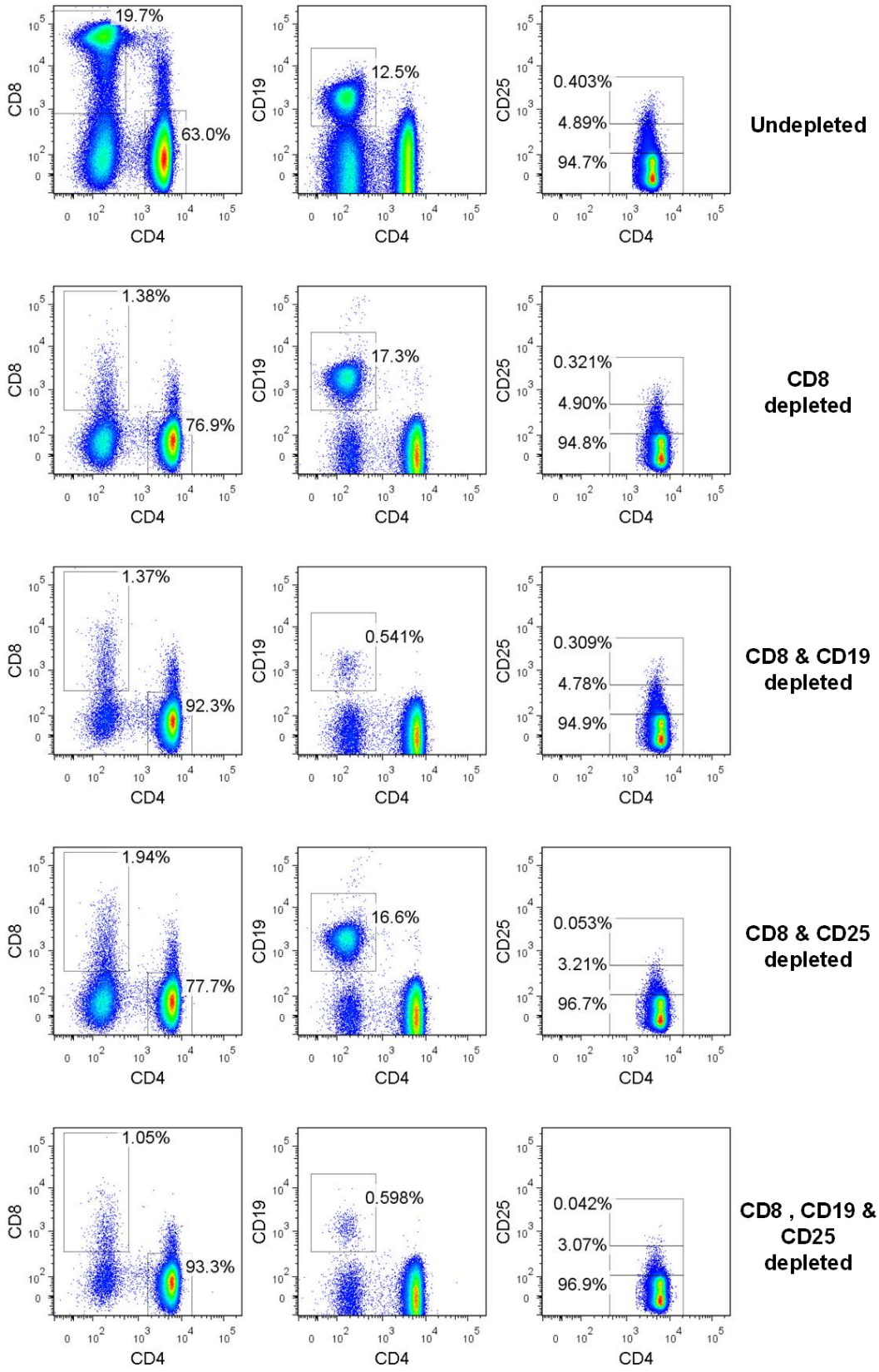

Figure 2.2 Representative dot plots to illustrate depletion of different lymphocyte subsets using the Dynabead® system.

2.3.5.2 Donor membrane proteins

The appropriate membrane proteins were used at two different concentrations in the assay and diluted in AIMV10 media to either 1µg/ml or 0.2µg/ml so the final concentration in the assay was 0.5µg/ml and 0.1µg/ml respectively.

2.3.5.3 Viral cocktail and CD3/CD28 beads as positive controls

A viral cocktail was used as a positive control for antigen processing and presenting in the assay. The cocktail comprised three protein antigens that the majority of individuals in the general population are likely to have been exposed to: Varicella Zoster Virus glycoprotein E (VZV gE, Prospec, Rehovot, Israel) and Cytomegalovirus pp65 and glycoprotein B (CMV pp65 and CMV gB, Abcam, Cambridge, UK). VZV gE and CMV gB were used at a concentration of 0.03µg/ml and CMV pp65 was used at 0.003µg/ml. All viral proteins were combined and diluted in AIMV10.

CD3/CD28 human T activator beads (Life Technologies) were used as a polyclonal stimulus as a way of checking T cell viability and the ability to produce IFNγ. The beads were used according to the manufacturer's instructions with 10µl of bead solution being added to each well.

2.3.5.4 Preparing the ELISpot plate

The same batch of IFNγ ELISpot kit (MABTECH, Nacka Strand, Sweden) was used for every patient sample. 96 well plates with a PVDF membrane were pre-coated with anti-IFNγ capture antibody by the manufacturer. The plates were washed twice with 200µl of sterile PBS and then blocked with 100µl AIMV10 medium at room temperature for two hours to prevent any non-specific binding. Blocking solution was then removed and 100µl of the donor membrane proteins and viral cocktail were added to the plate. Wells containing only AIMV10 were also set up as an un-stimulated control to measure any non-specific IFNγ that was produced by the cells. Wells were always set up in triplicates for each condition apart from the CD3/CD28 beads where only one well was used for each sample of PBMC. In all wells that did not have membrane proteins, the solubilising solution that the membrane proteins were dissolved in was added at an equivalent concentration to account for any toxic effects that this carrier solution may have on the PBMC. Wells with only AIMV10, 0.2µg/ml membrane proteins or viral cocktail without any PBMC were also set up as negative controls.

Once the antigens had been added to the plate, 100µl of well mixed PBMC from each of the depletion conditions was dispensed directly into the centre of each well. The ELISpot plate was then wrapped in foil to prevent evaporation and incubated for 24 hours at 37°C, 5% CO_2.

2.3.5.5 Adding the detection antibody

PBMC were removed from the ELISpot plate with a flick and 200µl of ddH_2O was added to each well for 2 minutes to lyse any residual cells. This step was repeated and then each well was washed 5 times with 200µl PBS and tapped dry. An anti-IFNγ detection antibody conjugated to alkaline phosphatase (ALP) was diluted to 1:200 in PBS with 0.5% FCS and 100µl was added to each well. The plate was then wrapped in foil and incubated at room temperature for 1.5-2 hours.

Each well was then washed 5 times in PBS, tapped dry and 100µl of 0.45µm filtered substrate solution 5-bromo-4-chloro-3-indolyl-phosphate/nitro blue tetrazolium (BCIP/NBT) was added to each well. The plate was washed well with tap water to stop the reaction once defined spots had appeared in the wells (approximately 30 seconds). Plates were then dried overnight.

2.3.5.6 Analysing the ELISpot plates

Spots on the ELISpot plates were counted using an automated counting system (AID ELISpot reader system, Strassberg, Germany). As a quality control measure, each well was checked to make sure the spot count was accurate. The mean spot count for each triplicate condition was calculated and the mean spot count in the un-stimulated wells was subtracted from this. The frequency of CD4+ cells in each depletion condition was calculated using the flow cytometry staining data in conjunction with the PBMC count post depletion to calculate the number of IFNγ spots per million CD4+ T cells. A sample was deemed reactive to the donor membrane proteins or viral cocktail if it produced ≥ 25 IFNγ+ spots per million CD4+ lymphocytes after the subtraction of background.

Throughout the thesis, the pattern of reactivity when either CD8+&CD19+ cells, CD8+&CD25+ cells or CD8+, CD19+ & CD25+ cells were depleted was defined using the same criteria used in Shiu et al. and are as follows:

B dependence (Bdep): If the number of IFNγ spots per million CD4+ T cells was reduced by ≥20%, or did not reach above ≥25 spots per million CD4+ lymphocytes when CD19+ cells were depleted, the sample was deemed B dependent.

B regulation (Breg): If the number of IFNγ spots reached above the ≥25 spots per million CD4+ lymphocytes cut off, or increased by ≥20% when CD19+ cells were depleted, the sample was deemed B regulated.

Treg (Treg): If the number of IFNγ spots reached above the ≥25 spots per million CD4+ lymphocytes cut off, or increased by ≥20% when CD25+ cells were depleted, the sample was deemed T regulated.

Bnon: Any change in the number of IFNγ spots per million CD4+ T cells observed post CD19+ cell depletion was not large enough to meet the criteria above.

2.3.6 Blocking IL-10 in the IFNγ ELISPOT assay

The ELISpot was carried out as described in section 2.3.5 using PBMC from leukocyte cones with CMV gB as the stimulating antigen. Anti- IL-10 or the appropriate isotype control were added to the wells at a concentration of 10µg/ml to measure the effect that blocking IL10 had on IFNγ production pre and post CD19+ cell depletion.

2.4 Flow cytometry

2.4.1 General flow cytometry method

Flow cytometry is used heavily throughout this thesis for both surface and intracellular staining. A general protocol was followed for all flow cytometry with appropriate modifications being made to suit the assay where necessary. All antibodies were titrated to determine the optimum volume per test to use. In many instances, the optimum concentration of antibody to be used had been established by previous members of the supervisor's laboratory before this thesis began. Table 2.5 summarises details of all of the antibodies used in this thesis. Antibodies were made up into cocktails on the day of staining. The FACS staining buffer used was PBS+30% human AB serum or PBS+30% FCS if IgM was included in the staining cocktail.

Cells were transferred to a 96 deep well plate and washed in 300µl FACS staining buffer at 500g for 5 minutes, 4 °C. All subsequent wash steps were carried out using these parameters. The cells were then re-suspended in 50µl of antibody stain cocktail and incubated for 30 minutes at 4°C in the dark. Cells were washed twice in 400µl cold PBS to remove any unbound antibody, and re-suspended in 200µl of cold Live Dead solution (Life Technologies) and incubated for 30 minutes at 4 °C in the dark. Excess Live dead dye was removed by washing the cells twice in 400µl of cold PBS+ 2% FCS (FACS wash buffer). PBMC were then re-suspended in 200µl of a 1% PFA solution (Alfa Aesar, Karlsruhe, Germany) and incubated for 10 minutes at 4°C in the dark. The cells were then washed once in 400µl of FACS wash buffer and re-suspended in 300µl of FACS wash buffer before being transferred into 5ml polystyrene tubes and stored at 4°C in the dark ready for acquisition. PBMC were always acquired on the flow cytometer within 24 hours of staining.

Table 2.3 List of flow cytometry antibodies used throughout thesis

Reagent	Clone	Catalogue #	Manufacturer	Address	Volume/test (µl)
Anti-human CD19 APC eFluor®780	HIB19	47-0199	eBioscience	Hatfield, UK	1
Anti-human IgG V450	G18-145	561299	BD Biosciences	Oxford, UK	5
Anti-human IgM APC	MHM-88	314510	Biolegend	London, UK	5
Anti-Human CD27 PerCP-eFluor®710	O323	46-0279	eBioscience	Hatfield, UK	2
Streptavidin PE	NA	12-4317	eBioscience	Hatfield, UK	0.2
Streptavidin BV421	NA	405226	Biolegend	London, UK	0.4
Anti-Human CD4 FITC	RPA-T4	11-0049	eBioscience	Hatfield, UK	0.25
Anti-Human CD4 APC	OKT-4	17-0048	eBioscience	Hatfield, UK	1
Mouse IgG2a, k PE	G155-178	555574	BD Biosciences	Oxford, UK	1
MS IgG2a isotype control Pac Blue	NA	MG2A28	Life Technologies	Paisley, UK	0.5
Anti-human CD38 Qdot®605	HIT2	Q10053	Life Technologies	Paisley, UK	0.4
Anti-human CD10 APC	HI10a	332777	BD Biosciences	Oxford, UK	2
Mouse IgG1 k, isotype control PE-Cy7	P3.6.2.8.1	25-4714	eBioscience	Hatfield, UK	0.25
Mouse IgG1 k isotype control FITC	P3.6.2.8.1	11-4714	eBioscience	Hatfield, UK	0.25
Anti-Human CD25 PE	BC96	12-0259	eBioscience	Hatfield, UK	2
Anti-human CD39 PE-Cy7	eBioA1	25-0399	eBioscience	Hatfield, UK	0.25
Mouse IgG1 k Isotype Control PE	P3.6.2.8.1	12-4714	eBioscience	Hatfield, UK	1

Anti-human CD5 PE-Cy7	UCHT2	25-0059	eBioscience	Hatfield, UK	0.25
Anti-human CD8 Qdot®605	3B5	Q10009	Life Technologies	Paisley, UK	0.2
Anti-Human CD14 Pac Blue	TuK4	MHCD1428	Life Technologies	Paisley, UK	0.5
Anti-human CD38 PE-Cy7	HIT2	25-0389	eBioscience	Hatfield, UK	1
Anti-Human CD24 FITC	eBioSN3	11-0247-42	eBioscience	Hatfield, UK	2
Anti-human CD154 PE	24-31	310805	Biolegend	London, UK	1
Anti-human CD45RB (MEM55) FITC	MEM-55	Ab18239	Abcam	Cambridge, UK	1.25
Anti-human CD45RB (MEM55) PE	MEM-55	310204	Biolegend	London, UK	2
Anti-Human IL-10 PE-Cy7	JES3-9D7	501419	Biolegend	London, UK	5
Anti-Human IFNγ PerCP- Cy5.5	4S.B3	45-7319-41	eBioscience	Hatfield, UK	5
Live dead Fixable Dye Aqua	NA	L34957	Life Technologies	Paisley, UK	200 (stock diluted 1:1000)
Rat IgG1 isotype (for anti-IL-10)	RTK2071	400416	Biolegend	London, UK	5
Anti-human BAFFr (CD268) FITC	11C1	316904	Biolegend	London, UK	1.25
Anti-human CD86 PerCP eFluor®710	IT2.2	46-0869-42	eBioscience	Hatfield, UK	1.25
Anti-human HLA DR FITC	L243	11-9952-42	eBioscience	Hatfield, UK	1.25
Ant- human TACI PerCP	165604	FAB1741C	Bio-Techne	Abingdon, UK	10
Anti-human TACI PE	165604	FAB1741P	Bio-Techne	Abingdon, UK	10
Anti-Human CD10 PE Cy7	H110a	312213	Biolegend	London, UK	1.25

2.4.2 Intracellular cytokine staining

Cell cultures were set up to replicate the conditions of the ELISpot but carried out in round bottomed 96 well plate without a membrane. CMV gB at a concentration of 0.3µg/ml was used as the stimulating agent. 1µl of Brefeldin A (eBioscience, Hatfield, London), was added to the cultures for the last 5 hours of incubation to facilitate the accumulation of cytokines within the cell. Triplicate wells of each condition were pooled and washed twice in FACS wash buffer and surface staining was carried out as described in 2.4.1.

Cells were then fixed in 100µl of IC fixation buffer (eBioscience) for 20 minutes at room temperature in the dark. Cells were washed once in 400µl of permeabilisation buffer (eBioscience) and then incubated for 20 minutes at room temperature in the dark in 100 µl of permeabilisation buffer that contained the anti-IL-10 and anti-IFNγ antibodies or the appropriate isotype controls. Cells were washed once in 400µl of permeabilisation buffer and then again in 400µl of FACS wash buffer. Cells were then immediately acquired on the flow cytometer.

2.4.3 Acquisition on flow cytometer

OneComp eBeads (eBioscience) were used to make single stain controls for compensation before each new acquisition. Anti-CD25 PE and CD14 Pacific Blue were used as a substitute for streptavidin PE and streptavidin BV421. 1 drop of OneComp ebeads was incubated with 1µl of the appropriate antibody and incubated at 4°C for 20 minutes in 5ml polystyrene tubes. Unbound antibody was washed off in 2ml FACS buffer at 500g for 5 minutes and re-suspended in 300µl FACS buffer ready for acquisition. Acquisition was carried out on a Fortessa LSR II flow cytometer (Becton Dickinson) using DIVA software (Becton Dickinson). Application settings were used to help account for the changes in laser power over time. Data was analysed using Flowjo software (Tree Star Inc, Ashland, OR, USA).

2.5 Detection of antigen binding B cells

The basic principle of this method is based on antigen specific B cells binding a biotinylated antigen which can then be visualised on the flow cytometer using streptavidin conjugated to a fluorochrome. The addition of a B cell phenotyping panel allows the phenotype of the antigen binding B cells to be determined. This method was initially developed using a CMV gB antigen which was biotinylated in-house. The method was then applied to a patient setting where ready-made biotinylated Pure™ HLA proteins were used.

2.5.1 Biotinylating the CMV gB protein

0.18mg of pure HCMV glycoprotein B (CMV gB) protein (abcam, Cambridge, UK) at 1.0mg/ml in 0.5% Tris HCL buffer was exchanged into PBS buffer using a Zeba™Spin desalting column (Thermo Scientific). The Zeba™Spin column was placed in a 15ml tube and washed four times by loading 200µl of PBS and centrifuging at 500g for 2 minutes. 180µl of CMV gB protein was loaded onto the column followed by a 40µl PBS stacker. The column was placed in a fresh 15ml tube and centrifuged at 500g for 2 minutes. The CMV gB protein was removed from the bottom of the 15ml tube and placed in a 1.5ml Eppendorf tube ready for biotinylation using an EZ-Link®Sulfo-NHS-biotin biotinylation kit (Thermo Scientific).

The biotinylation of the CMV gB was carried out according to manufacturer's instructions. A 20 molar excess of biotin was used in order to ensure that every viral protein was biotinylated. Briefly: 1mg of biotin was reconstituted in 224µl of ultrapure water and a 12.2µl aliquot was mixed with the CMV gB and incubated for 30 minutes at room temperature. Excess biotin was removed by inserting the mixture into a 0.1-0.5ml Slide-A-Lyzer® dialysis cassette (Thermo Scientific) and immersing it in 500ml sterile PBS for 2 hours at room temperature, followed by a replenishment of the PBS and an overnight incubation at 4°C. The CMV gB protein was then removed from the dialysis cassette using a 1ml syringe, aliquoted into 5µl volumes and stored at -20°C.

2.5.2 Determining the efficiency of the biotinylation process

In order to check that all of the CMV gB protein had been biotinylated, the biotinylated protein was run through an SDS PAGE gel with or without prior incubation with 0.1unit of streptavidin (SIGMA-ALDRICH) for 30 minutes at room temperature. The biotinylated CMV gB was mixed 1:1 with 1x Laemli sample buffer (BIO-RAD, Hemel Hempstead, UK) and a 30µl volume was immediately loaded into a ready-made 10% SDS PAGE gel (BIORAD). 5µl of a 10kb – 250kb protein ladder (Promega,

Southampton, UK) was also added to one of the lanes. The gel was run at 100 volts for approximately 100 minutes using the running buffer detailed in Table 2.4.

Once the gel had finished running, it was removed from its cask and fixed for 30 minutes in 100ml of the fixing solution detailed in Table 2.5. 3ml of Coomassie blue stock solution was then added to the fixing solution and the gel was stained for 25-40 minutes (see Table 2.6). The staining solution was then removed and the gel was incubated for 2.5 hours in de-stain solution which is detailed in Table 2.7. Figure 2.3 shows that 100% of the CMV gB was biotinylated as the CMV gB-biotin-streptavidin complex can be seen as a large molecule at the very top of the gel in lane 4, with no protein detected at the 25kDa mark where both the CMV gB and CMV gB biotin can be seen in lanes 2 and 3 respectively.

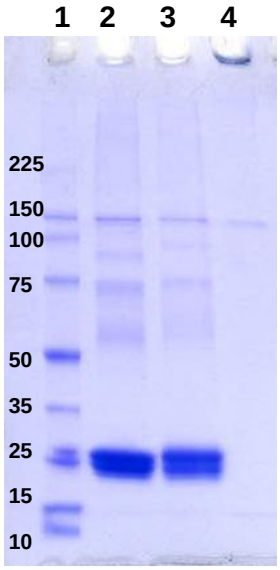

Figure 2.3 Determining the biotinylation efficiency
The biotinylated CMV gB was incubated with streptavidin for 30 minutes at room temperature and then run on an SDS PAGE and stained with coomassie blue. Lane 1: Protein ladder (10-225kDa). Lane 2: CMV gB, Lane 3: CMV gB+biotin, Lane 4: CMV gB+biotin +streptavidin. The bands at ~ 25kDa represent the CMV gB virus. In lane 4, a protein band is visible at the very top of the gel where the streptavidin has formed a large complex with the biotinylated CMV gB. The lack of a band present at ~25kDa suggests that there are no CMV gB molecules present in the solution that have not been biotinylated. The BCA assay was used as described in section 2.3.2 to determine the concentration of the biotinylated CMV gB.

Table 2.4 Recipe for 10x SDS PAGE running buffer

Reagent	Quantity to dissolve in 1L ultrapure water(g)
Tris 25mM (Sigma-Aldrich)	30.28
Glycine 192 mM (Sigma-Aldrich)	144g
SDS 0.1% (Sigma-Aldrich)	10g

Table 2.5 Recipe for fixing solution for Coomassie blue staining

Reagent	Volume (ml)
Methanol (Thermo Scientific)	50
Acetic acid (SIGMA ALDRICH)	10
Deionised H_20	40

Table 2.6 Recipe for Coomassie blue stock solution

Reagent	Quantity
Coomassie Blue R-250 (Thermo Scientific)	1.5g
Methanol	50ml
Acetic acid	30ml

Table 2.7 Recipe for de-staining solution for Coomassie blue staining

Reagent	Volume (ml)
Methanol	45
Acetic acid	10
Deionised H_20	45

2.5.3 Phenotyping antigen binding B cells by flow cytometry

The biotinylated antigen was diluted to the optimal concentration in AIMV media with 10% FCS and kept on ice. Each different antigen that was used was titrated prior to use in order to determine the optimal concentration that would lead to effective binding of antigen specific B cells with minimal background binding. This is detailed in the relevant sections of chapter 4.

Whilst working on ice at all times to prevent the internalisation of the viral or HLA proteins by the B cells, 1-5x10^6 PBMC were re-suspended in 200µl of cold biotinylated antigen solution and incubated for 30 minutes on ice in a 96 well round bottom plate. Unbound protein was then washed off by adding 300µl of cold PBS and centrifuging at 500g for 5 minutes, re-suspending the cells and washing them again. The PBMC were then stained with a B cell phenotyping panel using the method described in section 2.4.1, with an amendment to the protocol that all incubations were carried out on ice and not in the refrigerator.

2.6 Determining if the antigen binding is specific.

2.6.1 Cold inhibition assay

PBMC were incubated with 0.35µg/ml biotinylated CMV gB as described in section 2.5.3. To competitively inhibit the binding of this protein to the BCR, non-biotinylated CMV gB was titrated into each sample from 0.0µg/ml to 14.0µg/ml. VZV gE was titrated into separate samples at the same concentrations to use as a negative control which should not affect antigen specific binding of the gB to the BCR. Subsequent steps of flow cytometry staining were carried out as described in section 2.4.1.

2.6.2 Blocking the BCR

PBMC were incubated with 0.35µg/ml biotinylated CMV gB as described in section 2.5.3. To block binding of the biotinylated CMV gB to the BCR, anti-human IgM/IgG Fab (H+L) (Jackson ImmunoResearch Laboratories inc, Westgrove, PA, USA) was titrated into each sample from 0.0µg/ml-6.4µg/ml. Subsequent steps of flow cytometry staining were as described in section 2.4.1.

2.6.3 Blocking the FcγRIIB receptor

PBMC were incubated with 0.35µg/ml biotinylated CMV gB as described in section 2.5.3. To check that the biotinylated CMV gB was not non-specifically binding to FCγRIIB (CD32) expressed on B cells, PBMC were incubated with anti-human CD32 (eBioscience) at a concentration of 10µg/ml for 30 minutes at 4°C and washed twice in AIMV 10% FCS prior to incubating with the biotinylated CMV gB. PBMC that had not been incubated with anti-human CD32 were used as a negative control. Subsequent steps of flow cytometry staining were carried out as described in section 2.4.1.

2.6.4 Single cell sorting for downstream sequencing and cloning of CMV gB binding B cells

PBMC from 3 leukocyte cones were incubated with CMV gB and stained as per the protocol detailed in section 2.5.3 and 2.4.1. PBMC were then passed through a FACS Aria III sorter, where single CMV gB binding, IgMhi B cells were collected in each well of a 96 well plate that contained SLYRT buffer (contains lysis buffer and reagents required for reverse transcription). The gating strategy and examples of the cells pre and post sort are shown in Figure 2.4. As the distinguishing feature of the CMV gB binding B cells was that they were IgMhi, it was decided that the cells that would be sorted would be CMV gB+ and IgMhi as shown in Figure 2.4. Index gating was set up on the sorter so the exact phenotype of each CMV gB binding B cell could be related back to its antibody production once the BCR sequence had been sequenced and

cloned. The 96 well plates were handed over to Verena Hehle who performed several rounds of PCR in order to amplify the genes from the single cells so they could be sent off for BCR sequencing. Once known, the BCR sequence was then integrated into a pVitro vector and transformed into *E.coli.* The plasmid DNA from the E.coli culture was then extracted using a Miniprep kit and transfected into 293T cells. Cell culture supernatants containing immunoglobulin were measured for their ability to bind the CMV gB in an ELISA.

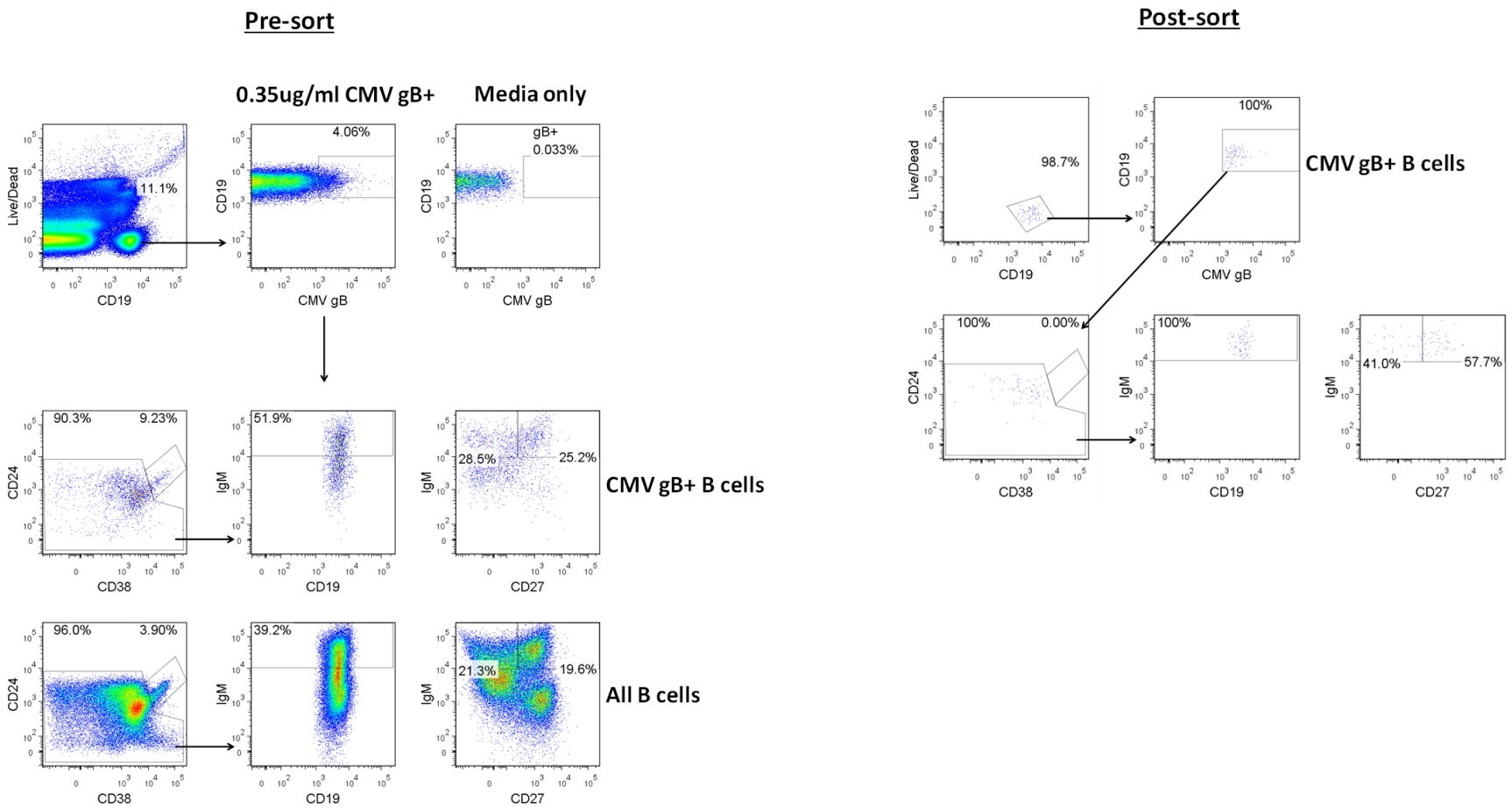

Figure 2.4 Gating strategy for single cell sorting with dot plots pre and post sort

2.7 Isolation of B cells and B cell subsets

2.7.1 Isolating B cells from PBMC

B cells were isolated from whole PBMC using a negative isolation magnetic bead kit (Miltenyi,Bergisch Gladbach, Germany) so the B cells were left as untouched as possible. According to the manufacturer's instructions: the PBMC were washed at 500g for 5 minutes in PBS+0.5% FCS and 2mM EDTA (MACS buffer), re-suspended in 40µl MACS buffer per $1x10^7$ PBMC plus 10µl of biotin-antibody cocktail per $1x10^7$ PBMC and incubated for 5 minutes at 4°C. 30µl MACS buffer per $1x10^7$ PBMC plus 20µl anti-biotin microbeads per $1x10^7$ PBMC was then added for a further incubation of 10 minutes at 4°C. The MACS column was washed three times and then the labelled cell suspension was passed through the column. The negative fraction containing the isolated B Cells was collected in a sterile tube, counted, and re-suspended in RPMI 10% FCS. B cells were stained to check their purity using flow cytometry (see figure 2.5). The average purity of the isolated B cells was 91.1%.

2.7.2 Isolating CMV gB B cells from isolated B cells

To isolate the CMV binding B cells from the CMV non-binding B cells, the isolated B cells were incubated with 200µl of cold CMV gB at a concentration of 0.35µg/ml, washed twice in cold MACS buffer at 500g for 5 minutes and then incubated with 0.1µl of streptavdin PE in 50µl MACS buffer for 30 minutes at 4°C. Excess streptavidin was washed off by washing twice in cold MACS buffer at 500g for 5 minutes. Cells were re-suspended in 80µl MACs buffer per $1x10^7$ total cells plus 20µl of Anti-PE microbeads per $1x10^7$ total cells and incubated for 15 minutes in the refrigerator. Cells were washed in 2ml MACS buffer, re-suspended in 500µl of MACS buffer and then passed through the pre-washed MACS column. The resulting CMV+ and CMV- fractions of cells were counted and re-suspended in AIMV10. Both fractions were stained to check their purity using flow cytometry (see dot plots in Figure 2.6).

2.7.3 Isolating CD27+ and CD27- B cells from isolated B cells

B cells were isolated as described in section 2.7.1, re-suspended in 80µl of MACS buffer per $1x10^7$ total cells. 20µl per 10^7 total cells of CD27 labelled magnetic beads (Miltenyi Biotec) were mixed with the cells, and incubated in the refrigerator for15 minutes. Cells were then washed in 2ml MACS buffer at 300g for 10 minutes and re-suspended in 500µl of MACS buffer. 500µl of MACS buffer was passed through an MS column (Miltenyi Biotec) followed by the magnetically labelled cells. The CD27- cells were collected in the flow through and the CD27+ cells were removed from the column

using the plunger provided with the column. Both CD27- and CD27+ B cell fractions were counted as described in section 2.2.2 and a small aliquot was removed for flow cytometry staining to check the purity of the cells. The average purity from these experiments was 75.7% for the CD27+ population and 94.15 % for the CD27- B cell population.

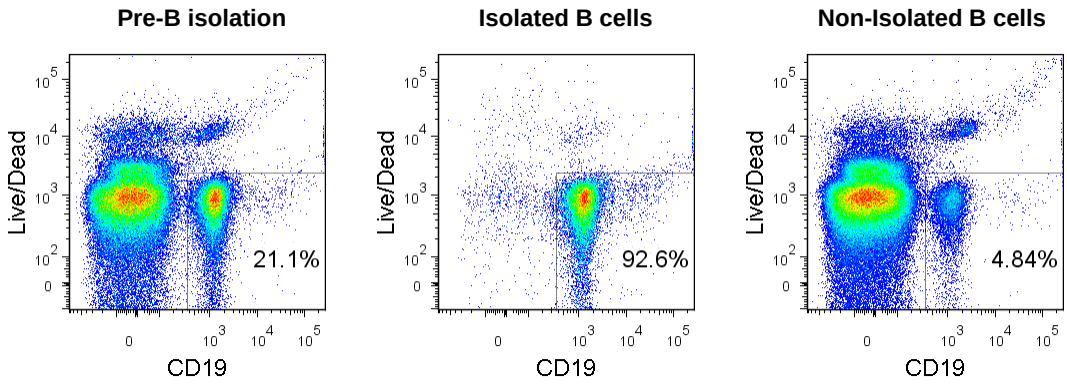

Figure 2.5 Example dot plots of cells pre and post B cell isolation

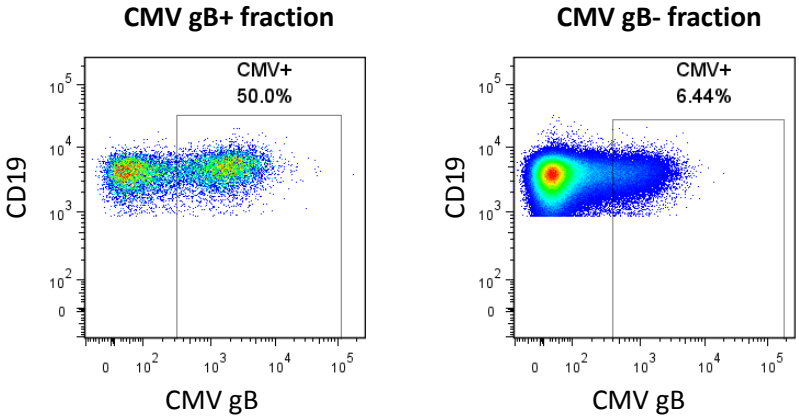

Figure 2.6 Dot plots of CMV gB binding B cell isolation using MACS beads.

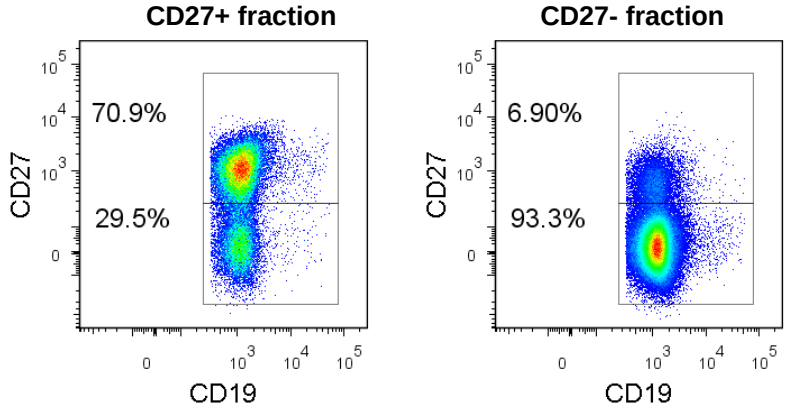

Figure 2.7 Example dot plots of CD27+/CD27- separation

2.8 Statistical analysis

All statistical analysis was performed using Graphpad Prism® software version 5. Paired samples were compared using a Wilcoxon matched pairs signed rank test with two tailed P values. Unpaired samples were compared using a Mann Whitney U test with two tailed P values. A Kruskal-Wallis test with Dunn's multiple comparison was used to compare more than two groups at a time. P values of <0.05 were considered significant.

3 Results part 1

3.1 Introduction

The major aim of this chapter was to establish that the patterns of reactivity to donor membrane proteins observed in the observational study reported in Shiu et al. could be reproduced in another cohort of patients whom fitted the diagnostic criteria for CAMR in a kidney transplant setting. This chapter addresses aims 1-3 in section 1.4.

Patients enrolled on the RituxiCAN C4 trial were chosen to be tested in the IFNγ ELISpot based on the criteria that they would be finished the trial within the timescale that this thesis required completion, as this would enable the correlation of the patterns of reactivity in the indirect IFNγ ELISpot with the clinical outcomes in these individuals. The IFNγ ELISpot will be carried out on PBMC samples on the remaining patients at a later date and added to the data presented in this thesis for publication.

The enrolment, end of phase I and end of phase II samples from patients that were consented into phase II of the trial were tested in the indirect IFNγ ELISpot. For those that were not randomised and went straight to phase III, the enrolment and end of year 1 samples were tested. Where samples from later time points were available, these were also tested in the IFNγ ELISpot at approximately yearly intervals. A full set of PBMC samples were not acquired for all patients, as some patients were withdrawn from the study due to either graft failure or the patient withdrawing consent. In such circumstances, the ELISpot was carried out on all available PBMC samples up until they stopped being collected. If a sample was not collected at the exact time point, for example 1 year, the next closest sample was tested in the IFNγ ELISpot.

3.2 Results

3.2.1 IFNγ production can be detected in response to donor membrane proteins

PBMC from each time point tested were depleted of either CD8+ cells, CD8+&CD19+ cells, CD8+&CD25+ or CD8+, CD19+&CD25+ cells (triple depletion) and then stimulated in the IFNγ ELISpot with donor membrane proteins as described in section 2.3.5. As one of the aims of this study was to broadly replicate the findings of Shiu et al. the proportions of reactive and non-reactive samples in all samples tested was analysed. Of the 104 samples thawed, from 33 patients, 97 were found to be viable. The number of IFNγ+ spots per million CD4+ lymphocytes produced by each CD8+ depleted PBMC sample when stimulated with either live donor membrane proteins or surrogate donor membrane proteins is shown in Figure 3.1. 18/97 (19%) samples were deemed reactive as their spot count was ≥25 IFNγ+ spots per million CD4+ lymphocytes. The remaining 79/97 (81%) samples were deemed non-reactive.

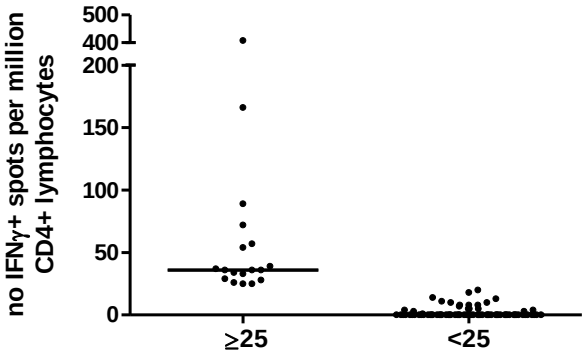

Figure 3.1 Response to donor membrane proteins of all samples tested in the indirect IFNγ ELISpot.

Spot counts shown are a mean of triplicate wells with background subtracted and multiplied up to give spot counts per million CD4+ lymphocytes. A total of 97 samples were tested: 18/97 were reactive, 79/97 were non-reactive. A reactive response was defined as ≥25 IFNγ+ spots per million CD4+ lymphocytes. Black bars on graph represent the median.

3.2.2 IFNγ production in response to donor membrane proteins is dependent on B cells

The criteria stated in section 2.3.5.6 of the material and methods was used to define whether each sample was 'reactive B dependent' or 'reactive B regulated' after in vitro depletion of CD19+ cells. Of the 18 samples that were deemed reactive, enough PBMC were available from 17 of them to deplete CD19+ cells. Figure 3.2 (a) shows the IFNy production pre and post CD19+ depletion in samples that were deemed 'reactive B dependent': IFNγ production was reduced by more than 20% post B cell depletion in all 17 of these samples.

In the 79 samples that were non-reactive, CD19+ cell depletion revealed that 6/79 samples could be classed as 'reactive B regulated'. IFNy production pre and post B cell depletion by these 6 samples is shown in Figure 3.2 (b).

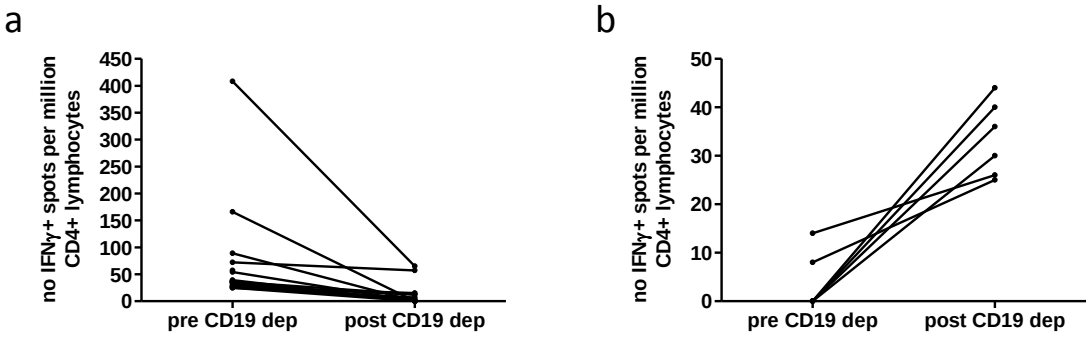

Figure 3.2 Impact of CD19+ depletion on IFNγ production
(a) Sufficient PBMC were available to deplete CD19+ cells from 17/18 reactive samples: IFNγ decreased post CD19+ cell depletion in all 17 samples. **(b)** Sufficient PBMC were available to deplete CD19+ cells from 76/79 non-reactive samples: IFNγ increased to ≥25 IFNγ+ spots per million CD4+ lymphocytes post CD19+ cell depletion in 6/76 of these samples.

3.2.3 Depleting CD25+ cells reveals IFNγ production in response to donor membrane proteins in a subset of samples.

Sufficient PBMC were available to deplete CD25+ cells from 80 of the 97 samples tested. CD25+ cell depletion lead to an increase in IFNγ production in 9/80 samples which were classed as 'reactive T regulated' based on the criteria stated in section 2.3.5.6 of the materials and methods section. IFNγ production pre and post CD25+ deletion in these samples is shown in Figure 3.3.

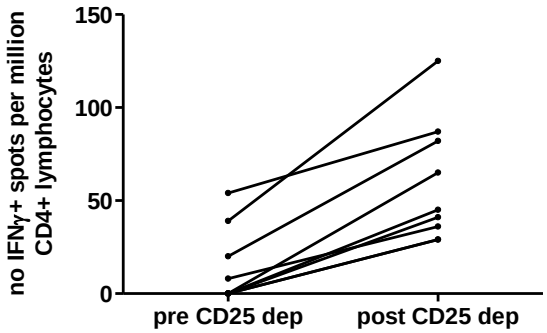

Figure 3.3 Impact of CD25+ cell depletion on IFNγ production
Sufficient PBMC were available to deplete CD25+ cells from 80 of the 97 samples tested. IFNγ production increased to ≥25 IFNγ+ spots per million CD4+ lymphocytes post CD25+ cell depletion in 9/80 samples shown here. 7/9 samples were non-reactive before CD25+ cell depletion.

3.2.4 Depleting CD19+ and CD25+ cells increases the frequency of samples that can be defined as reactive towards donor membrane proteins.

When the patterns of reactivity described above are considered together, the analysis reveals that 31/97 (32%) of the samples have the capacity to produce IFNγ in response to the donor membrane proteins. Figure 3.4 illustrates that samples can be sub-divided with regards to their reactivity whether it is revealed post CD19+ cell depletion (Breg) or post CD25+ cell depletion (Treg). These subgroups will be referred to in subsequent analysis throughout this thesis. Also included in this graph is the data from the triple depletion condition that was possible to test in 69/97 samples. This condition revealed reactivity in one sample that was previously non-reactive in all other depletion conditions. The two samples that were reactive Treg before CD25+ depletion are included In the CD8 dep column and one sample that was both Breg and Treg is included in the CD8 & CD19 dep column. 6/9 reactive Treg samples are therefore included in the CD8 & CD25 dep column.

A breakdown of the number of samples tested in the IFNγ ELISpot for each patient along with details of the time point is shown in Table 3.1. The data in this table illustrates how the pattern of reactivity in response to donor membrane preps changes over time. 18/33 patients had evidence of reactivity towards donor membrane proteins at 1 or more time points. It also highlights that in vitro depletion of CD19+ cells in individuals who have received Rituximab can still have an impact on IFNγ production. Included in this table is a summary of the DSA detected in the serum of each patient. If a patient has had a DSA detected at any time point post transplantation it has been recorded in this table. DSA were not necessarily detected at every time point that the serum was tested in the Luminex® assay in each patient. The time points at which the serum was tested was at the discretion of the clinical laboratory at each site and often does not match the time point tested in the IFNγ ELISpot. This therefore has not made it possible to directly correlate the presence of DSA with the pattern of reactivity in the IFNγ ELISpot. However, it can be highlighted that 29/33 patients tested had evidence of DSA post-transplant. 16/33 patients had evidence of both DSA and reactivity in the IFNγ ELISpot and 13/33 patients had evidence of DSA but no evidence of reactivity in the IFNγ ELISpot. 2/33 patients had no evidence of DSA but did have evidence of reactivity in the IFNγ ELISpot. The remaining 2/33 had no evidence of DSA or reactivity in the IFNγ ELISpot.

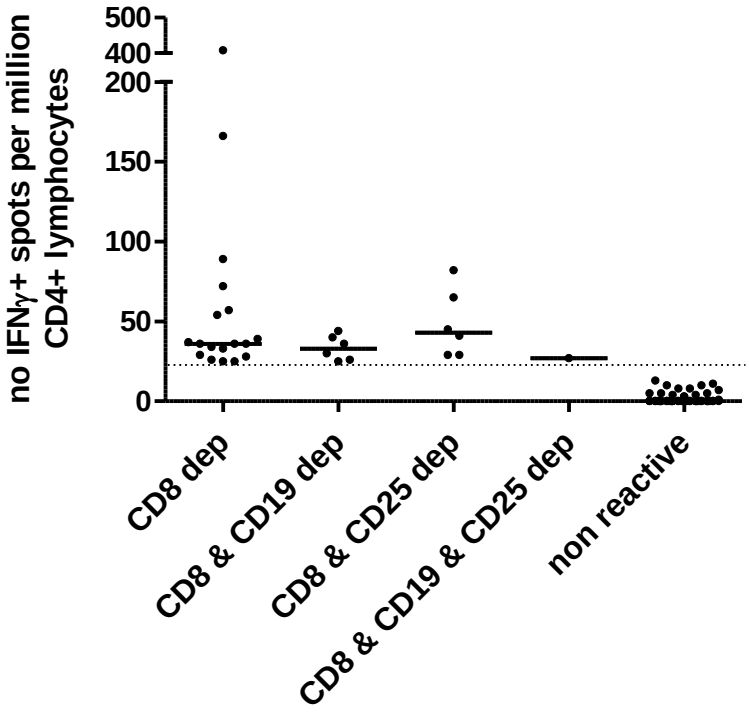

Figure 3.4 IFNγ response to donor membrane proteins
Depletion of CD19+ and CD25+ subsets (or a combination of the two) reveals reactivity in samples that were non-reactive when just CD8+ cells were depleted. One sample had an increase of IFNγ to ≥25 IFNγ+ spots per million CD4+ lymphocytes post CD19+ cell depletion and CD25+ cell depletion and has been included in the CD8&CD25 dep column on this graph. Black bars on graph represent the median. Dep is an abbreviation of depleted.

Table 3.1a Summary of all samples from West London Renal centre tested in the IFNγ ELISpot

Patient ID	Class I DSA	Class II DSA	In phase II?	Timepoint ELISpot tested	Response to donor membrane proteins	Response to viral cocktail
W001	A1	DQ5	No	Baseline	Reactive	Reactive
W002			No	Baseline	Reactive, Bdep	Non-reactive
				9 mnths (Phase III)	N/A - cells not viable	
W003	A30, B63		No	Baseline	Non-reactive	Reactive, B/Treg
				6 mnths (Phase III)	Non-reactive	Reactive, B/Treg
				9 mnths (Phase III)	Non-reactive	Non-reactive
				21 mnths (Phase III)	Non-reactive	Reactive, Treg
				30 mnths (Phase III)	Non-reactive	Reactive, Bdep
W004	B44	DR53	No	Baseline	N/A - cells not viable	
				3 mnths (End phase I)	N/A - cells not viable	
				12 mnths (Phase III)	Reactive, Bdep	Reactive, Bdep
W005			No	Baseline	Non-reactive	Reactive, Breg
W006	A1	DR17	Yes no Ritux	Baseline	Reactive, Bdep	Non-reactive
				12 mnths (End phase I)	Reactive, Bdep	Reactive, Bdep, Treg
				15mnths (End phase II)	Reactive, Breg	Reactive, Bdep
				42 mnths (Phase III)	Non-reactive	Non-reactive
W008			Yes no Ritux	Baseline	Reactive, Treg	Reactive, Treg
				3 mnths (End phase I)	Non-reactive	Non-reactive
				6 mnths (End phase II)	Reactive B/Treg	Reactive, Bdep
				12 mnths (Phase III)	Non-reactive	Reactive, Breg
W009	B44	DQ8, DR4, DR53, DR51	No	Pre-recruitment	Non-reactive	Non-reactive
				Baseline	Non-reactive	Non-reactive
				10 mnths (Phase III)	Non-reactive	Reactive, Breg
				28 mnths (Phase III)	Reactive, Bdep	Reactive, Breg
W010	Cw7	DR53	Yes Ritux	Baseline	Reactive, Bdep	Reactive, Bdep
				5 mnths (End phase I)	Reactive, Breg	Reactive, Breg
				10 mnths (End phase II)	Reactive, Bdep	Reactive, Breg
W011	A2		No	Baseline	Non-reactive	Non-reactive
				12 mnths (Phase III)	Non-reactive	Non-reactive
W012		(DQ7, DQ8, DQ9)	No	Baseline	Non-reactive	Non-reactive
				12 mnths (Phase III)	Non-reactive	Non-reactive
W013		DR53, DQ7 (DQ6)	No	Baseline	Non-reactive	Reactive, Treg
				12mnths (Phase III)	Non-reactive	Reactive, Bdep
W014		DQ6, DQ7	No	Baseline	Non-reactive	Reactive, Breg
				3 mnths (end phase I)	Non-reactive	Reactive, Treg
				16mnths (Phase III)	Non-reactive	Reactive, Treg
				29 mnths (Phase III)	Non-reactive	Reactive, Bdep, Treg
W016			No	Baseline	Non-reactive	Reactive, Bdep
				3mnths (End phase I)	Non-reactive	Reactive, Treg
				6mnths (Phase III)	Non-reactive	Non-reactive
W017	A24, B60, B7		No	Baseline	Non-reactive	Non-reactive
				3mnths (End phase I)	Reactive, Bdep	Reactive, Bdep
				15mnths (Phase III)	Reactive, Breg	Reactive, Breg
				25mnths (Phase III)	Reactive, Bdep	Reactive, Treg

Table 3.1b Summary of all samples from Guy's Hospital tested in the IFNγ ELISpot

Patient ID	Class I DSA	Class II DSA	In phase II?	Timepoint ELISpot tested	Response to donor membrane proteins	Response to viral cocktail
G001	B8	DQ2	No	Baseline	Non-reactive	Reactive, Bdep
				4 mnths (End phase I)	Non-reactive	Non-reactive
				13 mnths (Phase III)	Reactive, Treg	Reactive, Breg, Treg
G002	A1		Yes no Ritux	Baseline	Reactive, Bdep	Reactive, Bdep
				3mnths (End phase I)	Non-reactive	Reactive, B/Treg
				6mnths (End phase II)	Non-reactive	Reactive, Bdep
				14mnths (Phase III)	Reactive, Bdep	Non-reactive
G003	B8		Yes Ritux	Baseline	Reactive, Breg	Non-reactive
				5mnths (End phase I)	Reactive, Breg,Treg	Reactive, Breg
				10 mnths (End phase II)	Non-reactive	Non-reactive
				24mnths (Phase III)	Non-reactive	Non-reactive
				37mnths (Phase III)	Non-reactive	Non-reactive
G004		DR51, DQ7	No	Baseline	Non-reactive	Non-reactive
				4 mnths (Withdrawal)	Non-reactive	Reactive, Breg, Treg
G006		DR7, DR53, DQ2	No	Baseline	Non-reactive	Non-reactive
				5mnths (End phase I)	Reactive, Bdep, Treg	Reactive, Treg
				8mnths (Phase III)	Non-reactive	Non-reactive
				11mnths (Phase III)	Non-reactive	Non-reactive
G007	A2	DR12	Yes no Ritux	Baseline	Non-reactive	Non-reactive
				4mnths (End phase I)	Non-reactive	Non-reactive
				7mnths (End Phase II)	Non-reactive	Non-reactive
G008	A11	DQ2	No	Baseline	Non-reactive	Non-reactive
				4mnths (End Phase I)	Non-reactive	Reactive, Breg
				10mnths (Phase III)	Non-reactive	Non-reactive
G009		DR13, DR52	Yes Ritux	Baseline	Non-reactive	Reactive, Treg
				5mnths (ritux 1mnth later)	Non-reactive	Reactive, Bdep, Treg
G010	A1	DR1, DP1, DP17	Yes Ritux	Baseline	Non-reactive	Reactive, Bnon
				5mnths (End phase I)	Non-reactive	Non-reactive
				10mnths (End phase II)	Non-reactive	Non-reactive
G012	A23, A2	DR53, DQ2, DR7, DR53	Yes Ritux	Baseline	Reactive, Treg	Reactive, Treg
				4mnths (End phase I)	Non-reactive	Non-reactive
				9mnths later (End phase II)	Non-reactive	Non-reactive
				15mnths (Phase III)	Non-reactive	Non-reactive
G013	Cw6		Yes no Ritux	Baseline	Reactive, Treg	Non-reactive
				4 mnths (End phase I)	Non-reactive	Reactive, Bdep
				7mnths (End Phase II)	Reactive, Bdep	Non-reactive
				13mnths (Phase III)	Non-reactive	Non-reactive
G014	A1, A2	DQ5	No	Baseline	Non-reactive	Non-reactive
				4mnths later (End phase I)	Non-reactive	Non-reactive
				14mnths (Phase III)	Non-reactive	Non-reactive
G015		DR52, DR14	No	Baseline	Non-reactive	Reactive, Bdep
				3mnths (End phase I)	Non-reactive	Non-reactive
				13mnths (Phase III)	Non-reactive	Reactive, Breg
G017	A23		Yes Ritux	Baseline	Reactive, Treg	Reactive, Treg
				13mnths (End phase I)	Reactive, Bdep	Reactive, Bdep
				19mnths (End Phase II)	Non-reactive	Non-reactive
G023		DQ7, DQ8, DQ9, DR53	Yes no Ritux	Baseline	Reactive, Bdep	Non-reactive
				4mnths (End phase I)	Reactive Treg	Reactive, Treg
				11mnths (End phase II)	Non-reactive	Non-reactive
G025		DQ2, DQ7,DR53	Yes Ritux	Baseline	Reactive, Bdep	Non-reactive
				4mnths (End phase I)	Non-reactive	Reactive, Bdep
				7mnths (End Phase II)	Reactive, Bdep	Non-reactive
G027	B8	DQ2, DQ6, DR51, DR3, DR16	Yes no Ritux	Baseline	Non-reactive	Non-reactive
				5mnths (End phase I)	N/A cells not viable	
				11mnths (End phase II)	Non-reactive	Non-reactive
G029		DR4, DR53	Yes Ritux	Baseline	Non-reactive	Non-reactive
				3mnths (End phase I)	N/A cells not viable	Non-viable
				6mnths (End phase II)	Reactive, Breg	Non-reactive

3.2.5 Similar patterns of reactivity observed in the response to donor membrane proteins are also observed in the response to a viral cocktail

Every sample tested in Figure 3.1 was also tested for their response to a cocktail of viral antigens that the majority of individuals should have been exposed to and are known to induce both a humoral and a T cell response: CMV pp65, CMV gB and VZV gE (Manikkavasagan et al., 2010, Vyse et al., 2009, Sylwester et al., 2005, Pötzsch et al., 2011, Gonczol and Plotkin, 2001, Arvin, 2008). This served as a control to assess the antigen processing and presenting ability of those individuals who did not produce IFNγ in response to donor membrane proteins. As with the donor membrane protein stimulated samples, different patterns of reactivity were seen in response to the viral cocktail. Samples were assigned a pattern of reactivity according to the criteria stated in section 2.3.5.6 of the materials and methods. Figure 3.5 shows the number of reactive samples revealed with each depletion condition and those that did not respond to the viral cocktail in any depletion condition. When just CD8+ cells were depleted, IFNγ was produced in response to the viral cocktail in 30/97 samples. IFNγ production was reduced upon in vitro depletion of CD19+ cells in 18/30 of these samples. 6/30 of these samples showed evidence of B regulation and 9/30 showed evidence of T regulation. In 2 of these samples, evidence of both B regulation and T regulation was observed and are detailed in Table 3.1.

7/97 samples only showed evidence of reactivity when CD19+ cells were depleted and 8/97 non-reactive samples responded to the viral cocktail when CD25+ cells were depleted. 3/97 samples responded to the viral cocktail only in the triple depleted condition when both CD19+ and CD25+ cells were depleted. Therefore in total, 48/97 (49%) samples showed evidence of reactivity to the viral cocktail.

Importantly, 22/79 of the samples that were non-reactive to the donor membrane proteins when just CD8+ T cells were depleted, responded to the viral cocktail. This suggests that there is not a global defect in the antigen processing and presenting capability of the patients that these samples were derived from. Additionally, only 8/18 of the samples that produced IFNγ in response to donor membrane proteins when only the CD8+ cells were depleted also responded to the viral cocktail, thus supporting the hypothesis that an antigen specific response is being observed in the patients with regards to their reactivity to donor membrane proteins.

39/97 samples were globally hypo-responsive and did not produce IFNγ in response to either donor or viral antigens in any of the depletion conditions. It is worth noting that due to limited PBMC availability for some samples, CD19 depletion was possible in

35/39 samples, CD25 depletion possible in 29/39 and triple depletion possible in 24/39 samples so it is possible that in some samples reactivity would have been revealed if all of the depletion conditions had been possible.

Finally, the pattern of reactivity observed in response to donor membrane proteins was not always mirrored in the response to the viral cocktail suggesting that B cells may play a different role in the immune response depending on the antigen (Table 3.1.).

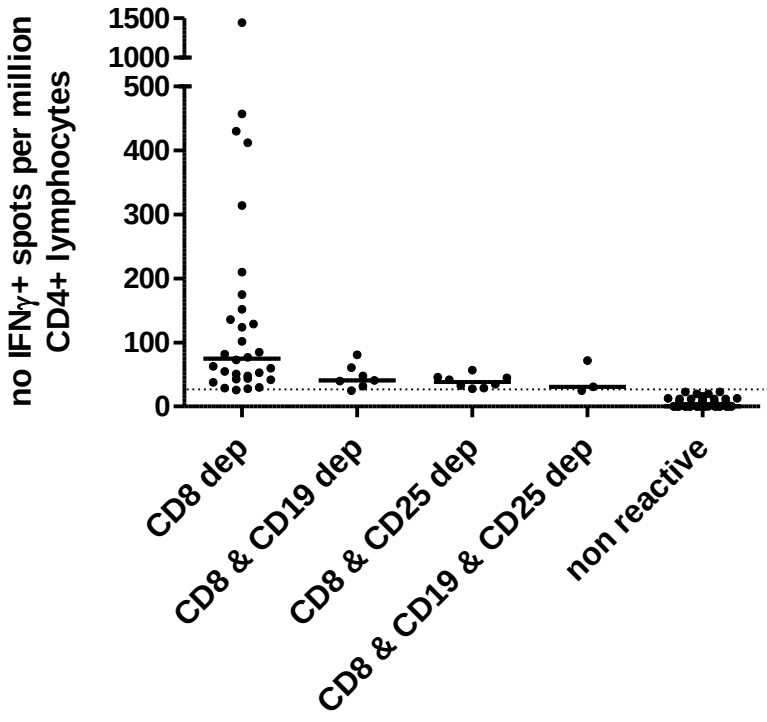

Figure 3.5 IFNγ production in response to a viral protein cocktail
Samples were incubated with a viral cocktail at the same time as the donor membrane proteins. A reactive response was defined as ≥25 IFNγ+ spots per million CD4+ lymphocytes and is marked by the dotted line. Each depletion condition is shown along the X-axis. Samples were grouped according to the depletion condition where a response was observed. If a sample was both B regulated and T regulated, it has been included in the B regulated column only.

3.2.6 B cell phenotype does not correlate with pattern of reactivity in the indirect IFNγ ELISpot

Because all of the reactive samples that were depleted of CD19+ cells showed B cell dependent IFNγ production, it was hypothesised that the B cell phenotype in these samples may differ from those that were non-reactive. The phenotype of the B cells at enrolment were therefore correlated with the pattern of reactivity in the IFNγ ELISpot at enrolment. There were no reactive Breg samples at enrolment so in this analysis the non-reactive group contains all samples that were non-reactive when only CD8+ T cells were depleted. Analyses of later time points has not been included because a) some patients received Rituximab and therefore were depleted of B cells and b) the majority of the samples from those that were not given Rituximab were non-reactive. Patient W004 could not be used in any analysis that involved just enrolment samples as their enrolment PBMC sample was non-viable upon thawing. Figure 3.6 shows the initial gating strategy that was used prior to any panel specific analysis: doublets were gated out using FSC-W versus FSC-A, followed by non-live cells. Lymphocytes were defined as CD14-. An example of the gating strategy used for the B cell phenotyping panel is shown in Figure 3.7. Both a patient enrolled on the RituxiCAN C4 trial and a Leukocyte cone are shown (Fig 3.7 (a) and 3.7 (b) respectively). Isotype control antibodies were used to guide the gating for the CD1d+, CD5+ and CD10+ populations as illustrated in Fig 3.7 (a).

Figures 3.8 and 3.9 show a comparison between the phenotype of the B cells of each enrolment sample and whether the samples were reactive or non-reactive when just CD8+ cells were depleted. Figure 3.8 shows that no differences in the frequency of CD19+ cells (Fig 3.8 (a)) or naïve, intermediate and transitional B cells (Fig 3.8 (b), (c) & (d)) were found between reactive and non-reactive samples ($P > 0.05$). Additionally, no difference was found in the frequency of CD27+ or CD27- B cells, or the ratio of these two subsets between the reactive and non-reactive samples (Fig 3.9 (a), (b) & (c), $P > 0.05$).

The phenotype of regulatory B cells has been reported to include the expression CD10, CD5 and CD1d (Blair et al., 2010, Ma et al., 2014), so the frequency of naïve, intermediate and transitional B cells that expressed these markers was analysed. No difference was found between the reactive and non-reactive samples (Fig 3.10).

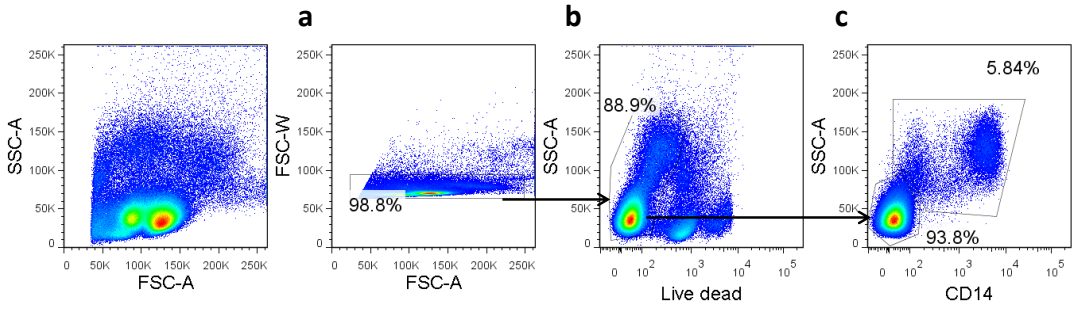

Figure 3.6 General gating strategy for phenotyping T and B cells.
The initial gating strategy to define the live lymphocytes was used for both the T and B cell phenotyping panels. Doublets were gated out **(a)**, followed by the dead cells **(b)**. Lymphocytes were defined as CD14- **(c)**.

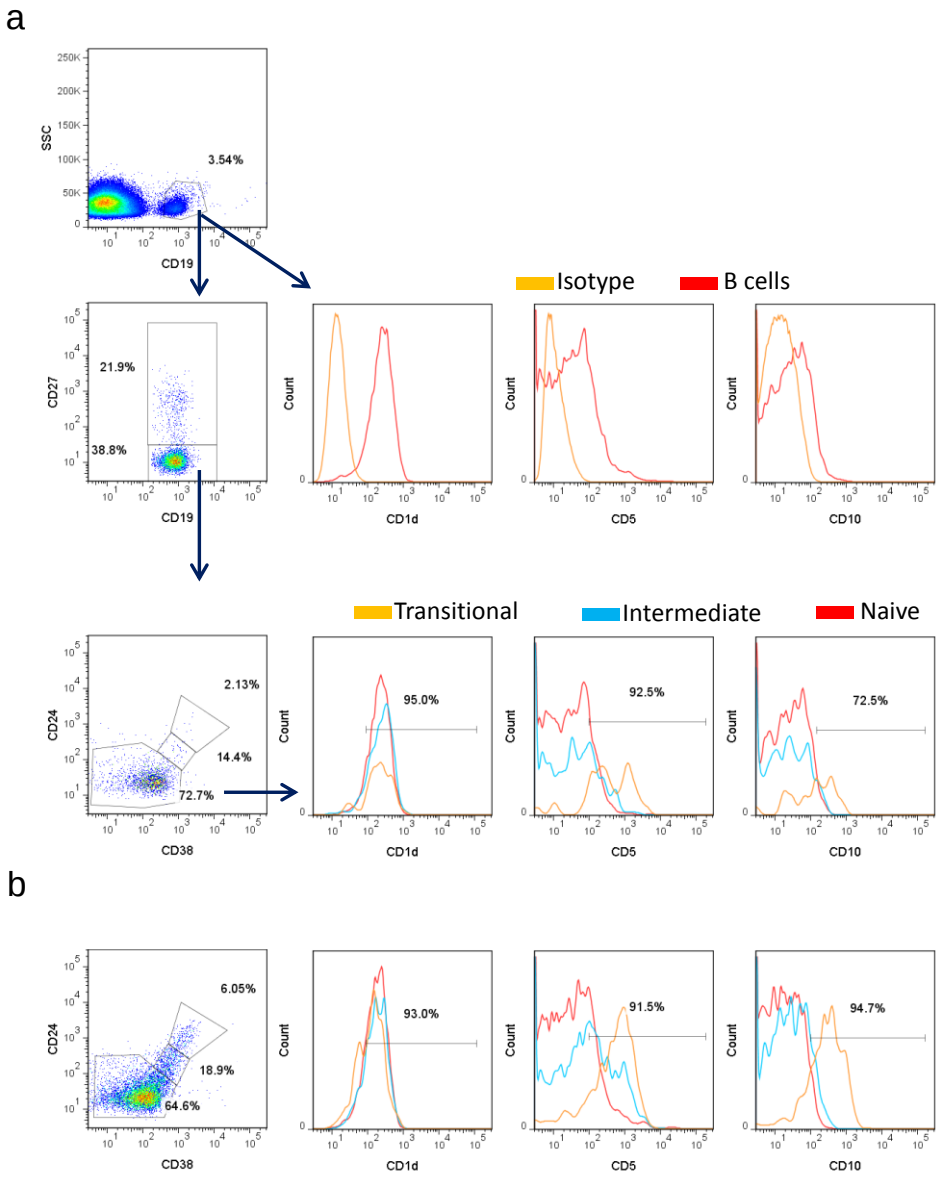

Figure 3.7 Gating strategy for B cell phenotyping
(a) B cells were defined as CD19+ lymphocytes and then divided into CD27+ (memory) and CD27- (non-memory) subsets. Within the CD27- population, the B cells were further divided into naïve (CD38loCD24lo), intermediate (CD38intCD24int) and transitional subsets (CD38hiCD24hi). CD1d, CD5 and CD10 expression was gated on using the isotype control as a guide and then applied to each CD27- cell subset. **(a)** Shows representative plots from a CAMR patient and **(b)** shows representative plots from a Leukocyte cone to highlight the difference observed in the transitional population.

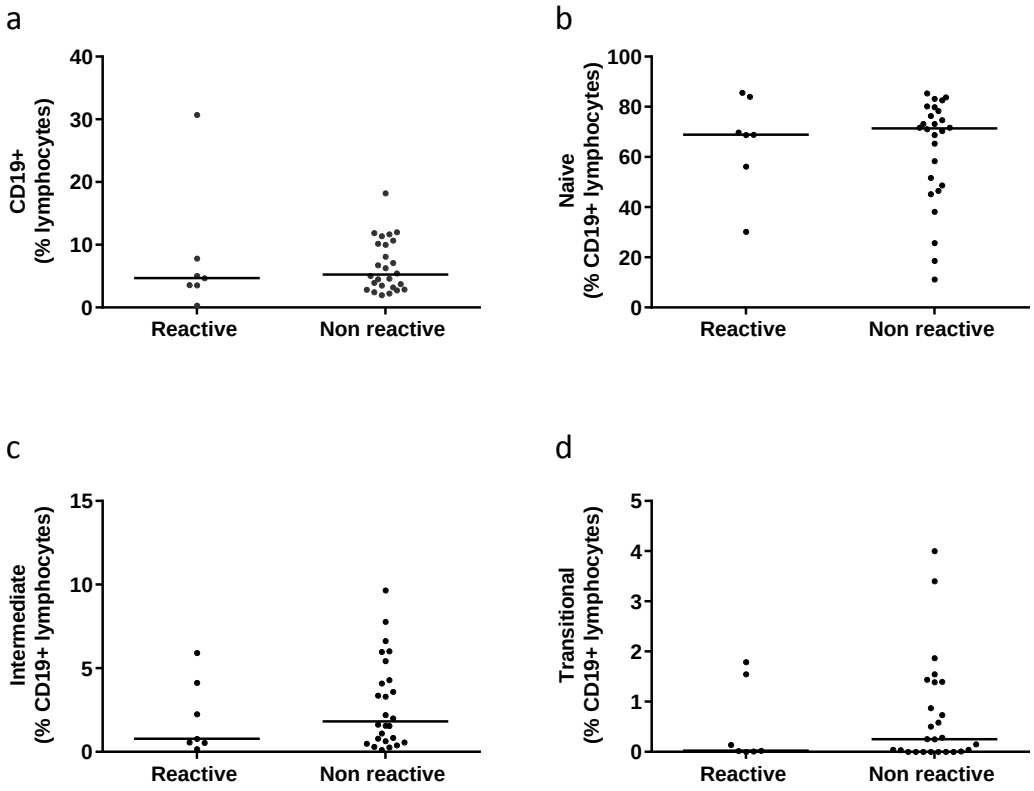

Figure 3.8 Correlation of B cell frequencies and phenotypes with reactivity in the IFNγ ELISpot at enrolment

The frequency of CD19+ cells and CD19+ subsets (Naïve **(a)**, Intermediate **(b)** and Transitional **(c))** were compared in enrolment samples grouped according to reactivity to donor membrane proteins when just CD8+ cells were depleted. CD19+ cells are expressed as frequency of lymphocytes. Naïve, Intermediate and Transitional subsets are expressed as frequency of CD19+ lymphocytes. Black line represents the median. Samples were compared using a Mann Whitney U test. P>0.05 for all graphs.

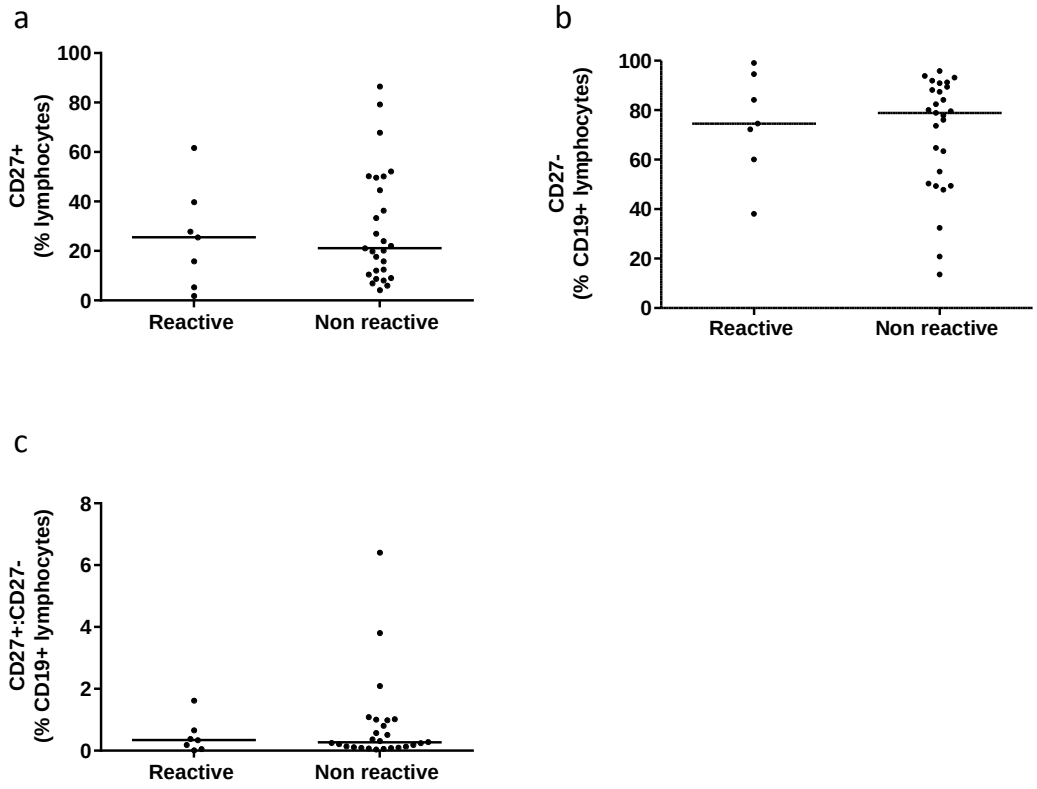

Figure 3.9 Correlation of CD27+ and CD27- B cell subset frequencies with reactivity in the IFNγ ELISpot at enrolment

The frequency of CD27+ **(a)** and CD27- **(b)** B cells was compared in enrolment samples grouped according to reactivity to donor membrane proteins when just CD8+ cells were depleted. The ratio of CD27:CD27- B cells was compared between the two groups **(c).** CD27+ and CD27- subsets are expressed as frequency of CD19+ lymphocytes. Black line represents the median. Samples were compared using a Mann Whitney U test. P>0.05 for all graphs.

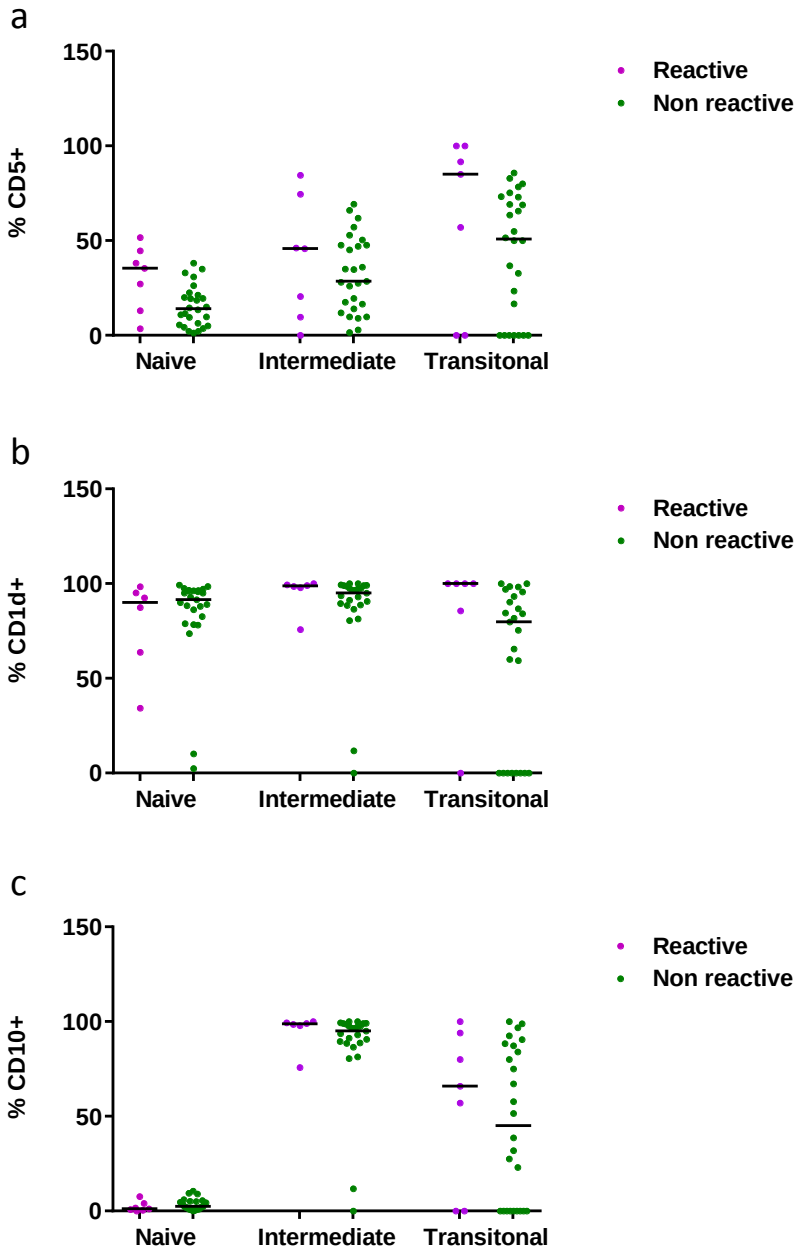

Figure 3.10 Correlation of CD5+, CD1d+ and CD10+ cell frequencies with reactivity in the IFNγ ELISpot at enrolment

Enrolment samples were grouped according to reactivity to donor membrane proteins when just CD8+ cells were depleted. Black line represents the median. Reactive and non-reactive samples were compared for CD5, CD1d and CD10 expression on each B cell subset (Naïve, Intermediate and transitional) using a Mann Whitney U test. P>0.05 for all analyses.

3.2.7 T cell phenotype does not correlate with patterns of reactivity in the indirect IFNγ ELISpot.

At the same time as the B cell phenotyping and IFNγ ELISpot, PBMC were also stained with a T cell panel principally to characterise surface marker expression associated with regulatory T cells**.** CD4+ T cells were separated into CD25hi, CD25+ and CD25- subsets. The co-expression of CD25 and CD39 on CD4+ T cells was also analysed and CD25hiCD39+ cells were gated on, as this is a Treg subset that has recently been reported in the literature (Grant et al., 2014, Deaglio et al., 2007, Dwyer et al., 2010, Salcido-Ochoa et al., 2010). Example FACS plots of a RituxiCAN C4 patient and a leukocyte cone are shown in Figure 3.11 (a) and (b) respectively.

The T cell phenotype was correlated with the pattern of reactivity observed in the IFNγ ELISpot when CD25+ cells were depleted. Samples from all time points were used in this analysis and grouped as follows: a) non-reactive, which includes samples that were 'reactive B regulated', b) 'reactive, Treg' which are samples that responded to donor membrane proteins only when CD25+ cells were depleted c) reactive, which are samples that responded to donor membrane proteins when only CD8+ cells were depleted and includes 1 sample that also had evidence of T cell regulation. No differences were observed in the frequency of T cell subsets and the pattern of reactivity in the IFNγ ELISpot (Fig 3.12, $P>0.05$). In addition, no differences were observed when the reactive sample that was T regulated was included in the 'reactive Treg' group ($P>0.05$).

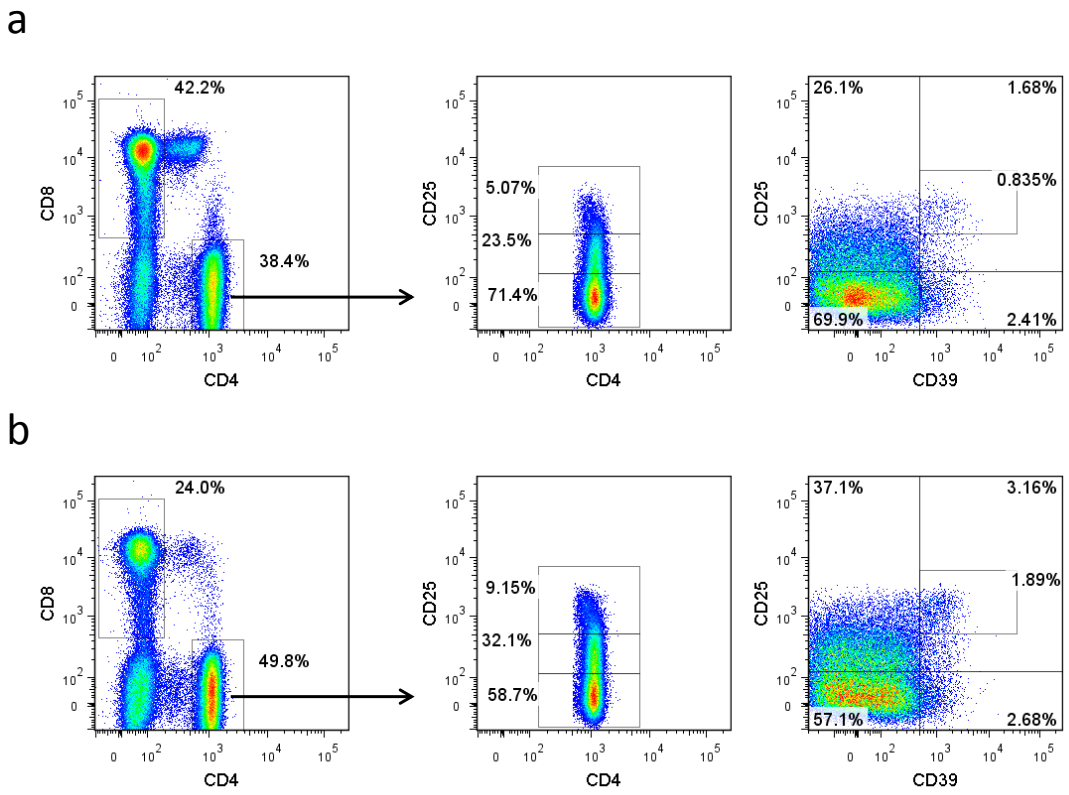

Figure 3.11 Gating strategy for T cell phenotyping

CD4+ T cells were gated on, followed by either CD25hi to define Tregs, or a quadrant gate was used to divide the CD4+ T cells into four populations based on their CD25 and CD39 expression. Within the quadrant gate, a specific population of Tregs were gated on based on their high expression of CD25 and positive expression of CD39 (CD25hiCD39+ Tregs). **(a)** is an example of a CAMR patient, **(b)** is an example of a leukocyte cone.

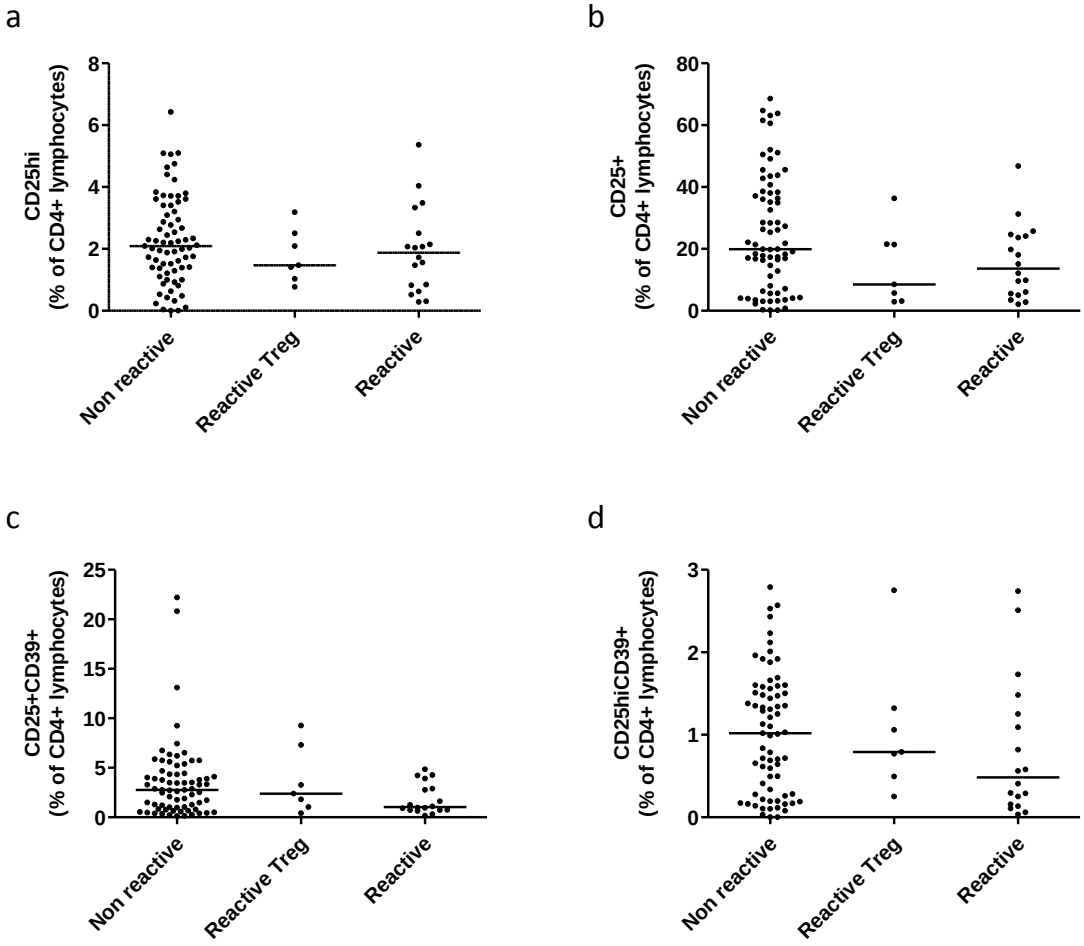

Figure 3.12 Comparison of frequency of T cell subsets between samples grouped according to their pattern of reactivity in IFNγ production upon CD25+ depletion.
The frequency of four different T cell subsets was compared between all samples grouped according to IFNγ production in response to donor membrane proteins pre and post CD25+ cell depletion: 1. Non-reactive, which includes samples that were 'reactive B regulated', 2. 'Reactive, Treg' which are samples that responded to donor membrane proteins only when CD25+ cells were depleted; 3. Reactive, which are samples that responded to donor membrane proteins when only CD8+ cells were depleted and includes 1 sample that also had evidence of T cell regulation. **(a)** CD25hi T cells, **(b)** CD25+ T cells, **(c)** CD25+CD39+ T cells **(d)** CD25hiCD39+ T cells. All subsets expressed as frequency of CD4+ lymphocytes. Black lines on graph represent the median. Groups compared using a Kruskal-Wallis test with a Dunn's multiple comparison test. P>0.05 for all analyses.

3.2.8 Patients who produced IFNγ in response to donor membrane proteins at enrolment did not pass phase I.

Data from the observational study reported in Shiu et al has produced some interesting correlations with clinical outcome. Although somewhat complex, these correlations suggest that the pattern of reactivity in the ELISpot can be used to predict the clinical outcome (manuscript in preparation). Following on from these findings, similar correlations were made with the clinical outcomes of the patients enrolled on the RituxiCAN trial. An in depth clinical analysis is being prepared for publication, but for the purpose of this thesis, it was decided that the clinical outcome at the end of phase I would be correlated with the in vitro measured parameters, as at this point in the trial all patients had been subjected to the same treatment protocol. Figure 3.13 shows the clinical course reported as estimated glomerular filtration rate (eGFR) for each of the patients included in Figure 3.1. There were three potential outcomes at the end of phase I: a) the patient's creatinine stabilised and they transitioned to phase III where they continued on optimised therapy and a PBMC sample was taken every 3 months, b) the patient's creatinine did not stabilise and they were consented and randomised into phase II where they continued on optimal therapy with or without the addition of Rituximab or c) the patient was ineligible for phase 2 on account of the eGFR falling to <20mls/min, or they did not reach the end of phase I due to graft failure.

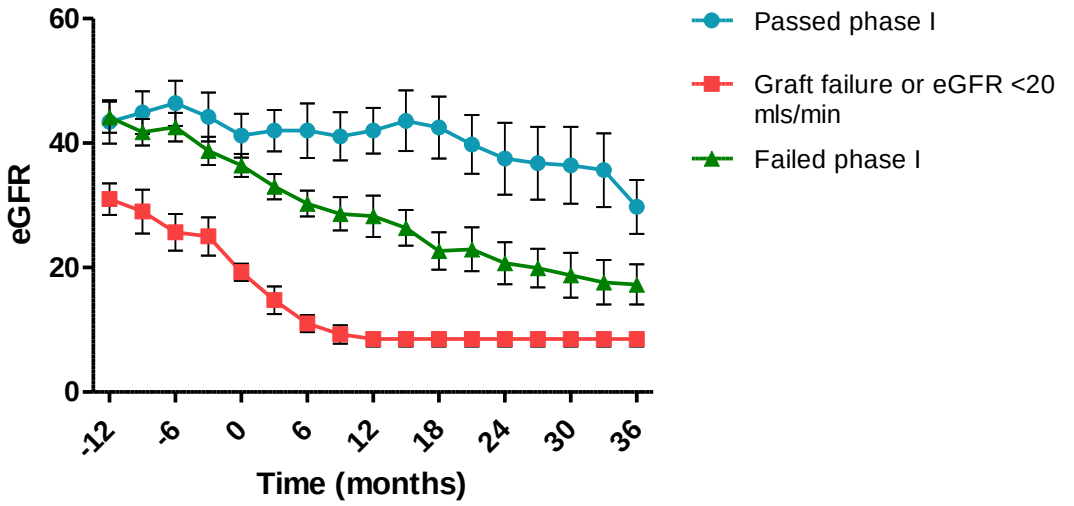

Figure 3.13 Estimated glomerular filtration rates over time of patients enrolled on the RituxiCAN C4 trial.

Patients were divided into three groups based on their outcome at the end of phase I. Passed phase I: the patient's creatinine stabilised and they transitioned to phase III where they continued on optimised therapy and a PBMC sample was taken every 3 months (n=10). Failed phase I: the patient's creatinine did not stabilise and they were eligible for randomisation (requiring second consent) into phase II where they continued on optimal therapy with or without the addition of Rituximab (n=18). Graft failure or eGFR<20mls/min: the patient did not reach the end of phase I due to graft failure, or at the end of phase I the eGFR had fallen below 20mls/min, making them ineligible for the randomisation phase (n=4). Data for figure obtained from A. Dorling and modified for this thesis to only include patients that have been tested in the IFNγ ELISpot in Figure 3.1.

The pie charts in Figure 3.14 illustrate the proportions of patients who responded to donor membrane proteins in the IFNγ ELISpot at enrolment and their corresponding pattern of reactivity with regards to CD19+ and CD25+ cell depletion.

9/10 (90%) patients who passed phase I were non-reactive to donor membrane proteins and remained non-reactive after subsequent CD19+ or CD25+ depletions. Sufficient PBMC were not available from two of these non-reactive patients to do subsequent CD25+ cell depletions. 1/10 of these samples (10%) was reactive.

50% of patients that failed phase I showed evidence of reactivity to donor membrane proteins when they were enrolled onto the trial: 5/18 patients (28%) were reactive with a B dependent IFNγ response. 4/18 (22%) patients were non-reactive when only CD8+ cells were depleted, but 1/4 (5%) had a B regulated IFNγ response and 3/4 (17%) had a T regulated IFNγ response. The remaining 9/18 patients (50%) were non-reactive and did not change upon depletion of CD19+ or CD25+ cells, however sufficient PBMC were not available from one of these non-reactive patients to do subsequent CD19+ and CD25+ cell depletions.

3/4 (75%) of the patients who experienced graft failure before the end of phase I did not respond to donor membrane proteins. 1/4 patients whose graft failed before the end of phase I responded to donor proteins. It is unknown whether this response was B dependent as there was insufficient PBMC available from this sample to do the CD19+ cell depletion in the ELISpot.

The triple depletion condition did not impact IFNγ production in any of the Enrolment samples.

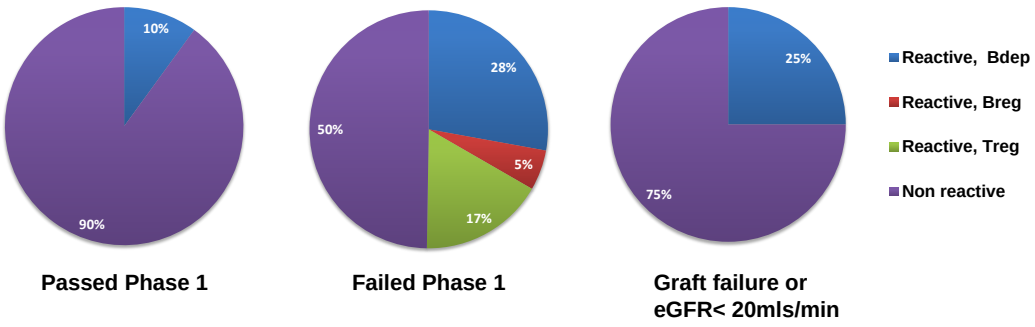

Figure 3.14 Correlating ELISpot reactivity at enrolment with clinical outcome
Patients were grouped according to those who passed phase I (n=10), failed phase I (n=18), or had their graft fail/had an eGFR <20mls/min during phase I (n=4).

3.2.9 B cell phenotype at enrolment does not correlate with clinical outcome at the end of phase I

The B cell phenotype of the enrolment samples was analysed according to the three groups described in Figure 3.14. This analysis includes two patients that did not pass phase I and had B cell phenotyping carried out on their samples but no ELISpot due to the lack of an appropriate surrogate donor. There was no difference observed between the overall frequency of CD19+ cells, the frequency of naïve, intermediate and transitional B cell subsets or the proportions of CD27+ and CD27- populations between the three groups (Fig 3.15 and 3.16). In addition, there was no difference observed between the frequency of CD1d+, CD5+ or CD10+ cells within the naïve, intermediate or transitional B cell subsets (Figure 3.17).

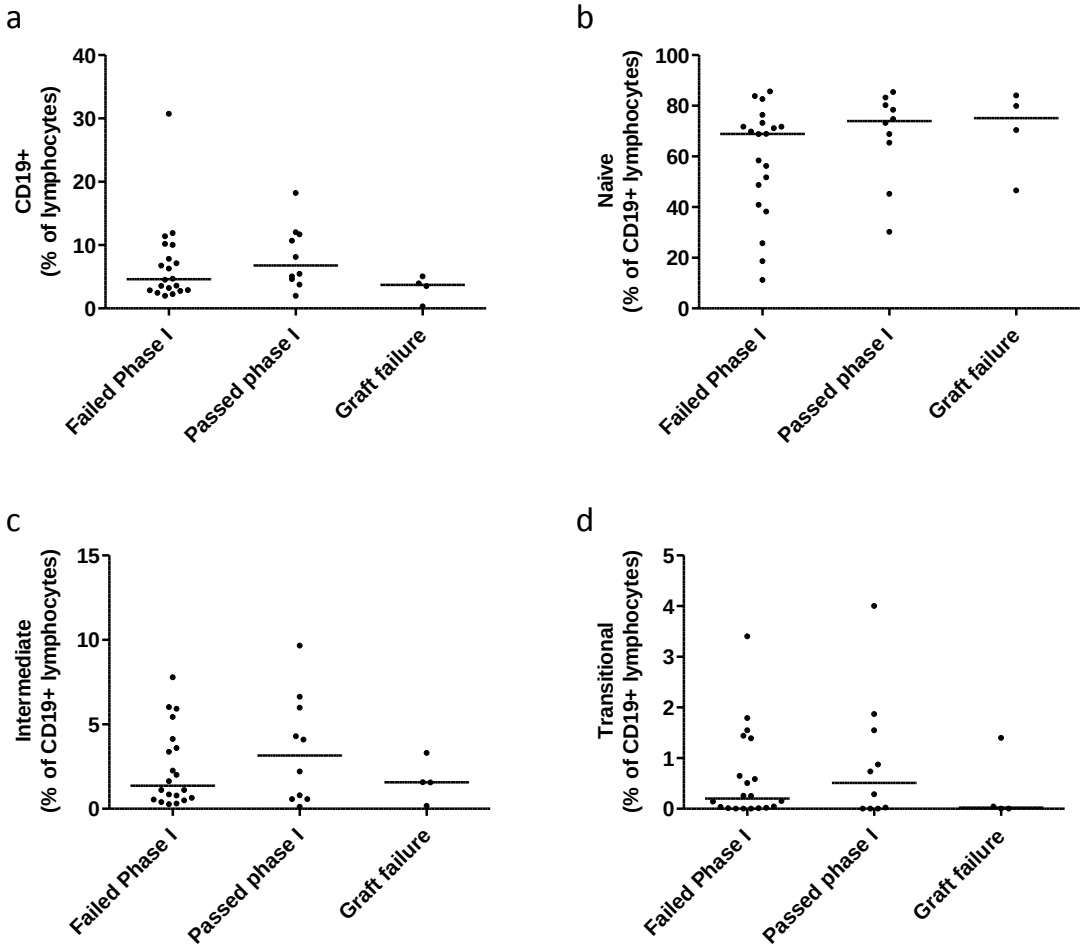

Figure 3.15 Comparison of the frequency of B cell subsets at enrolment with clinical outcome at the end of phase I

Patients were grouped according to those who failed phase I (n=20), passed phase I (n=10) or had their graft fail/had an eGFR <20mls/min during phase I (n=4). Black lines on graph represent the median. Groups compared using a Kruskal-Wallis test with a Dunn's multiple comparison test. P>0.05 for all analyses.

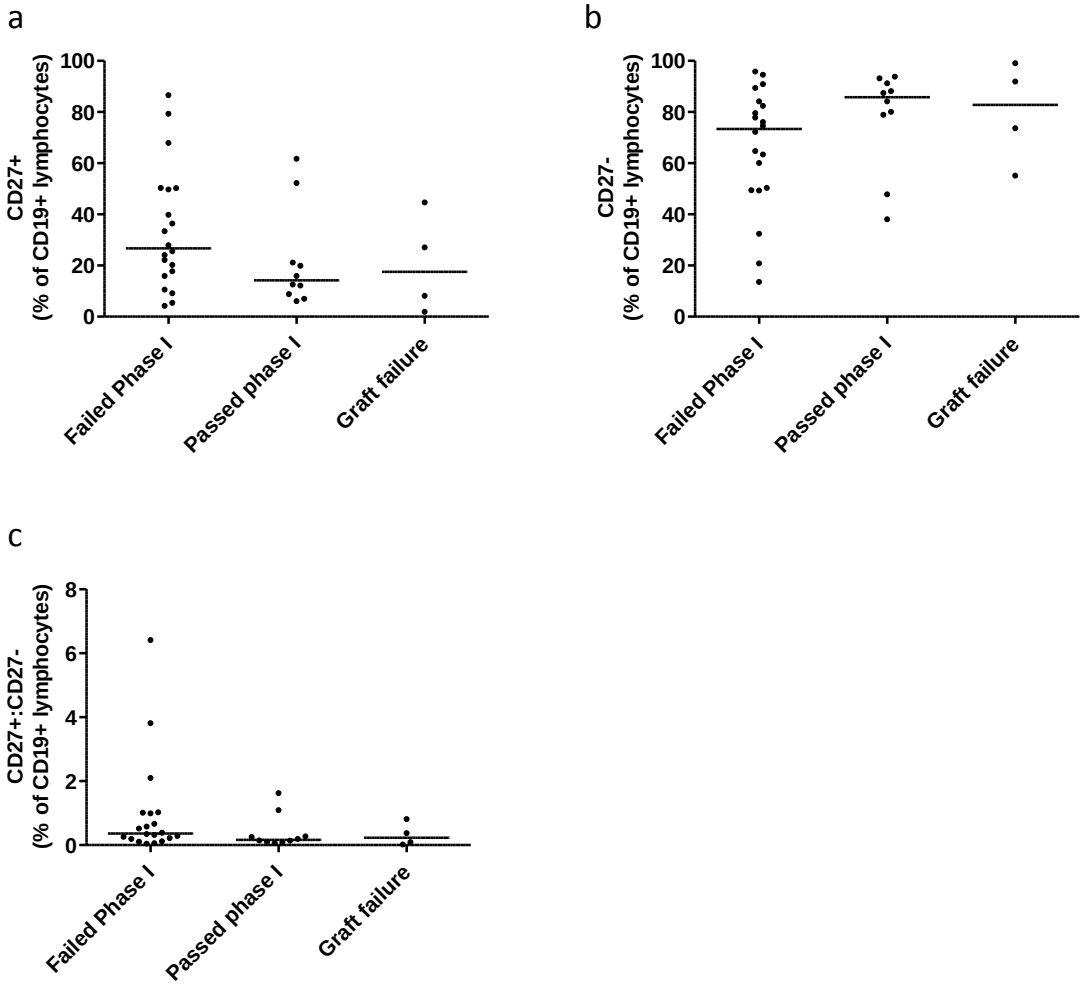

Figure 3.16 Comparison of CD27+ and CD27- B cell frequencies at enrolment with clinical outcome at the end of phase I

Patients were grouped according to those who failed phase I (n=20), passed phase I (n=10) or had their graft fail/ had an eGFR <20mls/min during phase I (n=4). Black lines on graph represent the median. Groups compared using a Kruskal-Wallis test with a Dunn's multiple comparison test. P>0.05 for all analyses.

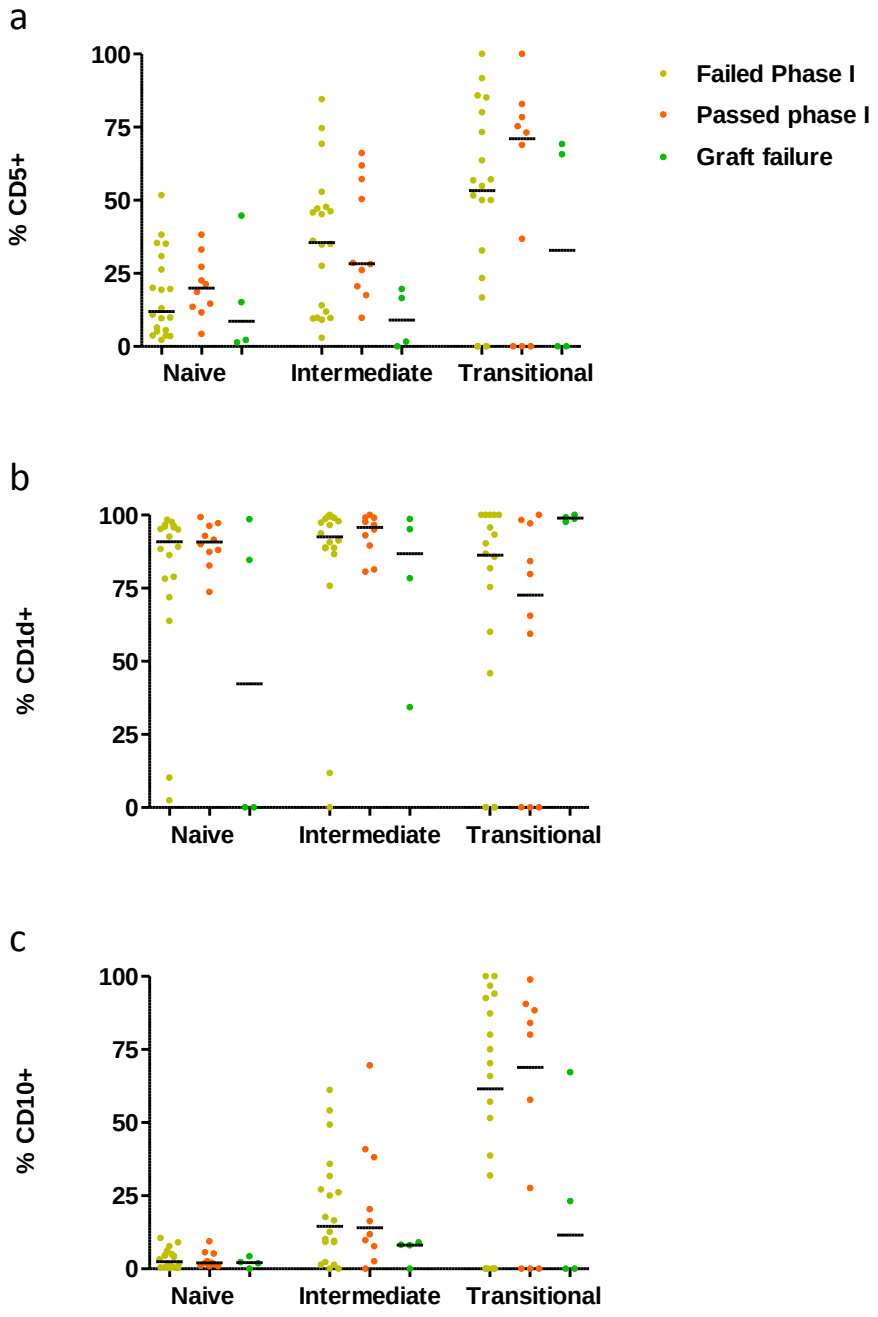

Figure 3.17 Comparison of the frequency of CD5+ cells, CD1d+ cells and CD10+ cells within the naive, intermediate and transitional B cell subsets at enrolment with clinical outcome at end of phase I

Patients were grouped according to those who failed phase I (n=20), passed phase I (n=10) or had their graft fail/ had an eGFR <20mls/min during phase I (n=4). Frequency of CD5 **(a)**, CD1d **(b)** or CD10 **(c)** expressed on each B cell subset (Naïve, Intermediate or Transitional) was compared between the three groups of patients. Black lines on graph represent the median. Groups compared using a Kruskal-Wallis test with a Dunn's multiple comparison test. P>0.05 for all analyses.

3.2.10 Patients who did not pass phase I have a lower frequency of CD4+CD25+ T cells than those who passed phase I

As in section 3.2.9, the T cell phenotype of the enrolment sample from each patient was correlated with the clinical outcome at the end of phase I. No differences were found between the two groups with regards to the frequency of CD4+ lymphocytes or the regulatory T cell subsets when defined as either CD4+CD25hi, CD4+CD25+CD39+ or CD4+CD25hiCD39+ (Fig 3.18(a), (b) (d) & (e)). However, patients who did not pass phase I were found to have a lower frequency of effector CD4+CD25+ T cells than those who did pass phase I (Fig 3.18 (c) P=0.0060).

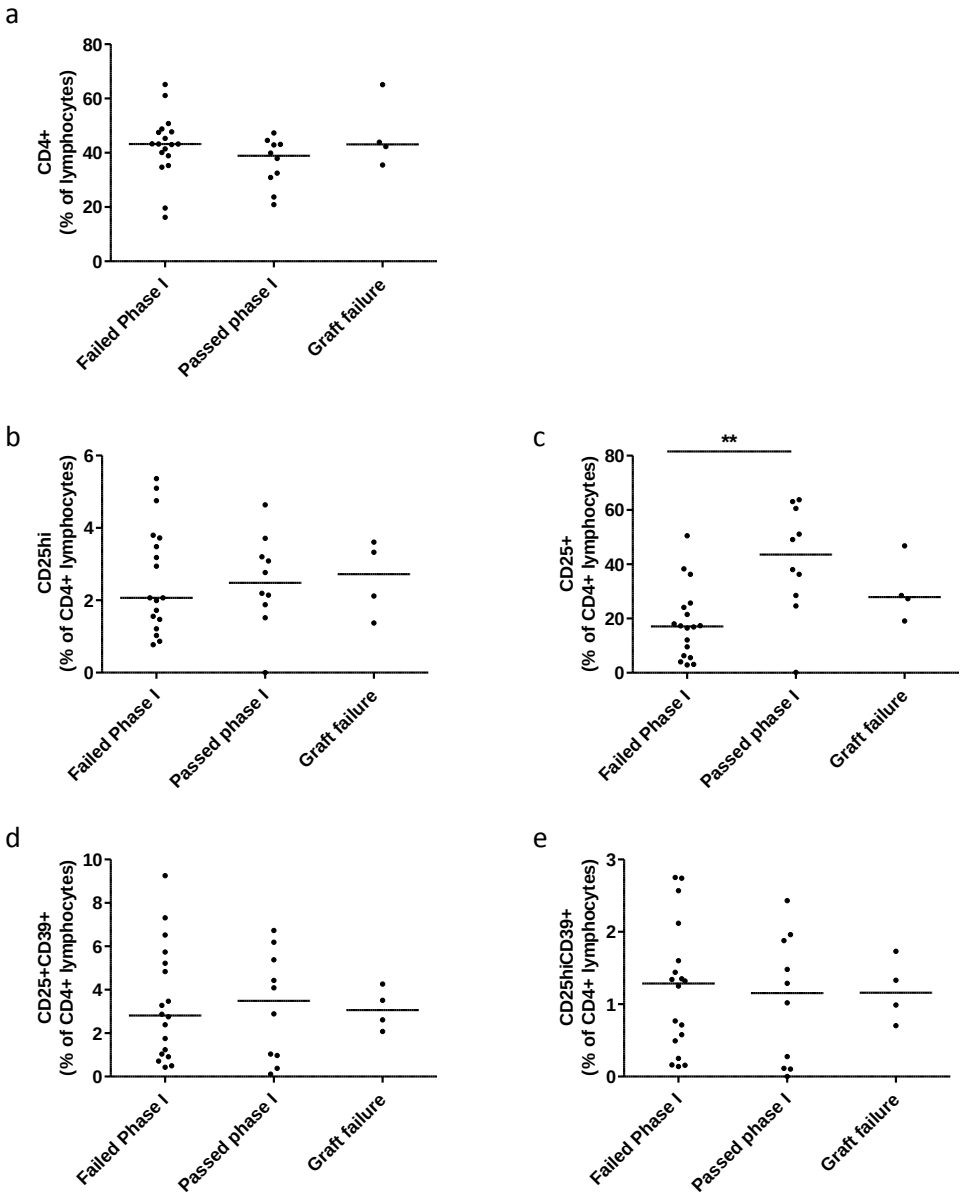

Figure 3.18 Comparison of frequency of CD4+ T cells and CD4+ T cell subsets at enrolment with clinical outcome at end of phase I

Patients were grouped according to those who failed phase I (n=18), passed phase I (n=10) or had their graft fail/ had an eGFR <20mls/min during phase I (n=4). The frequency of T cell subsets was compared between the three groups. **(a)** CD4+ T cells **(b)** CD25hi T cells, **(c)** CD25+ T cells, **(d)** CD25+CD39+ T cells **(e)** CD25hiCD39+ T cells. CD4+ T cells expressed as frequency of lymphocytes, all other subsets expressed as frequency of CD4+ lymphocytes. Black lines on graph represent the median. Groups compared using a Kruskal-Wallis test with a Dunn's multiple comparison test. Patients who did not pass phase I were found to have a lower frequency of effector CD4+CD25+ T cells than those who did pass phase I (P= 0.0060). P>0.05 for all other analyses.

3.2.11 Correlating B cell phenotype in patients enrolled on the RituxiCAN C4 trial with Leukocyte cones

The B cell phenotype of the enrolment samples was compared to the phenotype of 12 leukocyte cones to assess whether there were any gross differences between renal transplant patients with healthy volunteers. The leukocyte cones had been frozen in Liquid nitrogen for 3 years before being stained for flow cytometry in order to replicate, as close as possible, the conditions that the RituxiCAN C4 trial samples had been stored under as this may have had an effect on some B cell populations or the expression of certain cell surface markers. Figure 3.19 shows that the frequency of CD19+ cells in the enrolment samples is significantly lower than in the leukocyte cones (P=0.0004).

When the frequency of different B cell populations were compared between the leukocyte cones and the enrolment samples, the analysis revealed that the leukocyte cones have a higher frequency of transitional and intermediate B cell subsets compared to the enrolment samples (Fig. 3.20 (a) and (b), P=0.0105 and P=0.0079 respectively). No significant differences were found between the two groups with regards to the frequency of naïve cells or memory cells (CD27+) (Fig. 3.20 (c) and (d)).

The frequency of CD5+ cells was highest in the transitional population and lowest in the naïve population in both the enrolment samples and the leukocyte cones. However within each population, there was a significantly lower representation of CD5+ cells in the enrolment samples compared to the leukocyte cones (Fig 3.21 (a), P <0.0001 for all three populations). In both the enrolment samples and the leukocyte cones, the frequency of CD1d+ cells was very similar on naïve and intermediate cells but slightly lower on the transitional cell population. However, the frequency of CD1d expressing cells within each population was higher in the enrolment samples than the leukocyte cones (Fig 3.21(b), P<0.0001 for naïve and intermediate, P=0.0407 for Transitional). Finally, a lower frequency of CD10+ cells in the transitional and intermediate populations was observed in the patients compared to the leukocyte cones (Fig 3.21 (c) P=0.0032 and 0.0020 respectively).

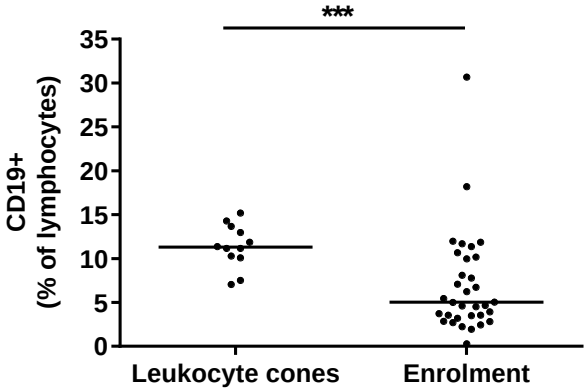

Figure 3.19 Comparison of CD19+ lymphocyte frequency between leukocyte cones and enrolment samples from patients enrolled on the RituxiCAN C4 trial

The patients have a lower frequency of CD19+ lymphocytes than Leukocyte cones, P=0.0004. Black lines on graph represent the median frequency, P value obtained using a Mann Whitney U test.

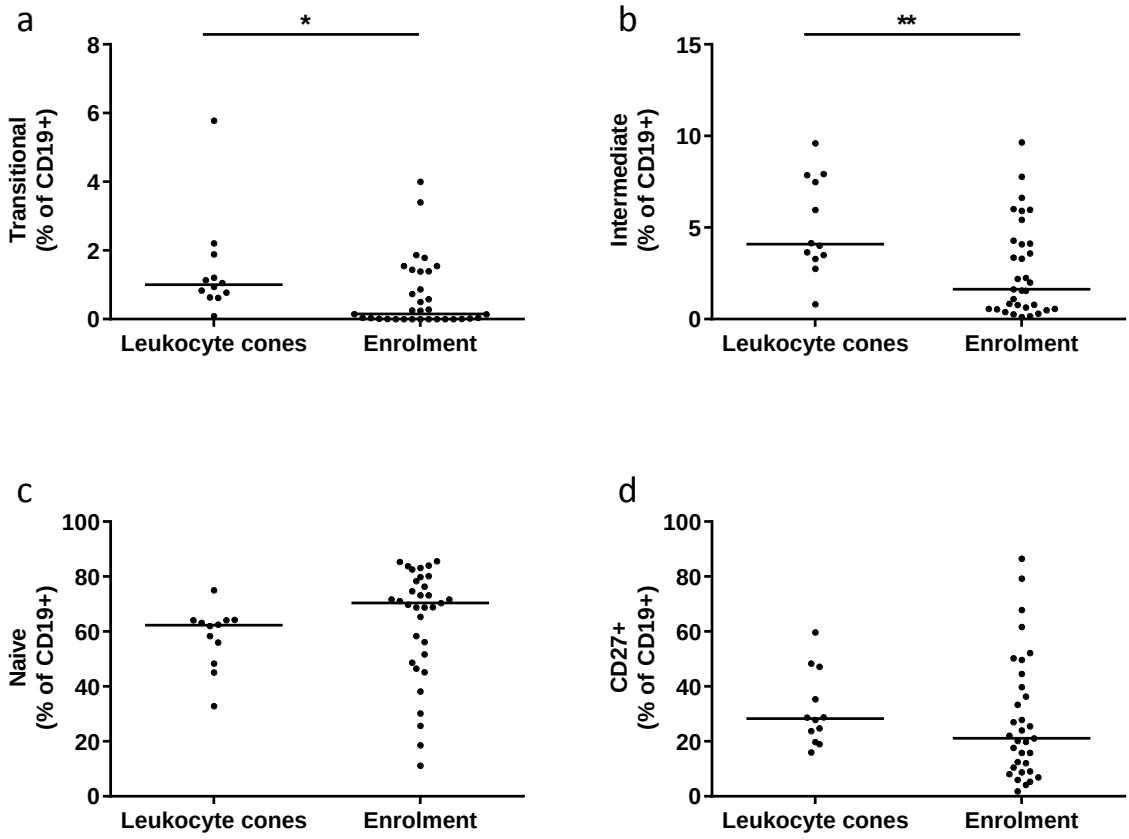

Figure 3.20 Comparison of B cell subset frequencies between leukocyte cones and enrolment samples from patients enrolled on the RituxiCAN C4 trial

(a) and **(b)**: transitional and intermediate B cells were found at lower frequencies in RituxiCAN C4 patients compared to leukocyte cones (P=0.0105 and P=0.0079 respectively). P>0.05 for Naïve and CD27+ subsets (**(c)** and **(d)**). Black lines represent the median. P values obtained using a Mann Whitney U test.

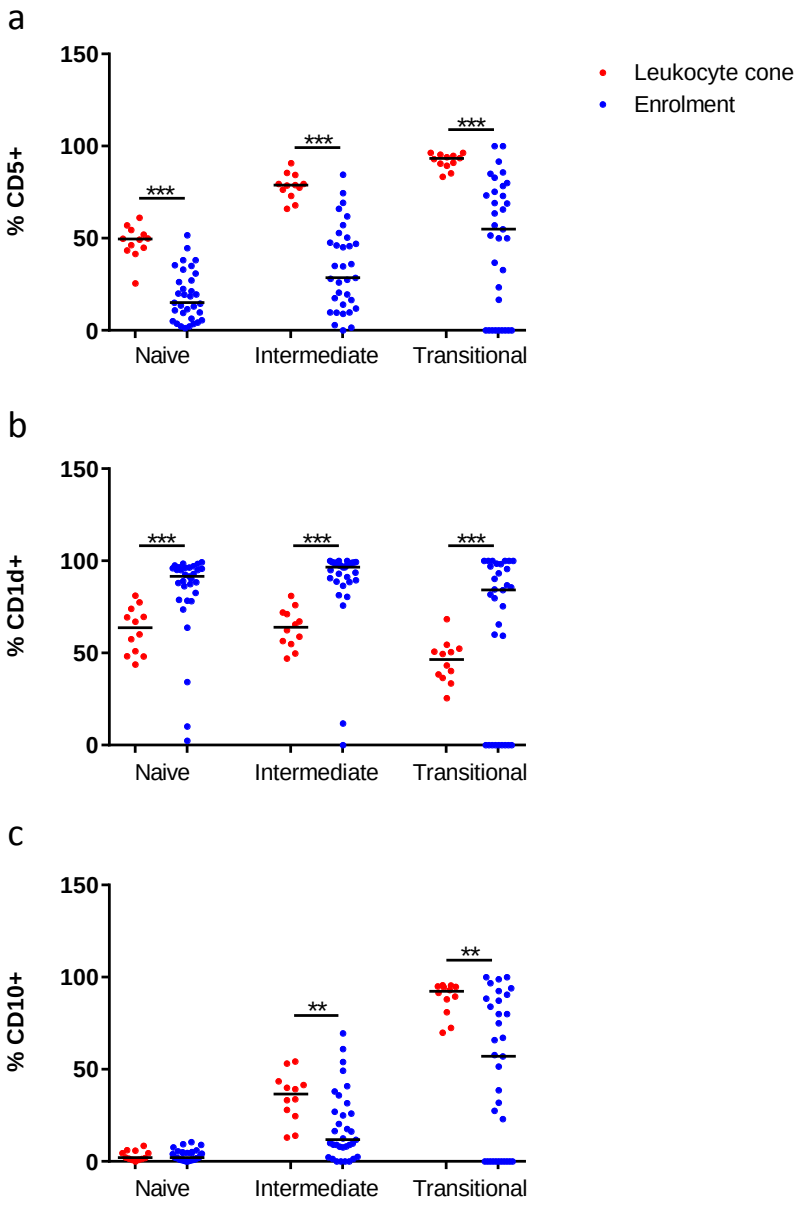

Figure 3.21 Comparison of CD5+, CD1d+ and CD10+ cell frequencies within the naive, intermediate and transitional subsets between leukocyte cones and enrolment samples from patients enrolled on the RituxiCAN C4 trial

(a) A lower frequency of CD5+ cells on all subsets (Naïve, Intermediate and Transitional) was measured in the enrolment samples compared to the leukocyte cones (P= < 0.0001 for all three subsets). **(b)** A higher frequency of CD1d+ cells was measured in the enrolment samples compared to the leukocyte cones (P<0.0001 for naïve and intermediate, P=0.0407 for transitional). **(c)** A lower frequency of CD10+ cells was measured in the intermediate and transitional cells in the enrolment samples compared to the leukocyte cones (P=0.0032 and 0.0020 respectively). P values obtained using a Mann Whitney U test.

3.2.12 B cell phenotypes post Rituximab

A delayed re-population of B cells post Rituximab treatment has previously been reported in cohorts of renal transplant patients with CAMR (Rostaing et al., 2009, Billing et al., 2012). One of the aims of this thesis was therefore to address how long this process would take in renal transplant recipients with CAMR enrolled onto the RituxiCAN C4 trial, and investigate whether there is preferential repopulation of a certain subset of B cells into the circulation before others. The absolute B cell numbers per µl of blood over time for each patient who was randomised into phase II are shown in Table 3.1. Data was collated from information collected from the clinical laboratories where blood samples were sent for routine monitoring. All available data has been included in this table. The patients have been grouped according to whether they received Rituximab or not. In the Rituximab treated group, there was a sharp decrease in B cell numbers between months 3 and 6 where the mean number of B cells/µl of blood reduced from 118 to 3. In contrast, the mean number of B cells per µl of blood in the non-Rituximab treated group increased from 76-93. The mean number of B cells in the Rituximab group remained low over the subsequent 36 months and were far from returning back to the numbers observed before Rituximab treatment.

B cells were stained by flow cytometry before and at several time points post Rituximab. In the majority of patients, very few events were detected in the CD19+ gate. Four patients who received Rituximab had enough B cells return to their peripheral blood to be able to do some basic phenotyping analysis. The B cell subsets were only phenotyped based on their CD27+ and CD27- expression as the small number of events was prohibitive to analysing the B cell subsets any further. In 3/4 patients, B002, G012 and G003, the B cells that were detectable in the circulation 12-19 months post enrolment were predominantly CD27+ (Fig 3.22 (b)). At later time points, this frequency declined and an increase in CD27- B cells was observed. By 33-39 months post enrolment, the frequency of CD27+ and CD27- B cells was more reflective of that measured at enrolment (Fig 3.22 (a) and (b)). The repopulation of the remaining patient (G017) at time point 1 was in contrast to the other patients as they had an equal distribution of CD27+ and CD27- B cells. However, a similar pattern was observed in all four patients between time points 1-3 where an overall decrease in CD27+ B cells and an increase in CD27- B cells was observed.

Table 3.2 B cell numbers over time in patients randomised in phase II

Rituximab administered ↓

Patient ID	No months post enrolment												
Rituximab	**0**	**3**	**6**	**9**	**12**	**15**	**18**	**21**	**24**	**27**	**30**	**33**	**36**
W010	90	23	0	4	5	6	9						
G003	203	89	13	19	2	17	10	2	4	1	5	10	2
G009	154	170	2										
G010	16	19	0										
G012	269	173	4	6	1	6	5	9	10	9	6		
G017	56	186	4	1		1	2		1		4		2
G025	224	164	1	1	2	5	1	2					
Mean	**145**	**118**	**3**	**6**	**3**	**7**	**5**	**4**	**5**	**5**	**5**	**10**	**2**
No Rituximab													
W006	630		517	758	287		143	142		288	321		275
W008	47	48	67		61	65	114	104	84	114		90	62
G002	49	148			100								
G007	36	17		19	34	11	20	21		16			
G011	21	40	16										
G013	133	160	189	230	172	165	196	179	241	204	190	186	217
G023	43	60		30									
G027	87	60	100	69	60	30							
Mean	**59**	**76**	**93**	**87**	**85**	**68**	**110**	**101**	**163**	**111**	**190**	**138**	**140**

Patients are grouped according to whether they received Rituximab or not. Numbers represent number of B cells per µl of blood. All available information is shown.

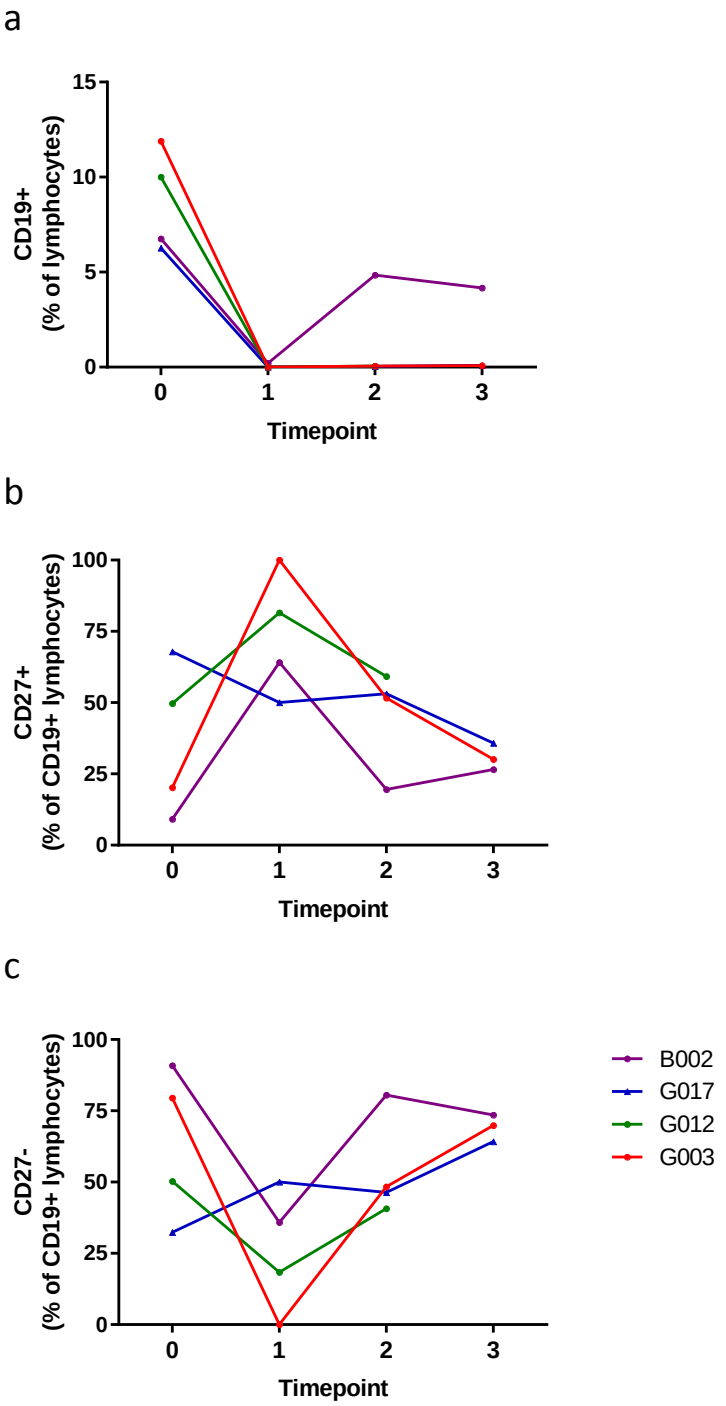

Figure 3.22 Frequency of CD19+ lymphocytes and CD27+ and CD27- B cell subsets pre and post Rituximab in four patients randomised in phase II

Rituximab was administered between time point 0 and 1. Time point 0 = enrolment, Time point 1 = 12-19 months post enrolment, Time point 2 = 24-29 months post enrolment,Time point 3 = 33-39 months post enrolment.

3.3 Key points in chapter 3

1. The B dependent, B regulated and T regulated patterns of IFNγ production in response to donor membrane proteins that were reported in Shiu et al. were reproduced in PBMC samples from the RituxiCAN C4 trial.

2. The patterns of reactivity in the IFNγ ELISpot did not correlate with the phenotype of B cell or Treg cell subsets.

3. IFNγ production at enrolment onto the RituxiCAN C4 trial correlated with clinical outcome at the end of phase I: The majority of patients who produced IFNγ in response to donor membrane proteins at enrolment had eGFRs that continued to decline post optimisation of oral immunosuppression.

4. PBMC from patients enrolled onto the RituxiCAN C4 clinical trial have significantly lower frequencies of circulating CD19+ cells and Intermediate and Transitional B cells than Leukocyte cones.

5. Rituximab mediated B cell depletion from the peripheral blood is highly effective in renal transplant recipients with CAMR. B cell numbers remained low up to 36 months post Rituximab administration. Upon B cell repletion, CD27+ memory B cells were the predominant B cell subset that could be detected in the majority of patients in whom phenotyping was possible.

3.4 Discussion

The indirect pathway of allorecognition has been known for over two decades and is regarded as the most important pathway for long-term outcomes in solid organ transplantation. Despite this, there is no reliable way of correlating indirect alloreactivity with clinical outcome and a routine clinical test that can be used to monitor indirect alloreactivity in transplant recipients is yet to be established.

In this chapter, a previously published IFNγ ELISpot assay used to measure indirect alloreactivity in renal transplant recipients with chronic rejection, was applied to a new cohort of patients with CAMR to establish whether this assay merits further development for use as a tool to study the relationship between the indirect pathway of allorecognition and the progression of CAMR (Shiu et al., 2015).

The group of patients studied were recruited onto the RituxiCAN C4 trial and were therefore a more uniform group of patients than used in the observational study published in Shiu et al. Alongside the initial aim of measuring the magnitude of the indirect alloreactive response to donor derived membrane proteins, was the aim of investigating the contribution that B cells make to this response as well as establishing if there was a role for Treg cells in regulating the indirect alloresponse. To this end, the contribution of B cells was measured in vitro by magnetic bead based depletion of CD19+ cells in the IFNγ ELISpot and in vivo by using Rituximab as a B cell depleting agent. The contribution of Treg cells was measured using in vitro depletion of CD25+ cells in the IFNγ ELISpot. In order to eliminate interference from the semi-direct or direct pathways in the IFNγ ELISpot, CD8+ T cells were in vitro depleted in every experiment. To complement the results from the IFNγ ELISpot, global phenotyping of the T and B cells in these patients was carried out. The analysis of the results focuses on the in vitro findings because at the time of writing this thesis, the RituxiCAN C4 clinical trial had not been completed, so in depth analyses of clinical outcomes have not been included. There was however the opportunity to study the effect that Rituximab treatment had on the depletion and subsequent reconstitution of the B cell population in this cohort of patients and to do some basic analyses with regards to the ELISpot pattern of reactivity at enrolment and how this related to the clinical outcome at the end of phase I of the trial.

3.4.1 The patterns of reactivity to donor membrane proteins detected in the RituxiCAN C4 cohort broadly replicates those reported in Shiu et al and highlight the complex and dynamic nature of the alloresponse

Shiu et al. reported that CD4+ IFNγ production in response to donor membrane proteins was both complex and dynamic in renal transplant recipients with chronic rejection (the Biopsy for cause-CAMR, or BFC-CAMR group). The data reported in this chapter broadly supports these findings as the same patterns of reactivity have been observed in the RituxiCAN C4 cohort. In Shiu et al. 36% of CD8+ depleted samples in the BFC-CAMR group produced IFNγ in response to donor membrane proteins compared to 19% of the RiuxiCAN C4 samples. When CD19+ cells were depleted from the samples that were hyporesponsive to donor membrane proteins when just CD8+ cells were depleted, IFNγ production was revealed in 18% of the BFC-CAMR samples compared to 8% in the RituxiCAN C4 samples. Similarly, when CD25+ cells were depleted from the hyporesponsive samples, IFNγ production was revealed in 34% of the BFC-CAMR samples and 9% of the RituxiCAN C4 samples (Shiu et al., 2015). The frequency of samples that display each pattern of reactivity is not the same in the two cohorts of patients, but there are limitations to the conclusions that can be made by making such gross comparisons, as the two groups were recruited using different criteria and the number of samples tested is not the same for each patient. The RituxiCAN C4 samples are from patients recruited onto a clinical trial and so therefore are more tightly defined and controlled than the BFC-CAMR group who were part of an observational study. Moreover, the RituxiCAN C4 patients all received the same treatment intervention of Tacrolimus and MMF in the first phase of the study and a subset of patients received Rituximab thereafter.

An appropriate way of using the data from both cohorts is to highlight that active cellular processes against donor antigens can be detected in the peripheral blood of renal transplant recipients with CAMR and that B cells are likely to be playing a role in facilitating this immune activation through processing and presenting donor antigen to indirect alloreactive CD4+ T cells. In the RituxiCAN C4 cohort, IFNγ production was dependent on the presence of B cells in 100% of the samples that responded to the donor membrane proteins when only CD8+ cells were depleted. Similarly, 76% of the reactive BFC-CAMR samples showed evidence of B cell dependent IFNγ production. The fact that the CD19+ depletion had such a dramatic effect on IFNγ production suggests that they were the dominant APCs in the culture. This is not surprising as others have previously shown that B cells are more efficient at processing and

presenting low concentrations of antigen than other APCs (Constant, 1999, Constant et al., 1995b, Constant et al., 1995a).

The data from both studies also highlights that there is a substantial proportion of samples that do not produce IFNγ in response to donor membrane proteins but that in some of these samples there is evidence of a regulated immune response towards donor antigens. Interestingly, some samples produce IFNγ when B cells are depleted suggesting that in these individuals, B cells are playing a regulatory role and that other APCs are active in these samples. Similarly, some samples produce IFNγ only when CD25+ cells are depleted from the PBMC mixture revealing that in these samples there are active anti-donor processes occurring but they are being kept in check by regulatory T cells. This evidence of immune regulation is not entirely unexpected as in a conventional immune response setting such as infection, the immune system is highly effective at clearing the pathogen whilst maintaining regulation so adverse pathology does not occur. Considering this point, it is perhaps more surprising that evidence of regulation could not be detected in more samples. This may be due to a technical limitation of this assay in that some effector cells may also have been depleted using the CD25+ Dynabeads, or it might be due to a fundamental lack of regulation in these patients which may have contributed to their progression to CAMR. The latter is hard to reconcile with the data as a whole because the majority of samples remain hyporesponsive to donor membrane proteins even when CD19+ or CD25+ cells are depleted. An IFNγ response to a cocktail of common viral proteins could be detected in some of these donor hyporesponsive samples and all samples produced IFNγ when polyclonally stimulated with anti-CD3/CD28 beads, so it is unlikely that the lack of response to donor membrane proteins is due to an intrinsic inability to respond to antigen or produce IFNγ. It is possible that the donor-specific CD4+ T cells were either in the graft or a draining lymph node at the time of blood draw as opposed to the peripheral blood. It is also possible that there was a response to donor antigen in these samples but the cytokine output was not IFNγ. The fact that the patients were all receiving potent immunosuppressive drugs may also impact the ability to detect a donor specific IFNγ response in vitro.

3.4.2 Evidence of donor specific reactivity at enrolment was mainly detected in patients who did not stabilise their graft function during phase I

The data in this study highlights that the response to donor membrane proteins is complex, but it also shows that the response is highly dynamic: each patient can display a different pattern of reactivity at each different time point. This constant changing in the dynamics of the alloresponse makes it difficult to determine which

subset of leukocytes to target in order to slow down the progression to graft loss. The data from the RituxiCAN C4 cohort does however suggest that evidence of donor specific reactivity- whether that be B cell dependent, B regulated or T regulated – is an indication that graft function will continue to decline and that these patients are refractory to optimised immunosuppression of TAC and MMF. 10/11 (91%) of the patients that showed evidence of donor specific reactivity at enrolment failed to stabilise their graft after optimal treatment was administered (end of phase I).

It must be noted that patients who did not pass phase I were divided into two different groups based on their graft function at the end of phase I. Patients whose kidney function failed to stabilise were eligible to be re-consented into phase II and those who had graft failure or an eGFR<20 mls/min during or at the end of phase I were withdrawn from the trial. It is perhaps surprising that only a small percentage of patients who produced IFNγ in response to donor derived proteins were found in the latter group, as it would follow that donor reactivity would lead to a poorer clinical outcome in all patients who did not pass phase I. It is possible however, that this group of patients were recruited onto the trial with an eGFR that was already lower than can benefit from intervention and that their poor renal function at enrolment was the major cause of the subsequent decline to graft failure, as opposed to any immunological mechanism (A.Dorling, personal communication).

3.4.3 Rituximab treatment leads to prolonged depletion of B cells from peripheral blood

Rituximab administration led to a prolonged reduction in B cell counts in the patients that were randomised to receive Rituximab in the RituxiCAN C4 trial. Such a prolonged reduction of B cells is not commonly seen in individuals who receive Rituximab for the treatment of Non-Hodgkin's Lymphoma, RA, SLE or Type I Diabetes, where B cells have been reported to re-populate the circulation by 12 months post Rituximab administration (Anolik et al., 2007b, Leandro et al., 2006, Palanichamy et al., 2009, Roll et al., 2006, Palanichamy et al., 2012, Pescovitz et al., 2009). It is possible that prolonged depletion of B cells post Rituximab is a feature of CAMR as previous studies that have included Rituximab as a treatment drug for CAMR or CAMR associated biopsy features have reported that B cells do not return to the circulation. Rostaing et al. reported that circulating B cells had not returned by 30 months post Rituximab administration (Rostaing et al., 2009) and Billing et al. reported that in 3/6 patients they treated with Rituximab, B cells remained completely depleted at their 12 month follow up, 1/6 had partial reconstitution and 2/6 had reconstituted their B cells (Billing et al., 2008).

Interestingly, the B cells that have been detected in the circulation of the RituxiCAN C4 patients are of a CD27+ memory phenotype which is in contrast to the phenotype of the B cells that re-populate the circulation in individuals treated with Rituximab for autoimmune diseases or Non-Hodgkin's Lymphoma, where re-population of the B cell compartment is in line with B cell ontogeny (Anolik et al., 2007b, Palanichamy et al., 2009, Roll et al., 2006). The first population to be detected in the peripheral blood post Rituximab therapy in these patients is of a transitional phenotype and a delayed reconstitution of the memory B cell population is often observed (Sidner et al., 2004, Roll et al., 2006, Anolik et al., 2007a). It is possible that the memory B cells detected in the peripheral blood of the RituxiCAN C4 patients post Rituximab originate from a pool of memory B cells that were never depleted by the Rituximab treatment (Kamburova et al., 2013). Alternatively, either CAMR itself, or the combination of Tacrolimus, MMF and Rituximab, may have a detrimental effect on B cell homeostasis post Rituximab treatment. The fact that the RituxiCAN C4 patients are being treated with immunosuppressant drugs Tacrolimus and MMF, in addition to the Rituximab, makes it difficult to directly compare B cell reconstitution in CAMR patients with those receiving treatment for Non-Hodgkins Lymphoma and autoimmune diseases. Whilst immunosuppressant drugs are used to treat some autoimmune diseases, Tacrolimus and MMF were not used in combination with Rituximab in the papers cited above. Similar results were found in a cohort of renal transplant recipients who received a single dose of Rituximab at the time of transplant; B cell numbers remained low for two years after Rituximab treatment. These patients did not have CAMR, but were also treated with Tacrolimus and MMF which suggests that it is the combination of these two immunosuppressant drugs that is preventing the reconstitution of B cells post Rituximab treatment (Kamburova et al., 2014).

Whether the administration of Rituximab in the RituxiCAN C4 CAMR patients has a favourable clinical outcome is yet to be determined as the RituxiCAN C4 trial is ongoing.

3.4.4 CD4+ T cell phenotype does not correlate with pattern of reactivity in the IFNγ ELISpot in RituxiCAN C4 patients

No correlations were found between the phenotype of T cell subsets and the ELISpot patterns of reactivity in the RituxiCAN C4 cohort of patients. This finding is not in agreement with the observational study by Shiu et al. where they reported that donor reactive samples (ie. those that produced IFNγ in response to donor membrane proteins when just CD8+ cells were depleted) had significantly higher frequencies of CD4+CD25+ T cells than those who were non-donor reactive, suggesting that these

samples had a higher frequency of activated effector T cells. Shiu et al. also reported that samples with a T regulated donor reactive response had significantly higher frequencies of CD4+CD25hi T cells. It is important to note however, that this data is based on samples from all of the cohorts studied in Shiu et al and not just the BFC-CAMR group. Interestingly, in the RituxiCAN C4 cohort a higher frequency of CD4+CD25+ T cells at enrolment was associated with a better clinical outcome at the end of phase I of the trial. This result is the opposite of what was predicted as it was expected that better clinical outcome would be associated with higher frequencies of CD4+CD25hi Treg cells. It does not appear that the positive clinical outcome in these patients is related to a reduction in the CD4+CD25+ subset or an increase in CD4+CD25hi cells between enrolment and the end of phase I as no obvious changes in the phenotype in either of these subsets were apparent in these samples.

3.4.5 Global phenotype of B cells at enrolment does not correlate with pattern of reactivity in IFNγ ELISpot or clinical outcome

No gross differences could be found in overall B cell phenotype at enrolment that distinguished the patients from one another in terms of their pattern of reactivity in the IFNγ ELISpot or their clinical outcome. This mirrors what was found in the observational study by Shiu et al. However, it was found that CAMR patients have lower frequencies of B cells than Leukocyte cones. Leukocyte cones are a source of PBMC derived from individuals who are blood donors and so in theory should be suitable to be used as healthy controls. Within the B cell population it was also found that CAMR patients have lower frequencies of transitional and intermediate populations than Leukocyte cones. Both of these findings are consistent with Shiu et al and others (Silva et al., 2012, Nova-Lamperti et al., 2016, Shiu et al., 2015, Nouel et al., 2014). Interestingly, it was found that CAMR patients have a higher proportion of CD1d expressing B cells than the Leukocyte cones. The reason for this remains unclear.

Correlating global phenotypes with an antigen specific response is a rather crude way of studying the immune system. The phenotype of individual allospecific B cells may not reflect that of the overall B cell population and may indeed correlate with the B cell dependent or B regulated patterns of reactivity. In the following chapter of this thesis, an assay to flow cytometrically detect antigen binding B cells was developed to help address this point.

3.4.6 Technical limitations of the IFNγ ELISpot and potential improvements

Whilst being one of the most sensitive immunological techniques available for detecting antigen specific responses, the ELISpot assay does have some limitations which could explain some of the variability that is seen in patient responses. For example, the fact that the response to donor membrane proteins was highly dynamic over time could be due to ever changing in vivo dynamics of the alloresponse or it could merely be a reflection of the alloreactive T and B cell clones that happened to be present in the vial of cells that was thawed on the day of the experiment. If a different composition of cells was added to the wells in the ELISpot, a different result may have been detected. This variability in results, as well as the high levels of background observed may be, in part, due to the fact that cryopreserved PBMCs were used for all of the experiments. Whilst this has the advantage that all patient samples can be tested on the same day with the same reagents, therefore reducing the impact of batch effects and other laboratory variables such as temperature and operator, it does lead to a freeze-thaw process which could potentially damage some of the antigen specific T and B cells and also lead to high number of non-antigen specific IFNγ spots being produced. Conducting these experiments using fresh blood would help preserve the antigen specific T and B cells and make it easier to resolve the antigen specific IFNγ producing T cells from the background.

3.4.7 Technical limitations of membrane proteins and potential alternatives

ELISpots have been used in many studies to determine the contribution that the indirect pathway of allorecognition makes to transplant rejection. Peptides containing known sequences of epitopes can be easily manufactured to study T cell responses, however, finding a readily available and economic source of HLA proteins to study the contribution that B cells make to the T cell alloresponse is more difficult. Many studies, including this one, have used cell membrane fragments as their source of HLA proteins (Baker et al., 2001, Benichou et al., 1999, Nadazdin et al., 2011, Nadazdin et al., 2010, Shiu et al., 2015, Breman et al., 2014). This has the advantage of being able to study the alloresponse to all alloantigens (including minor histocompatibility antigens) but the disadvantage of not knowing the exact composition or concentration of alloantigens that the cells are being exposed to. This limits the knowledge that can be gained from these antigens in terms of investigating whether the T cell or B cell population is skewed towards certain HLA epitopes or even HLA subtypes, eg. Class I or class II. In addition, if a membrane protein preparation has a particularly low yield of HLA molecules, a donor specific response could be missed due to insufficient antigen being used in the assay. Using surrogate donor membrane proteins enables patients who

had a cadaveric transplant to be studied in the ELISpot assay, however this also means that they are being stimulated with antigens that are not completely representative of the actual donor. In order to minimise any non-donor specific responses observed when using surrogate donors, patients were carefully matched with appropriate surrogate donors using their HLA antibody profiles and previous transplant history. Finally, the method used to manufacture the membrane proteins used in this thesis is laborious and highly dependent on the quality of the starting material. In addition, the solubilising solution required to dissolve these membrane fragments is toxic to cells and can have a detrimental effect in the ELISpot assay if too much is used. Breman et al demonstrated that HLA monomers could be used as an alternative to cell fragments to activate an HLA A2 specific T cell clone and the use of Pure™ HLA proteins will be described as an alternative source of intact HLA molecules in the next chapter of this thesis (Breman et al., 2014).

3.4.8 Limitations to the interpretation of the data

There are several limitations to the interpretation of the data in this chapter that must be noted. Firstly, it has been assumed that in the reactive B dependent samples, the B cells are processing and presenting the donor or viral antigens to CD4+ T cells. Shiu et al. has previously shown that when B cell activation was inhibited by adding Btk/Syk inhibitors to the cultures of the B dependent samples in the observational study, IFNγ production was diminished. In addition, IFNγ production was also diminished in these samples when the antigen processing and presentation pathway was targeted by adding leupeptin/pepstatin A/E64-d or an anti-class II antibody to the cultures. These experiments have not been repeated on the RituxiCAN C4 patient samples but it has been assumed that similar results would be seen if they were. It has also been assumed that the CD4+ T cells are the source of IFNγ when the number of IFNγ+ spots reached above the cut off of ≥ 25 IFNγ+ spots per million CD4+ T cells. This assumption is based on the rationale that if an antigen is added to a PBMC culture without any non-antigen specific stimulus, the cells that are activated to produce IFNγ should, in theory, be those that are specific to the antigen. By depleting CD4+ cells from ELISpots, it has been shown indirectly in other studies that using protein or peptide antigens elicits a CD4+ T cell response (Schmittel et al., 2001, Smith et al., 2001, McConkey et al., 2003, Arif et al., 2004) Since 92% of the CD8+ T cells were depleted from the cultures, it is unlikely that CD8+ T cells are producing the antigen specific IFNγ in the ELISpot system used here. Whilst depleting CD4+ T cells from the ELISpot may not definitively show that the CD4+ T cells are the source of the IFNγ it may be a worthwhile experiment to strengthen the evidence for making this

assumption. It is possible that the reduction in IFNγ observed when B cells are depleted is because the B cells themselves are the source of the IFNγ. Whilst B cells are not known as major IFNγ producing cells (unlike CD8+ and CD4+ T cells) this cannot be ruled out as a possibility as it has been shown in both mice and humans that B cells have the ability to produce IFNγ under certain stimulation conditions (Ganapamo et al., 2001, Lund, 2008, Gagro et al., 2006, Fillatreau, 2015). Recently, Olalekan et al demonstrated that development of proteoglycan induced arthritis in a mouse required the presence of IFNγ producing B cells, probably because they were able to inhibit in vivo differentiation of Tregs (Olalekan et al., 2015).

In samples where IFNγ production increased when either CD19+ cells or CD25+ cells were depleted it has been assumed that these cells were playing a regulatory role by suppressing IFNγ production. This is only indirect evidence of suppression of an antigen specific response, no attempt has been made in this chapter to perform suppression assays to directly demonstrate that the CD25hi or CD19+ populations that were depleted from the ELISpot assay are capable of suppressing CD4+ T cell IFNγ production in the presence of either donor membrane or viral proteins.

Finally, the contribution of the direct and semi-direct pathways have not been assessed in this study.

4 Results part 2

4.1 Introduction

The results in chapter one established that both B-dependent and B-regulated responses to donor membrane proteins in the IFNγ ELISpot could be observed in two independent cohorts of renal transplant recipients with chronic rejection: those from the observational study published by Shiu et al, and those enrolled onto the RituxiCAN C4 clinical trial and reported here. Analysis of the global phenotype of the B cells in both cohorts did not reveal any gross differences between the samples when grouped according to their pattern of reactivity in the IFNγ ELISpot. It was therefore hypothesised that differences between the samples may be detected in the antigen specific B cell compartment. Thus, the next step towards addressing the aims of this thesis was to investigate whether the phenotype of antigen specific B cells differed between samples that had a B dependent IFNγ response and those that had a B regulated IFNγ response. This chapter addresses aims 4 and 5.

4.1.1 Detection of antigen specific B cells by flow cytometry

Detecting antigen specific antibodies in an individual's serum using an ELISA is common practice for monitoring the response to a vaccine, such as Hepatitis B, and for the diagnosis and routine monitoring of many diseases such as rheumatoid factor in rheumatoid arthritis and HLA antibodies in transplantation. If a more specific and sensitive analysis of an antigen specific B cell compartment is required then an ELISpot is often used to enumerate the number of antibody producing cells that are specific to the antigen of interest (Cao et al., 2010, Crotty et al., 2004, Nanan et al., 2001). Although these techniques provide useful information, they only inform the investigator of the specificity and isotype of the antibodies that the B cell population of interest produces. They do not provide any insights into the phenotype of the B cells that were the precursors to those antibody producing cells.

As we are now able to divide B cells into functional subsets using a combination of cell surface markers such as CD38, CD24, CD10, CD27 and immunoglobulin isotype, it would be useful to be able to ascertain the phenotype of the B cells that are specific to the antigen of interest. This could prove useful in guiding the appropriate B cell targeted treatment for each individual depending on their antigen specific B cell phenotype. For example, depleting the HLA specific B cells that are antigen presenting cells in a patient with CAMR may lead to a reduced rate of rejection. Conversely, if an individual has an antigen specific B cell population that is of a regulatory phenotype, then depleting this population may increase the rate of rejection.

However, developing a reliable assay for flow cytometrically detecting and phenotyping antigen specific B cells comes with its own challenges. It is not surprising that the antibody is chosen to be detected over the antigen specific B cell, as serum antibodies are much more abundant in peripheral blood than antigen specific B cells, and the binding of an antigen in an ELISA to a specific antibody is a much 'cleaner' detection method than detecting an antigen specific B cell, where successful detection requires the specific binding of an antigen to the BCR, with minimal background binding of the antigen to either non-antigen specific BCRs or other receptors on the surface of that B cell. Other factors that need consideration are the requirement for the bound antigen-receptor complex to remain on the surface of the B cell for effective detection, and the potential for B cell-antigen complexes to form with two or more B cells binding to different epitopes on the same antigen (Moody and Haynes, 2008). The choice and preparation of the antigen is therefore very important to get right. For example, if the detection of an epitope specific B cell is desired, using a whole virus as the source of antigen would not be appropriate, as this would contain many epitopes that potentially several B cell clones could bind. A viral protein containing the epitope of interest would not completely eliminate this problem, but it is likely to yield much cleaner results. Correct preparation of the cells is also important in reducing the number of cells that will bind non-specifically to the antigen via Fc receptor bound antigen specific immunoglobulin (Irsch et al., 1995, Bell and Gray, 2003). Thorough washing of the cells prior to incubating with the antigen will reduce the number of antigen specific antibodies that bind to Fc receptors on B cells and other cell types (Hoven et al., 1989).

The first attempt to detect antigen binding B cells was by Julius et al in 1972 where antigen specific B cells from a mouse were FACS sorted using either fluorescent antigen to coat the B cells or the use of a fluorescent antigen specific antibody that would bind to antigen coated B cells (Julius et al., 1972). Many of the challenges in identifying an antigen specific B cell population in 1972 remain today and this has hampered progress in improving the assays employed to identify and phenotype a very specific antigen B cell population. As a result, the techniques used to flow cytometrically identify an antigen specific B cell population today are remarkably similar to those used 40 years ago, with most studies choosing to use either a fluorescently labelled or biotin labelled antigen to form a complex with the antigen specific BCR (Hoven et al., 1989, Nossal et al., 1978, Taylor et al., 2012, Doucett et al., 2005, Irsch et al., 1995, Pape et al., 2011, Pötzsch et al., 2011, Doria-Rose et al., 2009, Khaskhely et al., 2012, Leyendeckers et al., 1999) The majority of these studies have been

carried out in a murine setting, and those that have managed to identify an antigen specific B cell population in humans do not phenotype these cells in depth.

As similar patterns of reactivity to the cocktail of viral antigens were observed in the patients studied in Chapter 3, it was hypothesised that similar results would be obtained if this assay was performed using PBMC isolated from leukocyte cones. Viral proteins could be used as a model antigen to develop an assay which would enable the flow cytometric detection and phenotyping of viral protein specific B cells, in conjunction with determining the pattern of reactivity to the same viral protein in the IFNγ ELISpot. This approach had the advantage that the assay could be optimised before applying it to a patient setting and thereby reducing the use of valuable patient samples for this purpose. In addition, the results may be of interest to the transplant field in general, as the viral proteins used in this chapter are derived from viruses that are clinically relevant to transplant recipients.

4.2 Results

4.2.1 Developing a method to detect and phenotype CMV gB binding B cells

4.2.1.1 Leukocyte cones produce IFNγ when stimulated with CMV gB protein

Initially, the IFNγ ELISPOT assay was modified so the response to each individual viral protein that was used in the viral cocktail could be assessed. CMV gB, VZV gE and CMV pp65 were used individually, but at the same concentration used in the viral cocktail, to stimulate PBMC from 8 leukocyte cones. The response to each individual viral protein is shown in Figure 4.1. CMV gB induced IFNγ production in 4/8 individuals, with 3/4 of these individuals only producing IFNγ above the cut off of ≥25 IFNγ+ spots per million CD4+ lymphocytes when B cells had been depleted (Fig.4.1(a), (c) and (e)). In contrast, IFNγ production in response to CMV gB was B dependent in the remaining individual (Fig. 4.1(b)). CMV pp65 induced IFNγ above the cut off in 1/8 individuals tested, and this was only when B cells had been depleted (Fig.4.1 (e)). VZV gE induced IFNγ in 3/8 individuals tested, with 2/3 showing a B dependent response (Fig. 4.1(b) and (d)) and 1/3 individuals only producing IFNγ above the cut off when B cells were depleted (Fig.4.1(h)). These results clearly demonstrate that each individual responds differently to these three protein antigens in the IFNγ ELISpot assay. CMV gB was chosen as the model protein that would be used to develop the assay to detect antigen specific B cells as it elicited IFNγ production with both B dependent and B regulated patterns of reactivity in more of the cone samples than the CMV pp65 or the VZV gE.

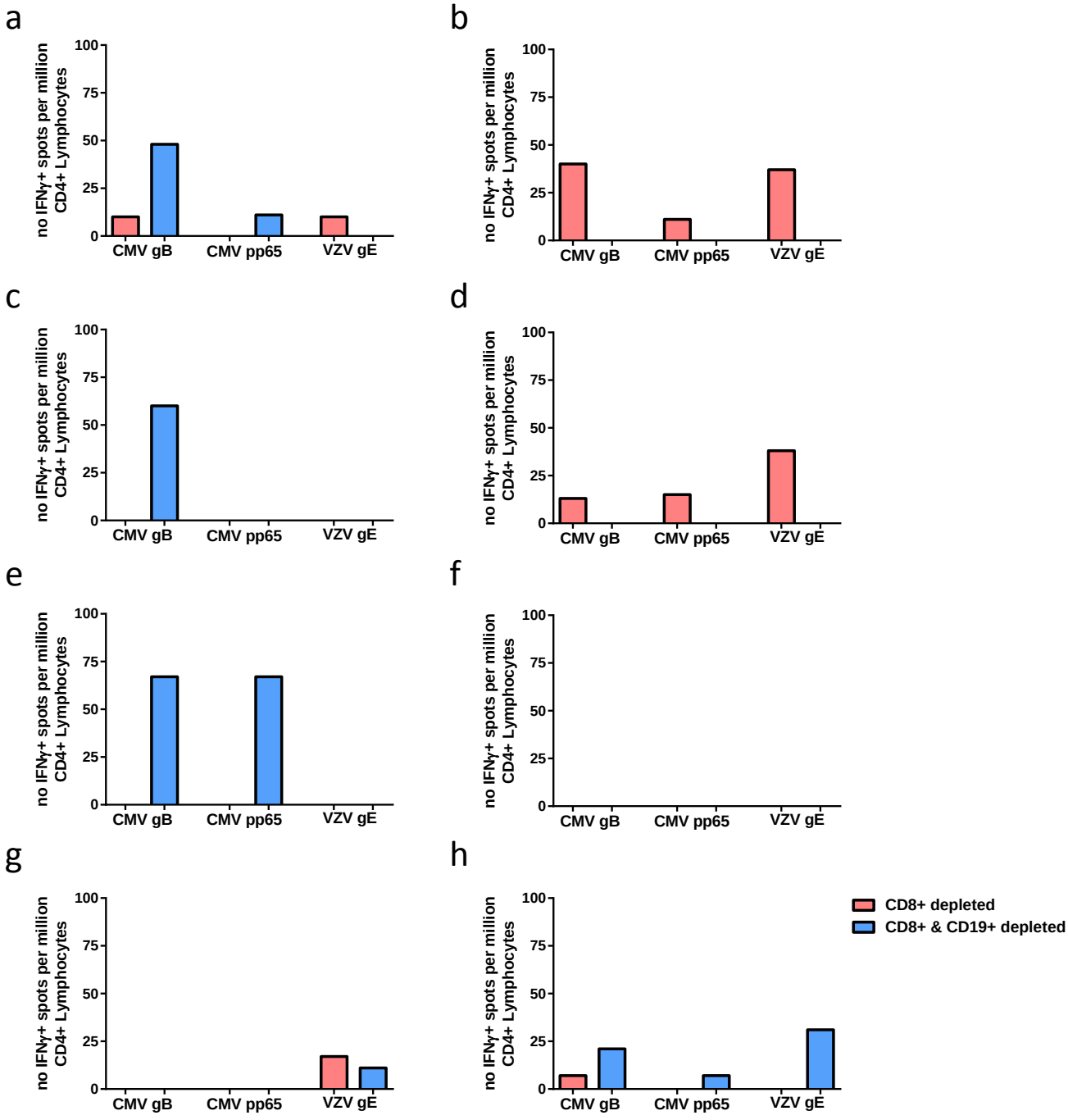

Figure 4.1 Patterns of reactivity in response to three viral proteins in the IFNγ ELISpot
(a-h) PBMC from 8 leukocyte cones were stimulated for 24 hours with either 0.03µg/ml CMV gB, 0.003 µg/ml CMV pp65 or 0.03 µg/ml CMV gE in a CD8+ (pink) or CD8+/CD19+ depleted (blue) ELISpot to investigate whether one of these protein antigens elicits a stronger IFNγ response than the others. A reactive response was defined as being ≥25 IFNγ+ spots per million CD4+ lymphocytes above background. Data represents number of IFNγ+ spots after background had been subtracted. Each graph represents one leukocyte cone.

4.2.1.2 CMV gB binding B cells can be detected using biotinylated CMV gB

Once it was established that CMV gB would be a good model protein to use, the assay to detect antigen binding B cells could be optimised. After a review of the literature, it was decided that incubating a biotinylated version of the CMV gB protein with PBMC and using streptavidin to visualise the B cells that bound the protein would be an appropriate method to try in the first instance. It was hypothesised that by using a biotinylated protein, as opposed to a directly fluorescently conjugated protein, the antigen binding population would be brighter and therefore more easily distinguished from the negative, non-antigen binding population.

The biotinylated CMV gB protein was incubated with PBMC from a leukocyte cone at increasing concentrations in order to find the optimal concentration of protein that allowed the detection of antigen binding B cells without excessive background binding. Figure 4.2 illustrates dot plots from this titration experiment comparing frequencies of antigen binding B cells in the B cell gate versus the non-B lymphocyte gate. Minimal binding was observed on the non-B lymphocytes. Any non-specific binding on these populations was used to guide the positioning of the gate to define a positive CMV gB binding B cell population. Figure 4.3 shows the median with range of the frequency of CMV gB binding B cells in the B cell gate (Fig. 4.3 (a)) compared with the non-B lymphocyte gate (Fig. 4.3 (b)) from 5 leukocyte cones. An increase in non-specific binding of the non B lymphocyte population was detected at 0.194µg/ml which increased with each upwards titration. An increase in CMV gB binding B cells was also observed from 0.194µg/ml to 0.785µg/ml. It was therefore decided that 0.384µg/ml would be the concentration of CMV gB to use in future experiments as this was deemed an acceptable compromise in order to detect as many CMV gB binding B cells as possible, without causing too much non-specific binding. For ease of use in future experiments, this concentration was rounded down to 0.35µg/ml.

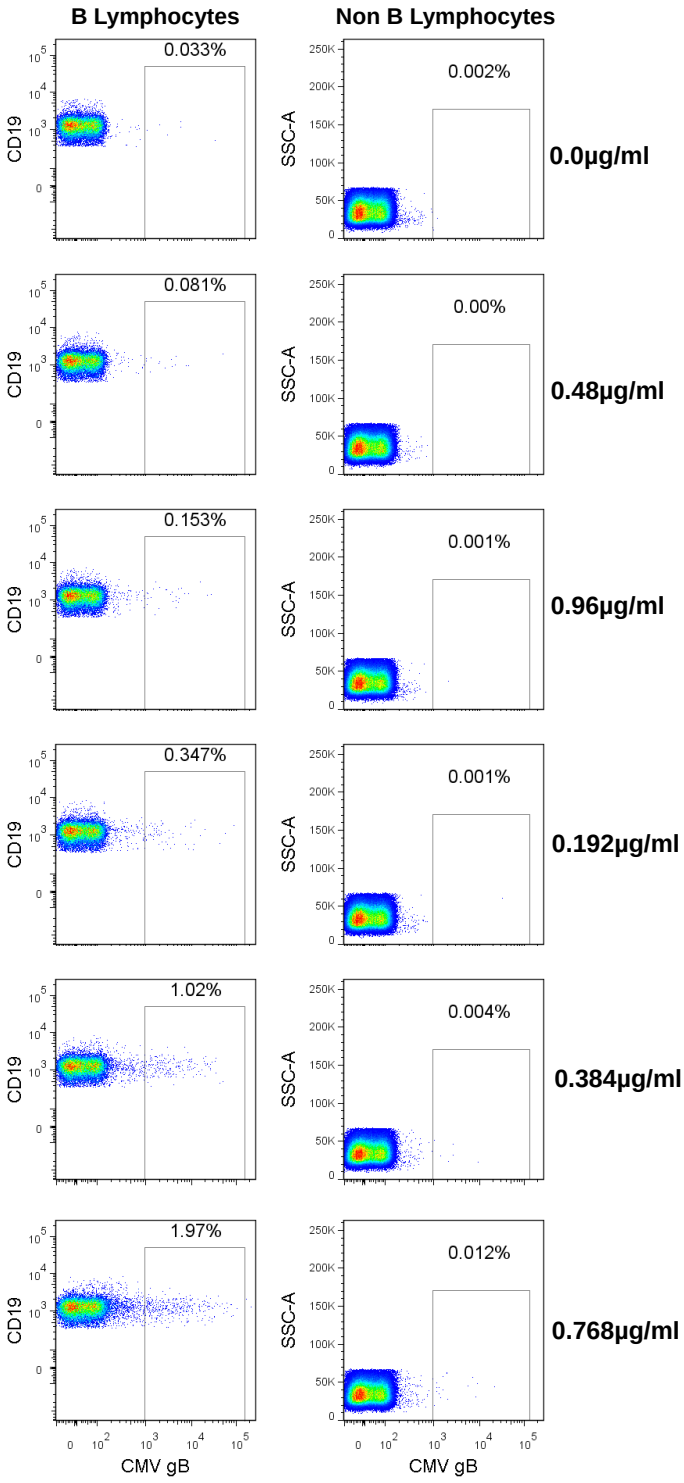

Figure 4.2 Example dot plots of CMV gB binding B cells
PBMC were incubated with increasing concentrations of biotinylated CMV gB (as indicated in figure) at 4°C and stained with CD19 APC-efluor 780 and streptavidin PE. Minimal binding was observed on non B lymphocytes. Any non-specific binding on these populations was used to guide the positioning of the gate to define a positive CMV gB binding B cell population.

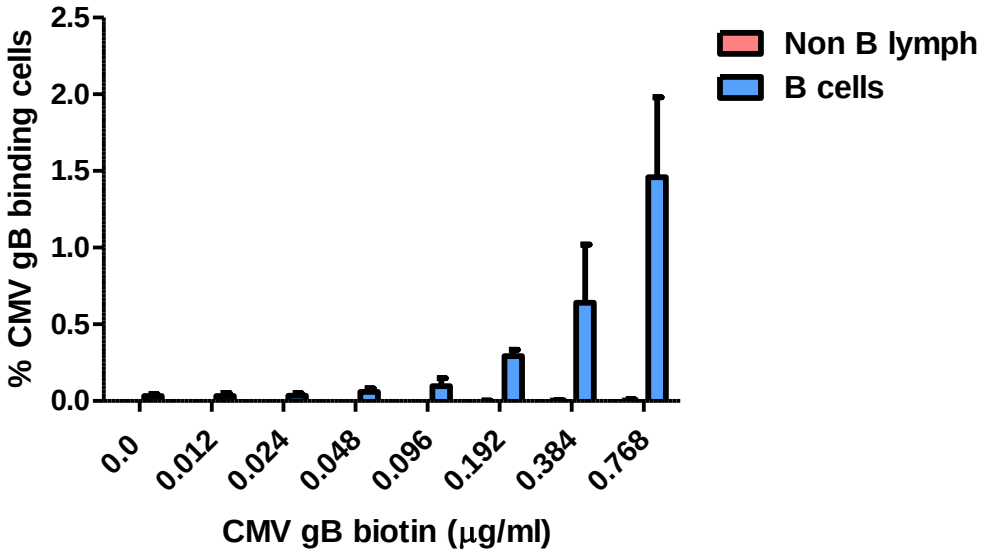

Figure 4.3 Detecting CMV gB binding B cells

PBMC from 5 leukocyte cones were incubated with increasing concentrations of biotinylated CMV gB at 4°C and stained with CD19 APC-efluor 780 and streptavidin PE in order to determine the optimum concentration required to detect CMV gB binding B cells. A titration effect was observed where increasing frequencies of CMV gB binding B cells could be detected when PBMC were incubated with higher concentrations of CMV gB. Minimal binding was observed on non-B lymphocytes: very small frequencies were observed when higher concentrations of CMV gB were used (0.192µg/ml-0.768µg/ml). The median frequency (with range) of CMV gB binding B cells and non B lymphocytes is shown in blue and pink respectively.

4.2.1.3 Biotinylated CMV gB binds the B cell receptor

In order to ascertain whether the binding of the CMV gB to the B cells was in an antigen specific manner, ie, binding to the B cell receptor, three different experiments were carried out. Firstly, the binding of B cells to biotinylated and non-biotinylated BSA was assessed. BSA was chosen as it is a readily available laboratory protein that the majority of humans should not be antigen exposed to, and therefore should not have a memory B cell response towards it. Figure 4.4 shows that in the two leukocyte cones that were tested (Fig. 4.4 (a) and (b)), antigen binding B cells were not detected when non-biotinylated CMV gB, non-biotinylated BSA or biotinylated BSA were incubated with the PBMC. This demonstrates that the events observed in the positive CMV gB gate were not due to the B cells binding non-specifically to the streptavidin, BSA, or the biotin respectively.

To check that the CMV gB was binding the cells directly and not forming a complex between CMV specific antibodies in the serum and CD32, the FCγRIIB receptor expressed on B cells, the biotinylated CMV gB was incubated with 10µg/ml of a blocking anti-CD32 antibody prior to incubation with the biotinylated CMV gB (Fig. 4.5). Blocking the Fc receptor did not impact the frequency of antigen binding B cells that were detected.

The role that CMV gB plays in viral entry remains unclear. Some studies report evidence to suggest that CMV gB binds directly to either epidermal growth factor receptor (EGFR) or platelet derived growth factor receptor (PDGFR) on the cell surface in order to facilitate cell entry (Soroceanu et al., 2008, Wang et al., 2003). Other studies have questioned these findings and report that although CMV gB is required for cell entry, it does not directly bind receptors on the cell surface (Isaacson et al., 2007, Vanarsdall et al., 2012, Wille et al., 2013). In order to confirm that the CMV gB used in this assay was binding the B cell receptor as opposed to any other receptor on the B cell, the B cell receptor was blocked using increasing concentrations of Fab anti-IgG/IgM whilst incubating the PBMC with the biotinylated CMV. The data shown in Figure 4.6 suggests that the CMV gB is binding the BCR as there is a clear titration effect; increased blocking of the BCR results in decreased binding of the CMV gB.

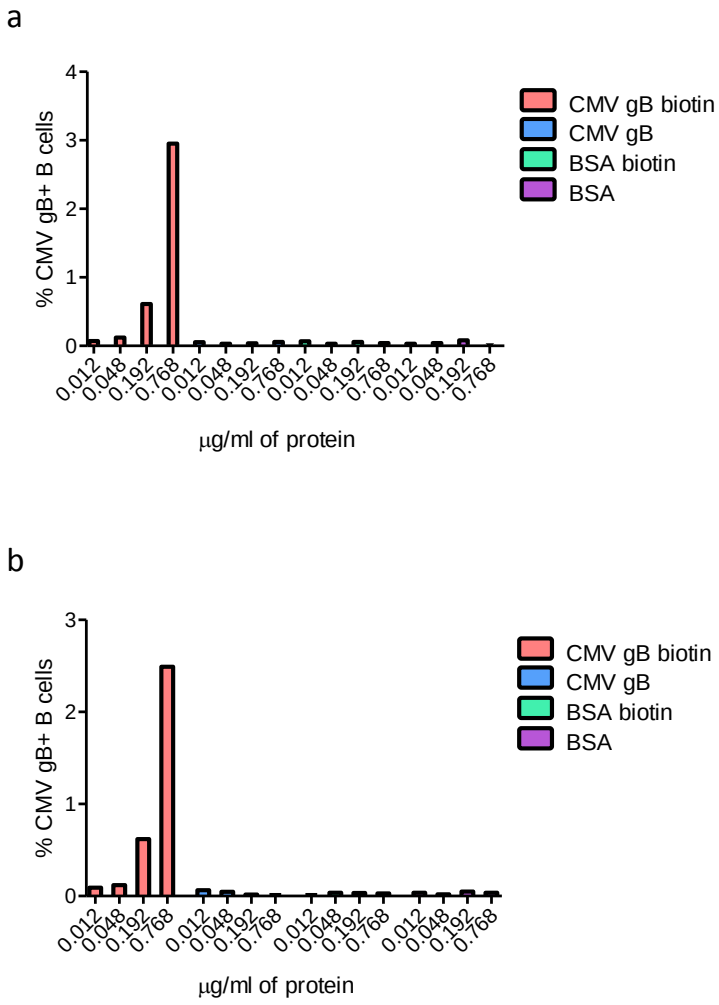

Figure 4.4 B cells do not bind streptavidin or biotin
PBMC from two different leukocyte cones **(a)** and **(b)** were incubated with increasing concentrations of either biotinylated CMV gB (pink) non biotinylated CMV gB (blue), biotinylated BSA (green) or non-biotinylated BSA (purple) for 30 minutes on ice and then stained with CD19 APC-efluor 780 and streptavidin PE.

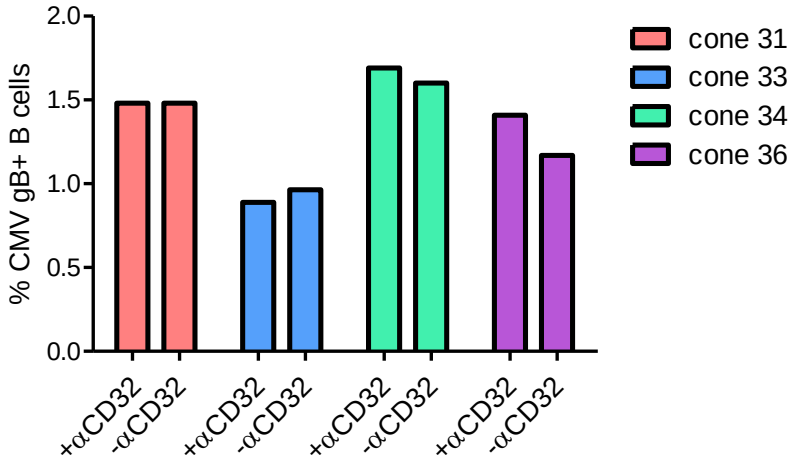

Figure 4.5 Blocking FCγRIIB does not reduce the frequency of CMV gB binding B cells detected

PBMC from four different cones (indicated as pink, blue, green or purple) were incubated with 10µg/ml anti-human CD32 for 30 minutes prior to incubation with biotinylated CMV gB for 30 minutes on ice. PBMC were then stained with CD19 APC-efluor 780 and streptavidin PE. Cones compared with and without αCD32 using a Wilcoxon matched pairs signed rank test, P = >0.05 for all cones.

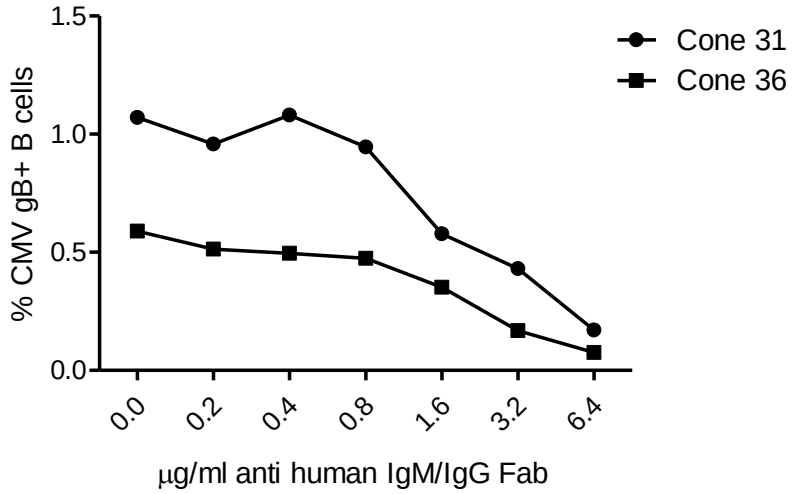

Figure 4.6 CMV gB binds the B cell receptor

PBMC from two different cones (as indicated by the square and circle) were co-incubated with 0.35μg/ml biotinylated CMV gB and increasing concentrations of anti-human IgM/IgG Fab (H+L) to block the BCR. PBMC were incubated for 30 minutes on ice and then stained with CD19 APC-efluor 780 and streptavidin PE.

4.2.1.4 CMV gB binding B cells are predominantly IgM+

Now confident that the CMV gB was binding the BCR, a panel of phenotyping antibodies was used to determine the phenotype of these CMV gB binding B cells in PBMC samples from 15 leukocyte cones. The PBMC were initially incubated with 0.35µg/ml biotinylated CMV gB, washed, and then stained with a combination of B cell surface markers CD19, CD27, IgM, IgG, CD24 and CD38. The median frequency of CMV gB binding B cells detected was 1.83% (range 1.04%-3.37%). For phenotyping analysis, all gates were drawn on the entire B cell population and then applied to the CMV gB binding B cell population. The B cells were initially divided into transitional ($CD24^{hi}CD38^{hi}$) and non-transitional B cells (everything else) (Fig 4.7 (c)). All subsequent gating was applied to only the non-transitional population and is shown in Figure 4.8.

The frequency of each CMV gB binding B cell subset was compared to the frequency of each B cell subset in the overall B cell population to determine whether the phenotype of CMV gB binding B cells is distinct from the overall B cell population. Figure 4.9 shows that the CMV gB binding B cells are predominantly of a non-transitional phenotype but are overrepresented in the transitional gate compared to the overall B cell population (P=0.0009). Within the non-transitional gate, the CMV gB binding B cells were found to be predominantly IgM+ and significantly underrepresented in the CD27+ and IgG+ populations when compared with the overall B cell population (Fig 4.10 (a) and (b), P=0.0054 and 0.0002 respectively). Interestingly, there was a significant overrepresentation of IgMhi B cells in the CMV gB binding population (Fig 4.10 (c), P=0.0001). Populations of B cells that are IgMhi include IgM+ memory B cells, T3 B cells and Marginal zone precursor B cells (Bemark, 2015). Therefore, to further characterise this population of CMV gB+ B cells, the co-expression of CD27, a memory marker on B cells, and IgM was analysed. Figure 4.11 shows that the frequency of both CD27+IgMhi B cells and CD27-IgMhi B cells were significantly higher in the CMV gB binding population than the overall B cell population (P=0.0003 and 0.0001 respectively). So although an overall underrepresentation of CD27+ cells in the CMV gB binding population was observed, when the co-expression of CD27 and IgM was analysed, the data suggests that CMV gB binding B cells are a mixed population consisting of both IgM+ memory B cells and possibly T3 or marginal zone precursor B cells.

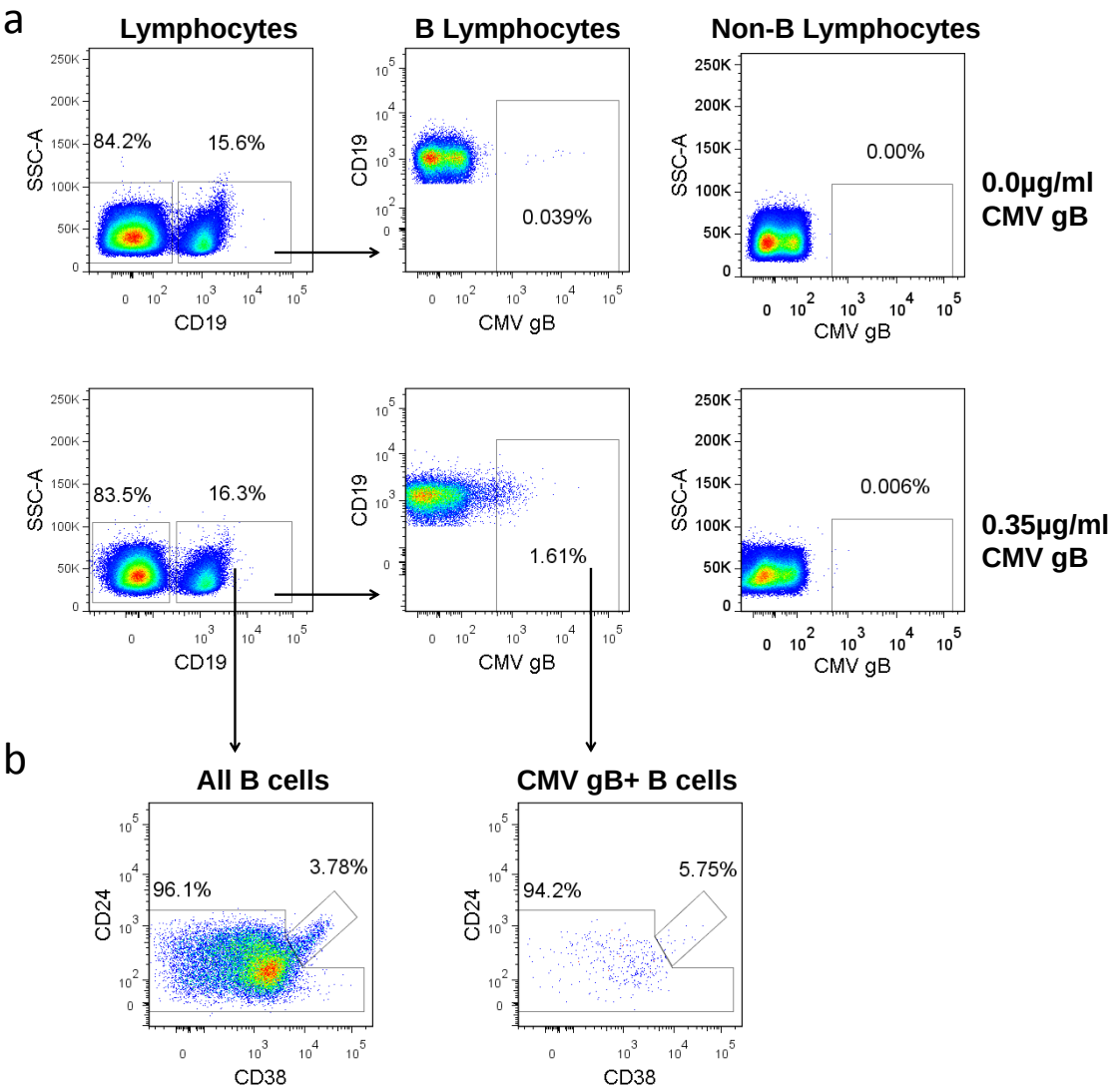

Figure 4.7 Gating strategy for phenotyping CMV gB binding B cells
(a) B cells were defined as CD19+ and CMV gB binding B cell were gated on using the negative control of 0.0µg/ml CMV gB and the non B lymphocytes population. **(b)** B cells were divided into two populations: transitional B cells ($CD24^{hi}CD38^{hi}$) and non-transitional B cells (everything else). Gates were initially drawn on the whole B cell population and then applied to the CMV gB+ population.

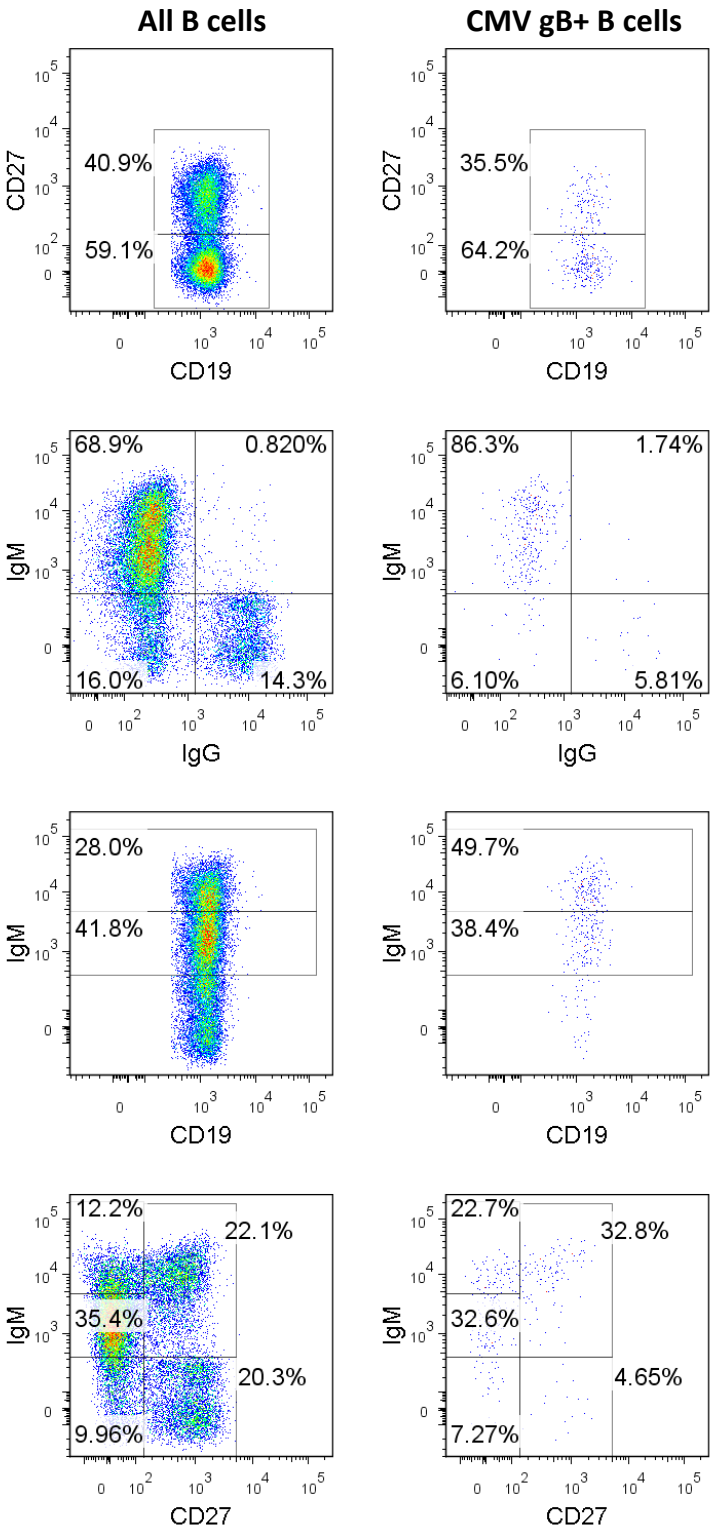

Figure 4.8 Dot plots to illustrate the gating strategy for phenotyping the CMV gB binding B cells

All gates were initially drawn on the whole non-transitional B cell population and then applied to the non-transitional CMV gB binding B cell population.

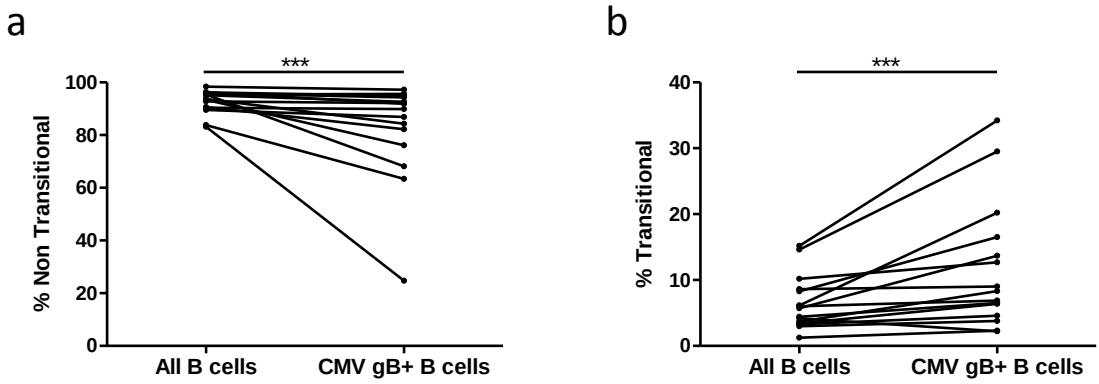

Figure 4.9 Frequency of non-transitional and transitional B cells in the overall B cell population compared to the CMV gB binding B cell population

(a) Non transitional B cells are underrepresented in the CMV gB binding B cell population (P= 0.0001). **(b)** Transitional B cells are overrepresented in the CMV gB binding population (P=0.0009). Each line on the graph represents a leukocyte cone (n=15). P values were obtained using a Wilcoxon matched pairs signed rank test.

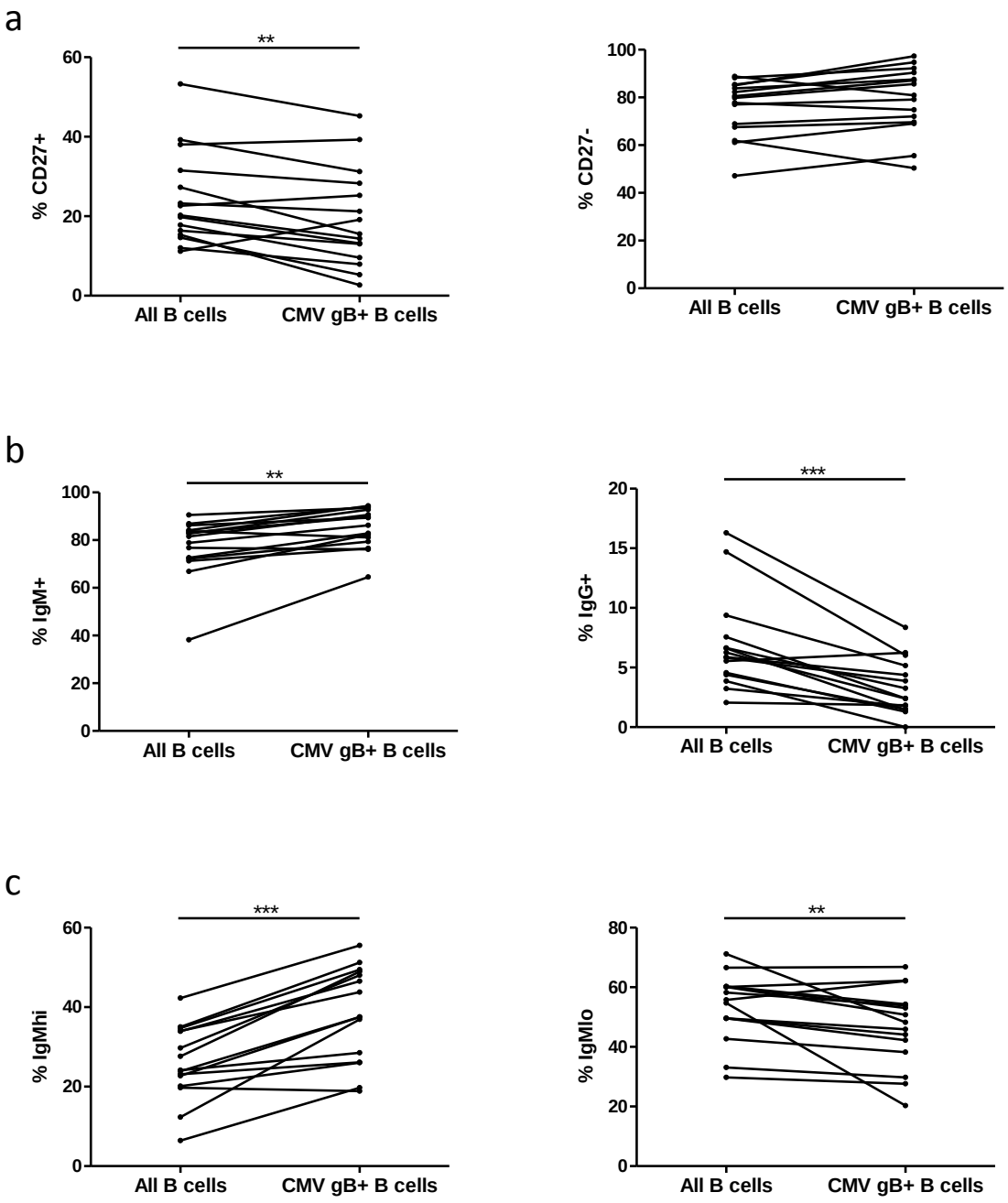

Figure 4.10 Frequency of different B cell subsets in the overall B cell population compared to the CMV gB+ B cell population

(a) CD27+ B cells are underrepresented in the CMV gB binding population (P=0.0054 for CD27+ and >0.05 for CD27-). **(b)** IgM+ B cells are overrepresented in the CMV gB+ population with a corresponding underrepresentation of IgG+ cells (P=0.0003 and 0.0002 respectively). **(c)** IgMhi B cells are overrepresented in the CMV gB+ population with a corresponding underrepresentation of IgMlo B cells (P=0.0001 and 0.0054 respectively). Each line on the graph represents a leukocyte cone (n=15). P values were obtained using a Wilcoxon matched pairs signed rank test.

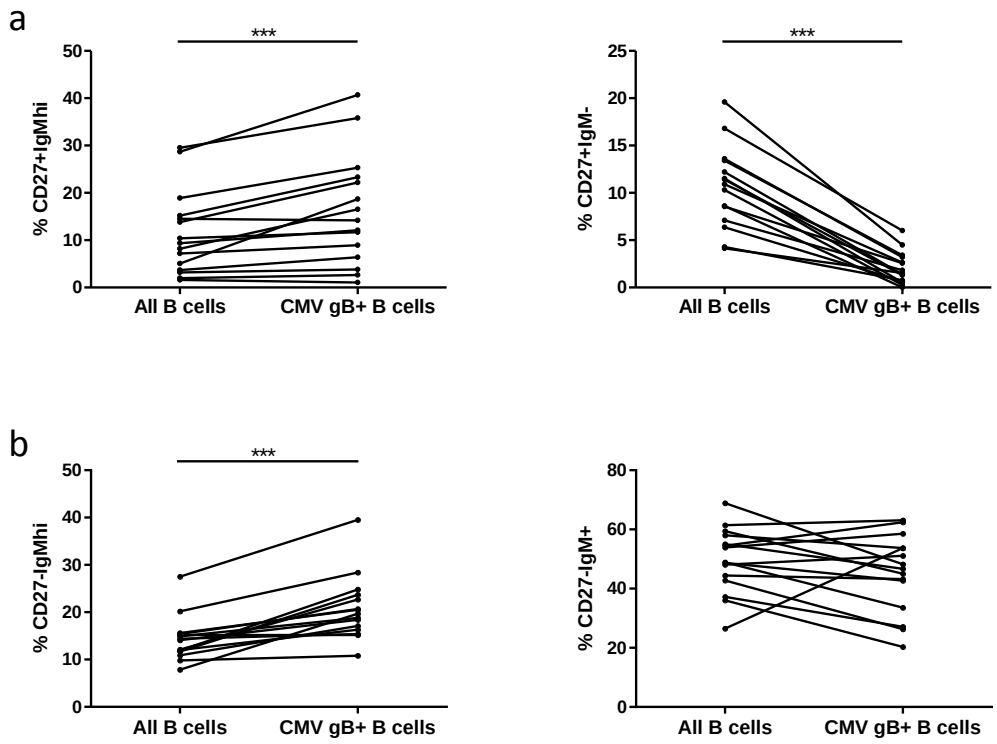

Figure 4.11 Frequency of IgM+ memory and naive subsets in the gB+ B cell population compared to the overall B cell population

(a) CD27+IgMhi are overrepresented in the CMV gB+ B cell population whilst CD27+IgM- are underrepresented (P=0.0003 and <0.0001 respectively). **(b)** CD27-IgMhi B cells are overrepresented (P=0.0001 for CD27-IgMhi and >0.05 for CD27-IgM+). Each line on the graph represents a leukocyte cone (n=15). P values were obtained using a Wilcoxon matched pairs signed rank test.

As recent publications in the literature have suggested that the expression of CD45RB MEM55 (from here on in referred to as CD45RB) is a more specific marker of memory B cells than CD27, and also a defining marker of Transitional 3, or marginal zone (MZ) pre-cursor B cells in humans, CMV gB binding B cells were stained for CD45RB expression and compared to the overall B cell population to investigate whether the CD27-IgMhi population is enriched for T3 or MZ pre-cursor cells in the CMV gB binding B cell population (Bemark et al., 2012, Descatoire et al., 2014, Koethe et al., 2011, Bemark, 2015).

As described in Figure 1.3 in the introduction to this thesis, T3 cells are thought to be late stage transitional B cells that will either differentiate into naïve follicular B cells or MZ/IgM+ memory B cells. The expression of CD45RB is thought to distinguish MZ/IgM+ memory pre cursor B cells from transitioning cells that will mature into naïve follicular B cells. Figure 4.12 shows the distribution of CD45RB+ B cells within the different B cell subsets when defined according to IgM and CD27 expression. The majority of CD27+ B cells express CD45RB. Approximately 50% of CD27-IgMhi B cells express CD45RB (MZ B precursor cells). Very few IgM+ Naïve B cells express CD45RB.

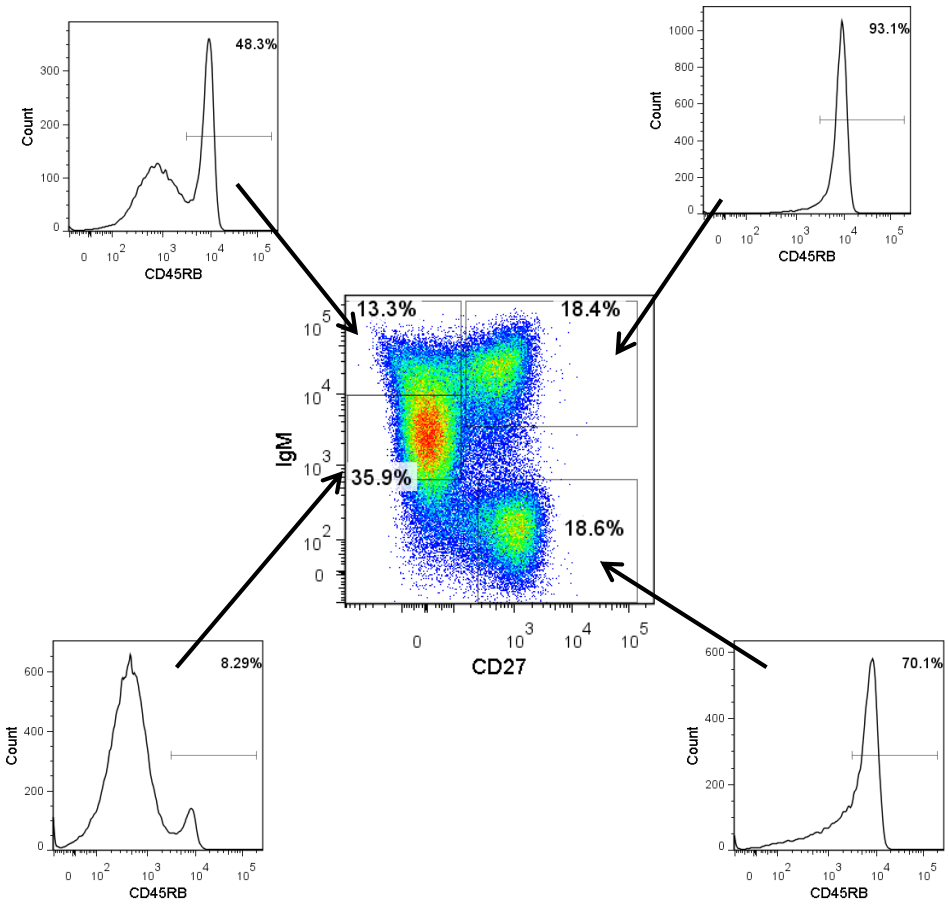

Figure 4.12 CD45RB MEM 55 expression on CD27+ and CD27- B cell populations. Representative staining on a leukocyte cone is shown. CD27+ and CD27- populations have been divided according to high (IgMhi), low (IgM+) or negative (IgM-) expression of IgM.

Figure 4.13 shows an example of a dot plot from a leukocyte cone that was incubated with CMV gB prior to staining with an antibody phenotyping panel. In this individual, the CMV gB binding B cells are overrepresented in both the CD45RB+IgMhi and CD45RB-IgMhi populations compared to the overall B cell population. When this analysis was carried out on 8 cone samples (Fig. 4.14), it showed that the CD45RB-IgMhi population was consistently overrepresented in the CMV gB binding population compared to the overall B cell population (Fig 4.14 (b), P=0.0078) and the CD45RB+IgMhi population was overrepresented in the CMV gB binding population in 5/8 cone samples (Fig 4.14 (a), P>0.05). The data suggests that the MZ/IgM+ memory precursor subset is not overrepresented in the CMV gB binding population as there was no difference found in the frequency of the CD27-CD45RB+ subset between the CMV gB binding population and the overall B cell population (Fig 4.14 (c), P>0.05) This data therefore demonstrates a trend that in the majority of individuals, the CMV gB binding B cell population is a mixed population of IgM+ memory B cells and IgMhi naïve follicular pre-cursor B cells. However, in some individuals, the phenotype of the CMV gB binding B cells is skewed towards an IgMhi naïve follicular pre-cursor phenotype. In addition, this analysis confirms that CMV gB binding B cells are not represented in the class switched memory population (IgM-CD45RB+) as they are underrepresented in this population in all individuals (P=0.0078).

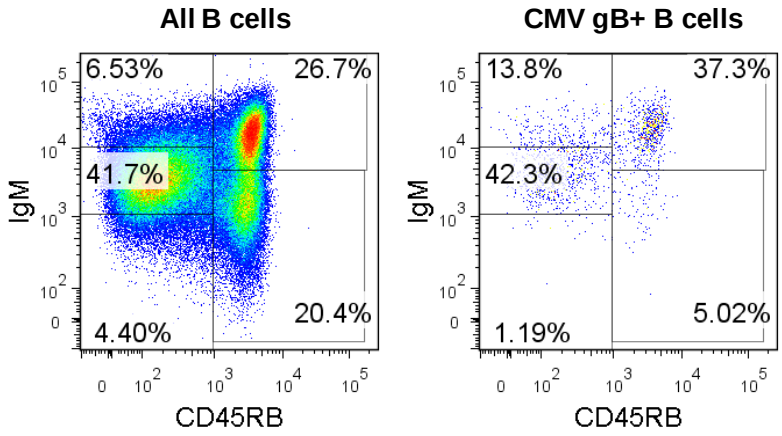

Figure 4.13 Dot plots to illustrate the gating strategy for IgM memory and naïve B cell populations based on CD45RB expression.
All gates were drawn on the non-transitional population of whole all the CD19+ cells (All B cells) and then applied to the CD19+ non transitional CMV gB+ population (CMV gB+ B cells).

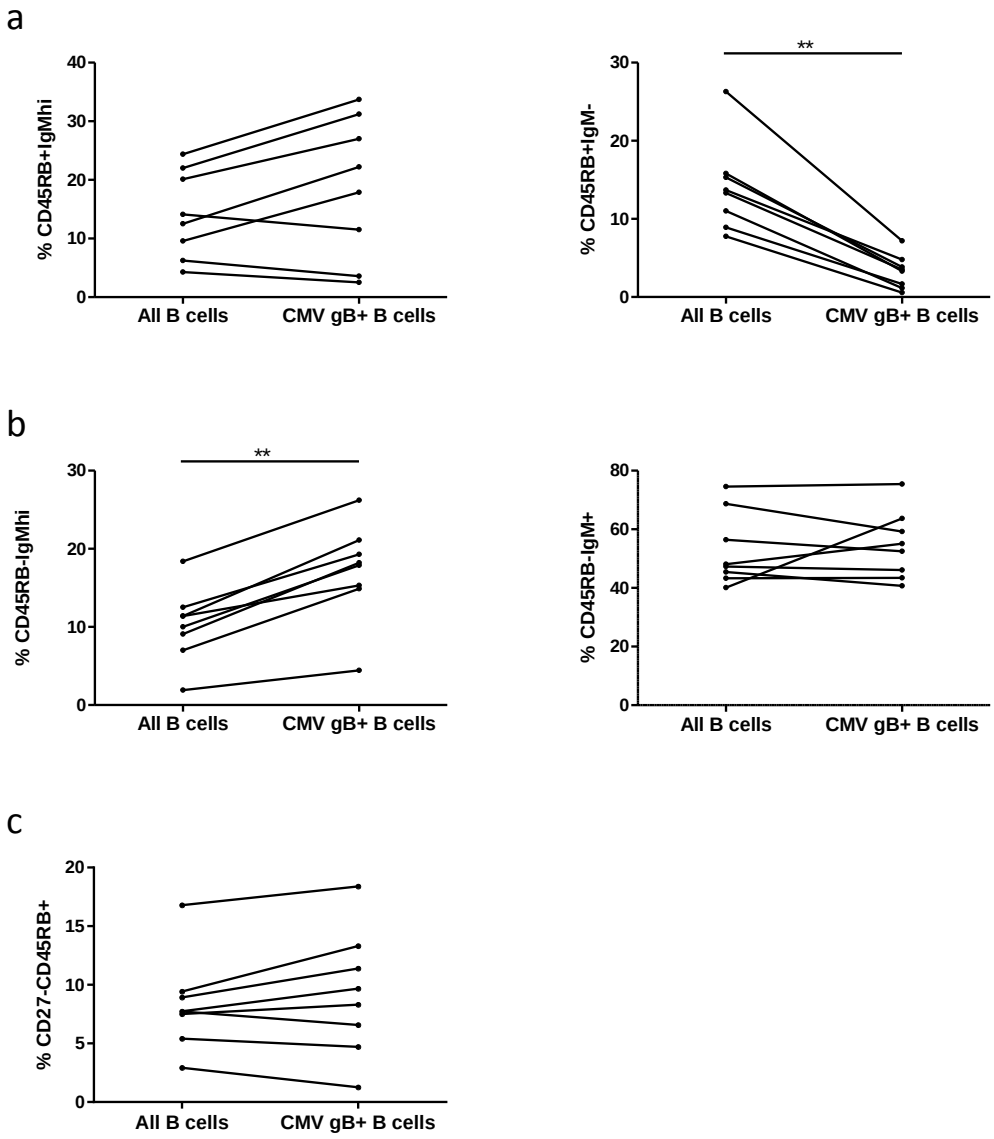

Figure 4.14 Frequency of IgM+ memory and naïve populations in the CMV gB binding B cell population compared to the overall B cell population according to CD45RB expression.

(a) CD45RB+IgMhi are overrepresented in the CMV gB+ B cell population in 5/8 leukocyte cones tested (P>0.05), whilst class switched CD45RB+IgM- are underrepresented in 8/8 (P= 0.0078). **(b)** CD45RB-IgMhi B cells are overrepresented in the CMV gB+ population in 8/8 (P=0.0078), whereas a slight trend towards underrepresentation of the CD45RB-IgM+ B cells in the CMV gB+ population can be observed (P>0.05). **(c)** CMV gB+ B cells are not overrepresented in the T3/MZ precursor population CD27-CD45RB+ (P>0.05). P values were obtained using a Wilcoxon matched pairs signed rank test.

4.2.1.5 Do CMV gB binding B cells make antibodies that bind to CMV gB?

When taken together the data presented in Figures 4.2-4.14 strongly suggests that B cells specific for CMV gB are binding the CMV gB protein via the B cell receptor. This binding can be blocked by using an anti-fab IgM/IgG antibody and the CMV gB binding B cells have a phenotype that is distinct from the overall phenotype of the B cell population. However, as the IgMhi phenotype of the antigen binding B cells was unexpected, it was decided that more experiments would be done to ascertain whether the antigen binding B cells are specific for just CMV gB or whether they would bind other proteins. This seemed particularly important since IgM is known for its broad specificity. A 'cold inhibition' assay was used where increasing concentrations of non-biotinylated CMV gB was incubated with PBMCs at the same time as 0.35µg/ml of biotinylated CMV gB for 30 minutes before staining the cells as in Figures 4.2-4.14. To test whether the binding to the biotinylated CMV gB could be inhibited by a different protein, and therefore ascertain whether the BCR binding to CMV gB was antigen specific, increasing concentrations of VZV gE were also incubated with PBMCs at the same time as 0.35µg/ml of biotinylated CMV gB. VZV gE was chosen for this purpose because it is derived from a virus that elicits an antibody response and that most people will have encountered. Therefore, most people should have a memory B cell response towards it (Manikkavasagan et al., 2010).

Figure 4.15 shows the results of this assay carried out on three different cones. The results indicate a complex picture: a high concentration of CMV gB was required to inhibit the binding of the biotinylated CMV gB to the B cells. The inhibition that was achieved was variable at different concentrations but the overall decrease in binding from an inhibiting concentration of 0 µg/ml to 14µg/ml was 37% in (a), 40% in (b) and 50% in (c). Incubating with VZV gE did cause a decrease in B cell binding, but the overall picture when the binding at 0µg/ml and 14µg/ml is compared, a 4% decrease in binding was observed in (a), a 64% increase in binding was observed in (b) and a 33% decrease in binding was observed in (c). Of note, the molecular weights of CMV gB and VZV gE are very similar so the level of inhibition is comparable between the two proteins at each concentration of 'cold' protein used.

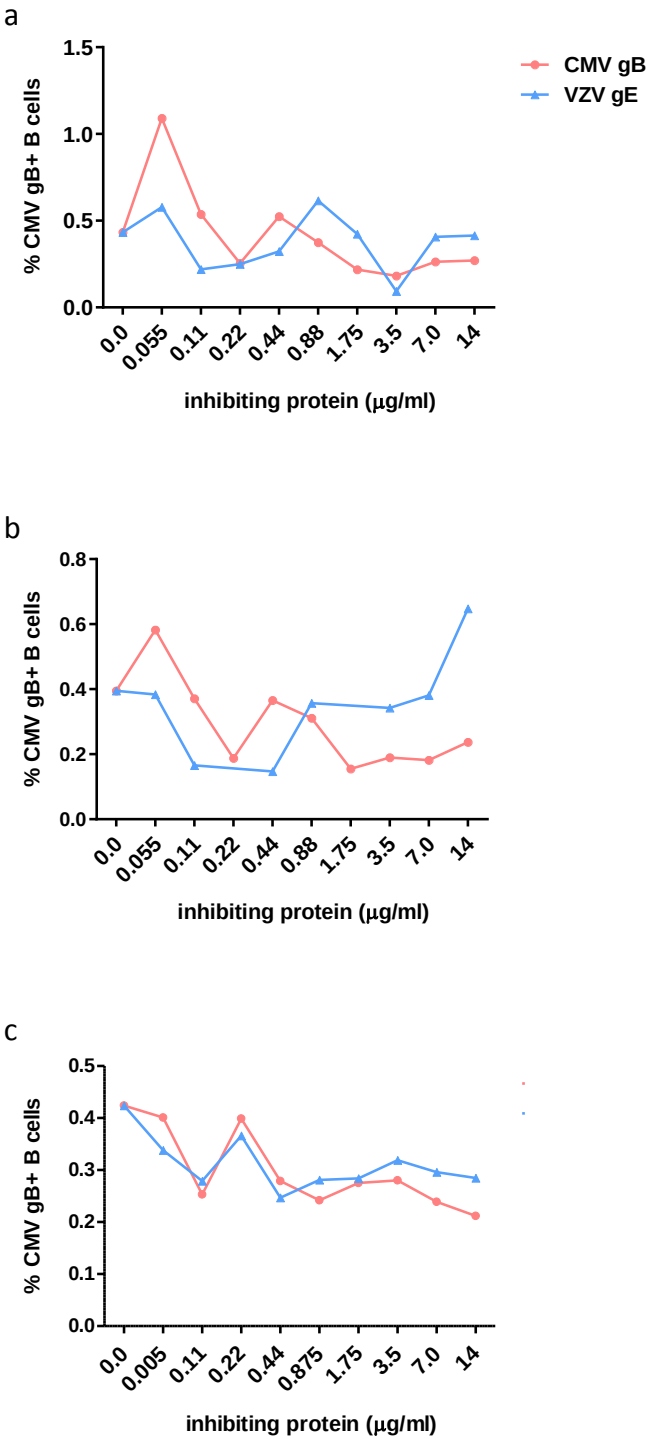

Figure 4.15 Binding of biotinylated CMV gB to B cells can be partially inhibited by non-biotinylated CMV gB

PBMC from three leukocyte cones **(a)**, **(b)** and **(c)**, were co-incubated with 0.35µg/ml biotinylated CMV gB and increasing concentrations of non-biotinylated CMV gB or non-biotinylated VZV gE as a control. PBMC were incubated for 30 minutes on ice and then stained with CD19 APC-efluor 780 and streptavidin PE.

Figure 4.15 suggests that the binding is only partially specific and it is likely that non-specific binding of the B cell receptor to the CMV gB protein is blurring the picture. It therefore seemed appropriate to investigate whether the CMV gB binding B cells were able to produce CMV gB specific antibodies that could bind CMV gB in an ELISA, as this would provide further evidence to support the hypothesis that the CMV gB binding B cells that were being detected by flow cytometry were indeed CMV gB specific. An opportunity arose to collaborate with Professor Jo Spencer which enabled deep sequencing of the BCR from single CMV gB binding B cells that had been sorted by flow cytometry. PBMC from 3 leukocyte cones were incubated with CMV gB and stained as per the protocol detailed in section 2.5.3. PBMC were then passed through a FACS machine where single CMV gB binding, IgMhi B cells were collected in each well of a 96 well plate. Once sequenced, the BCR was cloned and expressed first in *E.coli* and then finally in a mammalian cell system where supernatants containing antibodies could be measured for their ability to bind the CMV gB in an ELISA. The staining and sorting of the CMV gB+ B cells was performed by me and downstream analysis was performed by Dr Verena Hehle from the Spencer laboratory. The gating strategy and examples of the cells pre and post sort are shown in Figure 2.4.

Unfortunately, this series of experiments did not yield any positive results with regards to finding a clone that secreted antibodies that bound to an ELISA plate coated with CMV gB.

4.2.2 Applying the CMV gB binding assay to a renal transplant patient setting

Once the method to detect and phenotype antigen binding B cells was optimised, it was used to look for HLA binding B cells in a subset of patients enrolled on the RituxiCAN C4 trial.

Biotinylated and non-biotinylated versions of a Pure™ recombinant HLA A1:01 monomer protein (from here on in referred to as HLA A1) were sourced from Pure™ Proteins LLC. A patient that was enrolled on to the RituxiCAN C4 trial and who had an HLA A1 mismatched kidney transplant with sufficient PBMC samples available was identified (G002). It was important that the Pure™ HLA protein could be used in the ELISpot assay to induce IFNγ production as well as in the flow cytometric assay to detect HLA binding B cells. Therefore, the non-biotinylated HLA A1 was titrated to determine the optimal concentration required for the ELISpot and the biotinylated pure HLA A1 was titrated to determine the optimal concentration for detecting HLA binding B cells.

4.2.2.1 Pure HLA proteins can be used to elicit a B cell dependent IFNγ response

CD8+ or CD8+ & CD19+ depleted PBMC from a patient with an A1 mismatched kidney transplant were stimulated with increasing concentrations of HLA A1 from 0.0-0.5µg/ml, as per the ELISpot assay method described in section 2.3.5 of the materials and methods chapter. A reactive response was defined as ≥25 IFNγ spots per million CD4+ Lymphocytes and was observed in this patient. Figure 4.16 shows the number of IFNγ+ spots per million CD4+ lymphocytes before and after the background spots were subtracted (Fig. 4.16 (a) and (b) respectively). A titration effect could be seen where the spot count decreased as the concentration of HLA A1 increased. Figure 4.16 also shows that IFNγ production was dependent on B cells. An example of an ELISpot well for both depletion conditions is shown in Figure 4.17.

A leukocyte cone (Cone 23) was used as a control to investigate whether the HLA A1 protein would stimulate IFNγ production in a non-transplant recipient. The sex and pregnancy history of this individual is unknown. However, as they are a registered blood donor, they will not have experienced a prior sensitisation event due to blood transfusion or transplantation. The ELISpot was set up at the same time as the patient and stimulated in exactly the same way. Figure 4.18 shows the number of IFNγ+ spots per million CD4+ lymphocytes before and after the background spots were subtracted (Fig 4.18 (a) and (b) respectively). This leukocyte cone did not produce IFNγ in response to the HLA A1 protein, regardless of whether B cells were present. In order

to show that this was an antigen specific response to the HLA A1, both patient (G002) and leukocyte cone (Cone 23) were stimulated in separate wells from the HLA A1 with CMV gB in the same assay. Figure 4.19 shows that a reactive response that was dependent on the presence of B cells was observed in Cone 23 but G002 did not react to the viral protein. Based on the results from these experiments and availability of reagents, it was decided that 0.05µg/ml, 0.1µg/ml and 0.2µg/ml would be used in each experiment if there was enough PBMCs, as it was hypothesised that there would be variability in the response to different concentrations of the Pure™ HLA proteins between the patients.

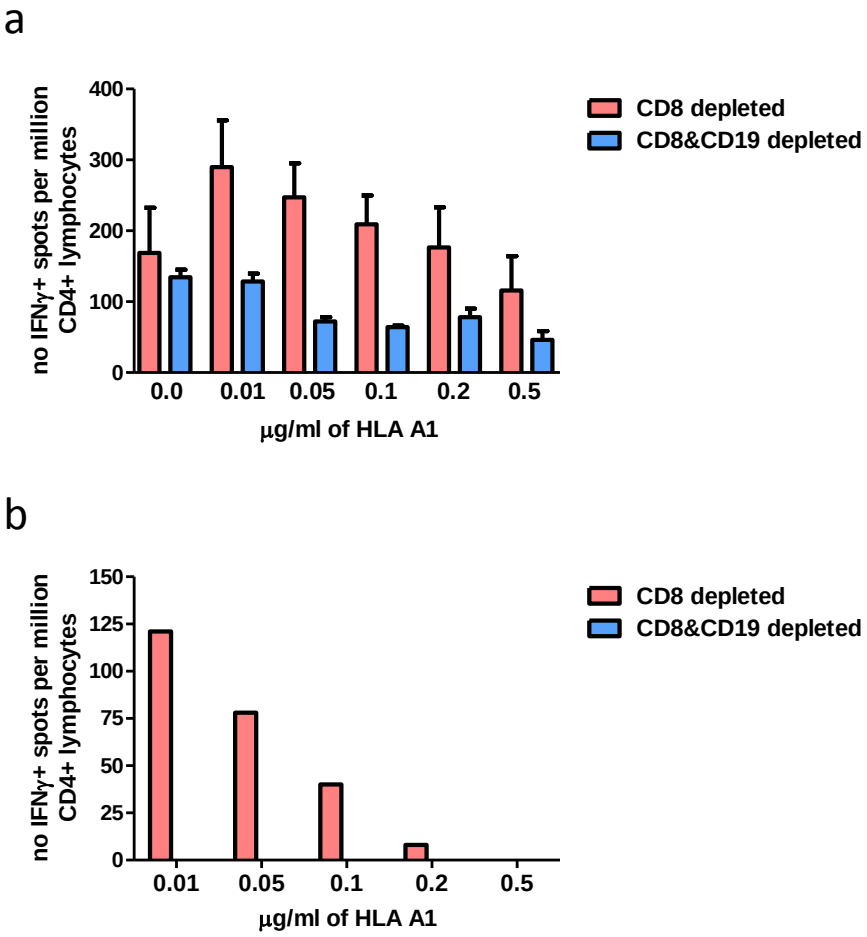

Figure 4.16 Titrating the Pure™ HLA A1 to determine the optimal concentration to induce antigen specific IFNγ in the indirect ELISpot assay

PBMC from a patient enrolled on the RituxiCAN trial who had an A1 mismatched transplant was used. The background IFNγ spot count shown in **(a)** as 0.0µg/ml HLA A1 was subtracted from each stimulation concentration. Spot counts per million CD4+ lymphocytes minus the background are shown in **(b).** A reactive response was defined as ≥25 IFNγ+ spots per million CD4+ lymphocytes. The mean of triplicate wells with SEM is displayed in **(a).**

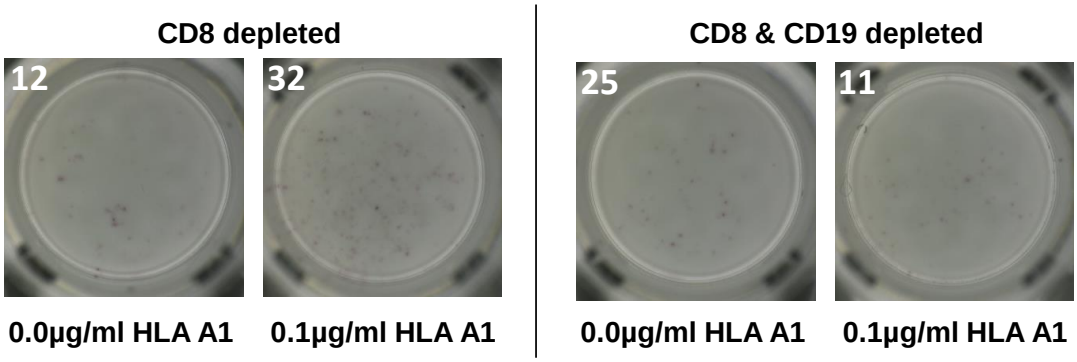

Figure 4.17 Example of ELISpot wells
Un-stimulated (0.0µg/ml HLA A1) control and 0.1µg/ml HLA A1:01 conditions with CD8 depleted PBMC and CD8 & CD19 depleted PBMC from a patient with an A1 mismatched transplant are shown. Raw spot count is in white.

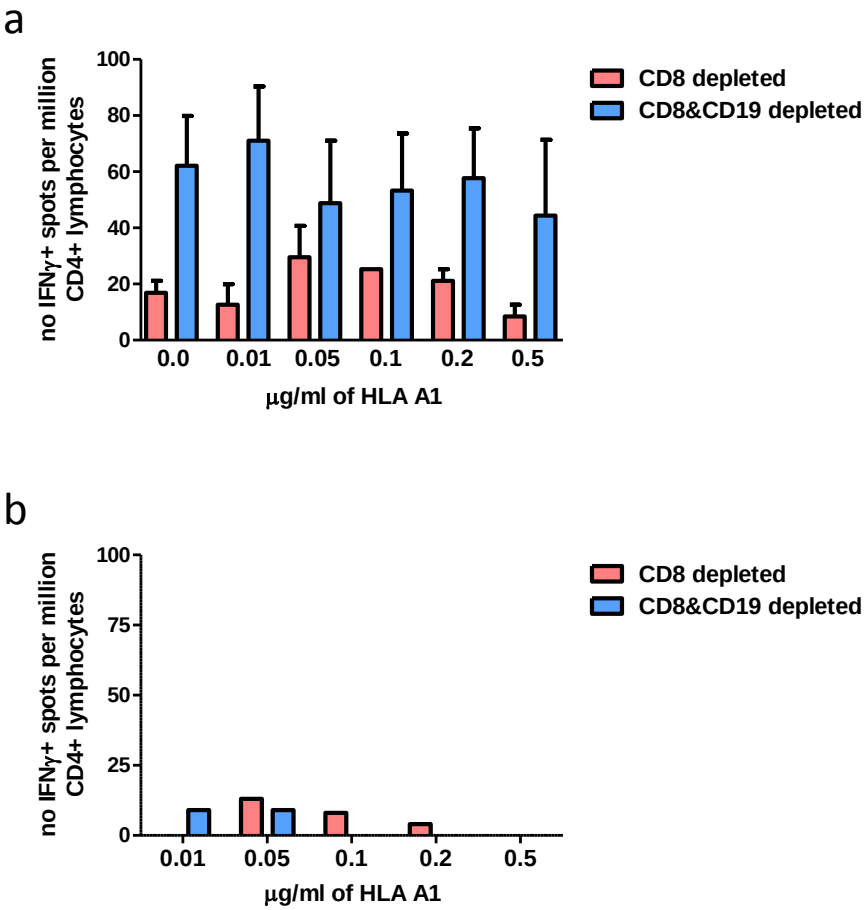

Figure 4.18 Titrating Pure HLA A1 into the indirect ELISpot assay to assess reactivity status of a non-transplant individual

PBMC from a Leukocyte cone were used. The background IFNγ spot count shown in **(a)** as 0.0µg/ml HLA A1 was subtracted from each stimulation concentration. **(b)** Spot counts per million CD4+ lymphocytes minus the background are shown in **(b)**. A reactive response was defined as ≥25 IFNγ+ spots per million CD4+ lymphocytes. The mean of triplicate wells with SEM is displayed in **(a).**

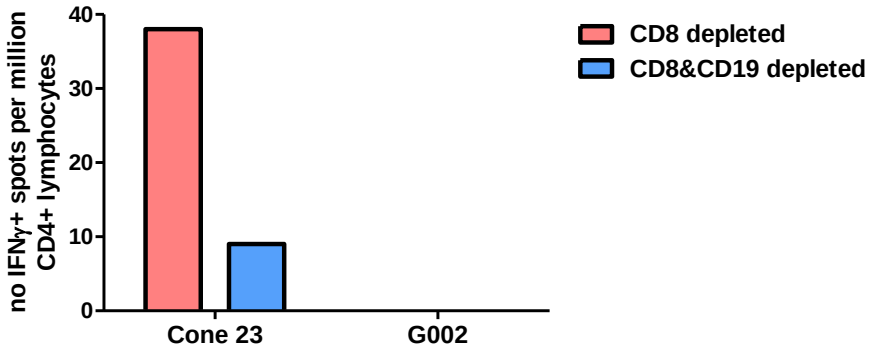

Figure 4.19 Reactivity to viral antigen cocktail in patient G002 compared to Cone 23
CD8+ or CD8+ & CD19+ depleted PBMC from Leukocyte Cone 23 and G002 were stimulated with CMV gB as a control for antigen processing and presentation for the HLA A1 ELISpot. Results shown are post subtraction of background IFNγ+ spots. A reactive response was defined as ≥25 IFNγ+ spots per million CD4+ lymphocytes.

4.2.3 HLA binding B cells can be detected in renal transplant recipients and leukocyte cones

Next, the optimal concentration of HLA A1 required to detect HLA binding B cells was investigated. The biotinylated HLA A1 protein was titrated from 0.0µg/ml to 2.0µg/ml and used in the antigen binding B cell detection assay developed in section 4.2.1. HLA A1 binding B cells above background were detected in the same patient and time point used in Figure 4.16, G002. Figure 4.20 shows the flow cytometric dot plots from each concentration of biotinylated HLA A1 used. As with the CMV gB binding B cell experiments in section 4.2.1, the non-B lymphocyte gate was used as a guide to determine the concentration at which the non-specific binding started to increase. Figure 4.21 shows the frequency of HLA A1 binding B cells detected with each concentration of biotinylated HLA A1 used compared with the frequency of HLA binding non-B lymphocytes. The frequency of HLA A1 binding B cells detected when PBMC were incubated with all concentrations of biotinylated HLA A1 used was above the background events detected when 0.0µg/ml HLA A1 was used. However little difference was observed in the frequency detected between 0.125µg/ml and 0.5µg/ml. Background events in the non-B lymphocyte population were only detected once the concentration of biotinylated HLA A1 reached 1.0µg/ml. It was therefore decided that the biotinylated HLA proteins would be titrated in subsequent experiments in 0.1µg/ml increments from 0.1µg/ml to 0.4µg/ml. The concentration that yielded the highest frequency of HLA binding B cells was chosen for further analysis. If PBMC were limited, only 0.2µg/ml and 0.3µg/ml were used.

As with the HLA A1 ELISpot, the same experiment was carried out using PBMC from a leukocyte cone to investigate whether HLA A1 B cells could be detected in an individual who had not received an A1 mismatched kidney transplant. Flow cytometric dot plots from this experiment are shown in Figure 4.22 and the frequency of HLA A1 binding B cells and HLA A1 binding non-B lymphocytes is displayed in Figure 4.23. The data shows that HLA A1 binding B cells were only detected above ≥0.5µg/ml HLA A1 and a corresponding increase in non-specific binding to the non-B lymphocytes was also observed. Although the concentration of HLA A1 required to detect HLA binding B cells was higher in the leukocyte cone than in the patient, the results suggest that HLA specific B cells can be detected in non-transplant recipients. Due to this finding it was decided that the IFNγ ELISpot and the HLA binding B cell assay would be carried out on several leukocyte cones at the same time as testing further patient samples.

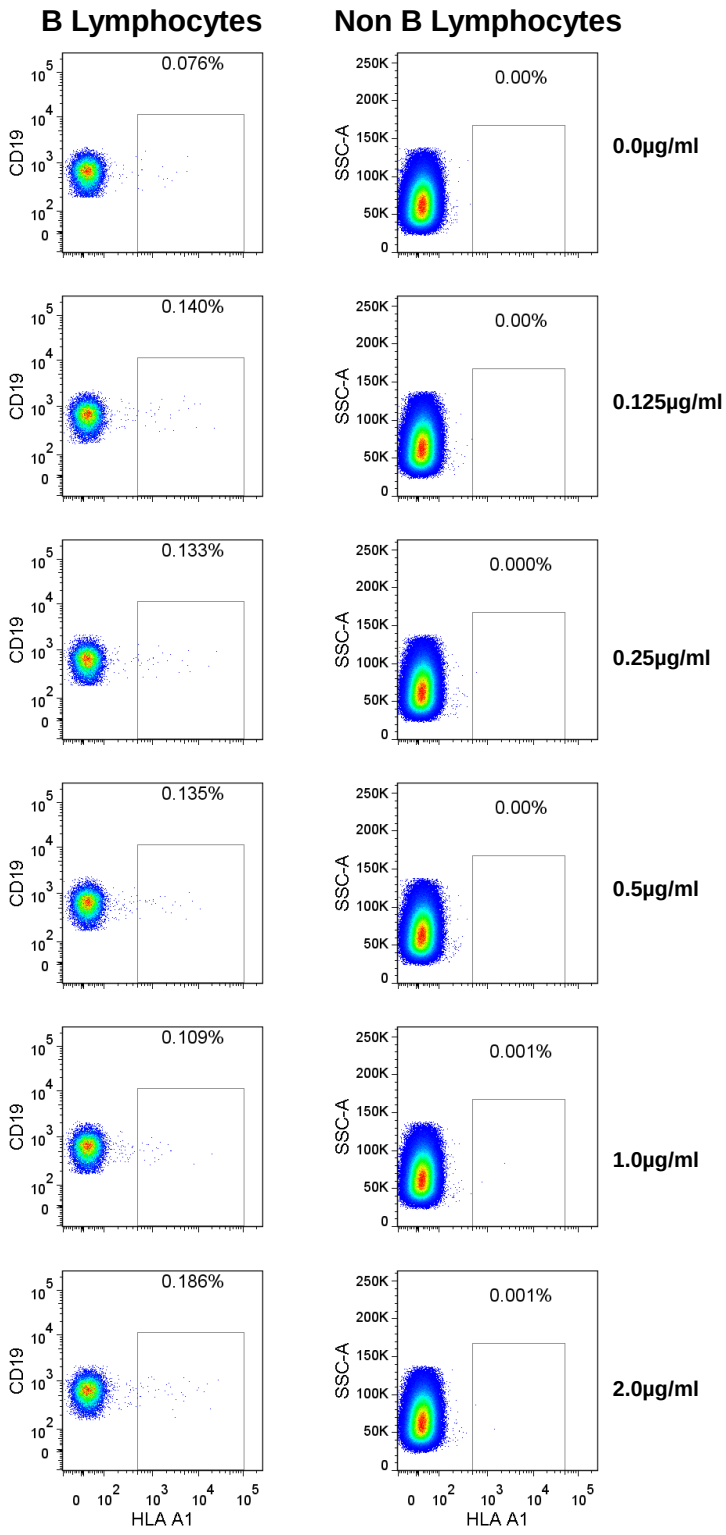

Figure 4.20 Dot plots to illustrate HLA A1 binding B cells in an HLA A1 mismatched kidney transplant patient.

PBMC from a patient with an HLA A1 mismatched transplant were incubated with increasing concentrations of biotinylated HLA A1 from 0.0µg/ml – 2.0µg/ml at 4°C and stained with CD19 APC-efluor 780 and streptavidin PE.

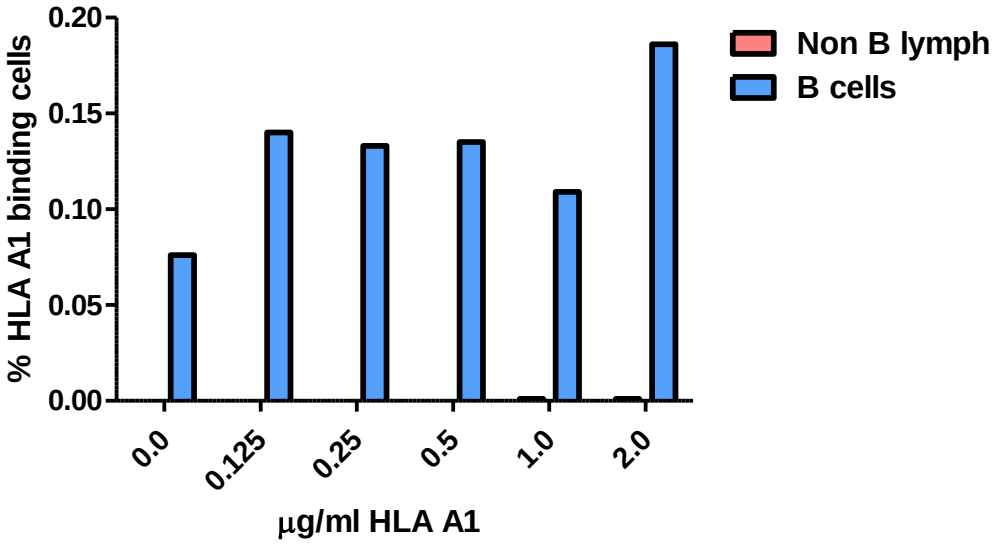

Figure 4.21 Detecting HLA A1 binding B cells in a renal transplant recipient
PBMC from a patient with an HLA A1 mismatched transplant were incubated on ice with increasing concentrations of biotinylated HLA A1 from 0.0µg/ml – 2.0µg/ml and stained with CD19 APC-efluor 780 and streptavidin PE in order to determine what concentration is optimal for detecting HLA A1 binding B cells. HLA A1 binding B cells are detected above background at ≥0.125µg/ml. Graph highlights that non-specific binding begins to occur in the non-B lymphocyte population when a concentration of ≥1.0µg/ml is used

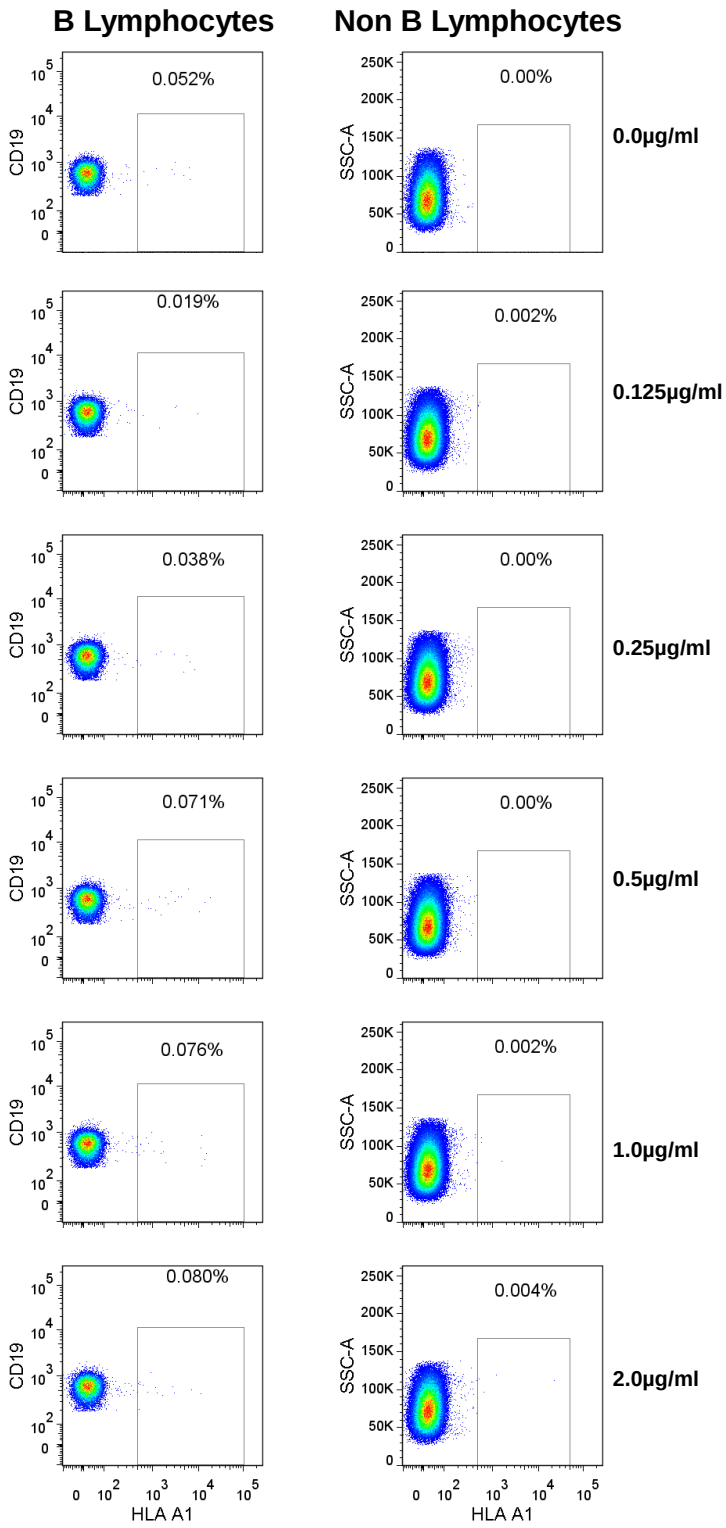

Figure 4.22 Dot plots to illustrate HLA A1 binding B cells in a leukocyte cone
PBMC from a leukocyte cone were incubated with increasing concentrations of biotinylated HLA A1 from 0.0µg/ml – 2.0µg/ml at 4°C and stained with CD19 APC-efluor 780 and streptavidin PE.

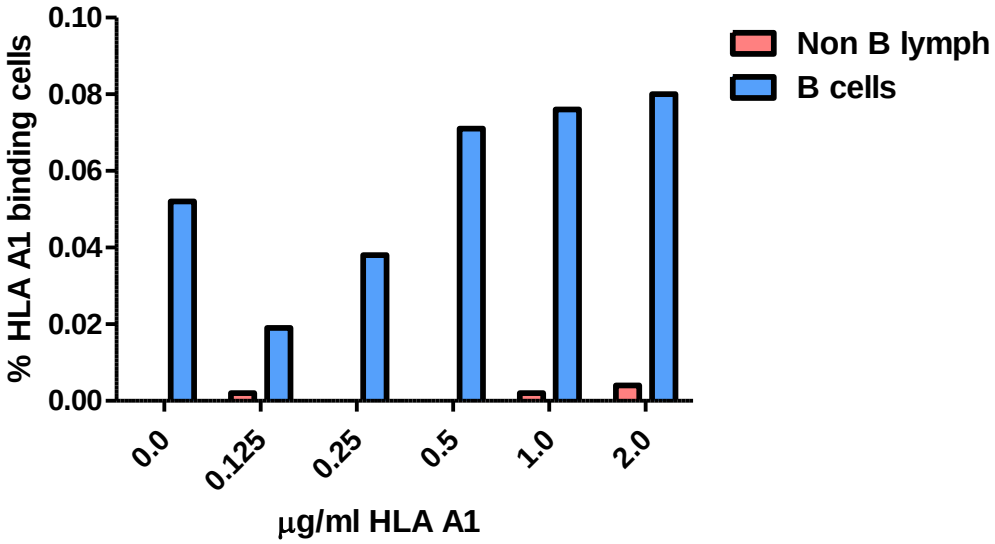

Figure 4.23 Detecting HLA binding B cells in a leukocyte cone
PBMC from a leukocyte cone were incubated on ice with increasing concentrations of biotinylated HLA A1 from 0.0µg/ml – 2.0µg/ml and stained with CD19 APC-efluor-780 and streptavidin PE. HLA A1 binding B cells are detected above background at ≥0.5µg/ml**.** Non-specific binding occurs in the non-B lymphocyte population at 0.125µg/ml, 1.0 µg/ml and 2.0 µg/ml is used.

4.2.3.1 Background events can be reduced by using a rigorous gating strategy and streptavidin BV421

Whilst conducting these experiments it became apparent that the level of background events detected could interfere with any phenotyping analysis as only a small frequency of HLA A1 binding B cells was detected above background. This problem was not an issue when detecting CMV gB binding B cells in section 4.2.1 as a much higher frequency of B cells bound the CMV gB protein. Fluorescent minus one (FMO) controls for each of the fluorochromes used in the B cell phenotyping panel in section 4.2.1 were set up to discover what fluorochrome had the least amount of spectral overlap from the other fluorochromes in the panel. Figure 4.24 shows the frequency of events detected in the channel for each individual fluorochrome, when that fluorochrome was removed from the staining mixture. The graph indicates that after compensation has been applied, the PE channel has the most amount of spectral overlap from the other channels and that the Pacific Blue channel has the least amount of spectral overlap. The stain panel was therefore altered to a) change the fluorochrome conjugated to streptavidin from PE to BV421 (a very bright fluorochrome that is detected in the pacific blue channel) and b) to incorporate CD45RB PE into the same panel and remove IgG V450.

In addition, the gating strategy used in section 4.2.1 was changed and a two-step gating strategy shown in Figure 4.25 was adopted in order to eliminate as many dead B cells as possible. This reduced the number of background events that were detected when 0.0µg/ml HLA A1 was incubated with the PBMC. As the presence of background events could not be completely eliminated, a cut off was used for deciding whether the phenotype of the HLA binding B cells could be assessed: both the number and frequency of events in the HLA binding B cell gate had to be at least double that detected in the background no antigen control gate.

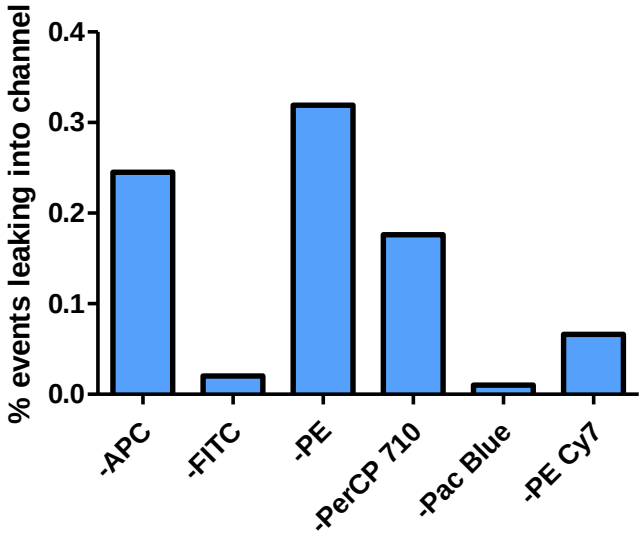

Figure 4.24 Using FMO controls to determine spectral overlap post compensation for each fluorochrome used in phenotyping the B cells

CD19+ cells were gated on and subsequent gates were drawn for each fluorochrome where the negative population ended. APC-efluor780 was used as the fluorochrome for CD19 detection so an FMO control was not used for this fluorochrome. X-axis labels represent the fluorochrome that was omitted from the antibody stain panel. Y-axis details the number of events that were detected in that channel when the fluorochrome was omitted.

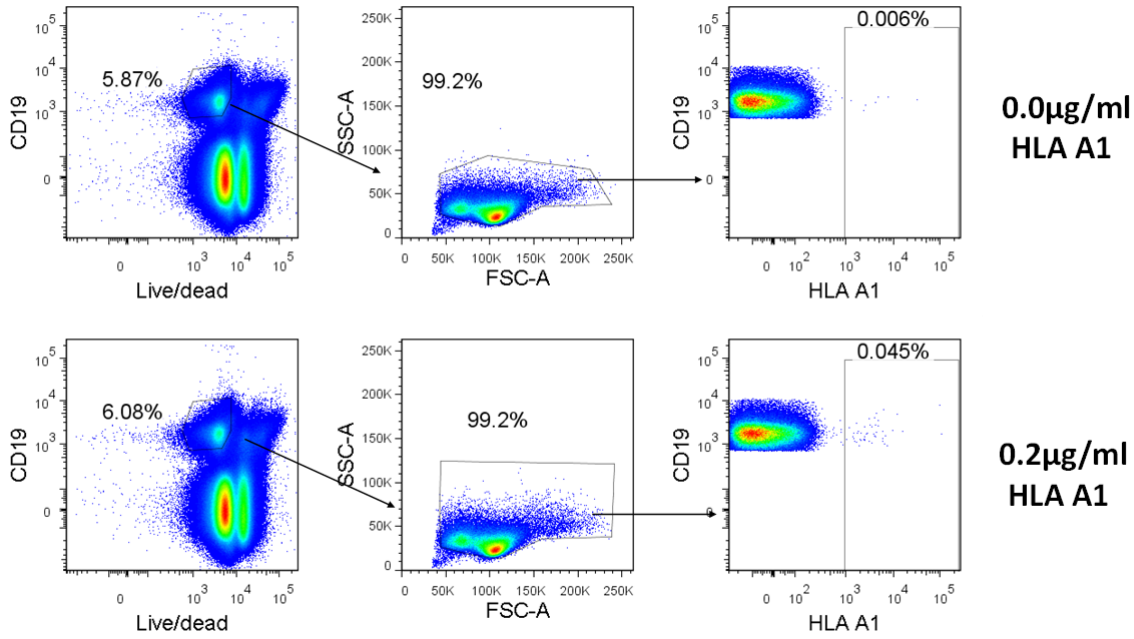

Figure 4.25 Example of gating strategy for detecting HLA binding B cells
Live B cells were first gated on using CD19 and a live-dead dye. The FSC-SSC profile was then used to remove any dead cells or debris that had not been stained with the live/dead dye before gating on the HLA A1+ positive population.

4.2.3.2 HLA A1 binding B cells are predominantly IgM+ memory

Once the assay had been optimised for detection of HLA A1 binding B cells in the RituxiCAN patients, patients enrolled on the trial who had an A1 mismatched transplant were identified and flow cytometry staining was carried out to detect and phenotype HLA A1 binding B cells in these patients. 11 PBMC samples from 4 patients with HLA A1 mismatched transplants were tested for the presence of HLA A1 binding B cells. HLA A1 binding B cells were detected in 4/11 samples, with a median frequency of 0.038% (range 0.02%-0.23%).

3/4 samples that had detectable HLA A1 binding B cells could go on to have their phenotype analysed because on average, the frequency of HLA A1 binding B cells was 3.3x that detected in the no antigen control (median 3.3x above background, range 2.85x-5.6x). All of these samples came from the same patient (G013).

An example of the gating strategy used is shown in Figure 4.26. This is the same patient sample that is shown in Figure 4.25 as the frequency of HLA A1 binding B cells is 5.6x that detected in the no antigen control. The dot plots in Figure 4.26 clearly show that the majority of HLA A1 binding B cells are non-transitional and are IgM+. In 3/3 samples the dominant HLA A1 binding B cell population was IgM+ memory B cells defined as either CD27+IgMhi (median 50.0%, range 45.7%-60%) or CD45RB+IgMhi (median 74.3%, range 65.7%-78.6%). In all samples, this population was overrepresented in these two IgM+ memory B cell gates in the HLA A1 binding B cell gate compared to the overall B cell population. The median frequency of CD27+IgMhi and CD45RB+IgMhi+ B cells was 6.2% (range 5.07%-6.62%) and 11.6% (range 9.94%-11.6%) respectively, although $p>0.05$ when a Wilcoxons signed rank test was performed.

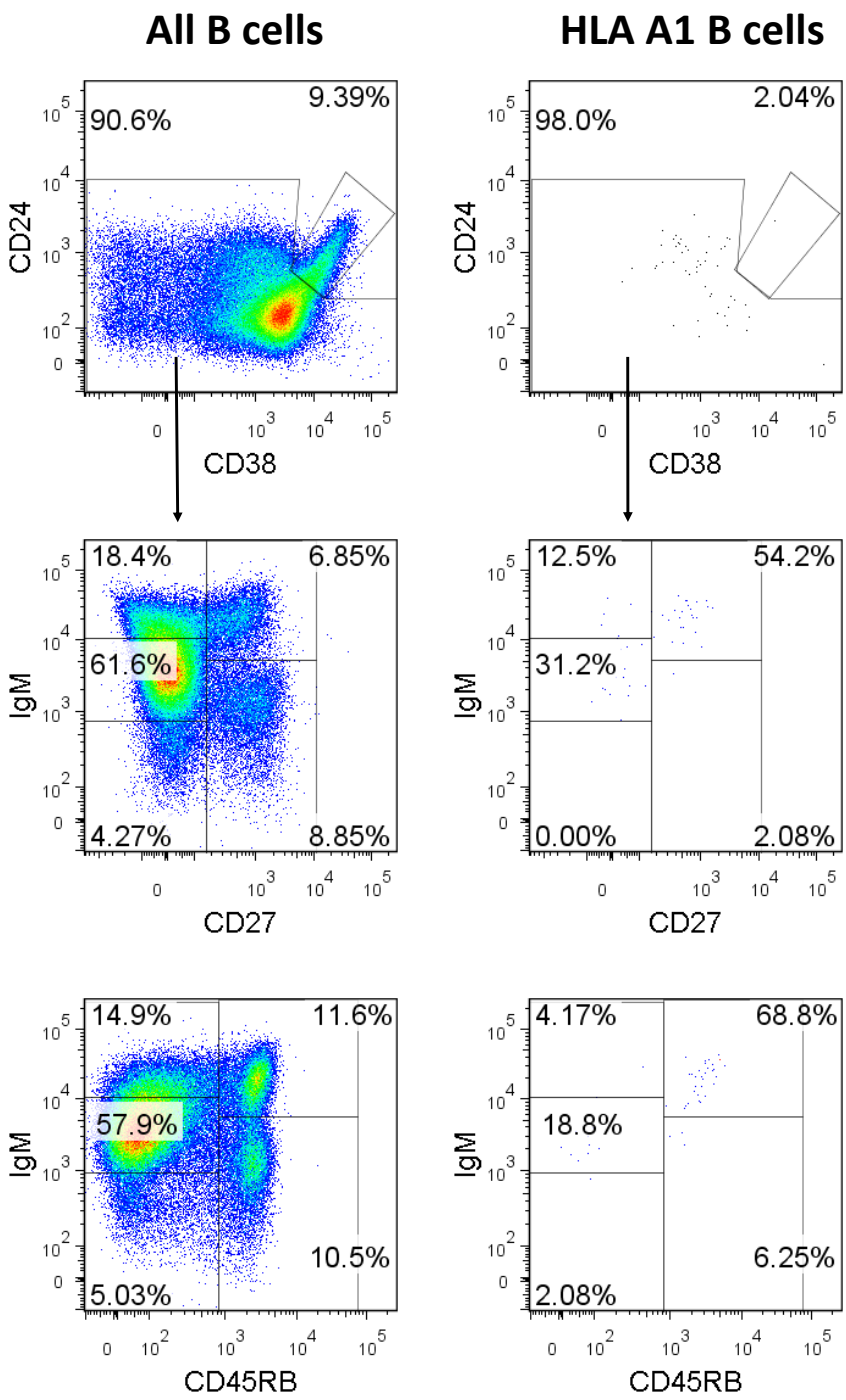

Figure 4.26 Example dot plots of the phenotype of HLA A1 binding B cells
Gates were drawn on the whole B cell population and then applied to the HLA A1 binding population. CD19+ cells were first divided into transitional and non-transitional B cells according to CD24 and CD38 expression. All subsequent gates were only applied to the non-transitional population as indicated by the black arrows. Non-transitional B cells were then divided into subsets based on CD27 and IgM expression, or CD45RB and IgM expression.

4.2.3.3 HLA A2 and HLA DR4 binding B cells are predominantly IgM+ and either predominantly IgM+ memory, or IgM+ naive

Due to the promising findings using an A1 protein, Pure™ proteins HLA A*02:01 and HLA DR*04:02 (from here on in referred to as HLA A2 and HLA DR4 respectively), were obtained as a gift from Prof. Robert Higgins and Dr. Sunil Daga (Warwick University, UK). Patients enrolled onto the RituxiCAN C4 trial that had either HLA A2 or HLA DR4 mismatched transplants were identified. HLA A2 and HLA DR4 binding B cells were detected and phenotyped using the protocol that had been optimised for detecting the HLA A1 binding B cells. As with the HLA A1, the Pure HLA A2 and DR4 proteins were titrated from 0.1µg/ml-0.4µg/ml in each experiment in order to increase the chance of detecting HLA binding B cells. If PBMC were limited, only 0.2µg/ml and 0.3µg/ml were used. Figure 4.27 (a) shows an example of HLA A2 binding B cells that were detected using 0.3µg/ml biotinylated HLA A2 in a patient with an HLA A2 mismatched transplant. Figure 4.27 (b) shows an example of HLA DR4 binding B cells that were detected using 0.4µg/ml biotinylated HLA DR4.

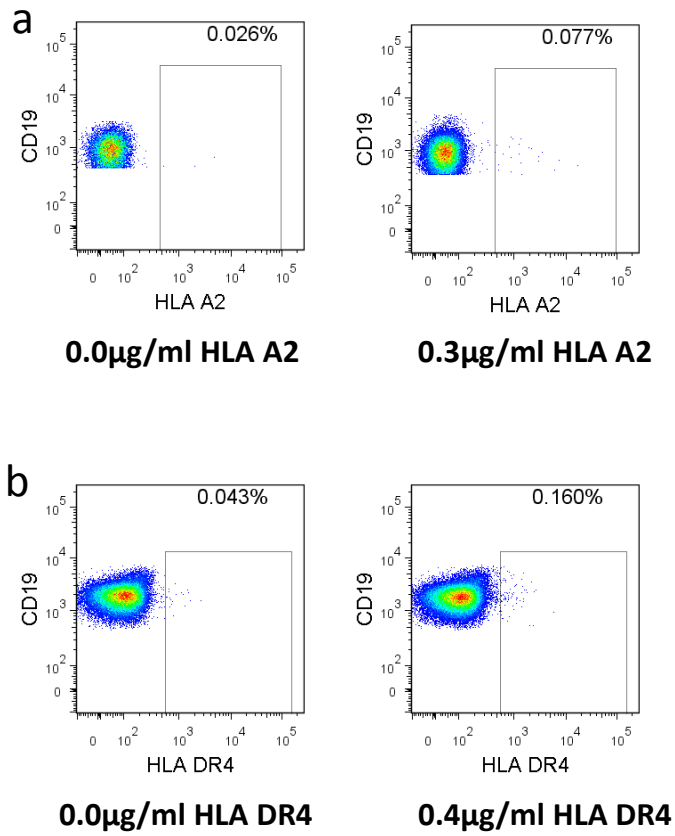

Figure 4.27 Example dot plots of A2 and DR4 binding B cells
Background events detected when PBMC were incubated with 0.0µg/ml HLA protein are shown alongside events detected when PBMC were incubated with either 0.3µg/ml HLA A2 protein **(a)**, or 0.4µg/ml HLA DR4 **(b)**.

HLA A2 binding B cells were detected in 13/26 samples from 8 patients, with a median frequency of 0.059% (range 0.011%-0.084%). 8/13 samples, from 4 patients, had a frequency of HLA A2 binding B cells that were more than double that found in the no antigen control gate. 3 samples had no events in the no antigen control and for the 5 samples that did, the frequency of HLA A2 binding B cells was on average 4.9x the background events (median 4.9x, range 2.69x-9.1x) and could be analysed for their phenotype. Figure 4.28 shows an example of the phenotype of the HLA A2 binding B cells. As with the HLA A1 binding B cells, the majority of the HLA A2 binding B cells were non transitional and IgM+. In 6/8 of the samples, the dominant phenotype of HLA A2 binding B cells was CD27+IgMhi (median 60.6%, range 45.5% – 71.4%) or CD45RB+IgMhi (median 65.1%, range 45.5%-76.2%). In 1/8 samples the largest population within the HLA A2 binding B cells was CD27-IgM+ and CD45RB-IgM+ (both 66.7%), and in the remaining sample, the HLA binding B cells were distributed throughout all of the B cell subsets and not of a distinct phenotype.

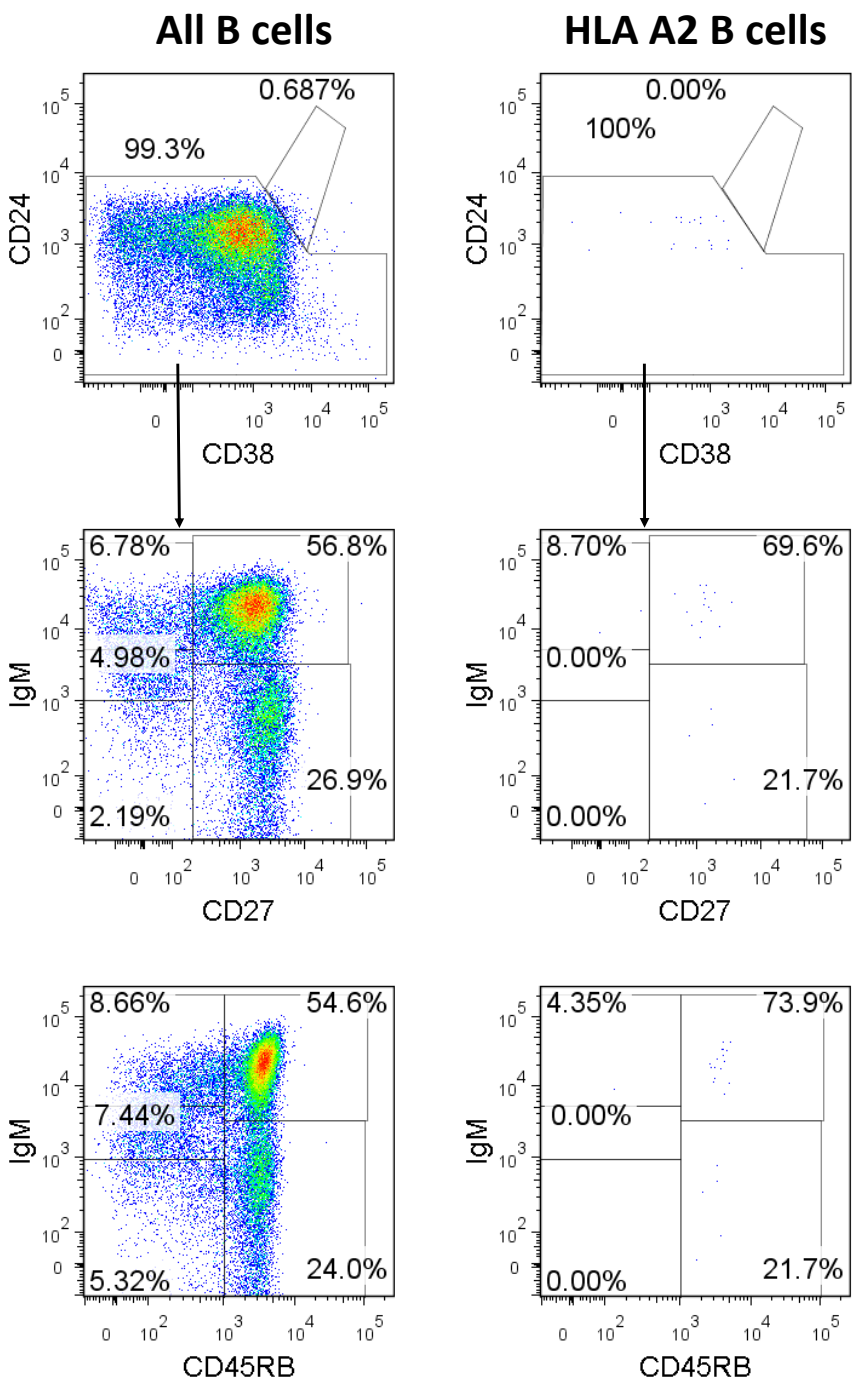

Figure 4.28 Example dot plots to show phenotype of HLA A2 binding B cells
Gates were drawn on the whole B cell population and then applied to the HLA A2 binding population. CD19+ cells were first divided into transitional and non-transitional B cells according to CD24 and CD38 expression. All subsequent gates were only applied to the non-transitional population as indicated by the black arrows. Non-transitional B cells were then divided into subsets based on CD27 and IgM expression, or CD45RB and IgM expression.

The exact same phenotyping panel was used when staining the HLA A2 binding B cells as with the A1 binding B cells. However, at the point when the HLA DR4 binding cells were being stained, the phenotyping panel was changed to incorporate antibodies for detecting CD86, BAFFr and HLA DR (rationale for this is detailed in chapter 5). As a compromise, CD24, CD38 and CD27 were removed from the panel and CD10 was added as a way of distinguishing transitional cells from non-transitional cells. Since in the majority of samples a higher proportion of HLA A1 and HLA A2 binding B cells expressed CD45RB than CD27, CD45RB was kept in the panel as the marker used for distinguishing memory from naïve. HLA DR4 binding B cells were detected in 4/11 samples from 3 patients with a median frequency of 0.12% (range 0.072%–0.28%). 3/4 samples, from 2 patients, had a frequency of HLA DR4 binding B cells that was more than double that of the no antigen control (median 3.7x background, range 2.5x-4.8x) and could be analysed for their phenotype. As with the HLA A1 and A2 binding B cells, the majority of HLA DR4 binding B cells were non transitional. Within the non-transitional gate, the dominant phenotype of HLA DR4+ binding B cells was naïve, CD45RB-IgM+ (median 50%, range 47.4% - 57.6%), with the remaining cells being distributed throughout the other populations.

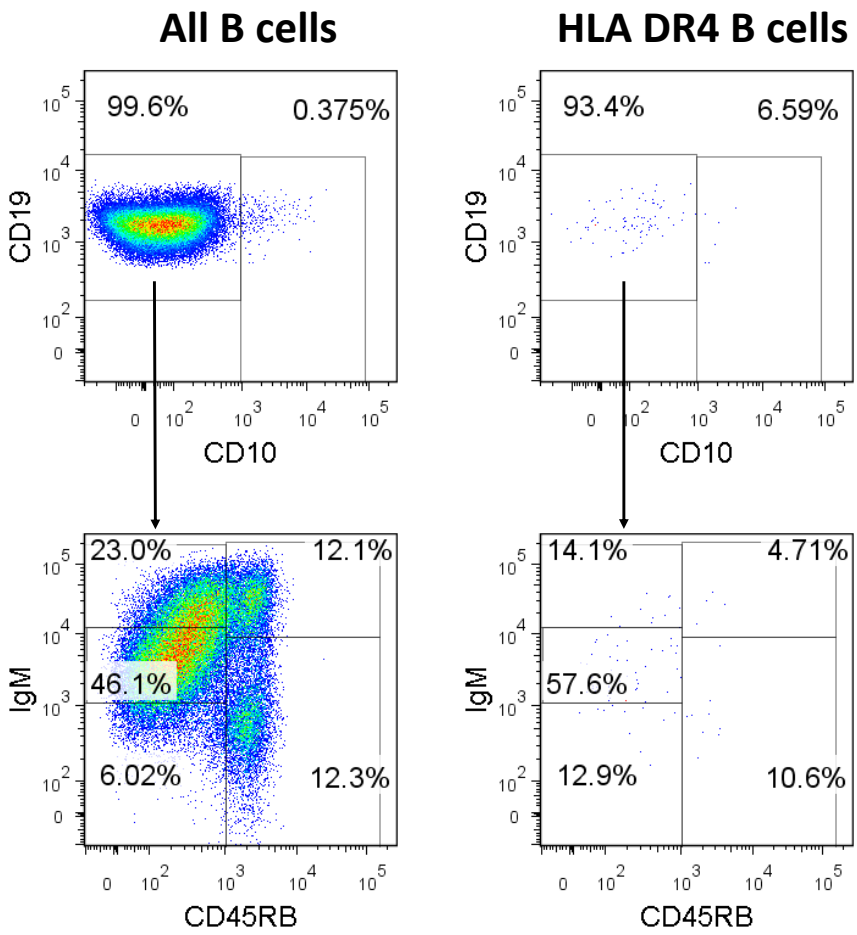

Figure 4.29 Example dot plot to show phenotype of HLA DR4 binding B cells
Gates were drawn on the whole B cell population and then applied to the HLA DR4 binding population. CD19+ cells were first divided into transitional and non-transitional B cells according to CD10 expression. All subsequent gates were only applied to the non-transitional population as indicated by the black arrows. Non-transitional B cells were then divided into subsets based on CD45RB and IgM expression

In total, 48 PBMC samples from 15 patients were analysed for the presence of HLA binding B cells and IFNγ production in response to the Pure HLA proteins. This data is summarised in Table 4.1. HLA binding B cells were detected in 21/48 samples with a median frequency of 0.070% (range 0.011%-0.28%). It was possible to analyse the phenotype of 14 of these samples. Figure 4.30 shows the phenotype of the HLA binding B cells compared to the overall B cell phenotype in all of the samples tested. B cells that have bound to the different HLA antigens used have been assigned a different colour on the graphs. It is clear that the phenotype of HLA binding B cells is not the same in all samples, but there are some general trends that can be observed. For example, when compared with the overall B cell population, CD45RB+IgMhi B cells are overrepresented in the HLA binding B cell population in 8/14 samples (57%) (Fig 4.30 (a), P=0.0494) and underrepresented in the CD45RB+IgM- population in 10/14 samples (71%) (Fig 4.30 (b), P=0.0166). CD45RB-IgMhi HLA binding B cells are underrepresented in 9/14 samples (64%) but this difference did not reach statistical significance (Fig 4.30 (c)). In the CD45RB-IgM+ HLA binding population, 6/14 samples (43%) are overrepresented compared to the overall B cell population, 7/14 samples (50%) are underrepresented and 1/14 samples (7%) hasn't changed (Fig 4.30 (d)). Similarly, in the CD45RB-IgM- HLA binding B cell population, 6/14 samples (42%) are overrepresented compared to the overall B cell population and 8/14 samples (57%) are underrepresented (Fig 5.15 (e)). It was possible to compare the frequency of the MZ/IgM+ memory pre-cursor population (CD27-CD45RB+) in the HLA A1 and HLA A2 mismatched samples. The Frequency of this population was overrepresented in 7/11 (64%) samples but this difference was not found to be significant (P>0.05).

In addition to the above comparisons, the phenotype of the HLA binding B cell population was compared to the phenotype of the events detected in the no antigen background control to confirm that the data from the cells that were incubated with the antigen did not mirror that in the no antigen control. This data can be found in Table 7.1 in the appendix.

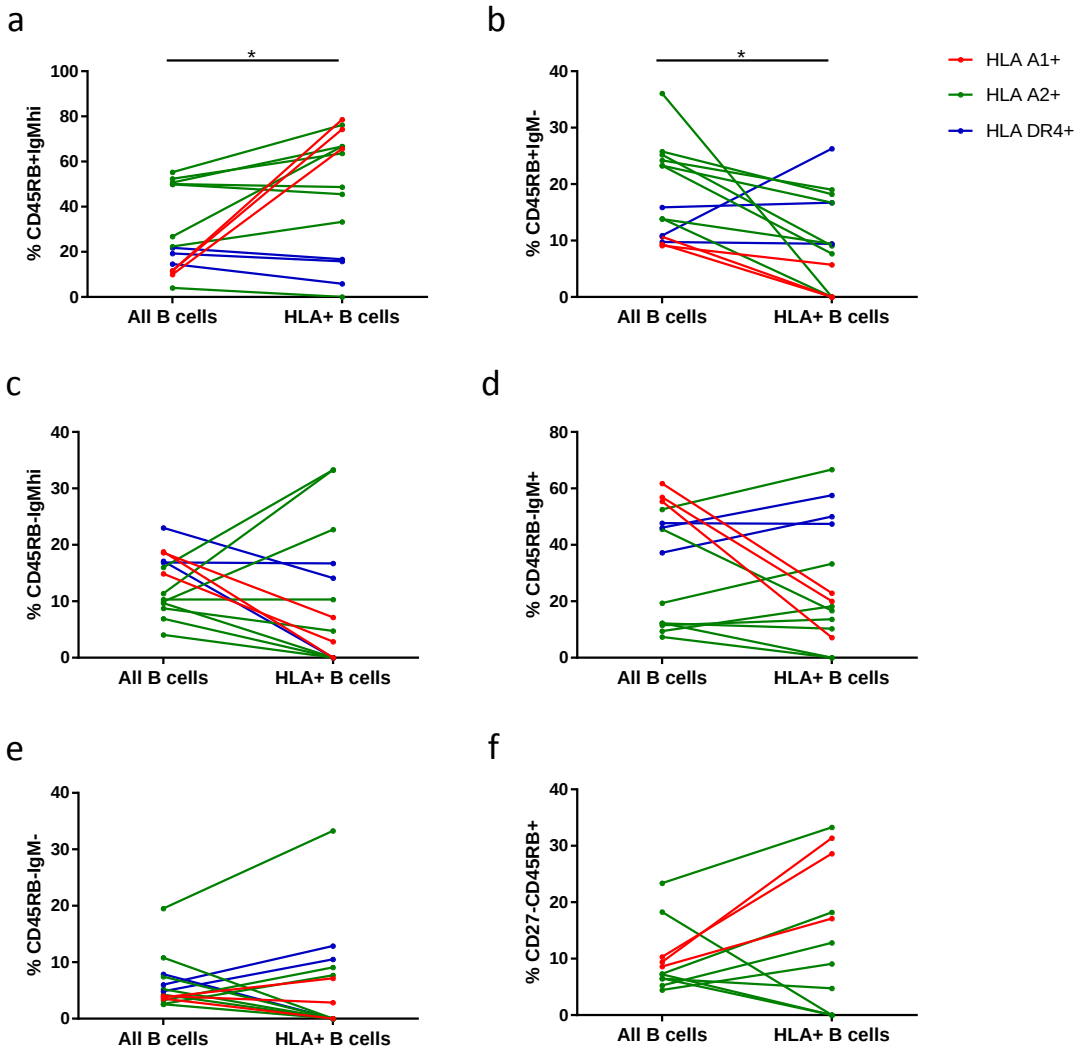

Figure 4.30 Phenotype of HLA binding B cells compared to the overall B cell population. **(a)** CD45RB+IgMhi are overrepresented in the HLA binding B cell population in 8/14 samples (P=0.0494). **(b)** Class switched CD45RB+IgM- are underrepresented in 10/14 samples (P=0.0166). **(c)-(f)** No significant differences were found between the HLA binding B cell population and the overall B cell population in the T3 naïve follicular B cell precursor subset **(c)**, IgM+naïve subset **(d)**, CD45RB-IgM- subset **(e)** or T3 MZ/IgM+ memory B cell precursor subset **(f)** (P>0.05). P values obtained using a Wilcoxon matched pairs signed rank test.

4.2.3.4 HLA binding B cells are not always associated with a history of circulating DSA.

Table 4.1 includes details of whether each patient has ever had evidence of circulating DSA to the mismatched antigen being tested in the HLA binding B cell assay. As DSA data was not available for each time point tested in the HLA binding B cell assay, it was only possible to group the patients based on whether they had DSA detectable at some point post-transplant. Table 4.1 also contains details of the IFNγ response that was observed in each sample. The data shows that in 5/15 patients, HLA binding B cells could be detected in patients who do not have a history of detectable DSA. 5/15 patients have both detectable HLA binding B cells and evidence of DSA and 2/15 patients have DSA but no detectable HLA binding B cells. Finally, 3/15 patients have no evidence of either HLA binding B cells or DSA. In addition, G014 has evidence of DSA specific for HLA A1 and HLA A2 but only has B cells that bound HLA A2 and not HLA A1.

2/15 patients have evidence of DSA and donor specific IFNγ production in the ELISpot. 4/15 patients have no evidence of DSA but did produce donor specific IFNγ at one or more time points when tested in the ELISpot.

7/48 samples have HLA binding B cells and evidence of donor specific reactivity in the IFNγ ELISpot. 5/48 samples have no detectable HLA binding B cells but evidence of donor specific reactivity in the IFNγ ELISpot.

The data in Table 4.1 indicates that within the limits of the three readouts presented here (DSA, HLA binding B cells and ELISpot reactivity) renal transplant patients with CAMR are, immunologically speaking, a highly heterogenous group. No patient has evidence of all three readouts at the same time point tested but many have at least two of them.

Table 4.1 (Legend over page)

							Spot count/million CD4+ T cells	
PATIENT ID	Timepoint	Mismatch	Mismatch DSA?	% HLA+ B cells	ELISpot reactivity	Bdep/Breg/ Bnon	CD8+ dep	CD8/CD19+ dep
W006	05/02/2009	A1	Y	0	NR	Bnon	0	0
W006	09/11/2009	A1		0	NR	Bnon	0	0
W006	11/04/2011	A1		0	NR	Bnon	0	0
G002	04/02/2009	A1	Y	0.23	R	Bdep	121	0
G002	02/09/2009	A1		0	R	Bdep	39	0
G013	14/11/2011	A1	N	0.037	R	Bdep	65	0
G013	21/02/2013	A1		0.039	NR	Breg	0	82
G013	09/01/2014	A1		0.02	R	Bdep	110	0
G014	17/05/2012	A1	Y	0	NR	Bnon	0	0
G014	12/11/2012	A1		0	NR	Bnon	0	0
G014	12/12/2013	A1		0	NR	Bnon	0	0
W003	11/12/2008	A2	N	0.016	R	Bdep	55	11
W003	25/06/2009	A2		0.018	R	Bnon	67	66
W003	21/06/2010	A2		0.011	NR	Bnon	12	4
W004	25/06/2009	A2	N	0	R	Bdep	94	3
W004	07/12/2009	A2		0	R	Breg	45	56
W004	21/06/2010	A2		0	NR	Bnon	12	0
W008	10/07/2008	A2	N	0.084	NR	Bnon	0	0
W008	12/01/2009	A2		0.059	R	Bdep	30	0
W008	02/07/2009	A2		0.073	NR	Bnon	12	0
W008	24/09/2009	A2		0.063	NR	Bnon	2	0
W008	21/06/2010	A2		0.041	NR	Bnon	1	12
W008	10/01/2011	A2		0.07	R	Bdep	32	12
W010	07/12/2009	A2	N	0	NR	Bnon	0	0
W010	08/03/2010	A2		0	NR	Bnon	0	0
W011	30/11/2009	A2	Y	0.057	NR	Bnon	0	3
W011	08/11/2010	A2		0.079	NR	Bnon	0	0
W011	21/11/2011	A2		0	NR	Bnon	0	0
G007	09/05/2011	A2	Y	0.058	NR	Bnon	3	0
G007	09/12/2011	A2		0	R	Breg	100	132
G007	15/10/2012	A2		0	R	Bdep	794	258
G012	14/06/2012	A2	Y	0	NR	Bnon	0	0
G012	12/11/2012	A2		0	NR	Bnon	0	0
G012	03/04/2013	A2		0	NR	Bnon	0	0
G014	17/05/2012	A2	Y	0	NR	Bnon	0	6
G014	12/11/2012	A2		0	NR	Bnon	0	16
G014	12/12/2013	A2		0.07	NR	Bnon	0	0
W009	16/10/2009	DR4	Y	0.16	NR	Bnon	0	0
W009	07/02/2011	DR4		0.28	NR	Bnon	0	0
G019	05/07/2012	DR4	N	0	NR	Bnon	13	21
G019	17/01/2013	DR4		0.086	NR	Bnon	0	6
G019	18/07/2013	DR4		0	NR	Bnon	0	0
G011	07/10/2010	DR4	N	0	NR	Bnon	0	0
G011	24/03/2011	DR4		0	NR	Bnon	0	0
G011	29/06/2011	DR4		0.072	ELISpot not done			
W013	08/03/2010	DR4	N	0	NR	Bnon	0	0
W013	12/01/2009	DR4		0	NR	Bnon	23	0
W013	14/05/2009	DR4		0	NR	Bnon	0	0

Table 4.1 Summary of each sample tested for the presence of HLA binding B cells, presence of DSA and the response to Pure™ HLA proteins in the IFNγ ELISpot before and after CD19+ cell depletion.

Samples were grouped according to whether the frequency of HLA binding B cells was at least double that detected in the no antigen gate. White rows represent samples where no HLA binding B cells were detected, blue rows represent samples where HLA binding B cells were detected but the frequency was less than double that detected in the no antigen control. Pink rows represent samples where the frequency of HLA binding B cells was more than double that detected in the no antigen control. Patients were assigned Y if they had ever had evidence of circulating DSA or N if they had not. Each sample was assigned a pattern of reactivity in the IFNγ ELISpot assay. R = reactive. NR= non-reactive. Bdep = B dependent reactivity, Breg = B regulated reactivity Bnon = CD19+ depletion had no effect on IFNγ production. Patterns of reactivity were assigned using the criteria stated in section 2.3.5.6

4.2.3.5 A higher ratio of IgM+memory to IgM+naïve HLA binding B cells associates with IFNγ production in response to the pure HLA proteins.

As the phenotype of HLA binding B cells is not homogeneous, it was investigated whether any associations could be made between the skewed phenotypes in the different samples and the pattern of reactivity observed in the IFNγ ELISpot in response to the Pure™ HLA proteins. To be able to include all events in the HLA binding B cell gate, non-transitional B cells were grouped according to their expression of either CD27 or CD45RB and called either memory (CD27+/CD45RB+) or Naïve (CD27-/CD45RB-). The ratio of these populations was calculated to investigate whether the balance of memory to naïve B cells impacts the outcome in the IFNγ ELISpot (Table 4.2). The following observations were made:

1. 5/13 samples responded. All of these samples had a ratio of memory to naïve >1 when CD45RB is used as a memory marker. Therefore the dominant phenotype of their HLA binding B cells is memory. In 4/5 samples, this ratio is higher in the HLA binding B cells than the global B cell population.

2. 8/13 samples did not respond. 4/8 of these samples have a ratio of memory:naïve cells of <1 and 4/8 samples have a ratio of memory:naïve of >1. There is therefore no distinct pattern that defines a non-reactive sample when this analysis is used.

3. As the pattern of reactivity changes over time, the ratio of memory:naïve B cells in the HLA binding B cell population also changes. It was possible to observe in 3 patients how the change in ELISpot pattern of reactivity relates to the phenotype of the HLA binding B cells over time. Interestingly, at the second time point tested in G013, the pattern of reactivity shifts from B dependent to B regulated. At the same time the ratio of memory:naïve HLA binding B cells is reduced when memory B cells are defined using CD45RB, and becomes <1 when CD27 as the memory marker. The ratio of memory: naïve is <1 in the global B cell population at all time points. It is possible that in this patient, there was a temporary shift in the balance between the memory and naïve HLA binding B cells that lead to an overall regulated response to the HLA protein at the second time point. In W008, the pattern of reactivity in response to the HLA A2 Pure protein also changes overtime, however it is less clear how the ratio of memory:naïve HLA A2 binding B cells relates to this. When CD45RB is used

as the memory marker, the ratio of memory:naïve does not distinguish the reactive, B dependent samples from the other samples as 2 of the non-reactive samples have a higher ratio than time point 12/01/2009 which was reactive. However, when CD27 is used as a memory marker, the ratio of memory:naïve is highest in both of the reactive samples compared to the other time points. The same thing cannot be said for the global B cell population. Finally, in W009, both samples are non-reactive to the Pure HLA DR4 protein, and at both time points the ratio of memory:naïve HLA DR4 binding B cells remains <1.

Table 4.2 Summary of all samples analysed for their HLA phenotype detailing their pattern of reactivity I the IFNγ ELISpot and the ratio of memory:naïve B cells, in the HLA binding B cell population and the overall B cell population

Patient ID	Timepoint	Mismatch	ELISpot reactivity	Bdep/Bsup /Bnon	CD45RB+:CD45RB- (% of HLA+ B cells)	CD45RB+:CD45RB- (% of all B cells)	CD27+: CD27- (% of HLA+ B cells)	CD27+: CD27- (% of all B cells)
G013	14/11/2011	A1	R	Bdep	4.00	0.26	2.18	0.18
G013	21/02/2013	A1	R	Breg	2.50	0.24	0.67	0.15
G013	09/01/2014	A1	R	Bdep	3.67	0.29	1.00	0.18
W008	10/07/2008	A2	NR	Bnon	2.00	2.82	2.00	3.82
W008	12/01/2009	A2	R	Bdep	1.99	2.99	5.50	4.37
W008	02/07/2009	A2	NR	Bnon	1.20	3.07	3.40	5.14
W008	24/09/2009	A2	NR	Bnon	4.49	3.28	4.50	4.15
W008	10/01/2011	A2	R	Bdep	20.00	3.68	9.50	5.23
W011	30/11/2009	A2	NR	Bnon	0.20	0.22	1.00	0.28
G007	09/05/2011	A2	NR	Bnon	2.00	2.39	2.00	1.20
G014	12/12/2013	A2	NR	Bnon	0.50	0.56	0.00	0.12
W009	16/10/2009	DR4	NR	Bnon	0.18	0.32		
W009	07/02/2011	DR4	NR	Bnon	0.73	0.43		

Memory cells were defined using either CD45RB or CD27 expression

There are hints in the data above to suggest that the balance of memory to naïve B cells may impact the IFNγ response to Pure™ HLA proteins. As the dominant phenotype of the HLA binding B cells was often found to be either IgM+ memory or IgM+ naïve, the ratio of these two subsets was calculated by defining the IgM+ memory B cells as either CD27+IgMhi or CD45RB+IgMhi, and the IgM+ naïve cells as CD27-IgM+ or CD45RB-IgM+ (Table 4.3). A similar pattern is observed for G013 where a shift from B dependent to B regulated pattern of reactivity is associated with a reduction in the ratio of IgM+memory:IgM+naïve. Again, the data shows that when CD45RB is used as a memory marker the data from W008 does not fit a clear pattern. However, when CD27 is used to define IgM+ memory cells, the difference in the ratio of IgM+memory:IgM+naïve B cells between the reactive B dependent samples and the non-reactive samples is much greater. The same distinction is not observed in the overall B cell population. This suggests that in this patient, there may be a higher proportion of T3 or marginal zone precursors that are detected in the CD45RB+IgMhi population which makes it harder to resolve differences in the ratio of memory:naïve B cells. When using CD27 as the memory marker, these cells are omitted from the analysis as they fall into the CD27-IgMhi gate. CD27 was not used in the stain panel for the DR4 binding B cells, however, when using CD45RB as the memory marker, W009 has a ratio of IgM+memory:IgM+naïve B cells of <1 which is consistent with the results in table 4.2.

Table 4.3 Summary of all samples analysed for their HLA phenotype detailing their pattern of reactivity in the IFNγ ELISpot to pure HLA proteins and the ratio of IgM+memory to IgM+naïve cells in the HLA binding B cell population and the overall B cell population.

Patient ID	Timepoint	Mismatch	ELISpot reactivity	Bdep/Bsup /Bnon	CD45RB+IgMhi :CD45RB-IgM+ (% of HLA+ B cells)	CD45RB+IgMhi: CD45RB-IgM+ (% of all B cells)	CD27+IgMhi: CD27-IgM+ (% of HLA+ B cells)	CD27+IgMhi: CD27-IgM+ (% of all B cells)
G013	14/11/2011	A1	R	Bdep	3.72	0.15	1.91	0.08
G013	21/02/2013	A1	R	Breg	2.55	0.13	0.70	0.06
G013	09/01/2014	A1	R	Bdep	5.50	0.16	1.17	0.08
W008	10/07/2008	A2	NR	Bnon	2.00	2.14	2.00	2.67
W008	12/01/2009	A2	R	Bdep	2.36	2.22	7.00	2.97
W008	02/07/2009	A2	NR	Bnon	1.25	2.33	2.00	3.51
W008	24/09/2009	A2	NR	Bnon	3.49	2.75	3.00	3.06
W008	10/01/2011	A2	R	Bdep	16.01	3.43	7.50	4.26
W011	30/11/2009	A2	NR	Bnon	0.00	0.07	0.50	0.06
G007	09/05/2011	A2	NR	Bnon	2.00	1.02	2.00	0.56
G014	12/12/2013	A2	NR	Bnon	0.50	0.40	0.00	0.03
W009	16/10/2009	DR4	NR	Bnon	0.08	0.21		
W009	07/02/2011	DR4	NR	Bnon	0.33	0.30		

IgM+ memory cells were defined as CD45RB/CD27+IgMhi, and IgM+ naïve B cells were defined as CD45RB/CD27-IgM+. CD45RB/CD27-IgMhi B cells were not included.

4.2.3.6 Can HLA binding B cells be detected in individuals who do not have a mismatched kidney transplant to the HLA antigen in question?

The cross-reactivity of antibodies to non-DSA that has been widely reported make it very difficult to truly control the experiments described in this chapter (Süsal, 2015, Lachmann et al., 2009). Nevertheless, it was decided that where sufficient PBMC were available, the patients with A2 or DR4 mismatched kidneys would also be analysed for the presence of HLA A1 specific B cells and whether they produced IFNγ in response to the Pure™ A1 protein. In addition, PBMC from leukocyte cones were also tested.

A1 binding B cells could be detected in 2/9 patient samples (0.106% and 0.049%) and in 4/8 leukocyte cones with a median frequency of 0.14% (range 0.114%-0.303%). The frequency of HLA binding B cells from all samples tested is shown in Figure 4.31. The X axis label relates to the biotinylated HLA antigen that was used to detect the HLA binding B cells. Samples are grouped according to whether they are derived from a patient who has a kidney mismatched to that antigen, a patient who does not have a kidney mismatched to that antigen, or a leukocyte cone. Surprisingly, the group that has the highest detectable frequency of HLA binding B cells is the leukocyte cones, whom in theory should not be sensitised to HLA A1. However this difference was not found to be significant when the frequency of HLA A1 binding B cells detected in the patients with the A1 mismatched transplants was compared with the leukocyte cones using a Mann Whitney U test ($P>0.05$). The difference in frequency of HLA A1 binding B cells between the patients who had an HLA A1 mismatched transplant and those who did not was also not significant.

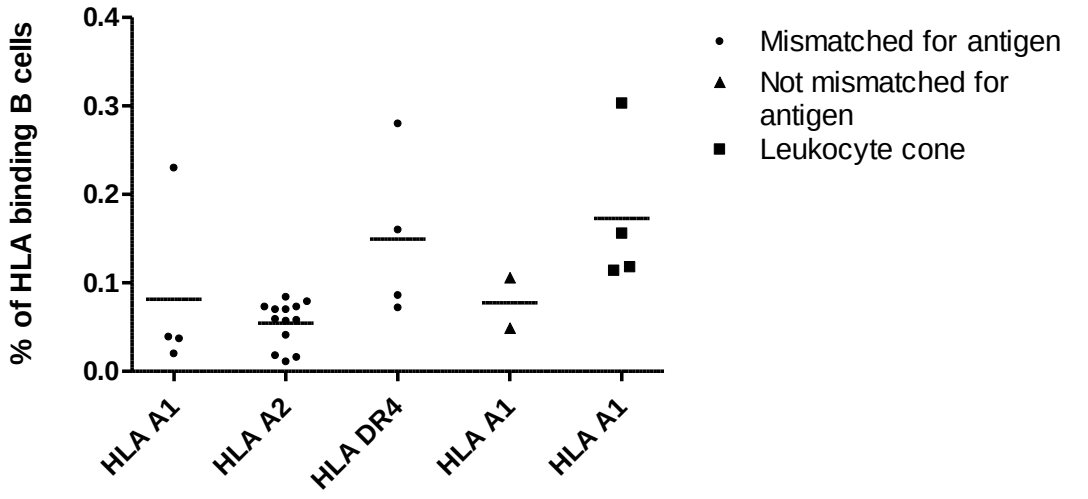

Figure 4.31 Frequency of HLA binding B cells in all sample groups tested.
Labels on X axis show the biotinylated HLA antigen that the PBMC were incubated with. Black circles are samples from patients who have a mismatched kidney to that antigen (n=4 for HLA A1, n=13 for HLA A2 and n=4 for HLA DR4). Black triangles are patients who do not have a mismatched kidney to HLA A1 (n=2). Black squares are samples from leukocyte cones who theoretically should not be sensitised to HLA A1. Black lines on graph represent the median. P>0.05 for all comparisons between groups using a Mann Whitney U test.

4.2.3.7 Do Pure HLA proteins elicit an IFNγ response in individuals who do not have an allograft that contains a mismatch for that Pure™ protein?

At the same time as staining the B cells from the leukocyte cones for HLA A1 binding B cells, the indirect IFNγ ELISpot assay was carried out using the same non-biotinylated Pure™ HLA A1 protein to see if similar results were observed in leukocyte cones as in the patients. In addition to this, if there were enough cells available, patients who had an A2 or DR4 mismatched kidney transplant were also stimulated with the Pure™ HLA A1 protein in the IFNγ ELISpot. The phenotype of the HLA A1 binding B cells was then correlated with the pattern of reactivity in the IFNγ ELISpot as in section 4.2.3.5.

HLA A1 binding B cells were detected in 2/9 patient samples tested and phenotyping was only possible in one of them as the other sample did not reach the cut-off previously defined where the frequency of HLA binding B cells must be at least double that detected in the no antigen control (Table 4.4). In the sample where the phenotype was analysed, 66.7% of the HLA binding B cells were either CD27+IgM- or CD45RB+IgM- and the remaining 33.3% were either CD27+IgMhi or CD45RB+IgMhi. This sample therefore did not contain any naïve HLA binding B cells and consistent with the results in section 4.2.3.5, this sample displayed a reactive, B dependent response to the HLA A1 protein in the IFNγ ELISpot. Two other patient samples produced IFNγ in response to the HLA A1 protein: one was B dependent and the other B regulated. HLA A1 binding B cells were not detected in either of these samples.

Table 4.4 Patients with A2 or DR4 mismatched kidney transplants tested for reactivity to HLA A1 Pure™ protein and presence of A1 binding B cells.

						Spot counts/million CD4+ T cells	
Patient ID	Timepoint	Mismatch	% HLA A1+ B cells	ELISPOT reactivity	Bdep/Breg /Bnon	CD8-	CD8& CD19-
W004	07/12/2009	A2	0.106	R	Bdep	43	0
W004	21/06/2010	A2	0	R	Breg	0	35
W010	07/12/2009	A2	0	R	Bdep	41	3
W011	21/11/2011	A2	0	NR	Bnon	0	0
W011	30/11/2009	A2	0	NR	Bnon	0	0
G012	12/11/2012	A2	0	NR	Bnon	0	0
G012	14/06/2012	A2	0	NR	Bnon	0	3
W013	12/01/2009	DR4	0.049	NR	Bnon	0	0
G019	17/01/2013	DR4	0	NR	Bnon	0	0

White rows represent samples where no HLA binding B cells were detected, blue rows represent samples where HLA binding B cells were detected but the frequency was less than double that detected in the no antigen control. Pink rows represent samples where the frequency of HLA binding B cells was more than double that detected in the no antigen control.

HLA binding B cells were detected in 4/8 of the leukocyte cones tested (Table 4.5). The majority of HLA A1 binding B cells in all leukocyte cones were non-transitional and of a naïve CD45RB-IgM+ or CD27-IgM+ phenotype (Table 4.6). The ratio of memory:naïve populations and IgM+memory:IgM+naïve was <1 for all samples. The distribution of each subset in the HLA A1 binding cell gate was similar to that of the overall B cell population in all Leukocyte cones. 1/4 of these samples produced IFNγ in response to the Pure HLA A1 in a B regulated manner. Two other samples also displayed a reactive B regulated response to the HLA A1 protein but HLA binding B cells could not be detected in these samples. This data is consistent with that of the patients where if the dominant HLA binding B cell population is naïve, a non-reactive response or reactive B regulated response is observed in the IFNγ ELISpot. However, the phenotype of HLA binding B cells in many of the patient samples is distinct from the overall B cell population. This was not observed in the Leukocyte cones. It is therefore possible that the HLA binding B cells detected in the leukocyte cones may not be clonally expanded antigen specific B cells but just non-specific naïve B cells that have bound the antigen in this assay.

Table 4.5 Leukocyte cones tested for reactivity to A1 Pure protein and the presence of A1 binding B cells

				Spot counts/million CD4+ T cells	
Cone ID	% HLA A1+ B cells	ELISPOT reactivity	Bdep/Breg /Bnon	CD8-	CD8& CD19-
Cone 23	0.156	R	Breg	26	126
Cone 26	0.303	NR	Bnon	0	0
Cone 27	0	R	Breg	0	32
Cone 28	0	NR	Bnon	0	0
Cone 29	0	R	Breg	0	41
Cone 34	0.118	NR	Bnon	0	0
Cone 35	0.114	NR	Bnon	0	0
Cone 36	0	NR	Bnon	0	0

White rows represent samples where no HLA binding B cells were detected, Pink rows represent samples where the frequency of HLA binding B cells was more than double that detected in the no antigen control.

Table 4.6 Phenotype of HLA A1 binding B cells compared to the overall B cell population in leukocyte cones.

a

Cone ID	ELISpot reactivity	Bdep/Breg /Bnon	CD45RB+:CD45RB- (% of HLA+ B cells)	CD45RB+:CD45RB- (% of all B cells)	CD45RB+IgMhi :CD45RB-IgM+ (% of HLA+ B cells)	CD45RB+IgMhi: CD45RB-IgM+ (% of all B cells)
Cone 23	R	Breg	0.25	0.27	0.23	0.21
Cone 34	NR	Bnon	0.1	0.14	0	0.04
Cone 35	NR	Bnon	0.43	0.43	0.34	0.31

b

Cone ID	ELISpot reactivity	Bdep/Breg /Bnon	CD27+: CD27- (% of HLA+ B cells)	CD27+: CD27- (% of all B cells)	CD27+IgMhi: CD27-IgM+ (% of HLA+ B cells)	CD27+IgMhi: CD27-IgM+ (% of all B cells)
Cone 26	NR	Bnon	0.21	0.19	0.2	0.14

(a) Leukocyte cones that were stained with CD45RB. **(b)** One Leukocyte cone that was stained with CD27 as a memory marker and not CD45RB.

4.3 Key points in chapter 4

1. CMV gB B cells can be detected using biotinylated CMV gB protein.

2. CMV gB binding B cells are predominantly IgMhi and are a mixed population of IgM+ memory B cells and Transitional 3 B cells that will most likely differentiate into naïve follicular B cells.

3. HLA A1, HLA A2 and HLA DR4 binding B cells can be detected in renal transplant recipients using biotinylated Pure™ HLA proteins.

4. The majority of HLA binding B cells have an IgM+ phenotype. Most patient samples have a dominant phenotype of HLA binding B cells that is either CD27/CD45RB+IgMhi memory or CD27/CD45RB-IgM+ naïve.

5. Pure™ HLA proteins can be used to induce IFNγ production that is dependent on the presence of B cells in the indirect IFNγ ELISpot assay. A higher ratio of IgM+ memory to IgM+ naïve HLA binding B cells is associated with a B dependent IFNγ response to the Pure™ proteins when CD27 is used as the marker to define memory.

6. HLA A1 binding B cells can be detected in the peripheral blood of individuals who have not received a kidney transplant (Leukocyte cones). The majority of these B cells are of a naïve, IgM+ phenotype and are not distinct from the overall B cell population.

7. A subset of Leukocyte cones tested produced IFNγ in response to the Pure™ HLA A1 protein. IFNγ production showed a B regulated pattern of reactivity in these individuals.

4.4 Discussion

In chapter 3, evidence of B cell dependent reactivity towards donor membrane proteins was found in CAMR patients recruited on to the RituxiCAN C4 trial. No differences were found in the global B cell phenotype of these patient's at enrolment compared to those that did not have a B cell dependent response. At later time points in the trial, evidence of B regulated reactivity towards the donor membrane proteins was also found in some samples. This lead to the hypothesis that, if no differences could be detected in the global phenotype of the B cells, then perhaps the differences lay within the antigen specific populations, in this case the donor HLA specific B cell population. An assay to detect antigen specific B cells that was compatible with the indirect IFNγ ELISpot was therefore developed to address this hypothesis. A model system using CMV gB was used to optimise the assay in order to preserve the valuable patient samples. This assay was then translated to a patient setting using Pure HLA proteins.

4.4.1 Antigen binding B cells can be detected flow cytometrically using biotinylated recombinant proteins

After a review of the literature it was decided that using biotinylated CMV gB combined with streptavidin PE would be the best way of detecting CMV binding B cells (Doucett et al., 2005, Amanna and Slifka, 2006). Several experiments were carried out to determine that the antigen was binding the B cells via the BCR as opposed to non-specifically binding other molecules on the surface of the B cells, or even via CMV specific antibodies in the human AB serum that was used. Whilst confident that these results demonstrated that the antigen was binding the BCR, it was not possible to show that this binding was completely specific for CMV gB. A cold inhibition assay that was designed to demonstrate that the binding was specific for CMV gB was inconclusive as incubation with increasing concentrations of a different non-biotinylated viral antigen, VZV gE, had a similar effect on the level of binding of the biotinylated CMV gB to the non-biotinylated CMV gB. Some studies that have flow cytometrically detected antigen specific B cells have shown that those B cells can also be induced to make antibodies that bind to the same antigen in an ELISA. This was therefore investigated further by single cell sorting the CMV gB binding B cells, sequencing and cloning their BCRs and transfecting 293T cells so they would secrete antibodies that could be tested in a CMV gB ELISA for their specificity. This set of experiments did not yield any positive results, so whether the BCRs that are binding the CMV gB are exclusively specific for just CMV gB remains unclear and limits the interpretations that can be made from the data.

4.4.2 CMV binding B cells are predominantly IgM+ and overrepresented in the IgMhi populations when compared to the global B cell phenotype

The frequency of CMV gB binding B cells detected ranged from 1.04% - 3.37% (median 1.83%) in the 15 leukocyte cones tested. This figure is higher than that reported in Potzsch et al. where a directly fluorescently labelled CMV gB was used to detect 0.33%-1.4% CMV gB binding B cells in the circulation of 15 HCMV seropositive individuals. However, this difference in results could be explained by the fact that the frequency of CMV gB binding B cells reported by Potzsch et al. is restricted to just the CD27+ IgG+ B cell population, where they showed that the frequency of CD27+IgG+ CMV binding B cells was higher in HCMV seropositive individuals than seronegative individuals. Although not highlighted in the text of the paper, the figure that is included of the FACS plots shows that the frequency of CD27+IgG- B cells that bind the CMV gB protein is in fact almost double that of the CD27+IgG+ population (Pötzsch et al., 2011). Importantly, the same result was also detected in HCMV seronegative patients in this paper, a finding that is relevant to the interpretation of the data in this thesis, as the HCMV status of the leukocyte cones used here is not known. The results reported in Potzsch et al therefore support those reported in this thesis, where the majority of CMV gB binding B cells were found to be IgM+.

Interestingly, the population that was most overrepresented in the CMV gB binding B cell gate compared to the overall B cell population was the IgMhi B cells. The IgMhi B cells were further subdivided according to the expression of the memory markers CD27 and CD45RB which revealed that both CD27+IgMhi and CD27-IgMhi B cells were overrepresented in the CMV gB binding B cell gate compared to the overall B cell population. In contrast, only CD45RB-IgMhi B cells, and not CD45RB+IgMhi B cells, were overrepresented in the CMV gB binding gate compared to the overall B cell population. Interestingly, the CD27-CD45RB+ MZ/IgM+ memory precursor B cells were also not enriched in the CMV gB binding population. Therefore, when considered together, the phenotyping data suggests that CMV gB binding B cells are enriched in the IgM+ memory population and the T3 naïve follicular pre cursor B cell population. This result was largely unexpected due to the fact that CD27+IgM+ (IgM+ memory B cells) are widely reported to be specific for polysaccharide antigens, such as those found on pneumococcal bacteria, and that they are considered by many researchers in the field to develop independently from the rest of the B cell population (Capolunghi et al., 2013, Kruetzmann et al., 2003, Carsetti et al., 2005). However, it has been previously reported that IgM+ memory B cells specific for tetanus toxoid, rhesus antigen and rotavirus like particles are enriched in human peripheral blood and that

switched memory B cells are underrepresented compared to the global B cell population, thus demonstrating that IgM+ memory B cells specific for a wide range of pathogens can be detected (Della Valle et al., 2014, Herrera et al., 2014, Rojas et al., 2008). Moreover, Della-Valle et al. demonstrated that both CD27- and CD27+ IgM+ cells specific for rhesus antigen had somatically mutated variable regions that were clonally related to each other, and the CD27+IgG+ rhesus antigen specific subset (Della Valle et al., 2014). Very recently, Dauby et al. reported that HCMV binding B cells in chronically infected individuals are activated CD27+CD21hi memory B cells (Dauby et al., 2015). Unfortunately, they did not look at the isotype of these cells so the data is not directly comparable to the data in this thesis, but it would be interesting to investigate whether the CD27+IgM+ CMV binding B cell population found in this thesis also express CD21 at high levels.

It is difficult to investigate the kinetics of the B cell response in humans as this requires access to secondary lymph organs and is also made more complicated by the fact that humans aren't kept in controlled environments, where the primary and secondary antigen encounters can be controlled. Studies in animals must therefore be used to help understand the B cell response. In the last 5 years or so studies in mice have shed light on the kinetics of the germinal centre reaction and have revealed that IgM+ memory cells specific for protein antigens are formed within 2 days of primary antigenic challenge in the extrafollicular space, prior to the initiation of the germinal centre reaction (Weisel et al., 2016, Taylor et al., 2012, Pape et al., 2011, Dogan et al., 2009). In addition, IgM+ memory B cells have also been shown to be the products of early germinal centre reactions (Dogan et al., 2009).

Pape et al. showed that the IgM+ memory B cells were maintained at their original numbers for the duration of the experiment (500 days) whereas isotype switched memory B cells began to decline after 50 days. In this model, the switched memory B cells would re-enter a germinal centre reaction to form long lived plasma cells upon secondary encounter with antigen if the titre of switched serum Immunoglobulin was high. However, when the switched immunoglobulin titre declined, IgM+ memory B cells entered germinal centre reactions to form a new population of plasma blasts. It appears that the IgM+ memory B cells in this model were therefore acting as a long-lived reserve for the immune response (Pape et al., 2011). Dogan et al. showed that IgM+ memory cells that have emerged early on after formation of a germinal centre have the ability to reinitiate a germinal centre reaction to form class switched germinal centre B cells when boosted with antigen (Dogan et al., 2009). In contrast, Zuccarino-Catania

et al. showed that the fate of a memory B cell upon secondary exposure to antigen is independent of the isotype of the BCR that the memory B cell expresses but is instead dependent on its expression of co-stimulatory/inhibitory molecules CD80 and PDL-2; IgM+ memory B cells that did not express these molecules (double negatives) were able to form germinal centre B cells and differentiate into antibody secreting cells. However, IgM+ memory B cells that expressed both molecules (double positives) were not able to form a germinal centre reaction but very efficiently differentiated into isotype switched antibody secreting cells (Zuccarino-Catania et al., 2014).

From these papers, it is becoming apparent that during a primary immune response, there are 'multiple layers' of memory created, from the initial encounter of antigen, to the eventual differentiation and production of long lived plasma cells. IgM+ memory B cells, it seems, play a much wider role in this layering of memory than previously thought. It is possible here, that the CMV gB binding IgM+ memory B cells detected have come from two different sources: some are the products of an early germinal centre reaction and were derived from naïve follicular B cells, and some are the products of differentiation of the MZ/IgM+ memory B cell subset. Interestingly, the T3 subset thought to be the precursors to the naïve follicular B cells (CD27-CD45RB-IgMhi) were enriched in the CMV gB binding population but the T3 subset that is reported to be the pre-cursor to MZ/IgM+ memory B cells (CD27-CD45RB+IgMhi) was not. One could therefore speculate on a model with multiple layers whereby the MZ/IgM+ memory pre cursor B cells specific for CMV gB have all differentiated into mature CD27+CD45RB+IgMhi cells by adulthood, a theory considered plausible as this subset has been reported to be enriched in children (Bemark et al., 2013, Descatoire et al., 2014). At the same time, there continues to be a pool of naïve follicular pre-cursor B cells that are able to mature into naïve follicular B cells and subsequently be activated by the CMV gB antigen to form new IgM+ memory B cells, that originate from either an extrafollicular engagement with T cells, or an early germinal centre reaction.

4.4.3 HLA binding B cells detected using Pure™ HLA proteins are found at a much lower frequency in the peripheral blood than reported using other methods of detection

HLA binding B cells have previously been detected in the peripheral blood of renal transplant patients using two different methods to the one used in this thesis. Firstly, Frans Claas' group at Leiden university described a method in which HLA A*0201, HLA A*2402 and HLA B*0702 tetramers carrying peptides specific for either HIV gag or melanoma derived antigen MART-1 were used to detect a mean frequency of 4.65%

HLA binding B cells in the peripheral blood of renal transplant patients that had evidence of sensitisation due to the presence of circulating antibodies specific for the same HLA antigen as the tetramer used. They also detected HLA binding B cells in the peripheral blood of unsensitised individuals at an average frequency of 2.33%. (Zachary et al., 2007a, Mulder et al., 2001, Mulder et al., 2003, Zachary et al., 2007b). The second paper, published by John Paul Soulilou's group, used a method based on the Luminex® technology normally used to detect HLA specific antibodies in the circulation, where instead of incubating fluorescent dye impregnated HLA antigen coated polystyrene beads with serum, they incubated them with isolated B cells. Each HLA specific B cell population was then detected as a bead-cell rosette on the Luminex® machine. Using this method they detected a mean frequency of 1.29% and 0.6% HLA A*0201 binding B cells in sensitised renal transplant recipients and healthy volunteers respectively (Degauque et al., 2013). The mean frequency of HLA binding B cells of all the samples tested in this thesis from the patients with an HLA A1, HLA A2 or HLA DR4 mismatched kidney was 0.07%, and in the leukocyte cones it was 0.14%. There is therefore a large discrepancy between the frequency of HLA binding B cells that are detected in the circulation of both renal transplant recipients and healthy volunteers between the three methods used. This could be due to differences in both the specificity and sensitivity of each assay system, but also the individuals tested. For example, Zachary et al. tested their method on patients with end-stage renal disease and Degauque et al. used renal transplant recipients who had either stable graft function or antibody mediated rejection, but not chronic rejection. In terms of healthy control subjects, Zachary et al. used male subjects and Degauque et al. didn't specify any characteristics of their healthy volunteer population. Very little is known about the leukocyte cones used here, apart from that they are blood donors. It is possible that they have a sensitisation history from previous pregnancies as their sex is unknown. However, they will not have received a transplant or a blood transfusion.

It is likely that the tetramer method is the least specific of all of the techniques as the frequency of HLA binding B cells is very high considering that the B cell repertoire should, in theory, contain B cells with a BCR to every antigen that an individual will encounter. Little information is provided about the characteristics of the transplant patients in the study by Zachary et al. but it is possible that an individual undergoing an acute rejection episode may have a high frequency of HLA binding B cells, but it is

unlikely that an unsensitised healthy volunteer would truly have HLA binding B cells specific to just one HLA antigen at a frequency as high as 2.33%.

To really understand whether the variability of the results in these three studies is due to the different patients/healthy volunteer cohorts studied, or the technique itself, requires testing of the same sample using all three techniques. As a major aim of this thesis was to correlate the pattern of reactivity in the IFNγ ELISpot with the phenotype of the HLA binding B cells, the techniques used by Zachary et al. and Degauque et al. would not have been suitable for this purpose, as a tetramer or a polystyrene coated bead could not be used as the source of B cell stimulating antigen in the IFNγ ELISpot assay as they are large complexes which contain many more antigens than just the HLA molecule. In addition, multi-parameter flow cytometric analysis of the phenotype of the cells would not be compatible with the Luminex® bead method.

In an attempt to improve on the sensitivity and specificity of the tetramer based assay that was developed in the same department at Leiden University, Sebastian Heidt's group have used Pure™ HLA monomers to develop an ELISpot assay that can be used to detect both class I and class II specific memory B cells (Karahan et al., 2015b, Heidt et al., 2012). It would therefore be possible to validate the flow cytometric antigen binding B cell assay described in this thesis (which used HLA monomers from Pure™ proteins LLC) with the ELISpot assay developed by Heidt's group using the exact same source of HLA.

Two papers using this ELISpot assay to study renal transplant recipients have recently been published. Lucia et al. reported that the presence of donor HLA specific memory B cells in the periphery of renal transplant patients often correlated with the presence of DSA, but in some cases they were detected in the absence of DSA. This was particularly true when patients were tested before transplant; the presence of donor specific HLA memory B cells before transplant was associated with development of antibody mediated rejection, even when the patient was classed as negative for DSA (Lúcia et al., 2015). Snanoudj et al. carried out a very similar study in three groups of patients with end stage renal disease who were grouped according to whether they had circulating DSA and/or a previous sensitisation event such as a transplant or pregnancy. Consistent with Lucia et al., this study found that the presence of HLA specific memory B cells was strongly associated with a previous sensitisation event. However in contrast to the findings of Lucia et al, they also found that the presence of

HLA specific B cells was always associated with detectable circulating DSA (Snanoudj et al., 2015).

A common goal of the assays mentioned above is to highlight the weaknesses in just monitoring serum DSA as a means to measuring the sensitisation status of a patient before and after transplantation, and that developing a clinical test that gives an alternative readout of a patient's humoral sensitisation to HLA antigens may aid in the initial matching of recipient donor pairs pre-transplant, and in the subsequent management of rejection post-transplant (Karahan et al., 2015a). The focus of these studies is still very much on the antibody producing function of a B cell and does not shed any light on other contributions that B cells may be making to the alloimmune response. The data in this thesis, therefore, is highly novel in that it is uses the same HLA monomers as used in the studies mentioned above, but for the purpose of investigating the contribution that different B cell subsets may be making to the indirect T cell alloimmune response. Moreover, this thesis focusses on this response in a chronic rejection setting, whereas the studies mentioned above are mainly focussed on the pre-transplant and acute rejection stages.

4.4.4 HLA binding B cells are predominantly IgM+ and are either IgM+ naïve or IgM+ memory B cells

When the assay for detecting antigen binding B cells was applied to an HLA setting, it was found that the phenotype of HLA binding B cells detected in the patients and leukocyte cones was also IgM+. Although the results were more variable than the CMV gB binding B cells when the IgM+ cells were divided into different subsets according to CD45RB and IgM expression, general trends could be observed where the predominant phenotype of the of HLA binding B cells was either CD45RB+IgMhi memory population or CD45RB-IgM+ naïve. This data is supported by that of Degauque et al. where they reported that the HLA A1+ B cells that they detected using their antigen coated bead system were overrepresented in the non-class switched memory B cell population (CD27+IgD+) and underrepresented in the class switched B cell population when compared to the overall B cell population (Degauque et al., 2013). Based on the findings of the murine studies of the germinal centre reaction mentioned above, and studies in humans conducted by Ralf Kupper's group, one could speculate that the HLA binding IgM+ memory B cells detected in the RituxiCAN patients are either products of extrafollicular engagement with T cells, or early products of a germinal centre reaction (Pape et al., 2011, Dogan et al., 2009, Weisel et al., 2016, Seifert et al., 2015, Seifert and Küppers, 2009, Budeus et al., 2015). It is well established, that not all antibody secreting cells are long lived (Nutt et al., 2015). For example, it has

recently been shown in a cohort of patients with RA, that Rituximab treatment lead to a reduction in the levels of RA related antibodies, but not of tetanus toxoid specific or rotavirus specific antibodies (Herrera et al., 2014). This suggests that the maintenance of antibody titres to some antigens does not come from long lived plasma cells but from a continual activation of naïve or memory cells to produce short lived antibody secreting cells. It is therefore possible that the IgM+ memory B cells detected here represent the population of B cells that become activated to form new germinal centres once the IgG DSA titre has reduced to a certain level, as previously described in the mouse (Pape et al., 2011). Thus this re-activation of IgM+ memory B cells represents a new wave of immune activation (and antibody production) that could contribute to the destruction of the graft.

4.4.5 The ratio of IgM+ memory to IgM+ naïve B cells in the HLA binding B cell population may impact the IFNγ to Pure™ HLA proteins

The results in this chapter show that Pure™ HLA proteins can be used to stimulate an IFNγ response that is B cell dependent in some samples and B regulated in others. As with the results in chapter 3, where donor membrane proteins were used, this pattern of reactivity changed over time in the same patient. This provided the opportunity to correlate the IFNγ response with the phenotype of the HLA binding B cells. This analysis revealed that CD27 proved to be the best marker of memory for resolving any associations between the phenotype of the HLA binding B cells and the pattern of reactivity in response to the Pure™ HLA protein. When CD27 is used to define memory, the data suggests that a higher ratio of IgM+ memory cells to IgM+ naïve cells is associated with B dependent IFNγ production. It is possible that the balance of these two populations within the antigen specific B cell compartment has an effect on the outcome of the ELISpot, but where the balance lies is different in each patient. In one patient, a switch from B dependent IFNγ production to B regulated IFNγ production was associated with a switch from IgM+ memory B cells being the dominant phenotype in the HLA binding B cell population to IgM+ naïve B cells being the dominant population. In another patient, the IgM+ memory population was always more dominant than the IgM+ naïve population (the ratio of IgM+ memory:IgM+ naïve B cells was always at least 2), however, an increase in this ratio to 7 or above was associated with the IFNγ response switching from a non-reactive response to a reactive B dependent response at two time points.

There are of course limitations to the interpretation of the data due to the small number of patients that were studied. For example, the HLA A1 binding B cells were all overrepresented in the IgM+ memory population compared to the global B cell

population, but the samples that this data was derived from all came from the same patient. A much larger study is required to find more concrete patterns in the phenotype of the HLA binding B cells and how that relates to the pattern of reactivity in the IFNγ ELISpot. This would require a large panel of Pure™ HLA proteins to be used, and many patients with a variety of mismatched transplants. This was beyond the resources available for this thesis, but the preliminary data presented here will prove useful in designing such a study. In addition, the number of events in the HLA binding B cell gate is small which can result in small changes in phenotype (for example between the CD45RB+ and CD27+ populations) appearing very large when cell frequencies are compared as ratios as presented here. For the purpose of this thesis, no minimum number of events inside the HLA binding B cell gate was set. However a cut off was required that the number of events must be at least double that of the background gate in order to analyse the phenotype of the cells. The number of cells that could be stained was limited as the same sample was also used in the IFNγ ELISpot. To strengthen the robustness of the results in future studies, it would be wise to stain a much larger number of PBMCs in order to detect more events in the HLA binding B cell gate. To be able to achieve this whilst concomitantly carrying out the IFNγ ELISpot, freshly isolated PBMCs could be used to eliminate the problem encountered with cell loss due to the freeze/thaw procedure.

5 Results part 3

5.1 Introduction

One of the major aims of this thesis was to investigate the impact that the antigen specific B cells have on CD4+ T cell IFNγ production in the ELISpot assay. As patient samples were limited, the CMV gB model system was used to explore this aim. The experiments in this chapter were based around linking the IgM+ memory phenotype of CMV gB binding B cells with the ELISpot pattern of reactivity, with the aim of demonstrating that IgM+ memory B cells are the subset of B cells responsible for inducing antigen specific CD4+ IFNγ production. These experiments also sought to explore the mechanism by which B cells were regulating the IFNγ production in some samples.

A limitation of the ELISpot was discovered when the ELISpot was carried out on the same lymphocyte cone on a different day; the pattern of reactivity in response to the CMV gB was found to be variable. This could be due to a number of factors but most likely it is due to the freeze/thawing process and the number or frequency of CMV gB specific T and B cells that were contained within each vial of PBMCs that were frozen down. It was therefore decided that if the result of the ELISpot was to be correlated with results from a different assay, the same vial of cells must be thawed and used for both assays on the same day. In addition, any other experiments carried out would be interpreted independently of the results from previous assays carried out on the same leukocyte cone.

5.2 Results

5.2.1 B cell depletion leads to both B dependent and B regulated phenotypes in leukocyte cones when stimulated with CMV gB in the IFNγ ELISpot

The IFNγ ELISpot assay was carried out on CD8+ depleted PBMCs from the same 15 leukocyte cones used in Chapter 4 with CMV gB as the stimulating antigen. These ELISpots were carried out at the same time as the antigen binding B cell assay described in Chapter 4. Both reactive, B dependent and B regulated patterns of reactivity were observed. 3/15 of the leukocyte cones produced IFNγ above background when stimulated with CMV gB (Fig. 5.1 (a)). IFNγ production in 3/3 of these reactive cones was dependent on the presence of B cells (Fig. 5.1 (b)). A further 6 individuals became reactive to the protein post B cell depletion and were deemed B regulated (Fig. 5.1 (c)).

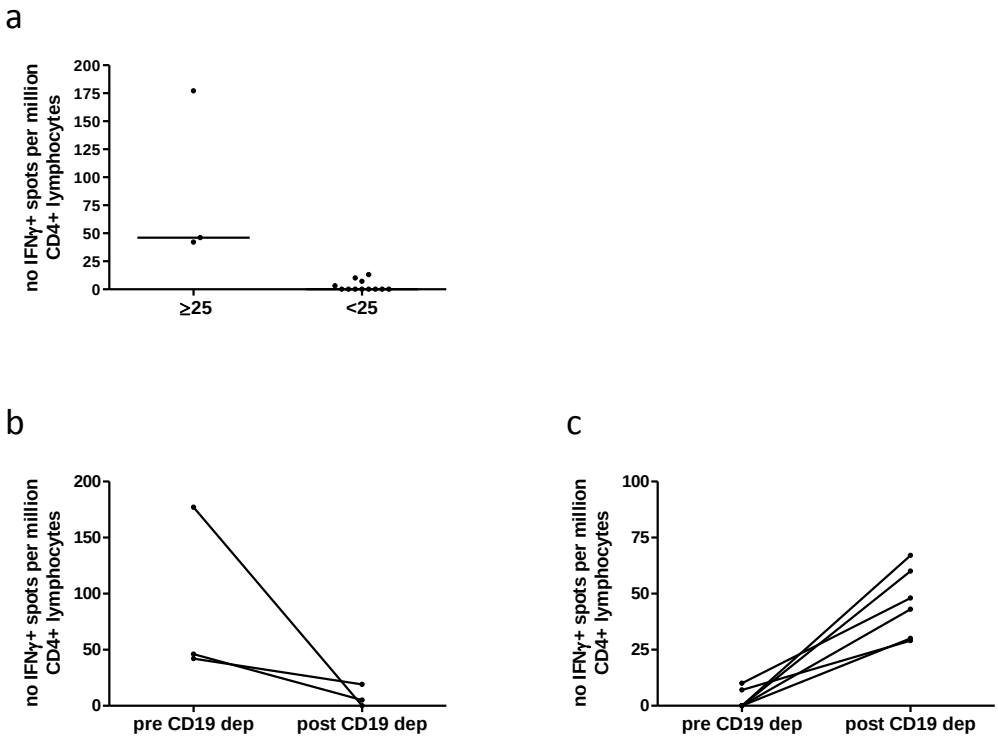

Figure 5.1 Impact of B cell depletion on 15 leukocyte cones when stimulated with CMV gB in the IFNγ ELISpot

(a) 3/15 individuals tested were deemed reactive when just CD8+ cells were depleted as they produced ≥25 IFNγ+ spots per million CD4+ lymphocytes. **(b)** When CD8+ and CD19+ cells were depleted, B dependency was revealed in these 3 individuals as IFNγ production decreased to <25 IFNγ+ spots per million CD4+ T cells in all 3 of these reactive individuals. **(c)** When CD8+ and CD19+ cells were depleted from the 12/15 non-reactive individuals, IFNγ increased to ≥25 IFNγ+ spots per million CD4+ T cells in 6/12 of them revealing B regulated reactivity.

5.2.2 CMV gB binding B cell phenotype does not correlate with the pattern of reactivity in the IFNγ ELISpot

It was hypothesised that the phenotype of the CMV gB binding B cells may correlate with the pattern of reactivity in response to CMV gB in the IFNγ ELISpot. The 15 leukocyte cones tested in 5.2.1 were therefore grouped according to the three patterns of reactivity observed; reactive, B dependent (n=3), reactive, B regulated (n=6) and non-reactive (n=6). The phenotype of their CMV gB binding B cells was compared between the three groups (Fig 5.2).

No significant differences were found between the three groups with respect to the frequency of transitional and non-transitional populations, IgM+ and IgG+ expressing populations or CD27 expressing populations (Fig. 5.2 (a), (b) & (c), $P>0.05$). No significant correlations were found when this analyses was extended to comparing the different B cell subsets according to their dual expression of IgM and CD27 (Fig. 5.2 (d) & (e), $P>0.05$). Similarly no correlations were found when the phenotype of the global B cell population was compared between the three groups (Fig. 5.3, $P>0.05$). In addition, no differences were found between the ratios of CD27+:CD27- or CD27+IgMhi:CD27-IgM+ populations in either the CMV gB binding B cell population or the global B cell population (Fig 5.4, $P>0.05$). All data was analysed using a Kruskall Wallis test with Dunns multiple comparison.

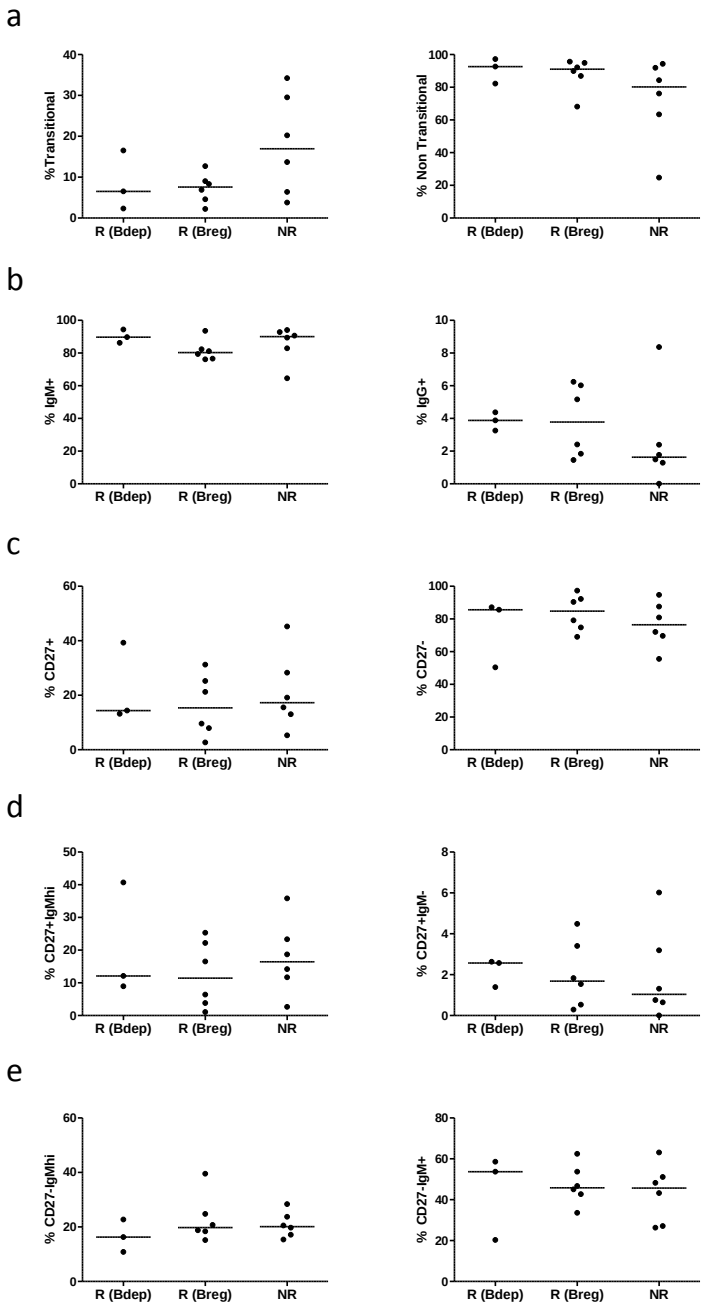

Figure 5.2 Correlating the phenotype of CMV gB binding B cells with the pattern of reactivity in the IFNγ ELISpot.

Leukocyte cones were grouped according to their pattern of reactivity to CMV gB in the IFNγ ELISpot. R (Bdep) = reactive, B dependent; R (Breg) = reactive, B regulated; NR = non-reactive. The frequencies of each B cell subset within the CMV gB binding B cell gate was compared between the three groups using a Kruskall Wallis test with Dunns multiple comparison test ($p>0.05$ for all analyses). Black line on graphs represents the median.

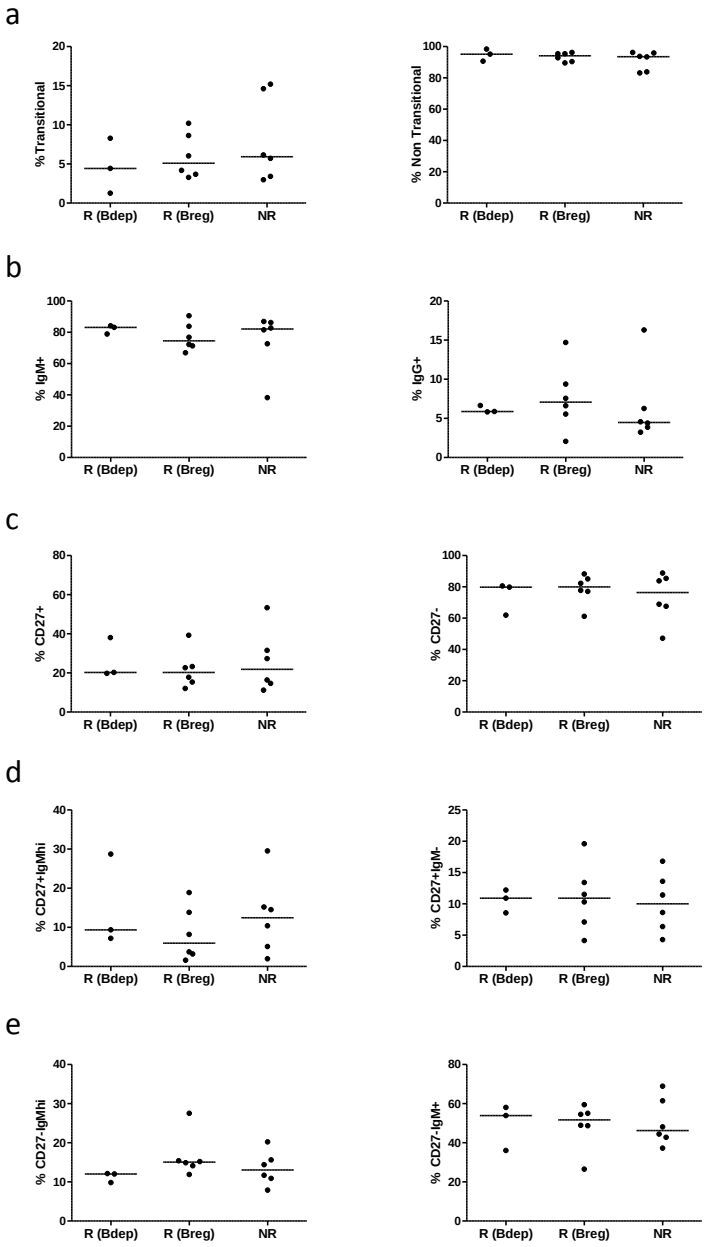

Figure 5.3 Correlating the phenotype of the global B cell population with the pattern of reactivity in the IFNγ ELISpot.

Leukocyte cones were grouped according to their pattern of reactivity to CMV gB in the IFNγ ELISpot. R (Bdep) = reactive, B dependent; R (Breg) = reactive, B regulated; NR = non-reactive. The frequencies of each B cell subset within the CD19+ gate was compared between the three groups using a Kruskall Wallis test with Dunns multiple comparison test ($p>0.05$ for all analyses). Black line on graphs represents the median.

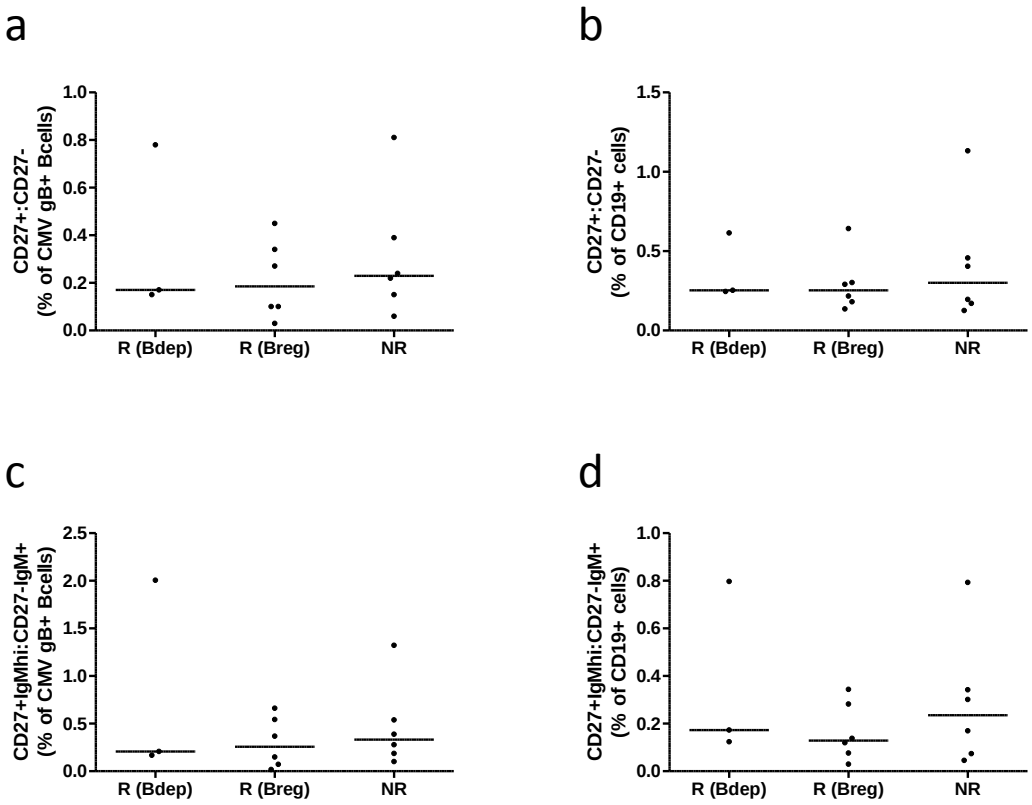

Figure 5.4 Correlating the ratio of memory to naïve or IgM+ memory to naïve B cells with the pattern of reactivity in IFNγ ELISpot

Leukocyte cones were grouped according to their pattern of reactivity to CMV gB in the IFNγ ELISpot. R (Bdep) = reactive, B dependent; R (Breg) = reactive, B regulated; NR = non-reactive. The ratio of memory to naïve B cells (CD27+:CD27-) in both the CMV gB binding population **(a)** and the global B cell population **(b)** was compared between groups. The ratio of IgM+ memory and IgM+ naive B cells (CD27+IgMhi:CD27-IgM+) in both the CMV gB binding Population **(c)** and the global B cell population **(d)** was compared between groups. Groups were compared using a Kruskall Wallis test with Dunns multiple comparison test ($p>0.05$ for all analyses). Black line on graphs represents the median.

5.2.3 Using an experimental approach to dissect the role that B cells play in producing different patterns of reactivity in the IFNγ ELISpot.

As the analysis carried out in section 5.2.2 did not reveal any straightforward correlations between the ELISpot pattern of reactivity and CMV gB binding B cell phenotype, a series of experiments was conducted with the aim of gaining an insight into why different samples display different patterns of reactivity to an antigen in the IFNγ ELISpot.

5.2.3.1 Do B cells suppress IFNγ production in the CMV gB ELISpot assay by secreting IL-10?

IL-10 production is one of the defining characteristics of regulatory B cells and it is required to suppress a T cell response (Blair et al., 2010, Flores-Borja et al., 2013, Iwata et al., 2011, Das et al., 2012b, Carter et al., 2012, Cherukuri et al., 2014, Bouaziz et al., 2010). An IL-10 blocking antibody was therefore added to the CMV gB ELISpot assay to assess whether blocking IL-10 would mirror the effect observed when B cells were depleted and a Breg response was observed. Figure 5.5 shows the results from 5 different leukocyte cones. When B cells are present and IL-10 is blocked, IFNγ always increases. When B cells are depleted and IL-10 is blocked, IFNγ production increases further, but to varying degrees depending on the individual. The cones in Figure 5.5 (a) and (b) have a reactive, B regulated response to the CMV gB when IL-10 is not blocked. There appears to be an additive effect on IFNγ production when IL-10 is blocked and B cells are depleted because the increase in IFNγ production post B cell depletion is similar in the isotype control wells and the anti-IL-10 wells when B cells are depleted. This suggests that in these two cones B cells may not be acting through IL-10 production to suppress IFNγ production, as it would be unlikely to see the additive effect of blocking IL-10 and depleting B cells if this was the case. Interestingly, this additional increase in IFNγ was also observed in the individuals represented in Fig. 5.5 (c) and (d), despite there being no evidence of B regulation in the isotype control wells. The cone in Figure 5.5 (e) has a reactive, B dependent response to the CMV gB protein, however when B cells are depleted in the presence of the IL-10 blocking antibody, the B dependency is not apparent, in fact there is a slight increase in IFNγ production. It appears that in this sample, the effect of blocking IL-10 is so powerful that it drowns out any contribution that the B cells are making to the IFNγ production.

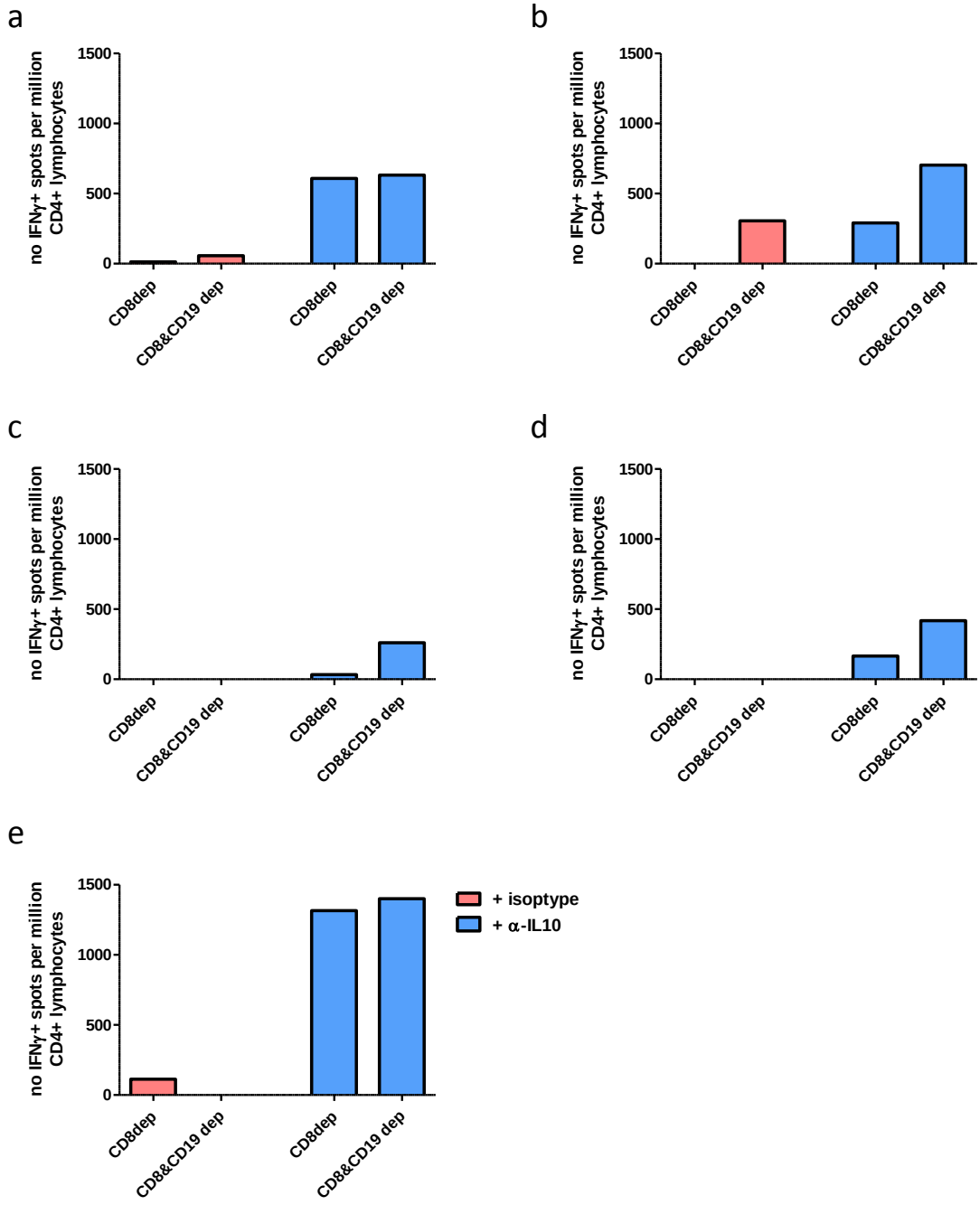

Figure 5.5 Blocking IL-10 in the IFNγ ELISpot
CMV gB stimulated, CD8+ and CD8+/CD19+ depleted IFNγ ELISpots were set up in the presence of an anti-IL10 blocking antibody or the appropriate isotype control. Each graph represents one leukocyte cone (**(a)-(e)**). Pink bars represent the isotype control wells and blue bars represent the wells where IL-10 blocking antibody was added. IFNγ spots per million CD4+ T cells of ≥ 25 was considered a response.

5.2.3.2 Intracellular cytokine staining is not sensitive enough to detect T or B cell derived IFNγ or IL-10 but does detect IFNγ+ NK cells.

Figure 5.5 suggests that B cells may not be suppressing IFNγ production via an IL-10 mediated mechanism, however, the data does not definitively show this. Intracellular cytokine staining was therefore carried out in PBMC that were cultured under the same conditions used in the ELISpot to investigate further. This also served as an opportunity to confirm that the IFNγ reduction seen in B cell dependent samples was not because B cells were producing the IFNγ. Cell cultures were set up to replicate the conditions used in the ELISpot wells with the modification that Brefeldin A was added 5 hours before the end of the 24 hour incubation. Polyclonal stimulus anti-CD3/CD28 beads were used as a control, as per the ELISpot protocol.

Table 5.1 and 5.2 show the results obtained from 5 leukocyte cones tested. The results indicate that intracellular staining is not a sensitive enough technique to detect antigen specific T cell IFNγ production, as IFNγ production was only detected when the PBMC were stimulated polyclonally (Table 5.1). However, concomitant ELISpots were not carried out to confirm this. A very small proportion of NK cells were detected above background as IFNγ+ in 3/5 individuals when CD8 cells were depleted (median 0.272%, range 0.154%-0.418%) and 3/5 when CD8/CD19 cells were depleted (median 0.174% and range 0.115-0.94%) (Table 5.1). Whether the NK cells are being activated by the antigen, for example via TLRs, or are just non-specifically producing IFNγ from the freeze thawing and culturing process remains unclear, but it is an important finding that requires further investigation. A similar proportion of NK cells were IFNγ+ as the CD4+ T cells when anti-CD3/CD28 beads were used (median 7.33%, range 4.43%-10.46% for CD4+T cells and median 5.8%, range 2.966%-14.328% for NK cells). B cells did not make IFNγ in the presence of either stimulus.

IL-10+ cells were not detected in the B, T or NK cell populations when stimulated with CMV gB. IL-10+ T cells were detected in 5/5 individuals when polyclonally stimulated with anti-CD3/CD28 beads (median 1.622, range 0.53%-5.271% for CD8 depleted, median 1.644%, range 0.715%-6.58% for CD8+&CD19+ depleted). When a Wilcoxon pairs signed rank test was used to compare this population pre and post B cell depletion, no difference was found ($P>0.05$). A very small proportion of IL-10+ NK cells was detected in 2/5 individuals when stimulated with anti-CD3/CD28 beads, although these individuals differed between the CD8+ and CD8+&CD19+ conditions.

Table 5.1 IFNγ production in response to CMV gB measured by intracellular staining.

	B cells			CD4+ T cells			NK cells		
Cone ID	Media	CMV gB	CD3/CD28	Media	CMV gB	CD3/CD28	Media	CMV gB	CD3/CD28
Cone 27	0	0	0.128	0	0	8.53	0.006	0.272	1.98
Cone 28	0	0	0.026	0	0	4.43	0.161	0.418	6.793
Cone 32	0	0	0	0	0	7.33	0	0.154	4.11
Cone 34	0.012	0	0	0	0	4.52	0	0	5.8
Cone 35	0	0	0.07	0	0	10.46	0.94	0.54	12.449
Cone 27	NA			0.041	0	8.63	0	0.115	2.966
Cone 28				0	0.084	7.9	0.152	0.174	14.328
Cone 32				0	0	8.71	0.298	0	5.82
Cone 34				0	0	4.84	0	0	6.674
Cone 35				0	0	12.11	0.474	0.94	12.037

Figures represent the percentage of IFNγ+ events detected after different stimulation conditions. CD8 depleted PBMC are in pink, CD8/CD19 depleted PBMC are in blue. An isotype control was used to gate on IFNγ+ cells within B cells (CD19+), CD4 T cells (CD3+CD4+) and NK cells (CD3-CD56+) and the frequency of isotype control+ events was subtracted from the frequency of IFNγ+ events.

Table 5.2 IL-10 production in response to CMV gB measured by intracellular staining.

	B cells			CD4+ T cells			NK cells		
Cone ID	Media	CMV gB	CD3/CD28	Media	CMV gB	CD3/CD28	Media	CMV gB	CD3/CD28
Cone 27	0	0	0.027	0	0	2.259	0.014	0	0
Cone 28	0	0	0.147	0	0	1.662	0	0	0.023
Cone 32	0	0	0.148	0	0	0.889	0	0	0
Cone 34	0	0	0.136	0	0	0.53	0	0	0
Cone 35	0	0	0.352	0	0	5.271	0	0	0.061
Cone 27	NA			0.042	0	2.484	0.048	0	0
Cone 28				0	0	1.644	0	0	0
Cone 32				0	0	0.715	0	0	0.038
Cone 34				0	0	1.203	0	0	0.092
Cone 35				0	0	6.58	0	0	0

Figures represent the percentage of IL-10+ events detected after different stimulation conditions. CD8 depleted PBMC are in pink, CD8/CD19 depleted PBMC are in blue. An isotype control was used to gate on IL-10+ cells within B cells (CD19+), CD4 T cells (CD3+CD4+) and NK cells (CD3-CD56+) and the frequency of isotype control+ events was subtracted from the frequency of IL-10+ events.

5.2.3.3 Enriching for different B cell populations impacts reactivity to the CMV gB antigen

As the intracellular staining was not deemed suitable for using in an antigen specific system, a different approach was taken. This involved modifying the ELISpot in a series of depletion and add back experiments of different B cell subsets in order to dissect out the role that each B cell subset plays in the ELISpot assay. It seemed logical to start with attempting to deplete the CMV gB binding B cells as this would be the best way of directly showing that the antigen binding B cell population is impacting IFNγ production in the ELISpot.

Several attempts were made using FACS sorting as a way of depleting populations from PBMC as this is the best way to obtain pure populations of different subsets of cells. However, it was deemed that this technique was incompatible with the ELISpot as it rendered the cells un-responsive and incapable of producing IFNγ.

In an attempt to overcome this problem and to conserve the T cells, PBMC were passed through the sorter and the relevant B cell population was sorted and collected before being added back to CD8+ & CD19+ depleted PBMC that had not been passed through the sorter. However, this approach did not improve IFNγ production.

With a lack of success using FACS sorting, a compromise was made by using magnetic beads to isolate or deplete different B cell populations. This is a more gentle approach but the populations obtained are less pure. Initially, the CMV gB binding B cells were isolated from the whole B cell population using anti-PE magnetic beads which would bind to the B cell-gB-Streptavidin PE complex. This only resulted in a 50% pure population (see Figure 2.6 for dot plot). It was therefore decided that this approach would not yield robust enough results, as a much purer population of the CMV gB binding B cells would be necessary to categorically demonstrate that they are the B cells that are influencing IFNγ production. As an alternative, it was decided that the hypothesis that different B cell subsets impact IFNγ production in different ways would be tested. This was done by using anti-CD27 magnetic beads to separate the B cells into CD27+ (memory) and CD27- (naïve) populations. Separating the B cells into subsets according to the co-expression of IgM and CD27 would have been more ideal given the results described in Chapter 4, however this approach was deemed unsuitable as it would have involved using antibodies that bound the IgM BCR and therefore potentially would have interfered with the subsequent binding and

internalisation of the CMV gB protein in the ELISpot assay, or possibly have polyclonally activated the B cells.

B cells were initially isolated by negative selection and then incubated with anti-CD27 labelled magnetic beads and passed through a magnetic column. The CD27- B cells were collected in the flow through and the CD27+ cells were removed from the column.

Each fraction was counted and added back to CD8+&CD19+ depleted PBMC and used in the ELISpot assay. The number of CD27- and CD27+ B cell fractions were added back to the PBMC according to the frequency of these subsets in the whole PBMC population, which was obtained from previous phenotyping of these cones. This resulted in populations of PBMC that were enriched for either CD27+ or CD27- B cells as shown in Figure 5.6. Isolated CD19+ cells were also added back to CD8+&CD19+ depleted PBMC to illustrate that the same result in the ELISpot assay is obtained when CD19+ cells are depleted and then added back.

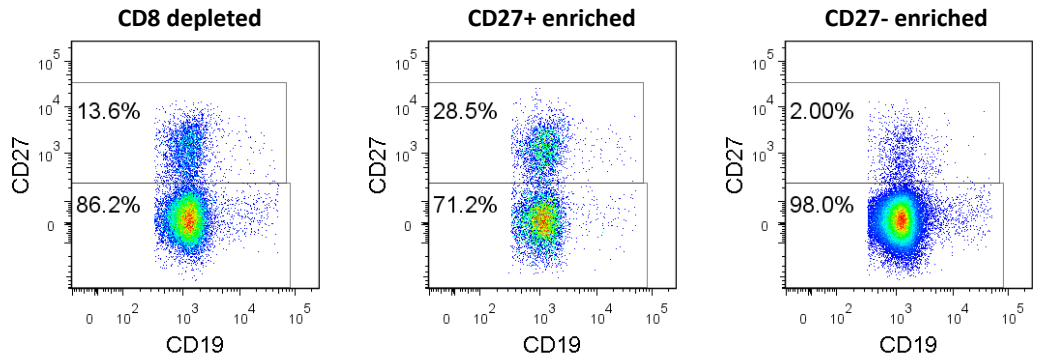

Figure 5.6 Example dot plots post CD27+ and CD27- B cell enrichment in the ELISpot wells

Figure 5.7 (a) and (b) shows two individuals that were non-reactive when CD19+ cells were either present or depleted. When the CD27+ enriched PBMC were added to the ELISpot, IFNγ production increased, a result that was not observed with the CD27- enriched PBMC. Of note, in (b) IFNγ increased to just shy of the cut off to be deemed a reactive response at 24 IFNγ spots per million CD4+ T cells. Additionally, Figure 5.7 (c) shows an individual who had a non-reactive, B regulated response that produced IFNγ when CD27+ enriched PBMC were added to the ELISpot, but not when the CD27- enriched PBMC were used. These results therefore suggest that CD27+ B cells support T cell IFNγ production and that CD27- B cells do not. The data from Figure 5.7 (c) also suggests that the CD27- B cell population may be suppressing T cell IFNγ production in this individual.

To investigate whether it is transitional B cells within the CD27- population that are responsible for suppressing the IFNγ production, CD10+ cells were depleted from isolated B cells. Both Dynabead® and MACS bead systems were used for this process but neither produced a level of CD10+ depletion that was satisfactory and so the ELISpot data that was produced from these experiments is not robust enough to include in this thesis.

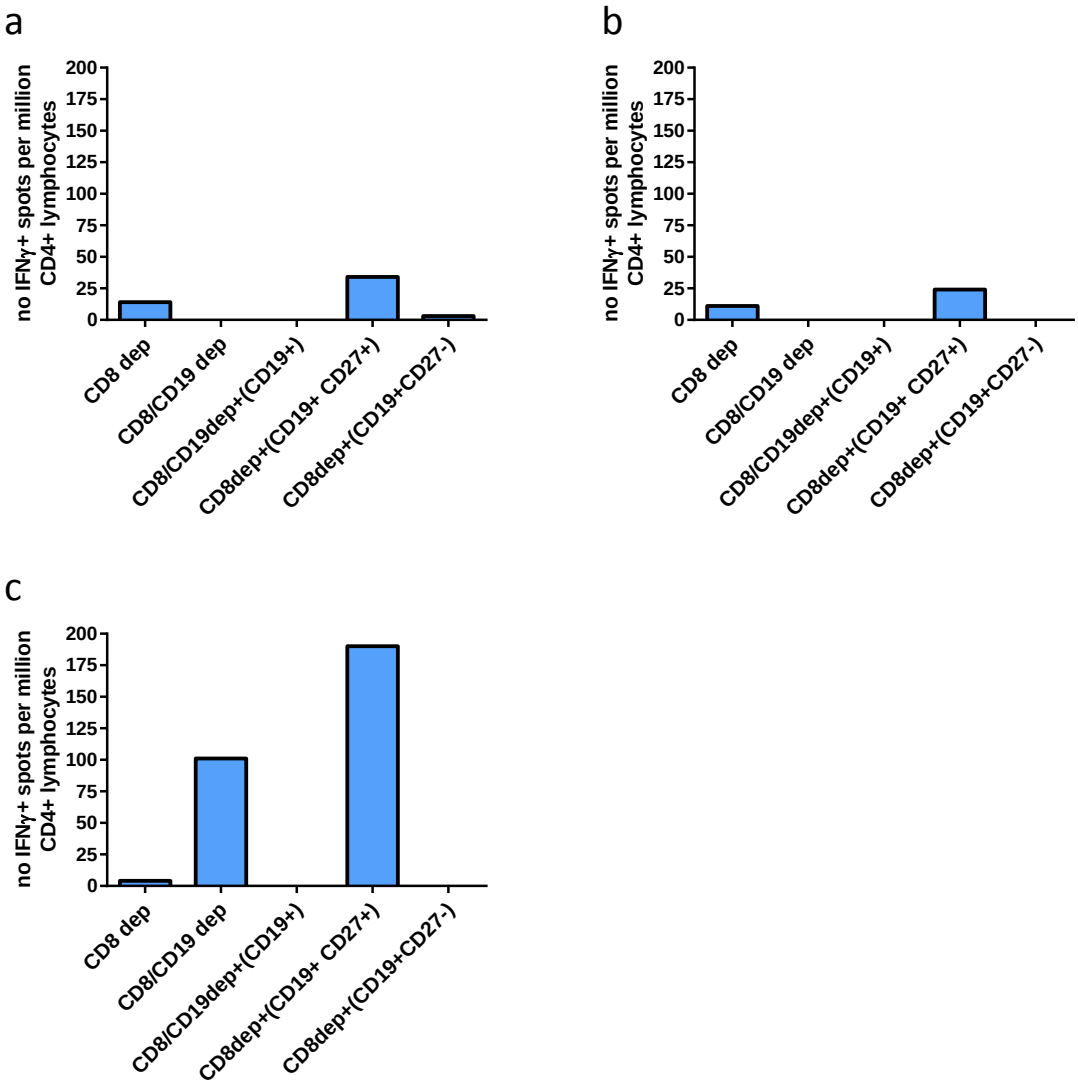

Figure 5.7 CD27+ B cells support IFNγ production in response to CMV gB.
(a-c) Each graph represents a different leukocyte cone. Adding isolated B cells back to the ELISpot reproduces the same result observed in just CD8 depleted B cells. Adding CD27+ B cell enriched PBMC supports IFNγ production: a substantial increase was observed in **(c)** and a moderate increase in IFNγ production was observed in **(a)** and **(b)**. Adding back CD27- B cell enriched PBMC does not support IFNγ production.

5.2.4 HLA DR and CD86 are expressed more brightly on CMV gB binding B cells compared to the overall B cell population

As the data presented in section 5.2.3.3 suggests that memory B cells support T cell IFNγ production, it was hypothesised that memory B cells may express molecules associated with antigen presentation at a higher level than naive B cells. Therefore, the surface level expression of HLA DR and CD86 on the CMV gB binding B cells and the whole B cell population was measured using flow cytometry (Fig. 5.8). The B cell phenotyping panel used in results chapter 4 was modified to include HLA DR and CD86, so CD24 and CD38 were omitted and replaced with CD10 to define transitional B cells. CD27 was removed and CD45RB was used to define memory B cells. In the majority of individuals, close to 100% of their B cells express HLA DR. This was observed in both the overall B cell population (median 99.7%, range 97.8-99.9%) and the CMV gB binding B cell population (median 99.5%, range 97.7-99.9%). When the frequency of HLA DR+ B cells within each subset was analysed, this revealed that there were no differences between the whole B cell population and the CMV gB binding B cell population, with the exception of the CD45RB+IgM- subset which had a lower proportion of B cells that were HLA DR+ in the CMV gB binding population (Fig. 5.9 (a), median 90.1% and range 73.7-100%, P=0.0049). The MFI (mean fluorescence intensity) of HLA DR expression is different on each B cell subset with CD45RB-IgMhi and CD45RB-IgM+ B cells expressing it most brightly (Fig. 5.9 (b)). Interestingly, HLA DR expression was brighter on the CMV gB binding B cell population than the overall B cell population in all B cell subsets apart from the CD45RB-IgM- subset (Fig. 5.10). This difference was most striking with the transitional population and memory populations CD45RB+IgMhi and CD45RB+IgM- (Fig. 5.10 (a),(b) &(c), P=0.0010 for all).

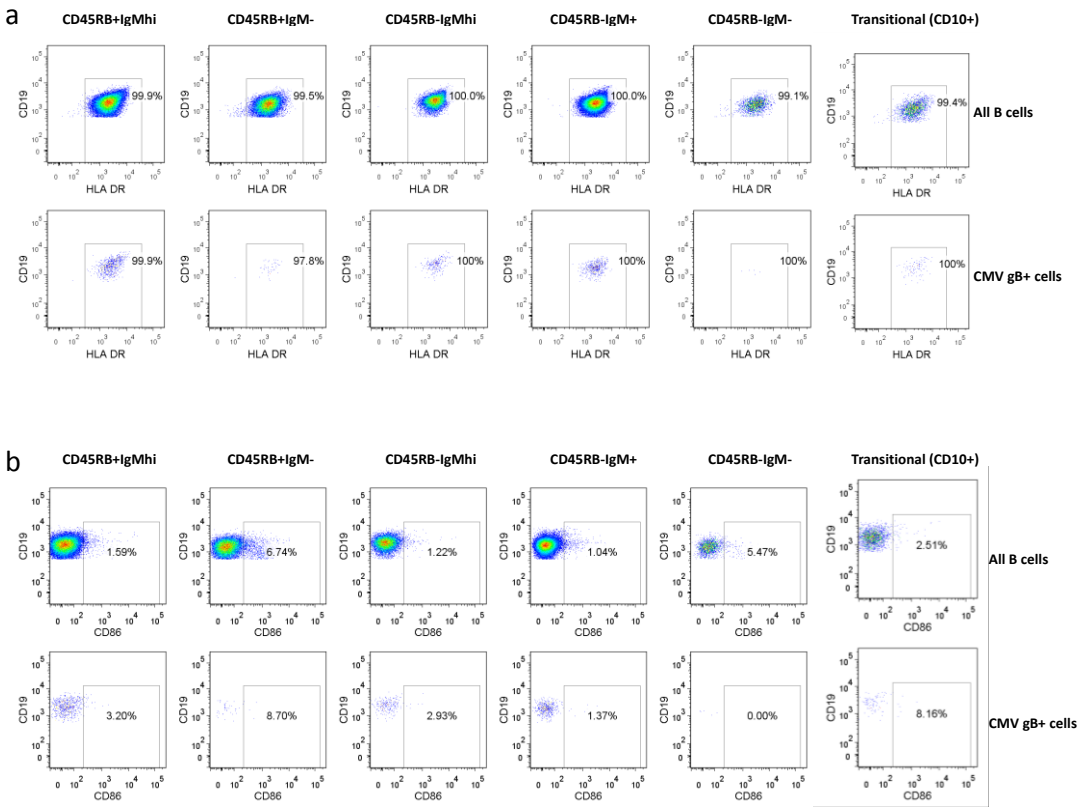

Figure 5.8 Representative dot plots of HLA DR (a) and CD86 (b) expression on B cells and CMV gB binding B cells.
B cells were initially divided into Transitional (CD10+) and non-transitional (CD10-). Non-transitional B cells were then divided further into subsets based on CD45RB and IgM expression. Each subset of non-transitional B cells is shown here.

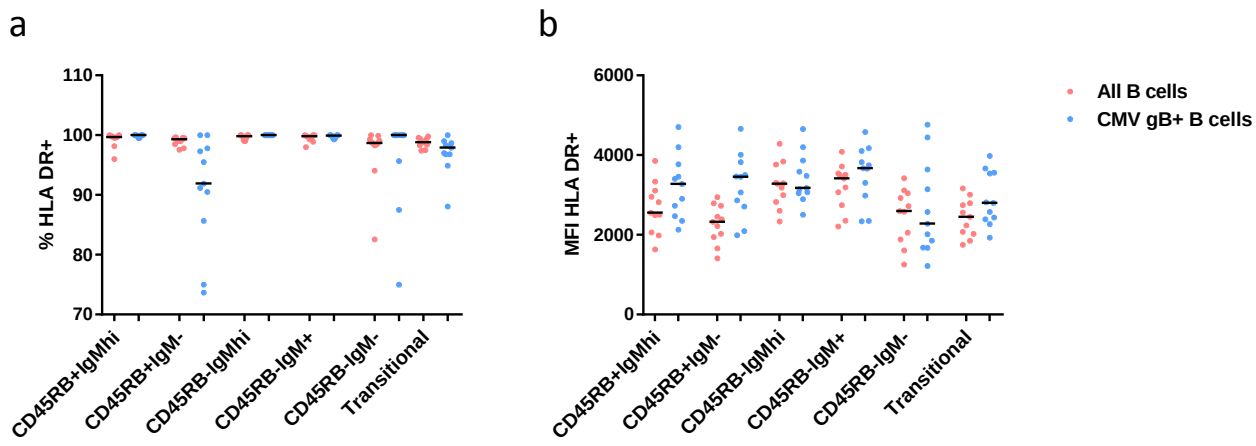

Figure 5.9 Expression of HLA DR on B cells and CMV gB binding B cells.
(a) HLA DR was gated on according to the isotype control and applied to each B cell subset within the CD19+ gate and the CMV gB binding B cell gate. **(b)** MFI of the HLA DR+ population within each B cell subset. Black lines represent the median of the 12 leukocyte cones tested.

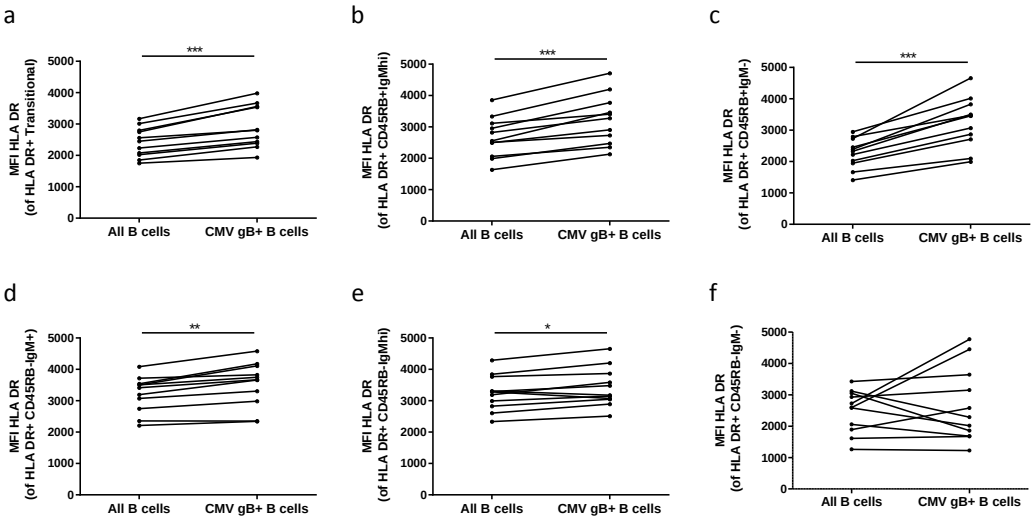

Figure 5.10 Comparison of HLA DR expression on B cell subsets within the whole B cell population and the CMV gB binding population

The mean fluorescence intensity of HLA DR expression on the different B cell subsets was compared between the overall B cell population and the CMV gB+ binding B cell population. HLA DR was expressed more brightly on the CMV gB binding population on all subsets apart from the CD45RB-IgM- subset. P = 0.0010 for **(a) (b)** and **(c)**, P= 0.0244 for **(d)**, P=0.0244 for **(e)**. P values obtained using a Wilcoxon matched pairs signed rank test.

A median of 2.4% (range 1.15-4.52) of B cells and 5.53% (range 2.7-11.2) of CMV gB+ B cells express CD86. Different B cell subsets contain different frequencies of CD86+ B cells (Fig 5.11 (a)). Switched memory B cells (CD45RB+IgM-) B cells contain the highest frequency of CD86+ B cells (median 6.59%, range 2.91-14.4%) and Naïve (CD45RB-IgM+) the least (median 1.04%, range 0.483-1.91%). The CMV gB binding B cell population contains a higher frequency of CD86+ B cells than the overall B cell population in all subsets apart from CD45RB-IgM- B cells (Fig. 5.12). This difference was most striking in the Transitional, IgM+ memory (CD45RB+IgMhi+) and naïve subsets (Fig. 5.12 (a), (b) and (d), P=0.0010 for all).

Figure 5.11 (b) shows that the MFI of CD86 expression was highest on the transitional B cells (median 27.1, range 15.5-53.6) and lowest on the CD45RB-IgMhi B cell subset (median 15.2, range 22.4-8.99). As with HLA DR expression, CD86 expression was brighter on the CMV gB binding B cell population compared to the overall B cell population in all B cell subsets apart from the CD45RB-IgM- subset (Fig. 5.13). This difference was most striking in the transitional and CD45RB-IgMhi populations (Fig. 5.13 (a) and (b), P=0.0010 for both).

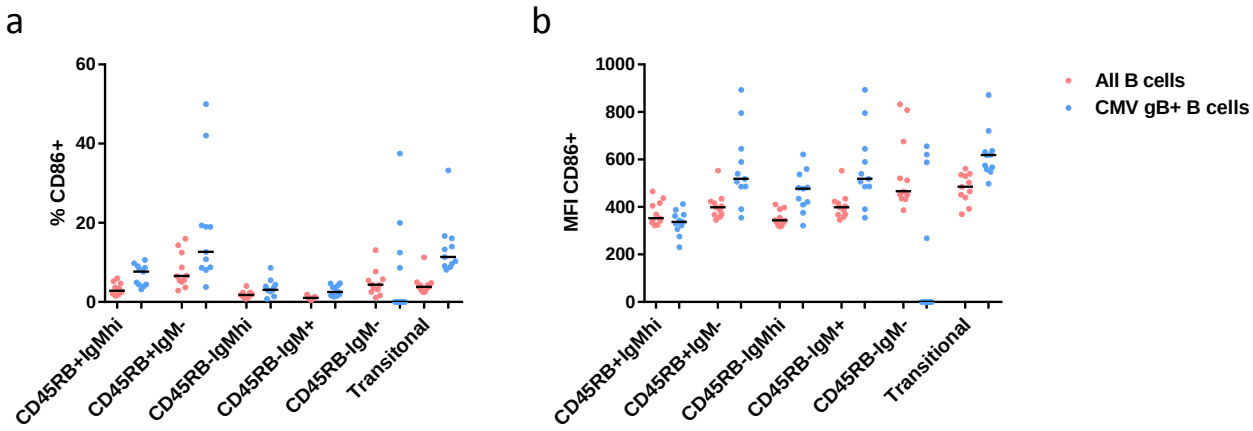

Figure 5.11 Expression of CD86 on B cells and CMV gB binding B cells.
(a) CD86 was gated on according to the isotype control and applied to each B cell subset within the CD19+ gate and the CMV gB binding B cell gate. **(b)** MFI of the CD86+ population within each B cell subset. Black lines represent the median of the 12 leukocyte cones tested.

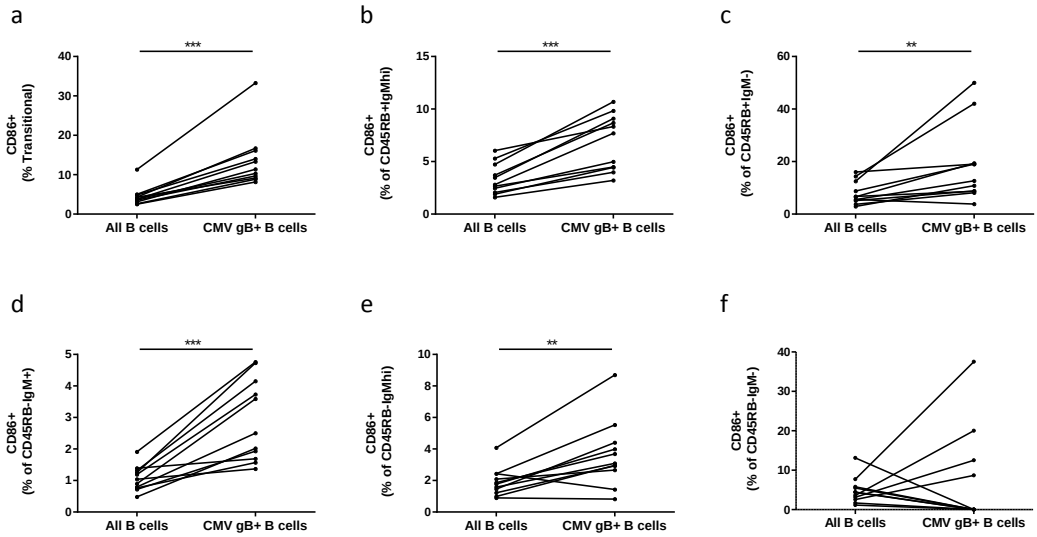

Figure 5.12 Comparison of CD86+ B cell subsets within the whole B cell population and the CMV gB binding population.

The frequency of CD86 expressing cells in the different B cell subsets was compared between the overall B cell population and the CMV gB+ binding B cell population. The CMV gB binding population had more CD86+ cells than the overall B cell population in all subsets apart from the CD45RB-IgM- population. P= 0.0010 for **(a)**, **(b)** and **(d)**, P= 0.0020 for **(c)**, P=0.0068 for **(e)**. P values obtained using a Wilcoxon matched pairs signed rank test.

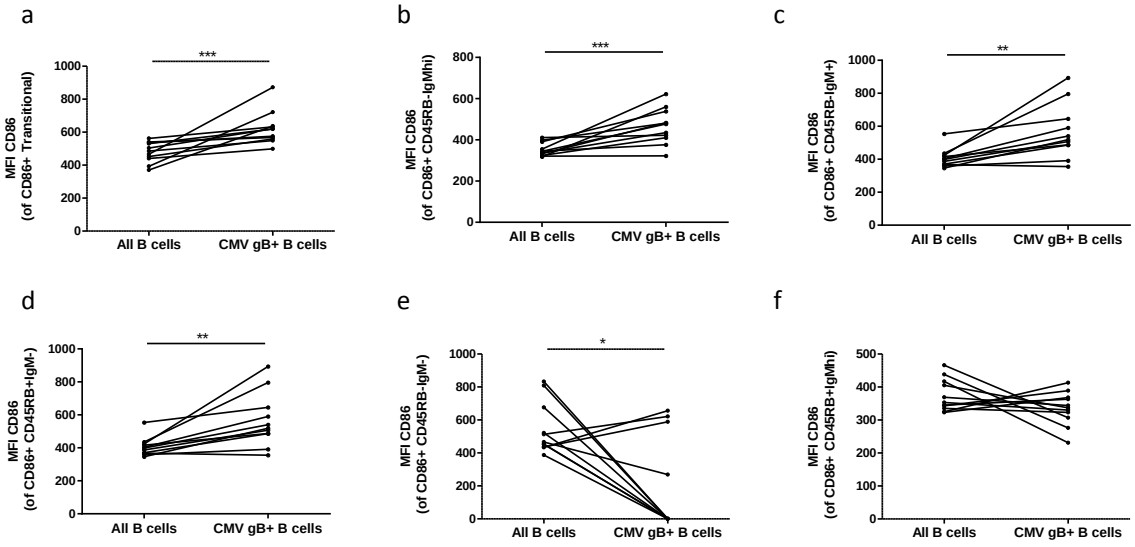

Figure 5.13 Comparison of CD86 expression on B cell subsets within the whole B cell population and the CMV gB binding population

The mean fluorescence intensity of CD86 expression on the different B cell subsets was compared between the overall B cell population and the CMV gB+ binding B cell population. CD86 was expressed more brightly on the CMV gB binding population on the CD45RB+IgM- **(a)**, CD45RB-IgM+ **(b)** and CD45RB-IgMhi **(c)** populations. P=0.0020 for **(a)** and **(b)**, P=0.0010 for **(c)**. P values obtained using a Wilcoxon matched pairs signed rank test.

5.2.5 BAFFr is not differentially expressed on different B cell subsets.

Therapeutic agents that target B cells are not limited to Rituximab. For example, Belimumab, a monoclonal antibody specific for BAFF receptor (BAFFr), is currently being used in a clinical trial to prevent kidney transplant rejection (Clinicaltrials.gov.uk identifier NCT01536379). Atacicept, a fusion protein that binds B cell survival factors BAFF and APRIL, has been used in a number of clinical trials to treat RA, SLE and MS with varying degrees of success (van Vollenhoven et al., 2011), Clinicaltrials.gov.uk identifier NCT01972568 & (Hartung and Kieseier, 2010), Clinicaltrials.gov.uk identifier NCT00642902).

Selectively depleting pathogenic B cell subsets and conserving those that are protective could potentially be a more beneficial treatment for chronic rejection than pan B cell depletion as is the case with Rituximab. Surface expression of BAFFr and TACI on different B cell subsets was therefore measured to investigate whether there is any potential to preferentially target specific B cell subsets with the use of either Belimumab or Atacicept.

PBMC were stained with the same antibody panel used in section 5.2.4 with BAFFr and TACI replacing HLA DR and CD86. Unfortunately, positive TACI staining could not be achieved despite titrating the antibody, staining different individuals, following recommendations by the manufacturer and using two different vials of TACI antibody conjugated to two different fluorochromes (Fig. 5.14 (a)).

The antibody for BAFFr however stained very clearly (Fig. 5.14 (b)). Figure 5.15 shows that the majority of individuals have BAFFr expressed on the vast majority of their B cells (median 99.4%, range 96.3-100%) with the exception of one individual who did not have BAFFr expressed on their B cells. A slightly lower frequency of transitional B cells expressed BAFFr (median 93.2, range 70.1-98.3). No difference in BAFFr expression was detected between the CMV gB binding B cell population and the overall B cell population (Fig. 5.15 (a) & (b)).

When the MFI was analysed, BAFFr was found to be most brightly expressed on Naïve B cells (CD45RB-IgM+, median 1205 and range 769-1915) and least on transitional B cells (Fig. 5.15 (b), median 771, range 394-1484, P=0.0010). Note, the individual who did not express BAFFr on their B cells was removed from the analysis used to derive these figures.

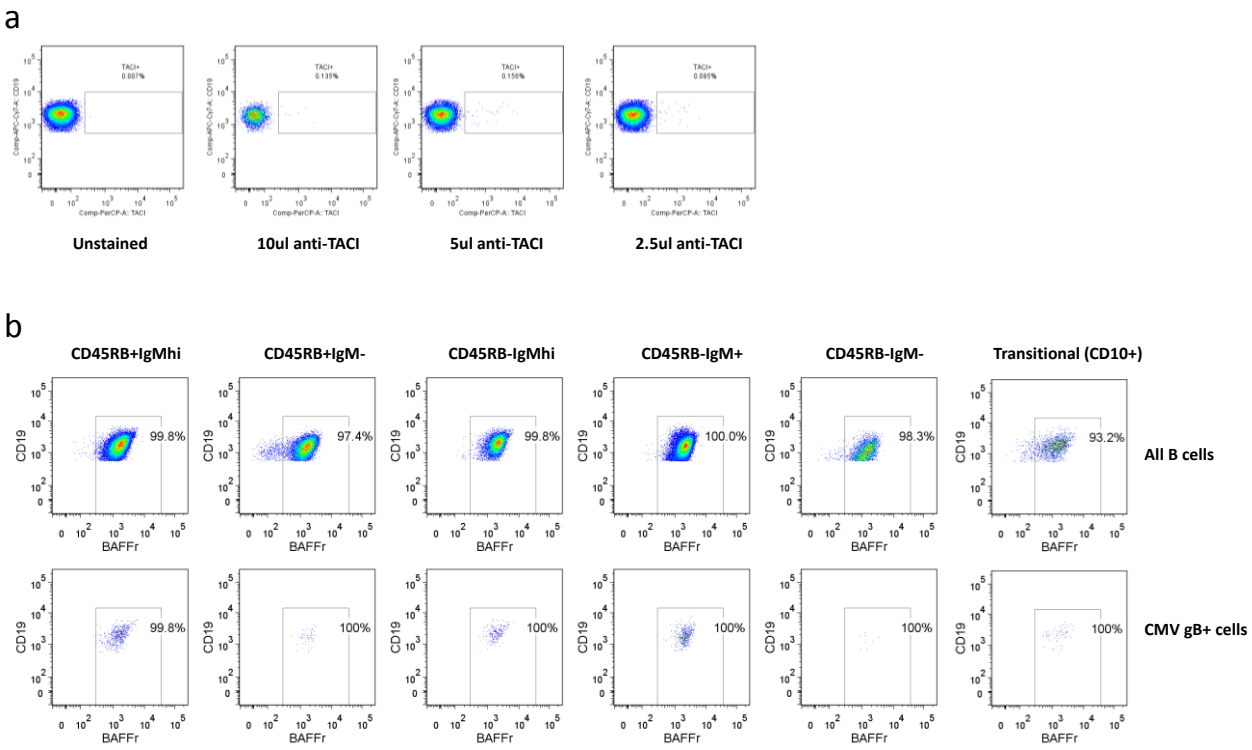

Figure 5.14 Representative dot plots of TACI and BAFFr expression on B cells and CMV gB binding B cells.
(a) Positive TACI events were not detected with any volume of antibody used. **(b)** For BAFFr staining analysis, B cells were initially divided into Transitional (CD10+) and non-transitional (CD10-). Non-transitional B cells were then divided further into subsets based on CD45RB and IgM expression. Each subset of non-transitional B cells is shown here.

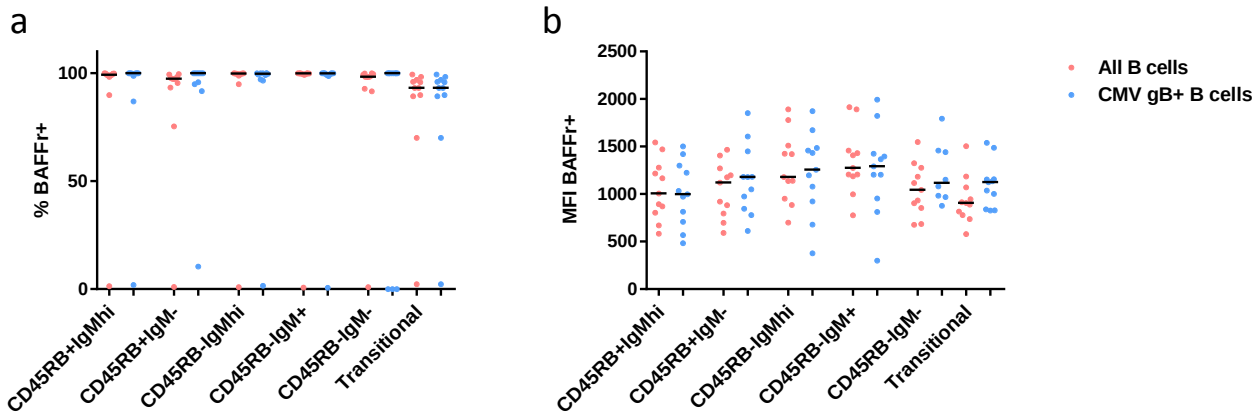

Figure 5.15 Expression of BAFFr on B cells and CMV gB binding B cells
(a) BAFFr was gated on according to the isotype control and applied to each B cell subset within the CD19+ gate and the CMV gB binding B cell gate. **(b)** The MFI represents the BAFFr+ population of each of the subsets. Black lines represent the median of the 12 leukocyte cones tested.

5.3 Key points in Chapter 5

1. The phenotype of CMV gB binding B cells does not correlate with the pattern of reactivity observed when PBMC from leukocyte cones are stimulated with CMV gB in the IFNγ ELISpot.

2. When B cells are depleted and IL-10 is blocked in the IFNγ ELISpot, IFNγ production is greater than when B cells are present and IL-10 is blocked.

3. Enriching for CD27+ B cells in the IFNγ ELISpot leads to increased IFNγ production whereas enriching for CD27- B cells does not.

4. Class switched memory B cells, IgM+ memory B cells and Transitional B cells contain greater frequencies of CD86 expressing B cells than naïve B cells. CMV gB binding B cells contain a higher proportion of CD86 expressing B cells in all subsets than the overall B cell population (apart from CD45RB-IgM-), and both HLA DR and CD86 are more brightly expressed on CMV gB binding B cells compared to the overall B cell population.

5. BAFFr is not differentially expressed on B cell subsets or between the CMV gB binding B cell population and the overall B cell population.

5.4 Discussion

The major aim of the final results chapter of this thesis was to investigate further the results obtained in chapters 3 and 4. Gathering in vitro mechanistic data to build an argument is always challenging. Here, various strategies were tried to investigate the impact that different B cell subsets have on the outcome of the IFNγ ELISpot assay. Due to limited patient material, frozen aliquots of PBMCs from a cohort of leukocyte cones were used in combination with CMV gB to conduct these experiments. It became apparent that a major limitation of this approach was that the pattern of reactivity observed in the IFNγ ELISpot would differ in the same sample when thawed on different days. To make use of the data collected, whilst not compromising the integrity of it, it was decided that the data would only be interpreted on an individual experiment basis. All assays conducted on the vial of cells that was thawed could be correlated with each other, but assays conducted on different days could not. For example, where the CMV gB binding B cell phenotyping data was correlated with the pattern of reactivity, these assays were set up on the same day from the same starting suspension of PBMCs.

Blocking IL-10 in the ELISpot assay revealed that IL-10 is suppressing the production of IFNγ from many cells. When B cells were depleted in addition to blocking IL-10, IFNγ always increased, regardless of whether the initial pattern of reactivity was B regulated or not. These results suggest that B cells may be partially suppressing IFNγ production in an IL-10 independent manner as their depletion heightened any effects that were observed when just the IL-10 blocking antibody was used. However, the involvement of B cell derived IL-10 could not be ruled out, so intracellular staining was used to try and detect B cell specific IL-10 when PBMC were stimulated in the same way as in the ELISpot assay. Unfortunately, it was very difficult to detect B cell derived IL-10 or T cell derived IFNγ. Intracellular staining is not as sensitive technique as the ELISpot, which is often regarded as the most sensitive technique for detecting antigen specific responses, and this result may just be evidence of that. It does not prove that B cells or T cells were not secreting IL-10 or IFNγ in response to the CMV gB protein as concomitant ELISpots were not carried out at the same time. However, an important finding of these experiments that requires further investigation is that a small percentage of NK cells produced IFNγ in response to the CMV gB. It is important to determine whether this level of IFNγ production is just background or if it would reach above the threshold used in the IFNγ ELISpot to determine whether a sample responded to the antigen or not (ie. ≥ 25 IFNγ+ spots per million CD4+ T cells). In

future, it may be wise to add in the depletion of CD56+ cells to produce more robust results. Using freshly isolated PBMC or introducing a resting phase post thaw would help reduce the level of background IFNγ produced and therefore make it easier to resolve an antigen specific CD4+ T cell response.

As no correlations could be found with this type of analysis, an experimental approach was taken to investigate whether different subsets of B cells could support or suppress T cell IFNγ production. Progress with these experiments was hampered by inadequate depletion of various subsets and the downstream effects that these depletions had. To support the hypothesis that the effects in the ELISpot are mediated by antigen specific B cells, the ideal experiment would be to compare the pattern of reactivity in the IFNγ ELISpot when just CMV gB binding B cells were added compared to the non-CMV gB binding B cell population. Whilst FACS sorting is the best way to obtain a pure population, the stress-effects of this technique on the cells appeared to be incompatible with the ELISpot assay, as no IFNγ was produced even when all PBMCs used in the assay, apart from the B cells, were not passed through the sorter. As an alternative, the Miltenyi MACS beads system was used to isolate the CMV gB binding B cell population, but the purity of the population obtained was approximately 50%. This was not deemed sufficient for the purpose of the experiment as this would not definitively show that it was the CMV gB binding B cells mediating the effects observed in the ELISpot assay. It was therefore decided that a less specific approach would be taken and an enrichment of different B cell subsets would be used in the ELISpot assay. Again, compromises were made with this approach as IgM could not be used as a marker to separate the different B cell populations, because this would involve directly binding the B cell receptor and therefore potentially influencing the results of the ELISpot assay. Instead, B cells were separated based on their expression of CD27. When the CD27+ B cell population was enriched in the ELISpot assay, IFNγ production was greater than when all B cells were present. However, when B cells were enriched for CD27- B cells, IFNγ production was not detected. From the three leukocyte cones tested in this assay, it was concluded that memory (CD27+) B cells support IFNγ production whereas naïve (CD27-) B cells do not. In addition, there was evidence to suggest in one individual that the CD27- B cell population was suppressing IFNγ production. With these results in mind, it was hypothesised that the memory B cell populations would express greater levels of molecules involved in antigen presentation and T cell activation. Therefore HLA DR and CD86 expression was measured on the different B cell subsets. Whilst the proportions of HLA DR+ B cells did not differ

between the different B cell populations, the level of expression was found to be least bright on the memory B cell populations. Class switched memory and IgM+ memory B cell subsets contained a greater frequency of CD86 expressing B cells than naïve B cells which has also been reported elsewhere (Nova-Lamperti et al., 2016). Greater expression of CD86+ within the memory B cell subset suggests that they will have greater antigen presenting capabilities than Naive B cells and supports the data from the ELISpots which suggest that the CD27+ B cell population supports CD4+ T cell IFNγ production. Interestingly, the CMV gB binding population was distinct from the overall B cell population in that it contained a higher frequency of B cells that expressed CD86, indicating that CMV gB binding B cells are in an activated state.

The transitional B cell population contained a higher frequency of CD86+ cells than the naïve CD45RB-IgM+ subset. The exact reason for this remains unclear but it has previously been published that CD86 expression on transitional B cells is required for effective suppression of T cell activation and proliferation (Blair et al., 2010, Khoder et al., 2014). Conversely, a recent study has shown that transitional B cells inhibit T cell activation due to the autocrine action of IL-10 which causes downregulation of CD86 on their surface. This data would suggest that B cells do not require CD86 expression to mediate their suppressive effects on T cells and in fact down-regulating CD86 on their surface may be the mechanisms by which they reduce T cell activation. Interestingly this study applied the relevance of this finding to a renal transplant setting and found that tolerant patients produced more IL-10 and had lower CD86 expression upon ligation of CD40 than patients with chronic rejection (Nova-Lamperti et al., 2016).

In addition to CD86 and HLA DR, the surface expression of BAFFr and TACI, two receptors for B cell survival cytokines, was compared between the overall B cell population and the CMV gB binding population. This was to investigate whether there was any therapeutic potential for targeting specific B cell subsets with monoclonal antibody therapies aimed at these receptors (Belimumab and Atacicept). BAFFr expression was found to be uniformly expressed on all B cell subsets. TACI was chosen to include in the stain panel over BCMA because BCMA is expressed at lower levels in peripheral blood B cells than TACI and TACI has previously been shown to be more highly expressed on memory B cell subsets, so it was of interest to see whether it was highly expressed on IgM+ memory B cells specifically (Salazar-Camarena et al., 2015, Darce et al., 2007). However, it was not possible to detect any TACI positive B cells using the two different antibodies purchased. Different

fluorochromes and staining protocols were used to optimise this staining but no signal was found.

6 Final discussion and future directions

6.1.1 Summary

CAMR is a major cause of graft loss in a renal transplant setting (Lamb et al., 2011). Currently, there is an unmet need in renal transplantation for effective treatments of CAMR, largely due to the fact that the mechanisms driving CAMR remain unclear. It is widely believed that donor specific antibodies mediate the damage observed upon biopsy because several studies have reported a correlation between the presence of donor specific antibody in the circulation and worse graft outcome (Lachmann et al., 2009, Campos et al., 2006, Worthington et al., 2003, Pelletier et al., 2002, Lee et al., 2002). Despite this strong correlation, there are many patients who maintain good graft function in the presence of circulating DSA, and others who have pathology consistent with CAMR, but no circulating DSA (Bartel et al., 2008, Hayde et al., 2014, Banasik et al., 2013, Campos et al., 2006, Lee et al., 2002). Moreover, there is insufficient mechanistic evidence in humans to definitively prove that DSA are the cause of CAMR.

The aim of this thesis was to build on the evidence published by Shiu et al. that suggested B cells can either support or regulate T cell activation via the indirect pathway of allorecognition, thereby driving the chronic rejection of renal transplants. This aim was initially addressed by using the indirect IFNγ ELISpot assay described in Shiu et al. to study a cohort of patients with CAMR who had been recruited onto the RituxiCAN C4 trial. As the patients had to meet eligibility criteria to be enrolled onto the trial, a more uniform population of patients was studied here than in Shiu et al. The IFNγ ELISpot data reported in this thesis supports the major findings of Shiu et al., that IFNγ production in response to donor derived antigens is influenced by different lymphocyte subsets in different patients, and sometimes within the same patient at different time points. IFNγ production in the RituxiCAN C4 patients was largely dependent on the presence of B cells. However, an IFNγ response was observed in some samples only when either B cells or CD25+ cells were depleted. These three patterns of reactivity were defined as B dependent (Bdep), B regulated (Breg), or T regulated (Treg). When the patterns of reactivity at enrolment were correlated with clinical outcome at the end of phase I of the trial, the majority of patients who displayed evidence of donor specific reactivity, whether that was with a Bdep, Breg or Treg pattern of reactivity, did not pass phase I (ie. their graft function did not stabilise). A small percentage of patients with evidence of donor specific reactivity at enrolment went on to pass phase I. Overall, these results suggest that cellular immune activity is

associated with a poorer clinical outcome, however an in depth analysis of all clinical data would have to be carried out to confirm this. Such analysis was beyond the scope of this thesis. As there were no correlations found between the pattern of reactivity in the IFNγ ELISpot and the global B cell phenotype, the relationship between IFNγ production and the antigen specific B cell population was investigated.

Biotinylated CMV gB was used as a model protein to facilitate the optimisation of the assay to flow cytometrically detect antigen binding B cells, before using biotinylated Pure™ HLA proteins to detect HLA binding B cells in patients who had kidney transplants mismatched to those antigens. Surprisingly, the dominant phenotype of antigen binding B cells in both the CMV gB and HLA systems was IgM+. CMV gB binding B cells were enriched in the IgM+ memory B cell population and the T3 CD27- IgMhi population in a cohort of leukocyte cones. HLA binding B cells were predominantly enriched in either the IgM+ memory or IgM+ naïve B cell populations. A higher ratio of IgM+ memory B cells to IgM+ naïve B cells was associated with a reactive, B dependent response to the mismatched HLA antigen in the IFNγ ELISpot, but a larger number of samples and patients need to be studied to confirm this finding. Finally, using the CMV gB+ antigen system to dissect out the contribution that different B cell subsets make to CD4+ T cell IFNγ production, B cells were separated based on their expression of the memory marker CD27. In three leukocyte cones tested, it appeared that IFNγ production was supported when CD27+ B cells were enriched, but not when CD27- B cells were enriched. In one leukocyte cone, the data suggested that the CD27- B cells may be suppressing the IFNγ response.

6.1.2 Future directions

The data in this thesis presents many avenues down which to explore unanswered questions. At present, a major limitation of the ELISpot assay is that the output is limited to one cytokine and it is impossible to know for certain which cell type is secreting the cytokine. A Fluorospot assay, which has the potential to give a readout of three cytokines, could be a way of partially overcoming this limitation (Janetzki et al., 2014). In a Fluorospot assay, fluorescently labelled detection antibodies are used to distinguish between the three different cytokines being produced. When the correct filters are applied, it is possible to visualise cells that are making more than one cytokine. This could be particularly useful to gain insights into the contribution that the B cells are making to the donor specific responses. For example, it would be possible to visualise in the B regulated samples, whether there is a decrease in IL-10 producing spots when B cells are depleted. This analysis could be extended to assessing the

change in dual or triple cytokine producing spots when just certain subsets of B cells are added to the cultures. For example, it may be possible to measure IFNγ secreting cells whilst simultaneously assessing the dual expression of IL10 and TNF-alpha in different B cell subsets (CD27+ versus CD27-). This data could be related to that reported in Cherukuri et al. where they found that the ability of a B cell to suppress a T cell response was based on the ratio of IL10:TNFα that it produces. Transitional B cells were found to be the subset that are best able to suppress and have a higher ratio of IL10:TNFα than naïve and memory B cells. This ratio was lower in patients who were rejecting their graft compared to those who had stable graft function (Cherukuri et al., 2014).

It has been assumed that B cells in the reactive B dependent samples are processing and presenting antigen to the CD4+ T cells. This assumption could be tested by using a transwell system in which the CD19+ cells are separated from the CD4+ T cells by a membrane and are therefore prevented from contacting each other. It could also be used to test the hypothesis that the B cells in the reactive B regulated samples require cell-cell contact to effectively suppress a T cell response, as this is controversially discussed in the literature (Blair et al., 2010, Khoder et al., 2014, Nova-Lamperti et al., 2016). As with the fluorospot assay, different B cell subsets could be added to the transwell system to investigate what effect the lack of cell-cell contact has on the ability of the CD27+ B cells to support CD4+ T cell IFNγ production. Or likewise what effect this has on the ability of the CD27- or transitional population to suppress.

Recent advances in the technology used to study cells at the single cell level could be taken advantage of in order to study the antigen specific B cell and T cell populations. With sufficient starting cell numbers it would be possible to single cell sort the HLA binding B cells from patients with CAMR and sequence their BCR to determine whether there is any evidence of specific clonal expansion. The B cell repertoire in this population could be compared to those detected in the no antigen ‘background’ gate and also compared between patients and non-sensitised healthy volunteers to see if a specific skewing of BCRs can be identified in the patients. This analysis could also be used to clonally relate the different IgMhi B cell subsets to establish whether the HLA or CMV gB binding B cells are a mixed pool of cells that originate from both MZ/IgM+ memory B and naïve follicular-germinal centre pathways of B cell differentiation.

To complement and strengthen the results obtained from the ELISpot, a flow cytometric T cell activation assay could be used to analyse donor specific CD4+ T

cells. It is possible to flow cytometrically detect and sort antigen specific CD4+ T cells, identified by their co-expression of CD154 and CD69, early on after in vitro stimulation with antigen (Estorninho et al., 2013, Chattopadhyay et al., 2005, Chattopadhyay et al., 2006). It would be interesting to investigate whether this assay could be applied to a transplant setting where HLA specific T cells are activated using Pure™ HLA proteins. By using microfluidic quantitative PCR methods for studying single cells, there is the potential to analyse the TCR repertoire and gene expression of single sorted indirect donor specific CD4+ T cells, thus providing information about the T cell response in renal transplant recipients with CAMR, which may prove useful in translating effective treatments into the clinic (Sanchez-Freire et al., 2012, Eugster et al., 2013). In addition, the antigen specific response could be studied in this assay in the presence or absence of B cells, and thus be used as a way of validating the results observed in the IFNγ ELISpot. It may also be possible to study the gene expression of the B cells to establish whether B dependent and B regulated patterns of reactivity can be distinguished from each other at the molecular level.

6.1.3 Conclusion

To conclude, the data in this thesis supports that found in Shiu et al and strengthens the argument for the involvement of a cell-mediated component in chronic rejection. Interest in the contribution that B cells make to chronic rejection is gaining momentum, however the major theme that runs through much of the research conducted around this topic remains focussed on a humoral component. There is some evidence from animal models that B cells contribute to chronic rejection in an antibody independent manner, and in humans, the outcome of the OuTSMART clinical trial should shed light on whether treatments targeting cellular rejection are an effective way of preventing the development of chronic rejection in individuals who are HLA antibody positive (Dorling et al., 2014, Tse et al., 2015, Zeng et al., 2014).

7 Appendix

				Expressed as % of HLA + B cells		Expressed as % of Non transitional HLA+ B cells					Expressed as % of Non transitional HLA+ B cells				
PATIENT ID	Timepoint	Mismatch	Antigen (µg/ml)	Transitional	Non Transitional	CD27+ IgMhi	CD27+ IgM-	CD27-IgMhi	CD27-IgM+	CD27- IgM-	CD45RB+ IgMhi	CD45RB+ IgM-	CD45RB-IgMhi	CD45RB-IgM+	CD45RB-IgM-
G013	14/11/2011	A1	0	18.2	81.8	11.1	0	0	66.7	22.2	11.1	22.2	0	44.4	22.2
G013	14/11/2011	A1	0.2	5.41	94.6	60	8.57	11.4	20	0	74.3	5.71	0	20	0
G013	21/02/2013	A1	0	28.6	71.4	40	20	20	20	0	80	0	0	20	0
G013	21/02/2013	A1	0.2	0	100	45.7	0	14.3	37.1	2.86	65.7	5.71	2.86	22.9	2.86
G013	09/01/2014	A1	0	0	100	0	0	0	50	50	0	0	0	50	50
G013	09/01/2014	A1	0.2	0	100	50	0	28.6	14.3	7.14	78.6	0	7.14	7.14	7.14
W008	10/07/2008	A2	0	0	0	0	0	0	0	0	0	0	0	0	0
W008	10/07/2008	A2	0.3	0	100	66.7	0	0	33.3	0	66.7	7.69	33.3	0	0
W008	12/01/2009	A2	0	0	100	14.3	71.4	14.3	0	0	0	28.6	28.6	0	42.9
W008	12/01/2009	A2	0.3	0	100	53.8	30.8	5.13	2.56	7.69	48.7	17.9	10.3	10.3	7.69
W008	02/07/2009	A2	0	0	100	50	0	0	50	0	50	0	0	50	0
W008	02/07/2009	A2	0.3	0	100	45.5	31.8	18.2	4.55	0	45.5	13.6	22.7	13.6	9.09
W008	24/09/2009	A2	0	0	100	50	0	50	0	0	100	0	0	0	0
W008	24/09/2009	A2	0.3	0	100	54.5	27.3	9.09	9.09	0	63.6	18.2	0	18.2	0
W008	10/01/2011	A2	0	0	100	66.7	33.3	0	0	0	66.7	33.3	0	0	0
W008	10/01/2011	A2	0.3	0	100	71.4	19	9.52	0	0	76.2	19	4.76	0	0
W011	30/11/2009	A2	0	0	0	0	0	0	0	0	0	0	0	0	0
W011	30/11/2009	A2	0.2	0	100	16.7	33.3	16.7	16.7	16.7	0	16.7	33.3	16.7	33.3
G007	09/05/2011	A2	0	0	100	0	0	100	0	0	100	0	0	0	0
G007	09/05/2011	A2	0.2	25	75	66.7	0	0	33.3	0	66.7	0	0	33.3	0
G014	12/12/2013	A1/A2	0	0	0	0	0	0	0	0	0	0	0	0	0
G014	12/12/2013	A1/A2	0.2	0	100	0	0	33.3	66.7	0	33.3	0	0	66.7	0
W009	16/10/2009	DR4	0	0	100						36.8	21.1	5.26	31.6	5.26
W009	16/10/2009	DR4	0.4	6.59	93.4						5.88	9.41	14.1	57.6	12.9
W009	07/02/2011	DR4	0	0	100						0	60	0	20	20
W009	07/02/2011	DR4	0.3	20.8	79.2						15.8	26.3	0	47.4	10.5
G011	29/06/2011	DR4	0	0	100						25	50	0	0	25
G011	29/06/2011	DR4	0.4	0	100						16.7	16.7	16.7	50	0

Figure 7.1 Table for no antigen control from section 4.2.3.3

8 Bibliography

AFZALI, B., LECHLER, R. I. & HERNANDEZ-FUENTES, M. P. 2007. Allorecognition and the alloresponse: Clinical implications. *Tissue Antigens,* 69**,** 545-556.

AFZALI, B., LOMBARDI, G. & LECHLER, R. I. 2008. Pathways of major histocompatibility complex allorecognition. *Current Opinion in Organ Transplantation,* 13**,** 438-444.

AGEMATSU, K., NAGUMO, H., SHINOZAKI, K., HOKIBARA, S., YASUI, K., TERADA, K., KAWAMURA, N., TOBA, T., NONOYAMA, S., OCHS, H. D. & KOMIYAMA, A. 1998. Absence of IgD-CD27(+) memory B cell population in X-linked hyper-IgM syndrome. *Journal of Clinical Investigation,* 102**,** 853-860.

AKALIN, E., DINAVAHI, R., DIKMAN, S., DE BOCCARDO, G., FRIEDLANDER, R., SCHROPPEL, B., SEHGAL, V., BROMBERG, J. S., HEEGER, P. & MURPHY, B. 2007. Transplant glomerulopathy may occur in the absence of donor-specific antibody and C4d staining. *Clinical Journal of the American Society of Nephrology,* 2**,** 1261-1267.

ALI, J., BOLTON, E., SAEB-PARSY, K., BRADLEY, J. A. & PETTIGREW, G. 2015. Targeting indirect pathway CD4 T-cell alloresponses in the prevention of chronic transplant rejection. *The Lancet,* 385**,** S17.

ALI, JASON M., NEGUS, MARGARET C., CONLON, THOMAS M., HARPER, INES G., QURESHI, M. S., MOTALLEBZADEH, R., WILLIS, R., SAEB-PARSY, K., BOLTON, ELEANOR M., BRADLEY, J. A. & PETTIGREW, GAVIN J. 2013. Diversity of the CD4T Cell Alloresponse: The Short and the Long of It. *Cell Reports*.

ALLEN, C. D. C., ANSEL, K. M., LOW, C., LESLEY, R., TAMAMURA, H., FUJII, N. & CYSTER, J. G. 2004. Germinal center dark and light zone organization is mediated by CXCR4 and CXCR5. *Nat Immunol,* 5**,** 943-952.

ALLEN, C. D. C., OKADA, T., TANG, H. L. & CYSTER, J. G. 2007. Imaging of Germinal Center Selection Events During Affinity Maturation. *Science,* 315**,** 528-531.

AMANNA, I. J. & SLIFKA, M. K. 2006. Quantitation of rare memory B cell populations by two independent and complementary approaches. *Journal of Immunological Methods,* 317**,** 175-185.

ANGELIN-DUCLOS, C., CATTORETTI, G., LIN, K.-I. & CALAME, K. 2000. Commitment of B Lymphocytes to a Plasma Cell Fate Is Associated with Blimp-1 Expression In Vivo. *The Journal of Immunology,* 165**,** 5462-5471.

ANOLIK, J. H., BARNARD, J., OWEN, T., ZHENG, B., KEMSHETTI, S., LOONEY, R. J. & SANZ, I. 2007a. Delayed memory B cell recovery in peripheral blood and lymphoid tissue in systemic lupus erythematosus after B cell depletion therapy. *Arthritis & Rheumatism,* 56**,** 3044-3056.

ANOLIK, J. H., FRIEDBERG, J. W., ZHENG, B., BARNARD, J., OWEN, T., CUSHING, E., KELLY, J., MILNER, E. C. B., FISHER, R. I. & SANZ, I. 2007b. B cell reconstitution after rituximab treatment of lymphoma recapitulates B cell ontogeny. *Clinical Immunology,* 122**,** 139-145.

ARANBURU, A., CECCARELLI, S., GIORDA, E., LASORELLA, R., BALLATORE, G. & CARSETTI, R. 2010. TLR ligation triggers somatic hypermutation in transitional B cells inducing the generation of IgM memory B cells. *Journal of Immunology,* 185**,** 7293-7301.

ARIF, S., TREE, T. I., ASTILL, T. P., TREMBLE, J. M., BISHOP, A. J., DAYAN, C. M., ROEP, B. O. & PEAKMAN, M. 2004. Autoreactive T cell responses show proinflammatory polarization in diabetes but a regulatory phenotype in health. *The Journal of Clinical Investigation,* 113**,** 451-463.

ARVIN, A. M. 2008. Humoral and Cellular Immunity to Varicella-Zoster Virus: An Overview. *Journal of Infectious Diseases,* 197**,** S58-S60.

AUCHINCLOSS, H., LEE, R., SHEA, S., MARKOWITZ, J. S., GRUSBY, M. J. & GLIMCHER, L. H. 1993. The role of "indirect" recognition in initiating rejection of skin grafts from major histocompatibility complex class II-deficient mice. *Proceedings of the National Academy of Sciences of the United States of America,* 90**,** 3373-3377.

AVERY, D. T., BRYANT, V. L., MA, C. S., DE WAAL MALEFYT, R. & TANGYE, S. G. 2008. IL-21-Induced Isotype Switching to IgG and IgA by Human Naive B Cells Is Differentially Regulated by IL-4. *The Journal of Immunology,* 181**,** 1767-1779.

BACHELET, T., NODIMAR, C., TAUPIN, J.-L., LEPREUX, S., MOREAU, K., MOREL, D., GUIDICELLI, G., COUZI, L. & MERVILLE, P. 2015. Intravenous immunoglobulins and rituximab therapy for severe transplant glomerulopathy in chronic antibody-mediated rejection: a pilot study. *Clinical Transplantation,* 29**,** 439-446.

BAGNARA, D., SQUILLARIO, M., KIPLING, D., MORA, T., WALCZAK, A. M., DA SILVA, L., WELLER, S., DUNN-WALTERS, D. K., WEILL, J.-C. & REYNAUD, C.-A. 2015. A Reassessment of IgM Memory Subsets in Humans. *The Journal of Immunology*.

BAKER, R. J., HERNANDEZ-FUENTES, M. P., BROOKES, P. A., CHAUDHRY, A. N., COOK, H. T. & LECHLER, R. I. 2001. Loss of direct and maintenance of indirect alloresponses in renal allograft recipients: Implications for the pathogenesis of chronic allograft nephropathy. *Journal of Immunology,* 167**,** 7199-7206.

BANASIK, M., BORATYŃSKA, M., KOŚCIELSKA-KASPRZAK, K., MAZANOWSKA, O., KRAJEWSKA, M., ZABIŃSKA, M., BARTOSZEK, D., MYSZKA, M., NOWAKOWSKA, B., DAWISKIBA, T., LEPIESZA, A., CHUDOBA, P. & KLINGER, M. 2013. The Impact of De Novo Donor-specific Anti-Human Leukocyte Antigen Antibodies on 5-Year Renal Transplant Outcome. *Transplantation Proceedings,* 45**,** 1449-1452.

BANNARD, O., HORTON, ROBERT M., ALLEN, CHRISTOPHER D. C., AN, J., NAGASAWA, T. & CYSTER, JASON G. 2013. Germinal Center Centroblasts Transition to a Centrocyte Phenotype According to a Timed Program and Depend on the Dark Zone for Effective Selection. *Immunity,* 39**,** 912-924.

BARTEL, G., REGELE, H., WAHRMANN, M., HUTTARY, N., EXNER, M., HÖRL, W. H. & BÖHMIG, G. A. 2008. Posttransplant HLA alloreactivity in stable kidney transplant recipients - Incidences and impact on long-term allograft outcomes. *American Journal of Transplantation,* 8**,** 2652-2660.

BATISTA, F. D. & HARWOOD, N. E. 2009. The who, how and where of antigen presentation to B cells. *Nature Reviews Immunology,* 9**,** 15-27.

BATISTA, F. D., IBER, D. & NEUBERGER, M. S. 2001. B cells acquire antigen from target cells after synapse formation. *Nature,* 411**,** 489-494.

BECKWITH, H. & LIGHTSTONE, L. 2014. Rituximab in Systemic Lupus Erythematosus and Lupus Nephritis. *Nephron Clinical Practice,* 128**,** 250-254.

BELL, J. & GRAY, D. 2003. Antigen-capturing cells can masquerade as memory B cells. *Journal of Experimental Medicine,* 197**,** 1233-1244.

BEMARK, M. 2015. Translating transitions – how to decipher peripheral human B cell development. *Journal of Biomedical Research,* 29**,** 264-284.

BEMARK, M., FRISKOPP, L., SAGHAFIAN-HEDENGREN, S., KOETHE, S., FASTH, A., ABRAHAMSSON, J., SVERREMARK-EKSTRÖM, E., ANDERSSON, B. A. & MELLGREN, K. 2013. A glycosylation-dependent CD45RB epitope defines previously unacknowledged CD27−IgMhigh B cell subpopulations enriched in young children and after hematopoietic stem cell transplantation. *Clinical Immunology,* 149**,** 421-431.

BEMARK, M., HOLMQVIST, J., ABRAHAMSSON, J. & MELLGREN, K. 2012. Translational Mini-Review Series on B cell subsets in disease. Reconstitution after haematopoietic stem cell transplantation - revelation of B cell developmental pathways and lineage phenotypes. *Clin Exp Immunol,* 167**,** 15-25.

BENICHOU, G., VALUJSKIKH, A. & HEEGER, P. S. 1999. Contributions of Direct and Indirect T Cell Alloreactivity During Allograft Rejection in Mice. *The Journal of Immunology,* 162**,** 352-358.

BENNETT, S. R. M., CARBONE, F. R., KARAMALIS, F., FLAVELL, R. A., MILLER, J. F. A. P. & HEATH, W. R. 1998. Help for cytotoxic-T-cell responses is mediated by CD40 signalling. *Nature,* 393**,** 478-480.

BERKOWSKA, M. A., DRIESSEN, G. J. A., BIKOS, V., GROSSERICHTER-WAGENER, C., STAMATOPOULOS, K., CERUTTI, A., HE, B., BIERMANN, K., LANGE, J. F., VAN DER BURG, M., VAN DONGEN, J. J. M. & VAN ZELM, M. C. 2011. Human memory B cells originate from three distinct germinal center-dependent and -independent maturation pathways. *Blood,* 118**,** 2150-2158.

BILLING, H., RIEGER, S., OVENS, J., SÜSAL, C., MELK, A., WALDHERR, R., OPELZ, G. & TÖNSHOFF, B. 2008. Successful treatment of chronic antibody-mediated rejection with IVIG and rituximab in pediatric renal transplant recipients. *Transplantation,* 86**,** 1214-1221.

BILLING, H., RIEGER, S., SÜSAL, C., WALDHERR, R., OPELZ, G., WÜHL, E. & TÖNSHOFF, B. 2012. IVIG and rituximab for treatment of chronic antibody-mediated rejection: a prospective study in paediatric renal transplantation with a 2-year follow-up. *Transplant International,* 25**,** 1165-1173.

BJORNSON, A. B. & DETMERS, P. A. 1995. The pentameric structure of IgM is necessary to enhance opsonization of Bacteroides thetaiotaomicron and Bacteroides fragilis via the alternative complement pathway. *Microbial Pathogenesis,* 19**,** 117-128.

BLAIR, P. A., NORENA, L. Y., FLORES-BORJA, F., RAWLINGS, D. J., ISENBERG, D. A., EHRENSTEIN, M. R. & MAURI, C. 2010. CD19(+)CD24(hi)CD38(hi) B cells exhibit regulatory capacity in healthy individuals but are functionally impaired in systemic Lupus Erythematosus patients. *Immunity,* 32**,** 129-40.

BOUAZIZ, J. D., CALBO, S., MAHO-VAILLANT, M., SAUSSINE, A., BAGOT, M., BENSUSSAN, A. & MUSETTE, P. 2010. IL-10 produced by activated human B cells regulates CD4(+) T-cell activation in vitro. *Eur J Immunol,* 40**,** 2686-91.

BRAUN, M. Y., MCCORMACK, A., WEBB, G. & BATCHELOR, J. R. 1993. Mediation of acute but not chronic rejection of MHC-incompatible rat kidney grafts by alloreactive CD4 T cells activated by the direct pathway of sensitization1. *Transplantation,* 55**,** 177-182.

BREMAN, E., VAN MIERT, P. P., VAN DER STEEN, D. M., HEEMSKERK, M. H., DOXIADIS, I. I., ROELEN, D., CLAAS, F. H. & VAN KOOTEN, C. 2014. HLA Monomers as a Tool to Monitor Indirect Allorecognition. *Transplantation,* 97**,** 1119-1127.

BRENNAN, T. V., JAIGIRDAR, A., HOANG, V., HAYDEN, T., LIU, F. C., ZAID, H., CHANG, C. K., BUCY, R. P., TANG, Q. & KANG, S. M. 2009. Preferential Priming of Alloreactive T Cells with Indirect Reactivity. *American Journal of Transplantation,* 9**,** 709-718.

BRINKMANN, M. M., SPOONER, E., HOEBE, K., BEUTLER, B., PLOEGH, H. L. & KIM, Y.-M. 2007. The interaction between the ER membrane protein UNC93B and TLR3, 7, and 9 is crucial for TLR signaling. *The Journal of Cell Biology,* 177**,** 265-275.

BROUARD, S., PALLIER, A., RENAUDIN, K., FOUCHER, Y., DANGER, R., DEVYS, A., CESBRON, A., GUILLOT-GUEGEN, C., ASHTON-CHESS, J., LE ROUX, S., HARB, J., ROUSSEY, G., SUBRA, J. F., VILLEMAIN, F., LEGENDRE, C., BEMELMAN, F. J., ORLANDO, G., GARNIER, A., JAMBON, H., LE MONIES DE SAGAZAN, H., BRAUN, L., NOËL, C., PILLEBOUT, E., MOAL, M. C., CANTARELL, C., HOITSMA, A., RANBANT, M., TESTA, A., SOULILLOU, J. P. & GIRAL, M. 2012. The Natural History of Clinical Operational Tolerance After Kidney Transplantation Through Twenty-Seven Cases. *American Journal of Transplantation,* 12**,** 3296-3307.

BROWN, K., SACKS, S. H. & WONG, W. 2011. Coexpression of Donor Peptide/Recipient MHC Complex and Intact Donor MHC: Evidence for a Link between the Direct and Indirect Pathways. *American Journal of Transplantation,* 11**,** 826-831.

BRYANT, V. L., MA, C. S., AVERY, D. T., LI, Y., GOOD, K. L., CORCORAN, L. M., MALEFYT, R. D. & TANGYE, S. G. 2007. Cytokine-mediated regulation of human B cell differentiation into Ig-secreting cells: Predominant role of IL-21 produced by CXCR5(+) T follicular helper cells. *Journal of Immunology,* 179**,** 8180-8190.

BUDEUS, B., SCHWEIGLE DE REYNOSO, S., PRZEKOPOWITZ, M., HOFFMANN, D., SEIFERT, M. & KÜPPERS, R. 2015. Complexity of the human memory B-cell compartment is determined by the versatility of clonal diversification in germinal centers. *Proceedings of the National Academy of Sciences,* 112**,** E5281-E5289.

BUGATTI, S., VITOLO, B., CAPORALI, R., MONTECUCCO, C. & MANZO, A. 2014. B Cells in Rheumatoid Arthritis: From Pathogenic Players to Disease Biomarkers. *BioMed Research International,* 2014**,** 681678.

BÖHMIG, G. A., EXNER, M., HABICHT, A., SCHILLINGER, M., LANG, U., KLETZMAYR, J., SÄEMANN, M. D., HÖRL, W. H., WATSCHINGER, B. & REGELE, H. 2002. Capillary C4d deposition in kidney allografts: A specific marker of alloantibody-dependent graft injury. *Journal of the American Society of Nephrology,* 13**,** 1091-1099.

CAMBRIDGE, G., LEANDRO, M. J., TEODORESCU, M., MANSON, J., RAHMAN, A., ISENBERG, D. A. & EDWARDS, J. C. 2006. B cell depletion therapy in systemic lupus erythematosus: Effect on autoantibody and antimicrobial antibody profiles. *Arthritis & Rheumatism,* 54**,** 3612-3622.

CAMERON, P. U., JONES, P., GORNIAK, M., DUNSTER, K., PAUL, E., LEWIN, S., WOOLLEY, I. & SPELMAN, D. 2011. Splenectomy associated changes in IgM memory B cells in an adult spleen registry cohort. *PLoS One,* 6.

CAMPOS, É. F., TEDESCO-SILVA, H., MACHADO, P. G., FRANCO, M., MEDINA-PESTANA, J. O. & GERBASE-DELIMA, M. 2006. Post-Transplant Anti-HLA Class II Antibodies as Risk Factor for Late Kidney Allograft Failure. *American Journal of Transplantation,* 6**,** 2316-2320.

CAO, Y., GORDIC, M., KOBOLD, S., LAJMI, N., MEYER, S., BARTELS, K., HILDEBRANDT, Y., LUETKENS, T., IHLOFF, A. S., KRÖGER, N., BOKEMEYER, C. & ATANACKOVIC, D. 2010. An optimized assay for the enumeration of antigen-specific memory B cells in different compartments of the human body. *Journal of Immunological Methods,* 358**,** 56-65.

CAPOLUNGHI, F., CASCIOLI, S., GIORDA, E., ROSADO, M. M., PLEBANI, A., AURITI, C., SEGANTI, G., ZUNTINI, R., FERRARI, S., CAGLIUSO, M., QUINTI, I. & CARSETTI, R. 2008. CpG drives human transitional B cells to terminal differentiation and production of natural antibodies. *Journal of Immunology,* 180**,** 800-808.

CAPOLUNGHI, F., ROSADO, M. M., SINIBALDI, M., ARANBURU, A. & CARSETTI, R. 2013. Why do we need IgM memory B cells? *Immunology Letters,* 152**,** 114-120.

CARSETTI, R., ROSADO, M. M., DONNANNO, S., GUAZZI, V., SORESINA, A., MEINI, A., PLEBANI, A., AIUTI, F. & QUINTI, I. 2005. The loss of IgM memory B cells correlates with clinical disease in common variable immunodeficiency. *Journal of Allergy and Clinical Immunology,* 115**,** 412-417.

CARTER, N. A., ROSSER, E. C. & MAURI, C. 2012. Interleukin-10 produced by B cells is crucial for the suppression of Th17/Th1 responses, induction of T regulatory type 1 cells and reduction of collagen-induced arthritis. *Arthritis Research and Therapy,* 14.

CASROUGE, A., ZHANG, S.-Y., EIDENSCHENK, C., JOUANGUY, E., PUEL, A., YANG, K., ALCAIS, A., PICARD, C., MAHFOUFI, N., NICOLAS, N., LORENZO, L., PLANCOULAINE, S., SÉNÉCHAL, B., GEISSMANN, F., TABETA, K., HOEBE, K., DU, X., MILLER, R. L., HÉRON, B., MIGNOT, C., DE VILLEMEUR, T. B., LEBON, P., DULAC, O., ROZENBERG, F., BEUTLER, B., TARDIEU, M., ABEL, L. & CASANOVA, J.-L. 2006. Herpes Simplex Virus Encephalitis in Human UNC-93B Deficiency. *Science,* 314**,** 308-312.

CASTILLO-TRIVINO, T., BRAITHWAITE, D., BACCHETTI, P. & WAUBANT, E. 2013. Rituximab in Relapsing and Progressive Forms of Multiple Sclerosis: A Systematic Review. *PLoS ONE,* 8**,** e66308.

CAYABYAB, M., PHILLIPS, J. H. & LANIER, L. L. 1994. CD40 preferentially costimulates activation of CD4+ T lymphocytes. *The Journal of Immunology,* 152**,** 1523-31.

CHAN, O. & J. SHLOMCHIK, M. 1998. A New Role for B Cells in Systemic Autoimmunity: B Cells Promote Spontaneous T Cell Activation in MRL-lpr/lpr Mice. *The Journal of Immunology,* 160**,** 51-59.

CHAN, O. T. M., HANNUM, L. G., HABERMAN, A. M., MADAIO, M. P. & SHLOMCHIK, M. J. 1999a. A Novel Mouse with B Cells but Lacking Serum Antibody Reveals an Antibody-independent Role for B Cells in Murine Lupus. *The Journal of Experimental Medicine,* 189**,** 1639-1648.

CHAN, O. T. M., MADAIO, M. P. & SHLOMCHIK, M. J. 1999b. B Cells Are Required for Lupus Nephritis in the Polygenic, Fas-Intact MRL Model of Systemic Autoimmunity. *The Journal of Immunology,* 163**,** 3592-3596.

CHATTOPADHYAY, P. K., YU, J. & ROEDERER, M. 2005. A live-cell assay to detect antigen-specific CD4+ T cells with diverse cytokine profiles. *Nature Medicine,* 11**,** 1113-1117.

CHATTOPADHYAY, P. K., YU, J. & ROEDERER, M. 2006. Live-cell assay to detect antigen-specific CD4+ T-cell responses by CD154 expression. *Nature Protocols,* 1**,** 1-6.

CHEN, L. C., DELGADO, J. C., JENSEN, P. E. & CHEN, X. 2009. Direct expansion of human allospecific FoxP3+CD4+ regulatory T cells with allogeneic B cells for therapeutic application. *J Immunol,* 183**,** 4094-102.

CHERUKURI, A., ROTHSTEIN, D. M., CLARK, B., CARTER, C. R., DAVISON, A., HERNANDEZ-FUENTES, M., HEWITT, E., SALAMA, A. D. & BAKER, R. J. 2014. Immunologic Human Renal Allograft Injury Associates with an Altered IL-10/TNF-α

Expression Ratio in Regulatory B Cells. *Journal of the American Society of Nephrology,* 25**,** 1575-1585.

CHESNEAU, M., MICHEL, L., DUGAST, E., CHENOUARD, A., BARON, D., PALLIER, A., DURAND, J., BRAZA, F., GUERIF, P., LAPLAUD, D.-A., SOULILLOU, J.-P., GIRAL, M., DEGAUQUE, N., CHIFFOLEAU, E. & BROUARD, S. 2015. Tolerant Kidney Transplant Patients Produce B Cells with Regulatory Properties. *Journal of the American Society of Nephrology*.

CHUNG, B. H., KIM, Y., JEONG, H. S., HONG, Y. A., CHOI, B. S., PARK, C. W., CHOI, Y. J., KIM, Y.-S. & YANG, C. W. 2014. Clinical outcome in patients with chronic antibody-mediated rejection treated with and without rituximab and intravenous immunoglobulin combination therapy. *Transplant Immunology,* 31**,** 140-144.

CIUBOTARIU, R., LIU, Z., COLOVAI, A. I., HO, E., ITESCU, S., RAVALLI, S., HARDY, M. A., CORTESINI, R., ROSE, E. A. & SUCIU-FOCA, N. 1998. Persistent allopeptide reactivity and epitope spreading in chronic rejection of organ allografts. *The Journal of Clinical Investigation,* 101**,** 398-405.

COLF, L. A., BANKOVICH, A. J., HANICK, N. A., BOWERMAN, N. A., JONES, L. L., KRANZ, DAVID M. & GARCIA, K. C. 2007. How a Single T Cell Receptor Recognizes Both Self and Foreign MHC. *Cell,* 129**,** 135-146.

COLVIN, R. B. 2007. Antibody-Mediated Renal Allograft Rejection: Diagnosis and Pathogenesis. *Journal of the American Society of Nephrology,* 18**,** 1046-1056.

COLVIN, R. B. & SMITH, R. N. 2005. Antibody-mediated organ-allograft rejection. *Nat Rev Immunol,* 5**,** 807-17.

CONDON, M. B., ASHBY, D., PEPPER, R. J., COOK, H. T., LEVY, J. B., GRIFFITH, M., CAIRNS, T. D. & LIGHTSTONE, L. 2013. Prospective observational single-centre cohort study to evaluate the effectiveness of treating lupus nephritis with rituximab and mycophenolate mofetil but no oral steroids. *Annals of the Rheumatic Diseases,* 72**,** 1280-1286.

CONLON, T. M., SAEB-PARSY, K., COLE, J. L., MOTALLEBZADEH, R., QURESHI, M. S., REHAKOVA, S., NEGUS, M. C., CALLAGHAN, C. J., BOLTON, E. M., BRADLEY, J. A. & PETTIGREW, G. J. 2012. Germinal center alloantibody responses are mediated exclusively by indirect-pathway CD4 T follicular helper cells. *Journal of Immunology,* 188**,** 2643-2652.

CONSORTIUM, M. S. 1999. Complete sequence and gene map of a human major histocompatibility complex. *Nature,* 401**,** 921-923.

CONSTANT, S., SANT'ANGELO, D., PASQUALINI, T., TAYLOR, T., LEVIN, D., FLAVELL, R. & BOTTOMLY, K. 1995a. Peptide and protein antigens require distinct antigen-presenting cell subsets for the priming of CD4+ T cells. *The Journal of Immunology,* 154**,** 4915-23.

CONSTANT, S., SCHWEITZER, N., WEST, J., RANNEY, P. & BOTTOMLY, K. 1995b. B lymphocytes can be competent antigen-presenting cells for priming CD4+ T cells to protein antigens in vivo. *Journal of Immunology,* 155**,** 3734-3741.

CONSTANT, S. L. 1999. B lymphocytes as antigen-presenting cells for CD4+ T cell priming in vivo. *Journal of Immunology,* 162**,** 5695-5703.

CRAWFORD, A., MACLEOD, M., SCHUMACHER, T., CORLETT, L. & GRAY, D. 2006. Primary T cell expansion and differentiation in vivo requires antigen presentation by B cells. *Journal of Immunology,* 176**,** 3498-3506.

CROTTY, S., AUBERT, R. D., GLIDEWELL, J. & AHMED, R. 2004. Tracking human antigen-specific memory B cells: A sensitive and generalized ELISPOT system. *Journal of Immunological Methods,* 286**,** 111-122.

DARCE, J. R., ARENDT, B. K., WU, X. & JELINEK, D. F. 2007. Regulated Expression of BAFF-Binding Receptors during Human B Cell Differentiation. *The Journal of Immunology,* 179**,** 7276-7286.

DAS, A., ELLIS, G., PALLANT, C., LOPES, A. R., KHANNA, P., PEPPA, D., CHEN, A., BLAIR, P., DUSHEIKO, G., GILL, U., KENNEDY, P. T., BRUNETTO, M., LAMPERTICO, P., MAURI, C. & MAINI, M. K. 2012a. IL-10-producing regulatory B cells in the pathogenesis of chronic hepatitis B virus infection. *Journal of Immunology,* 189**,** 3925-3935.

DAS, A., ELLIS, G., PALLANT, C., LOPES, A. R., KHANNA, P., PEPPA, D., CHEN, A., BLAIR, P., DUSHEIKO, G., GILL, U., KENNEDY, P. T., BRUNETTO, M., LAMPERTICO, P., MAURI, C. & MAINI, M. K. 2012b. IL-10–Producing Regulatory B Cells in the Pathogenesis of Chronic Hepatitis B Virus Infection. *The Journal of Immunology,* 189**,** 3925-3935.

DASS, S., VITAL, E. M. & EMERY, P. 2007. Development of psoriasis after B cell depletion with rituximab. *Arthritis & Rheumatism,* 56**,** 2715-2718.

DAUBY, N., SARTORI, D., KUMMERT, C., LECOMTE, S., HAELTERMAN, E., DELFORGE, M.-L., DONNER, C., MACH, M. & MARCHANT, A. 2015. Limited effector memory B cell response to envelope glycoprotein B during primary HCMV infection. *Journal of Infectious Diseases*.

DAVIS, D. M. 2007. Intercellular transfer of cell-surface proteins is common and can affect many stages of an immune response. *Nat Rev Immunol,* 7**,** 238-243.

DE, S. & BARNES, B. J. 2014. B cell transcription factors: Potential new therapeutic targets for SLE. *Clinical Immunology,* 152**,** 140-151.

DEAGLIO, S., DWYER, K. M., GAO, W., FRIEDMAN, D., USHEVA, A., ERAT, A., CHEN, J. F., ENJYOJI, K., LINDEN, J., OUKKA, M., KUCHROO, V. K., STROM, T. B. & ROBSON, S. C. 2007. Adenosine generation catalyzed by CD39 and CD73 expressed on regulatory T cells mediates immune suppression. *J Exp Med,* 204**,** 1257-65.

DEGAUQUE, N., NGONO, A. E., AKL, A., LEPETIT, M., CROCHETTE, R., GIRAL, M., LEPOURRY, J., PALLIER, A., CASTAGNET, S., DUGAST, E., GUILLOT-GUEGUEN, C., JACQ-FOUCHER, M., SAULQUIN, X., CESBRON, A., LAPLAUD, D., NICOT, A., BROUARD, S. & SOULILLOU, J.-P. 2013. Characterization of Antigen-Specific B Cells Using Nominal Antigen-Coated Flow-Beads. *PLoS ONE,* 8**,** e84273.

DELLA VALLE, L., DOHMEN, S. E., VERHAGEN, O. J. H. M., BERKOWSKA, M. A., VIDARSSON, G. & VAN DER SCHOOT, C. E. 2014. The Majority of Human Memory B Cells Recognizing RhD and Tetanus Resides in IgM+ B Cells. *The Journal of Immunology*.

DENG, S., MOORE, D. J., HUANG, X., LIAN, M.-M., MOHIUDDIN, M., VELEDEDEOGLU, E., LEE, M. K., SONAWANE, S., KIM, J., WANG, J., CHEN, H., CORFE, S. A., PAIGE, C., SHLOMCHIK, M., CATON, A. & MARKMANN, J. F. 2007. Cutting Edge: Transplant Tolerance Induced by Anti-CD45RB Requires B Lymphocytes. *The Journal of Immunology,* 178**,** 6028-6032.

DENT, A. L., SHAFFER, A. L., YU, X., ALLMAN, D. & STAUDT, L. M. 1997. Control of Inflammation, Cytokine Expression, and Germinal Center Formation by BCL-6. *Science,* 276**,** 589-592.

DESCATOIRE, M., WELLER, S., IRTAN, S., FEUILLARD, J., STORCK, S., GUIOCHON-MANTEL, A., BOULIGAND, J., MORALI, A., COHEN, J., JACQUEMIN, E., IASCONE, M., BOLE-FEYSOT, C., CAGNARD, N., WEILL, J. C. & REYNAUD, C. A. 2014. Identification of a human splenic marginal zone B cell precursor with NOTCH2-dependent differentiation properties. *Journal of Experimental Medicine,* 211**,** 987-1000.

DJAMALI, A., KAUFMAN, D. B., ELLIS, T. M., ZHONG, W., MATAS, A. & SAMANIEGO, M. 2014. Diagnosis and management of antibody-mediated rejection: Current status and novel approaches. *American Journal of Transplantation,* 14**,** 255-271.

DOGAN, I., BERTOCCI, B., VILMONT, V., DELBOS, F., MEGRET, J., STORCK, S., REYNAUD, C.-A. & WEILL, J.-C. 2009. Multiple layers of B cell memory with different effector functions. *Nat Immunol,* 10**,** 1292-1299.

DORIA-ROSE, N. A., KLEIN, R. M., MANION, M. M., O'DELL, S., PHOGAT, A., CHAKRABARTI, B., HALLAHAN, C. W., MIGUELES, S. A., WRAMMERT, J., AHMED, R., NASON, M., WYATT, R. T., MASCOLA, J. R. & CONNORS, M. 2009. Frequency and phenotype of human immunodeficiency virus envelope-specific B cells from patients with broadly cross-neutralizing antibodies. *Journal of Virology,* 83**,** 188-199.

DORLING, A. 2012. Transplant accommodation-are the lessons learned from xenotransplantation pertinent for clinical allotransplantation? *American Journal of Transplantation,* 12**,** 545-553.

DORLING, A., REBOLLO-MESA, I., HILTON, R., PEACOCK, J. L., VAUGHAN, R., GARDNER, L., DANZI, G., BAKER, R., CLARK, B., THURAISINGHAM, R. C., BUCKLAND, M., PICTON, M., MARTIN, S., BORROWS, R., BRIGGS, D., HORNE, R., MCCRONE, P., KELLY, J. & MURPHY, C. 2014. Can a combined screening/treatment programme prevent premature failure of renal transplants due to chronic rejection in patients with HLA antibodies: study protocol for the multicentre randomised controlled OuTSMART trial. *Trials,* 15**,** 30-30.

DOUCETT, V. P., GERHARD, W., OWLER, K., CURRY, D., BROWN, L. & BAUMGARTH, N. 2005. Enumeration and characterization of virus-specific B cells by multicolor flow cytometry. *J Immunol Methods,* 303**,** 40-52.

DUDLEY, C., POHANKA, E., RIAD, H., DEDOCHOVA, J., WIJNGAARD, P., SUTTER, C. & SILVA JR, H. T. 2005. Mycophenolate mofetil substitution for cyclosporine A in renal transplant recipients with chronic progressive allograft dysfunction: The "creeping creatinine" study. *Transplantation,* 79**,** 466-475.

DWYER, K. M., HANIDZIAR, D., PUTHETI, P., HILL, P. A., POMMEY, S., MCRAE, J. L., WINTERHALTER, A., DOHERTY, G., DEAGLIO, S., KOULMANDA, M., GAO, W., ROBSON, S. C. & STROM, T. B. 2010. Expression of CD39 by Human Peripheral Blood CD4+CD25+ T Cells Denotes a Regulatory Memory Phenotype. *American Journal of Transplantation,* 10**,** 2410-2420.

EDWARDS, J. C. W. & CAMBRIDGE, G. 2001. Sustained improvement in rheumatoid arthritis following a protocol designed to deplete B lymphocytes. *Rheumatology,* 40**,** 205-211.

EDWARDS, J. C. W., SZCZEPAŃSKI, L., SZECHIŃSKI, J., FILIPOWICZ-SOSNOWSKA, A., EMERY, P., CLOSE, D. R., STEVENS, R. M. & SHAW, T. 2004. Efficacy of B-Cell–Targeted Therapy with Rituximab in Patients with Rheumatoid Arthritis. *New England Journal of Medicine,* 350**,** 2572-2581.

EINECKE, G., SIS, B., REEVE, J., MENGEL, M., CAMPBELL, P. M., HIDALGO, L. G., KAPLAN, B. & HALLORAN, P. F. 2009. Antibody-mediated microcirculation injury is the major cause of late kidney transplant failure. *American Journal of Transplantation,* 9**,** 2520-2531.

ELGUETA, R., BENSON, M. J., DE VRIES, V. C., WASIUK, A., GUO, Y. & NOELLE, R. J. 2009. Molecular mechanism and function of CD40/CD40L engagement in the immune system. *Immunological Reviews,* 229**,** 152-172.

ELLIOTT, T. J. & EISEN, H. N. 1988. Allorecognition of purified major histocompatibility complex glycoproteins by cytotoxic T lymphocytes. *Proceedings of the National Academy of Sciences of the United States of America,* 85**,** 2728-2732.

ELLIOTT, T. J. & EISEN, H. N. 1990. Cytotoxic T lymphocytes recognize a reconstituted class I histocompatibility antigen (HLA-A2) as an allogeneic target molecule. *Proceedings of the National Academy of Sciences,* 87**,** 5213-5217.

ESTORNINHO, M., GIBSON, V. B., KRONENBERG-VERSTEEG, D., LIU, Y. F., NI, C., CEROSALETTI, K. & PEAKMAN, M. 2013. A novel approach to tracking antigen-experienced CD4 T cells into functional compartments via tandem deep and shallow TCR clonotyping. *Journal of Immunology,* 191**,** 5430-5440.

EUGSTER, A., LINDNER, A., HENINGER, A. K., WILHELM, C., DIETZ, S., CATANI, M., ZIEGLER, A. G. & BONIFACIO, E. 2013. Measuring T cell receptor and T cell gene expression diversity in antigen-responsive human CD4+ T cells. *Journal of Immunological Methods,* 400-401**,** 13-22.

FALCONE, M., LEE, J., PATSTONE, G., YEUNG, B. & SARVETNICK, N. 1998. B Lymphocytes Are Crucial Antigen-Presenting Cells in the Pathogenic Autoimmune Response to GAD65 Antigen in Nonobese Diabetic Mice. *The Journal of Immunology,* 161**,** 1163-1168.

FANGMANN, J., DALCHAU, R. & FABRE, J. W. 1992. Rejection of skin allografts by indirect allorecognition of donor class I major histocompatibility complex peptides. *The Journal of Experimental Medicine,* 175**,** 1521-1529.

FASSI, D. E., NIELSEN, C. H., KJELDSEN, J., CLEMMENSEN, O. & HEGEDÜS, L. 2008. Ulcerative colitis following B lymphocyte depletion with rituximab in a patient with Graves' disease. *Gut,* 57**,** 714-715.

FEHR, T., RÜSI, B., FISCHER, A., HOPFER, H., WÜTHRICH, R. P. & GASPERT, A. 2009. Rituximab and Intravenous Immunoglobulin Treatment of Chronic Antibody-Mediated Kidney Allograft Rejection. *Transplantation,* 87**,** 1837-1841.

FELIX, N. J., DONERMEYER, D. L., HORVATH, S., WALTERS, J. J., GROSS, M. L., SURI, A. & ALLEN, P. M. 2007. Alloreactive T cells respond specifically to multiple distinct peptide-MHC complexes. *Nat Immunol,* 8**,** 388-397.

FERRARI, S., GILIANI, S., INSALACO, A., AL-GHONAIUM, A., SORESINA, A. R., LOUBSER, M., AVANZINI, M. A., MARCONI, M., BADOLATO, R., UGAZIO, A. G., LEVY, Y., CATALAN, N., DURANDY, A., TBAKHI, A., NOTARANGELO, L. D. & PLEBANI, A. 2001. Mutations of CD40 gene cause an autosomal recessive form of immunodeficiency with hyper IgM. *Proc Natl Acad Sci U S A,* 98**,** 12614-12619.

FEUCHT, H. E., SCHNEEBERGER, H., HILLEBRAND, G., BURKHARDT, K., WEISS, M., RIETHMULLER, G., LAND, W. & ALBERT, E. 1993. Capillary deposition of C4d complement fragment and early renal graft loss. *Kidney International,* 43**,** 1333-1338.

FILLATREAU, S. 2015. Pathogenic functions of B cells in autoimmune diseases: IFN-γ production joins the criminal gang. *European Journal of Immunology,* 45**,** 966-970.

FILLATREAU, S., SWEENIE, C. H., MCGEACHY, M. J., GRAY, D. & ANDERTON, S. M. 2002. B cells regulate autoimmunity by provision of IL-10. *Nat Immunol,* 3**,** 944-50.

FLORES-BORJA, F., BOSMA, A., NG, D., REDDY, V., EHRENSTEIN, M. R., ISENBERG, D. A. & MAURI, C. 2013. CD19+CD24hiCD38hi B cells maintain regulatory T cells while limiting TH1 and TH17 differentiation. *Sci Transl Med,* 5.

FLYNN, K. & MULLBACHER, A. 1996. Memory alloreactive cytotoxic T cells do not require costimulation for activation in vitro. *Immunol Cell Biol,* 74**,** 413-420.

FULEIHAN, R., RAMESH, N., LOH, R., JABARA, H., ROSEN, R. S., CHATILA, T., FU, S. M., STAMENKOVIC, I. & GEHA, R. S. 1993. Defective expression of the CD40 ligand in X

chromosome-linked immunoglobulin deficiency with normal or elevated IgM. *Proceedings of the National Academy of Sciences,* 90**,** 2170-2173.

GAGRO, A., SERVIS, D., CEPIKA, A.-M., TOELLNER, K.-M., GRAFTON, G., TAYLOR, D. R., BRANICA, S. & GORDON, J. 2006. Type I cytokine profiles of human naïve and memory B lymphocytes: a potential for memory cells to impact polarization. *Immunology,* 118**,** 66-77.

GANAPAMO, F., DENNIS, V. A. & PHILIPP, M. T. 2001. CD19+ cells produce IFN-γ in mice infected with Borrelia burgdorferi. *European Journal of Immunology,* 31**,** 3460-3468.

GARSIDE, P., INGULLI, E., MERICA, R. R., JOHNSON, J. G., NOELLE, R. J. & JENKINS, M. K. 1998. Visualization of Specific B and T Lymphocyte Interactions in the Lymph Node. *Science,* 281**,** 96-99.

GASTON, R. S., CECKA, J. M., KASISKE, B. L., FIEBERG, A. M., LEDUC, R., COSIO, F. C., GOURISHANKAR, S., GRANDE, J., HALLORAN, P., HUNSICKER, L., MANNON, R., RUSH, D. & MATAS, A. J. 2010. Evidence for antibody-mediated injury as a Major determinant of late kidney allograft failure. *Transplantation,* 90**,** 68-74.

GATTO, D., WOOD, K. & BRINK, R. 2011. EBI2 Operates Independently of but in Cooperation with CXCR5 and CCR7 To Direct B Cell Migration and Organization in Follicles and the Germinal Center. *The Journal of Immunology,* 187**,** 4621-4628.

GOETZ, M., ATREYA, R., GHALIBAFIAN, M., GALLE, P. R. & NEURATH, M. F. 2007. Exacerbation of ulcerative colitis after rituximab salvage therapy. *Inflammatory Bowel Diseases,* 13**,** 1365-1368.

GONCZOL, E. & PLOTKIN, S. 2001. Development of a cytomegalovirus vaccine lessons from recent clinical trials. *Expert Opinion on Biological Therapy,* 1**,** 401-412.

GOOD, K. L., AVERY, D. T. & TANGYE, S. G. 2009. Resting Human Memory B Cells Are Intrinsically Programmed for Enhanced Survival and Responsiveness to Diverse Stimuli Compared to Naive B Cells. *The Journal of Immunology,* 182**,** 890-901.

GOOD-JACOBSON, K. L. & TARLINTON, D. M. 2012. Multiple routes to B-cell memory. *Int Immunol,* 24**,** 403-408.

GRANT, C. R., LIBERAL, R., HOLDER, B. S., CARDONE, J., MA, Y., ROBSON, S. C., MIELI-VERGANI, G., VERGANI, D. & LONGHI, M. S. 2014. Dysfunctional CD39POS regulatory T cells and aberrant control of T-helper type 17 cells in autoimmune hepatitis. *Hepatology,* 59**,** 1007-1015.

GRAY, D., BERGTHORSDOTTIR, S., VAN ESSEN, D., WYKES, M., POUDRIER, J. & SIEPMANN, K. 1997. Observations on memory B-cell development. *Seminars in Immunology,* 9**,** 249-254.

HAAS, M., SIS, B., RACUSEN, L. C., SOLEZ, K., GLOTZ, D., COLVIN, R. B., CASTRO, M. C. R., DAVID, D. S. R., DAVID-NETO, E., BAGNASCO, S. M., CENDALES, L. C., CORNELL, L. D., DEMETRIS, A. J., DRACHENBERG, C. B., FARVER, C. F., FARRIS III, A. B., GIBSON, I. W., KRAUS, E., LIAPIS, H., LOUPY, A., NICKELEIT, V., RANDHAWA, P., RODRIGUEZ, E. R., RUSH, D., SMITH, R. N., TAN, C. D., WALLACE, W. D. & MENGEL, M. 2014. Banff 2013 meeting report: Inclusion of C4d-negative antibody-mediated rejection and antibody-associated arterial lesions. *American Journal of Transplantation,* 14**,** 272-283.

HARPER, S. J. F., ALI, J. M., WLODEK, E., NEGUS, M. C., HARPER, I. G., CHHABRA, M., QURESHI, M. S., MALLIK, M., BOLTON, E., BRADLEY, J. A. & PETTIGREW, G. J. 2015. CD8 T-cell recognition of acquired alloantigen promotes acute allograft rejection. *Proceedings of the National Academy of Sciences,* 112**,** 12788-12793.

HARRISON, A. M., THALJI, N. M., GREENBERG, A. J., TAPIA, C. J. & WINDEBANK, A. J. 2014. Rituximab for Non-Hodgkin's Lymphoma: A Story of Rapid Success in Translation. *Clinical and translational science,* 7**,** 82-86.

HARTUNG, H.-P. & KIESEIER, B. C. 2010. Atacicept: targeting B cells in multiple sclerosis. *Therapeutic Advances in Neurological Disorders,* 3**,** 205-216.

HASAN, U., CHAFFOIS, C., GAILLARD, C., SAULNIER, V., MERCK, E., TANCREDI, S., GUIET, C., BRIÈRE, F., VLACH, J., LEBECQUE, S., TRINCHIERI, G. & BATES, E. E. M. 2005. Human TLR10 Is a Functional Receptor, Expressed by B Cells and Plasmacytoid Dendritic Cells, Which Activates Gene Transcription through MyD88. *The Journal of Immunology,* 174**,** 2942-2950.

HAYDE, N., BROIN, P. Ó., BAO, Y., DE BOCCARDO, G., LUBETZKY, M., AJAIMY, M., PULLMAN, J., COLOVAI, A., GOLDEN, A. & AKALIN, E. 2014. Increased intragraft rejection-associated gene transcripts in patients with donor-specific antibodies and normal biopsies. *Kidney International,* 86**,** 600-609.

HEIDT, S., ROELEN, D. L., DE VAAL, Y. J. H., KESTER, M. G. D., EIJSINK, C., THOMAS, S., VAN BESOUW, N. M., VOLK, H. D., WEIMAR, W., CLAAS, F. H. J. & MULDER, A. 2012. A Novel ELISPOT Assay to Quantify HLA-Specific B Cells in HLA-Immunized Individuals. *American Journal of Transplantation,* 12**,** 1469-1478.

HERRERA, D., ROJAS, O. L., DUARTE-REY, C., MANTILLA, R. D., ÁNGEL, J. & FRANCO, M. A. 2014. Simultaneous Assessment of Rotavirus-Specific Memory B Cells and Serological Memory after B Cell Depletion Therapy with Rituximab. *PLoS ONE,* 9**,** e97087.

HERRERA, O. B., GOLSHAYAN, D., TIBBOTT, R., OCHOA, F. S., JAMES, M. J., MARELLI-BERG, F. M. & LECHLER, R. I. 2004. A Novel Pathway of Alloantigen Presentation by Dendritic Cells. *The Journal of Immunology,* 173**,** 4828-4837.

HERZOG, S., RETH, M. & JUMAA, H. 2009. Regulation of B-cell proliferation and differentiation by pre-B-cell receptor signalling. *Nat Rev Immunol,* 9**,** 195-205.

HOFFMANN, F. & MEINL, E. 2014. B cells in Multiple Sclerosis: Good or bad guys? *European Journal of Immunology,* 44**,** 1247-1250.

HORNICK, P. I., MASON, P. D., YACOUB, M. H., ROSE, M. L., BATCHELOR, R. & LECHLER, R. I. 1998. Assessment of the contribution that direct allorecognition makes to the progression of chronic cardiac transplant rejection in humans. *Circulation,* 97**,** 1257-1263.

HOVEN, M. Y., DE LEIJ, L., KEIJ, J. F. K. & THE, T. H. 1989. Detection and isolation of antigen-specific B cells by the fluorescence activated cell sorter (FACS). *Journal of Immunological Methods,* 117**,** 275-284.

IRSCH, J., HUNZELMANN, N., TESCH, H., MERK, H., MAGGI, E., RUFFILLI, A. & RADBRUCH, A. 1995. Isolation and characterization of allergen-binding cells from normal and allergic donors. *Immunotechnology,* 1**,** 115-125.

ISAACSON, M. K., FEIRE, A. L. & COMPTON, T. 2007. Epidermal Growth Factor Receptor Is Not Required for Human Cytomegalovirus Entry or Signaling. *Journal of Virology,* 81**,** 6241-6247.

IWATA, Y., MATSUSHITA, T., HORIKAWA, M., DILILLO, D. J., YANABA, K., VENTURI, G. M., SZABOLCS, P. M., BERNSTEIN, S. H., MAGRO, C. M., WILLIAMS, A. D., HALL, R. P., ST CLAIR, E. W. & TEDDER, T. F. 2011. Characterization of a rare IL-10-competent B-cell subset in humans that parallels mouse regulatory B10 cells. *Blood,* 117**,** 530-541.

JANETZKI, S., RUEGER, M. & DILLENBECK, T. 2014. Stepping up ELISpot: Multi-Level Analysis in FluoroSpot Assays. *Cells,* 3**,** 1102-1115.

JONES, R. B. 2014. Rituximab in the Treatment of Anti-Neutrophil Cytoplasm Antibody-Associated Vasculitis. *Nephron Clinical Practice,* 128**,** 243-249.

JULIUS, M. H., MASUDA, T. & HERZENBERG, L. A. 1972. Demonstration that antigen-binding cells are precursors of antibody-producing cells after purification with a fluorescence-activated cell sorter. *Proc Natl Acad Sci U S A,* 69**,** 1934-1938.

KAMBUROVA, E. G., KOENEN, H. J. P. M., VAN DEN HOOGEN, M. W. F., BAAS, M. C., JOOSTEN, I. & HILBRANDS, L. B. 2014. Longitudinal Analysis of T and B Cell Phenotype and Function in Renal Transplant Recipients with or without Rituximab Induction Therapy. *PLoS ONE,* 9**,** e112658.

KARAHAN, G. E., CLAAS, F. H. J. & HEIDT, S. 2015a. Detecting the humoral alloimmune response: We need more than serum antibody screening. *Transplantation,* 99**,** 908-915.

KARAHAN, G. E., DE VAAL, Y. J. H., ROELEN, D. L., BUCHLI, R., CLAAS, F. H. J. & HEIDT, S. 2015b. Quantification of HLA class II-specific memory B cells in HLA-sensitized individuals. *Human Immunology,* 76**,** 129-136.

KELLY, L. M., PEREIRA, J. P., YI, T., XU, Y. & CYSTER, J. G. 2011. EBI2 Guides Serial Movements of Activated B Cells and Ligand Activity Is Detectable in Lymphoid and Nonlymphoid Tissues. *The Journal of Immunology,* 187**,** 3026-3032.

KHASKHELY, N., MOSAKOWSKI, J., THOMPSON, R. S., KHUDER, S., SMITHSON, S. L. & WESTERINK, M. A. J. 2012. Phenotypic analysis of pneumococcal polysaccharide-specific B cells. *Journal of Immunology,* 188**,** 2455-2463.

KHODER, A., SARVARIA, A., ALSULIMAN, A., CHEW, C., SEKINE, T., COOPER, N., MIELKE, S., DE LAVALLADE, H., MUFTUOGLU, M., FERNANDEZ CURBELO, I., LIU, E., MURARO, P. A., ALOUSI, A., STRINGARIS, K., PARMAR, S., SHAH, N., SHAIM, H., YVON, E., MOLLDREM, J., ROUCE, R., CHAMPLIN, R., MCNIECE, I., MAURI, C., SHPALL, E. J. & REZVANI, K. 2014. Regulatory B cells are enriched within the IgM memory and transitional subsets in healthy donors but are deficient in chronic GVHD. *Blood,* 124**,** 2034-2045.

KISSMEYER-NIELSEN, F., OLSEN, S., PETERSEN, V. P. & FJELDBORG, O. 1966. HYPERACUTE REJECTION OF KIDNEY ALLOGRAFTS, ASSOCIATED WITH PRE-EXISTING HUMORAL ANTIBODIES AGAINST DONOR CELLS. *The Lancet,* 288**,** 662-665.

KLEIN, U., CASOLA, S., CATTORETTI, G., SHEN, Q., LIA, M., MO, T., LUDWIG, T., RAJEWSKY, K. & DALLA-FAVERA, R. 2006. Transcription factor IRF4 controls plasma cell differentiation and class-switch recombination. *Nat Immunol,* 7**,** 773-782.

KLEIN, U., KÜPPERS, R. & RAJEWSKY, K. 1997. *Evidence for a Large Compartment of IgM-Expressing Memory B Cells in Humans*.

KLEIN, U., RAJEWSKY, K. & KÜPPERS, R. 1998. Human immunoglobulin (Ig)M+IgD+ peripheral blood B cells expressing the CD27 cell surface antigen carry somatically mutated variable region genes: CD27 as a general marker for somatically mutated (memory) B cells. *Journal of Experimental Medicine,* 188**,** 1679-1689.

KNECHTLE, S. J., KOLBECK, P. C., TSUCHIMOTO, S., COUNDOURIOTIS, A., SANFILIPPO, F. & BOLLINGER, R. R. 1987. HEPATIC TRANSPLANTATION INTO SENSITIZED RECIPIENTS: DEMONSTRATION OF HYPERACUTE REJECTION. *Transplantation,* 43**,** 8-12.

KOETHE, S., ZANDER, L., KÖSTER, S., ANNAN, A., EBENFELT, A., SPENCER, J. & BEMARK, M. 2011. Pivotal advance: CD45RB glycosylation is specifically regulated during human peripheral B cell differentiation. *Journal of Leukocyte Biology,* 90**,** 5-19.

KORTHAUER, U., GRAF, D., MAGES, H. W., BRIERE, F., PADAYACHEE, M., MALCOLM, S., UGAZIO, A. G., NOTARANGELO, L. D., LEVINSKY, R. J. & KROCZEK, R. A. 1993. Defective expression of T-cell CD40 ligand causes X-linked immunodeficiency with hyper-IgM. *Nature,* 361**,** 539-541.

KRUETZMANN, S., ROSADO, M. M., WEBER, H., GERMING, U., TOURNILHAC, O., PETER, H.-H., BERNER, R., PETERS, A., BOEHM, T., PLEBANI, A., QUINTI, I. & CARSETTI, R. 2003. Human Immunoglobulin M Memory B Cells Controlling Streptococcus pneumoniae Infections Are Generated in the Spleen. *J Exp Med,* 197**,** 939-945.

LACHMANN, N., TERASAKI, P. I., BUDDE, K., LIEFELDT, L., KAHL, A., REINKE, P., PRATSCHKE, J., RUDOLPH, B., SCHMIDT, D., SALAMA, A. & SCHONEMANN, C. 2009. Anti-human leukocyte antigen and donor-specific antibodies detected by luminex posttransplant serve as biomarkers for chronic rejection of renal allografts. *Transplantation,* 87**,** 1505-13.

LAKKIS, F. G. & LECHLER, R. I. 2013. Origin and Biology of the Allogeneic Response. *Cold Spring Harbor Perspectives in Medicine,* 3.

LAMB, K. E., LODHI, S. & MEIER-KRIESCHE, H. U. 2011. Long-Term Renal Allograft Survival in the United States: A Critical Reappraisal. *American Journal of Transplantation,* 11**,** 450-462.

LEANDRO, M. J., CAMBRIDGE, G., EHRENSTEIN, M. R. & EDWARDS, J. C. W. 2006. Reconstitution of peripheral blood B cells after depletion with rituximab in patients with rheumatoid arthritis. *Arthritis & Rheumatism,* 54**,** 613-620.

LECHLER, R. I. & BATCHELOR, J. R. 1982. Restoration of immunogenicity to passenger cell-depleted kidney allografts by the addition of donor strain dendritic cells. *Journal of Experimental Medicine,* 155**,** 31-41.

LEDERER, S. R., KLUTH-PEPPER, B., SCHNEEBERGER, H., ALBERT, E., LAND, W. & FEUCHT, H. E. 2001. Impact of humoral alloreactivity early after transplantation on the long-term survival of renal allografts. *Kidney International,* 59**,** 334-341.

LEDERMAN, S., YELLIN, M. J., KRICHEVSKY, A., BELKO, J., LEE, J. J. & CHESS, L. 1992. Identification of a novel surface protein on activated CD4+ T cells that induces contact-dependent B cell differentiation (help). *The Journal of Experimental Medicine,* 175**,** 1091-1101.

LEE, J., KUCHEN, S., FISCHER, R., CHANG, S. & LIPSKY, P. E. 2009. Identification and characterization of a human CD5+ pre-naive B cell population. *Journal of Immunology,* 182**,** 4116-4126.

LEE, P.-C., TERASAKI, P. I., TAKEMOTO, S. K., LEE, P.-H., HUNG, C.-J., CHEN, Y.-L., TSAI, A. & LEI, H.-Y. 2002. All chronic rejection failures of kidney transplants were preceded by the development of HLA antibodies. *Transplantation,* 74**,** 1192-1194.

LEE, S. M. Y., KOK, K.-H., JAUME, M., CHEUNG, T. K. W., YIP, T.-F., LAI, J. C. C., GUAN, Y., WEBSTER, R. G., JIN, D.-Y. & PEIRIS, J. S. M. 2014. Toll-like receptor 10 is involved in induction of innate immune responses to influenza virus infection. *Proceedings of the National Academy of Sciences,* 111**,** 3793-3798.

LEVESQUE, M. C. & ST CLAIR, E. W. 2008. B cell-directed therapies for autoimmune disease and correlates of disease response and relapse. *J Allergy Clin Immunol,* 121**,** 13-21; quiz 22-3.

LEYENDECKERS, H., ODENDAHL, M., LÖHNDORF, A., IRSCH, J., SPANGFORT, M., MILTENYI, S., HUNZELMANN, N., ASSENMACHER, M., RADBRUCH, A. & SCHMITZ, J. 1999. Correlation analysis between frequencies of circulating antigen-

specific IgG-bearing memory B cells and serum titers of antigen-specific IgG. *Eur J Immunol,* 29**,** 1406-1417.

LI, X. & ZHUANG, S. 2014. Recent advances in renal interstitial fibrosis and tubular atrophy after kidney transplantation. *Fibrogenesis & Tissue Repair,* 7**,** 15-15.

LINDAHL, K. F. & WILSON, D. B. 1977. Histocompatibility antigen-activated cytotoxic T lymphocytes. II. Estimates of the frequency and specificity of precursors. *The Journal of Experimental Medicine,* 145**,** 508-522.

LINDNER, S., DAHLKE, K., SONTHEIMER, K., HAGN, M., KALTENMEIER, C., BARTH, T. F. E., BEYER, T., REISTER, F., FABRICIUS, D., LOTFI, R., LUNOV, O., NIENHAUS, G. U., SIMMET, T., KREIENBERG, R., MÖLLER, P., SCHREZENMEIER, H. & JAHRSDÖRFER, B. 2013. Interleukin 21–Induced Granzyme B–Expressing B Cells Infiltrate Tumors and Regulate T Cells. *Cancer Research,* 73**,** 2468-2479.

LINTON, P.-J., BAUTISTA, B., BIEDERMAN, E., BRADLEY, E. S., HARBERTSON, J., KONDRACK, R. M., PADRICK, R. C. & BRADLEY, L. M. 2003. Costimulation via OX40L Expressed by B Cells Is Sufficient to Determine the Extent of Primary CD4 Cell Expansion and Th2 Cytokine Secretion In Vivo. *The Journal of Experimental Medicine,* 197**,** 875-883.

LINTON, P.-J., HARBERTSON, J. & BRADLEY, L. M. 2000. A Critical Role for B Cells in the Development of Memory CD4 Cells. *The Journal of Immunology,* 165**,** 5558-5565.

LIU, Z., COLOVAI, A. I., TUGULEA, S., REED, E. F., FISHER, P. E., MANCINI, D., ROSE, E. A., CORTESINI, R., MICHLER, R. E. & SUCIU-FOCA, N. 1996. Indirect recognition of donor HLA-DR peptides in organ allograft rejection. *The Journal of Clinical Investigation,* 98**,** 1150-1157.

LOMBARDI, G., SIDHU, S., BATCHELOR, J. R. & LECHLER, R. I. 1989. Allorecognition of DR1 by T cells from a DR4/DRw13 responder mimics self-restricted recognition of endogenous peptides. *Proceedings of the National Academy of Sciences,* 86**,** 4190-4194.

LOUIS, S., BRAUDEAU, C., GIRAL, M., DUPONT, A., MOIZANT, F., ROBILLARD, N., MOREAU, A., SOULILLOU, J.-P. & BROUARD, S. 2006. Contrasting CD25hiCD4+T Cells/FOXP3 Patterns in Chronic Rejection and Operational Drug-Free Tolerance. *Transplantation,* 81**,** 398-407.

LOVEGROVE, E., PETTIGREW, G. J., BOLTON, E. M. & BRADLEY, J. A. 2001. Epitope Mapping of the Indirect T Cell Response to Allogeneic Class I MHC: Sequences Shared

by Donor and Recipient MHC May Prime T Cells That Provide Help for Alloantibody Production. *The Journal of Immunology,* 167**,** 4338-4344.

LU, T. Y. T., NG, K. P., CAMBRIDGE, G., LEANDRO, M. J., EDWARDS, J. C. W., EHRENSTEIN, M. & ISENBERG, D. A. 2009. A retrospective seven-year analysis of the use of B cell depletion therapy in systemic lupus erythematosus at university college london hospital: The first fifty patients. *Arthritis Care & Research,* 61**,** 482-487.

LUND, F. E. 2008. Cytokine-producing B lymphocytes - key regulators of immunity. *Curr Opin Immunol,* 20**,** 332-338.

LUND, F. E., HOLLIFIELD, M., SCHUER, K., LINES, J. L., RANDALL, T. D. & GARVY, B. A. 2006. B Cells Are Required for Generation of Protective Effector and Memory CD4 Cells in Response to Pneumocystis Lung Infection. *The Journal of Immunology,* 176**,** 6147-6154.

LÚCIA, M., LUQUE, S., CRESPO, E., MELILLI, E., CRUZADO, J. M., MARTORELL, J., JARQUE, M., GIL-VERNET, S., MANONELLES, A., GRINYÓ, J. M. & BESTARD, O. 2015. Preformed circulating HLA-specific memory B cells predict high risk of humoral rejection in kidney transplantation. *Kidney International,* 88**,** 874-887.

MA, L., LIU, B., JIANG, Z. & JIANG, Y. 2014. Reduced numbers of regulatory B cells are negatively correlated with disease activity in patients with new-onset rheumatoid arthritis. *Clinical Rheumatology,* 33**,** 187-195.

MAGLIONE, P. J., SIMCHONI, N., BLACK, S., RADIGAN, L., OVERBEY, J. R., BAGIELLA, E., BUSSEL, J. B., BOSSUYT, X., CASANOVA, J. L., MEYTS, I., CERUTTI, A., PICARD, C. & CUNNINGHAM-RUNDLES, C. 2014. IRAK-4 and MyD88 deficiencies impair IgM responses against T-independent bacterial antigens. *Blood,* 124**,** 3561-3571.

MAMULA, M. J. & JANEWAY, C. A. 1993. Do B cells drive the diversification of immune responses? *Immunology Today,* 14**,** 151-152.

MANIKKAVASAGAN, G., DEZATEUX, C., WADE, A. & BEDFORD, H. 2010. The epidemiology of chickenpox in UK 5-year olds: An analysis to inform vaccine policy. *Vaccine,* 28**,** 7699-7705.

MATSUMOTO, M., BABA, A., YOKOTA, T., NISHIKAWA, H., OHKAWA, Y., KAYAMA, H., KALLIES, A., NUTT, STEPHEN L., SAKAGUCHI, S., TAKEDA, K., KUROSAKI, T. & BABA, Y. 2014. Interleukin-10-Producing Plasmablasts Exert Regulatory Function in Autoimmune Inflammation. *Immunity,* 41**,** 1040-1051.

MAUIYYEDI, S., DELLA PELLE, P., SAIDMAN, S., COLLINS, A. B., PASCUAL, M., TOLKOFF-RUBIN, N. E., WILLIAMS, W. W., COSIMI, A. B., SCHNEEBERGER, E. E. & COLVIN, R. B. 2001. Chronic humoral rejection: Identification of antibody-mediated chronic renal allograft rejection by C4d deposits in peritubular capillaries. *Journal of the American Society of Nephrology,* 12**,** 574-582.

MCCONKEY, S. J., REECE, W. H. H., MOORTHY, V. S., WEBSTER, D., DUNACHIE, S., BUTCHER, G., VUOLA, J. M., BLANCHARD, T. J., GOTHARD, P., WATKINS, K., HANNAN, C. M., EVERAERE, S., BROWN, K., KESTER, K. E., CUMMINGS, J., WILLIAMS, J., HEPPNER, D. G., PATHAN, A., FLANAGAN, K., ARULANANTHAM, N., ROBERTS, M. T. M., ROY, M., SMITH, G. L., SCHNEIDER, J., PETO, T., SINDEN, R. E., GILBERT, S. C. & HILL, A. V. S. 2003. Enhanced T-cell immunogenicity of plasmid DNA vaccines boosted by recombinant modified vaccinia virus Ankara in humans. *Nat Med,* 9**,** 729-735.

MIELKE, F., SCHNEIDER-OBERMEYER, J. & DÖRNER, T. 2008. Onset of psoriasis with psoriatic arthropathy during rituximab treatment of non-Hodgkin lymphoma. *Annals of the Rheumatic Diseases,* 67**,** 1056-1057.

MOLNARFI, N., SCHULZE-TOPPHOFF, U., WEBER, M. S., PATARROYO, J. C., PROD'HOMME, T., VARRIN-DOYER, M., SHETTY, A., LININGTON, C., SLAVIN, A. J., HIDALGO, J., JENNE, D. E., WEKERLE, H., SOBEL, R. A., BERNARD, C. C., SHLOMCHIK, M. J. & ZAMVIL, S. S. 2013. MHC class II-dependent B cell APC function is required for induction of CNS autoimmunity independent of myelin-specific antibodies. *J Exp Med,* 210**,** 2921-2937.

MONTECALVO, A., SHUFESKY, W. J., STOLZ, D. B., SULLIVAN, M. G., WANG, Z., DIVITO, S. J., PAPWORTH, G. D., WATKINS, S. C., ROBBINS, P. D., LARREGINA, A. T. & MORELLI, A. E. 2008. Exosomes as a short-range mechanism to spread alloantigen between dendritic cells during T cell allorecognition. *Journal of Immunology,* 180**,** 3081-3090.

MOODY, M. A. & HAYNES, B. F. 2008. Antigen-specific B cell detection reagents: Use and quality control. *Cytometry Part A,* 73**,** 1086-1092.

MOORE, J., MA, D., WILL, R., CANNELL, P., HANDEL, M. & MILLIKEN, S. 2004. A phase II study of Rituximab in rheumatoid arthritis patients with recurrent disease following haematopoietic stem cell transplantation. *Bone Marrow Transplant,* 34**,** 241-247.

MULDER, A., EIJSINK, C., KARDOL, M. J., FRANKE-VAN DIJK, M. E. I., VAN DER BURG, S. H., KESTER, M., DOXIADIS, I. I. N. & CLAAS, F. H. J. 2003. Identification, Isolation,

and Culture of HLA-A2-Specific B Lymphocytes Using MHC Class I Tetramers. *Journal of Immunology,* 171**,** 6599-6603.

MULDER, A., KARDOL, M. J., KAMP, J., UIT HET BROEK, C., SCHREUDER, G. M. T., DOXIADIS, I. I. N. & CLAAS, F. H. J. 2001. Determination of the frequency of HLA antibody secreting B-lymphocytes in alloantigen sensitized individuals. *Clinical and Experimental Immunology,* 124**,** 9-15.

MURAMATSU, M., KINOSHITA, K., FAGARASAN, S., YAMADA, S., SHINKAI, Y. & HONJO, T. 2000. Class switch recombination and hypermutation require activation-induced cytidine deaminase (AID), a potential RNA editing enzyme. *Cell,* 102**,** 553-563.

NADAZDIN, O., BOSKOVIC, S., MURAKAMI, T., O'CONNOR, D. H., WISEMAN, R. W., KARL, J. A., TUSCHER, J. J., SACHS, D. H., MADSEN, J. C., TOCCO, G., KAWAI, T., COSIMI, A. B. & BENICHOU, G. 2010. Phenotype, Distribution and Alloreactive Properties of Memory T Cells from Cynomolgus Monkeys. *American Journal of Transplantation,* 10**,** 1375-1384.

NADAZDIN, O., BOSKOVIC, S., WEE, S.-L., SOGAWA, H., KOYAMA, I., COLVIN, R. B., SMITH, R. N., TOCCO, G., O'CONNOR, D. H., KARL, J. A., MADSEN, J. C., SACHS, D. H., KAWAI, T., COSIMI, A. B. & BENICHOU, G. 2011. Contributions of Direct and Indirect Alloresponses to Chronic Rejection of Kidney Allografts in Nonhuman Primates. *The Journal of Immunology,* 187**,** 4589-4597.

NAGASAWA, T. 2006. Microenvironmental niches in the bone marrow required for B-cell development. *Nat Rev Immunol,* 6**,** 107-116.

NANAN, R., HEINRICH, D., FROSCH, M. & KRETH, H. W. 2001. Acute and long-term effects of booster immunisation on frequencies of antigen-specific memory B-lymphocytes. *Vaccine,* 20**,** 498-504.

NEMAZEE, D. 2006. Receptor editing in lymphocyte development and central tolerance. *Nat Rev Immunol,* 6**,** 728-40.

NEWELL, K. A., ASARE, A., KIRK, A. D., GISLER, T. D., BOURCIER, K., SUTHANTHIRAN, M., BURLINGHAM, W. J., MARKS, W. H., SANZ, I., LECHLER, R. I., HERNANDEZ-FUENTES, M. P., TURKA, L. A. & SEYFERT-MARGOLIS, V. L. 2010. Identification of a B cell signature associated with renal transplant tolerance in humans. *The Journal of Clinical Investigation,* 120**,** 1836-1847.

NG, Y. H., OBERBARNSCHEIDT, M. H., CHANDRAMOORTHY, H. C., HOFFMAN, R. & CHALASANI, G. 2010. B cells help alloreactive T cells differentiate into memory T cells. *Am J Transplant,* 10**,** 1970-80.

NOORCHASHM, H., NOORCHASHM, N., KERN, J., ROSTAMI, S. Y., BARKER, C. F. & NAJI, A. 1997. B-Cells Are Required for the Initiation of Insulitis and Sialitis in Nonobese Diabetic Mice. *Diabetes,* 46**,** 941-946.

NOORCHASHM, H., REED, A. J., ROSTAMI, S. Y., MOZAFFARI, R., ZEKAVAT, G., KOEBERLEIN, B., CATON, A. J. & NAJI, A. 2006. B Cell-Mediated Antigen Presentation Is Required for the Pathogenesis of Acute Cardiac Allograft Rejection. *The Journal of Immunology,* 177**,** 7715-7722.

NOSSAL, G. J. V., PIKE, B. L. & BATTYE, F. L. 1978. Sequential use of hapten-gelatin fractionation and fluorescence-activated cell sorting in the enrichment of hapten-specific B lymphocytes. *Eur J Immunol,* 8**,** 151-157.

NOUEL, A., SEGALEN, I., JAMIN, C., DOUCET, L., CAILLARD, S., RENAUDINEAU, Y., PERS, J.-O., LE MEUR, Y. & HILLION, S. 2014. B cells display an abnormal distribution and an impaired suppressive function in patients with chronic antibody-mediated rejection. *Kidney Int,* 85**,** 590-599.

NOVA-LAMPERTI, E., FANELLI, G., BECKER, P. D., CHANA, P., ELGUETA, R., DODD, P. C., LORD, G. M., LOMBARDI, G. & HERNANDEZ-FUENTES, M. P. 2016. IL-10-produced by human transitional B-cells down-regulates CD86 expression on B-cells leading to inhibition of CD4+T-cell responses. *Scientific Reports,* 6**,** 20044.

NUTT, S. L., HODGKIN, P. D., TARLINTON, D. M. & CORCORAN, L. M. 2015. The generation of antibody-secreting plasma cells. *Nat Rev Immunol,* 15**,** 160-171.

OCHIAI, K., MAIENSCHEIN-CLINE, M., SIMONETTI, G., CHEN, J., ROSENTHAL, R., BRINK, R., CHONG, ANITA S., KLEIN, U., DINNER, AARON R., SINGH, H. & SCIAMMAS, R. 2013. Transcriptional Regulation of Germinal Center B and Plasma Cell Fates by Dynamical Control of IRF4. *Immunity,* 38**,** 918-929.

OLALEKAN, S. A., CAO, Y., HAMEL, K. M. & FINNEGAN, A. 2015. B cells expressing IFN-γ suppress Treg-cell differentiation and promote autoimmune experimental arthritis. *European Journal of Immunology,* 45**,** 988-998.

OOSTING, M., CHENG, S.-C., BOLSCHER, J. M., VESTERING-STENGER, R., PLANTINGA, T. S., VERSCHUEREN, I. C., ARTS, P., GARRITSEN, A., VAN EENENNAAM, H., STURM, P., KULLBERG, B.-J., HOISCHEN, A., ADEMA, G. J., VAN DER MEER, J.

W. M., NETEA, M. G. & JOOSTEN, L. A. B. 2014. Human TLR10 is an anti-inflammatory pattern-recognition receptor. *Proceedings of the National Academy of Sciences,* 111**,** E4478-E4484.

OPATA, M. M., HOLLIFIELD, M. L., LUND, F. E., RANDALL, T. D., DUNN, R., GARVY, B. A. & FEOLA, D. J. 2015. B Lymphocytes Are Required during the Early Priming of CD4+ T Cells for Clearance of Pneumocystis Infection in Mice. *The Journal of Immunology,* 195**,** 611-620.

O'CONNOR, B. P., VOGEL, L. A., ZHANG, W., LOO, W., SHNIDER, D., LIND, E. F., RATLIFF, M., NOELLE, R. J. & ERICKSON, L. D. 2006. Imprinting the Fate of Antigen-Reactive B Cells through the Affinity of the B Cell Receptor. *The Journal of Immunology,* 177**,** 7723-7732.

PALANICHAMY, A., BARNARD, J., ZHENG, B., OWEN, T., QUACH, T., WEI, C., LOONEY, R. J., SANZ, I. & ANOLIK, J. H. 2009. Novel human transitional B cell populations revealed by B cell depletion therapy. *Journal of Immunology,* 182**,** 5982-5993.

PALANICHAMY, A., MUHAMMAD, K., ROLL, P., KLEINERT, S., DORNER, T. & TONY, H.-P. 2012. Rituximab Therapy Leads to Reduced Imprints of Receptor Revision in Immunoglobulin κ and λ Light Chains. *The Journal of Rheumatology,* 39**,** 1130-1138.

PALLIER, A., HILLION, S., DANGER, R., GIRAL, M., RACAPE, M., DEGAUQUE, N., DUGAST, E., ASHTON-CHESS, J., PETTRE, S., LOZANO, J. J., BATAILLE, R., DEVYS, A., CESBRON-GAUTIER, A., BRAUDEAU, C., LARROSE, C., SOULILLOU, J. P. & BROUARD, S. 2010. Patients with drug-free long-term graft function display increased numbers of peripheral B cells with a memory and inhibitory phenotype. *Kidney Int,* 78**,** 503-13.

PAPE, K. A., TAYLOR, J. J., MAUL, R. W., GEARHART, P. J. & JENKINS, M. K. 2011. Different B cell populations mediate early and late memory during an endogenous immune response. *Science,* 331**,** 1203-1207.

PAUS, D., PHAN, T. G., CHAN, T. D., GARDAM, S., BASTEN, A. & BRINK, R. 2006. Antigen recognition strength regulates the choice between extrafollicular plasma cell and germinal center B cell differentiation. *J Exp Med,* 203**,** 1081-1091.

PELLETIER, R. P., HENNESSY, P. K., ADAMS, P. W., VANBUSKIRK, A. M., FERGUSON, R. M. & OROSZ, C. G. 2002. Clinical significance of MHC-reactive alloantibodies that develop after kidney or kidney-pancreas transplantation. *American Journal of Transplantation,* 2**,** 134-141.

PEREIRA, J. P., KELLY, L. M., XU, Y. & CYSTER, J. G. 2009. EBI2 mediates B cell segregation between the outer and centre follicle. *Nature,* 460**,** 1122-1126.

PESCOVITZ, M. D., GREENBAUM, C. J., KRAUSE-STEINRAUF, H., BECKER, D. J., GITELMAN, S. E., GOLAND, R., GOTTLIEB, P. A., MARKS, J. B., MCGEE, P. F., MORAN, A. M., RASKIN, P., RODRIGUEZ, H., SCHATZ, D. A., WHERRETT, D., WILSON, D. M., LACHIN, J. M. & SKYLER, J. S. 2009. Rituximab, B-Lymphocyte Depletion, and Preservation of Beta-Cell Function. *New England Journal of Medicine,* 361**,** 2143-2152.

PICARD, C., VON BERNUTH, H., GHANDIL, P., CHRABIEH, M., LEVY, O., ARKWRIGHT, P. D., MCDONALD, D., GEHA, R. S., TAKADA, H., KRAUSE, J. C., CREECH, C. B., KU, C.-L., EHL, S., MAŕODI, Ĺ., AL-MUHSEN, S., AL-HAJJAR, S., AL-GHONAIUM, A., DAY-GOOD, N. K., HOLLAND, S. M., GALLIN, J., CHAPEL, H., SPEERT, D. P., RODRIGUEZ-GALLEGO, C., COLINO, E., GARTY, B.-Z., ROIFMAN, C., HARA, T., YOSHIKAWA, H., NONOYAMA, S., DOMACHOWSKE, J., ISSEKUTZ, A. C., TANG, M., SMART, J., ZITNIK, S. E., HOARAU, C., KUMARARATNE, D., THRASHER, A., DAVIES, E. G., BETHUNE, C., SIRVENT, N., DE RICAUD, D., CAMCIOGLU, Y., VASCONCELOS, J. U., GUEDES, M., VITOR, A. B., RODRIGO, C., ALMAŸAN, F., ḾENDEZ, M., AŕOSTEGUI, J. I., ALSINA, L., FORTUNY, C., REICHENBACH, J., VERBSKY, J. W., BOSSUYT, X., DOFFINGER, R., ABEL, L., PUEL, A. & CASANOVA, J.-L. 2010. Clinical Features and Outcome of Patients With IRAK-4 and MyD88 Deficiency. *Medicine,* 89**,** 403-425.

PLOSKER, G. & FIGGITT, D. 2003. Rituximab. *Drugs,* 63**,** 803-843.

PÖTZSCH, S., SPINDLER, N., WIEGERS, A. K., FISCH, T., RÜCKER, P., STICHT, H., GRIEB, N., BAROTI, T., WEISEL, F., STAMMINGER, T., MARTIN-PARRAS, L., MACH, M. & WINKLER, T. H. 2011. B cell repertoire analysis identifies new antigenic domains on glycoprotein b of human cytomegalovirus which are target of neutralizing antibodies. *PLoS Pathog,* 7.

RETH M, P. E., WIESE P, LOBEL L, ALT F.W 1987. Activation of Vkappa gene rearrangement in pre-B cells follows the expression of membrane-bound immunoglobulin heavy chains. *The EMBO Journal,* 6**,** 3299-3305.

REVY, P., MUTO, T., LEVY, Y., GEISSMANN, F., PLEBANI, A., SANAL, O., CATALAN, N., FORVEILLE, M., DUFOURCQ-LAGELOUSE, R., GENNERY, A., TEZCAN, I., ERSOY, F., KAYSERILI, H., UGAZIO, A. G., BROUSSE, N., MURAMATSU, M., NOTARANGELO, L. D., KINOSHITA, K., HONJO, T., FISCHER, A. & DURANDY, A.

2000. Activation-induced cytidine deaminase (AID) deficiency causes the autosomal recessive form of the hyper-IgM syndrome (HIGM2). *Cell,* 102**,** 565-575.

RICKERT, R. C. 2013. New insights into pre-BCR and BCR signalling with relevance to B cell malignancies. *Nat Rev Immunol,* 13**,** 578-591.

RIDGE, J. P., DI ROSA, F. & MATZINGER, P. 1998. A conditioned dendritic cell can be a temporal bridge between a CD4+ T-helper and a T-killer cell. *Nature,* 393**,** 474-478.

RIELLA, L. V., SAFA, K., YAGAN, J., LEE, B., AZZI, J., NAJAFIAN, N., ABDI, R., MILFORD, E., MAH, H., GABARDI, S., MALEK, S., TULLIUS, S. G., MAGEE, C. & CHANDRAKER, A. 2014. Long-term outcomes of kidney transplantation across a positive complement-dependent cytotoxicity crossmatch. *Transplantation,* 97**,** 1247-1252.

RIVERA, A., CHEN, C.-C., RON, N., DOUGHERTY, J. P. & RON, Y. 2001. Role of B cells as antigen-presenting cells in vivo revisited: antigen-specific B cells are essential for T cell expansion in lymph nodes and for systemic T cell responses to low antigen concentrations. *International Immunology,* 13**,** 1583-1593.

ROCCATELLO, D., SCIASCIA, S., ROSSI, D., ALPA, M., NARETTO, C., BALDOVINO, S., MENEGATTI, E., LA GROTTA, R. & MODENA, V. 2011. Intensive short-term treatment with rituximab, cyclophosphamide and methylprednisolone pulses induces remission in severe cases of SLE with nephritis and avoids further immunosuppressive maintenance therapy. *Nephrology Dialysis Transplantation,* 26**,** 3987-3992.

ROJAS, O. L., NARVÁEZ, C. F., GREENBERG, H. B., ANGEL, J. & FRANCO, M. A. 2008. Characterization of rotavirus specific B cells and their relation with serological memory. *Virology,* 380**,** 234-242.

ROLL, P., PALANICHAMY, A., KNEITZ, C., DORNER, T. & TONY, H.-P. 2006. Regeneration of B cell subsets after transient B cell depletion using anti-CD20 antibodies in rheumatoid arthritis. *Arthritis & Rheumatism,* 54**,** 2377-2386.

ROSTAING, L., GUILBEAU-FRUGIER, C., FORT, M., MEKHLATI, L. & KAMAR, N. 2009. Treatment of symptomatic transplant glomerulopathy with rituximab. *Transplant International,* 22**,** 906-913.

SAGOO, P., PERUCHA, E., SAWITZKI, B., TOMIUK, S., STEPHENS, D. A., MIQUEU, P., CHAPMAN, S., CRACIUN, L., SERGEANT, R., BROUARD, S., ROVIS, F., JIMENEZ, E., BALLOW, A., GIRAL, M., REBOLLO-MESA, I., LE MOINE, A., BRAUDEAU, C., HILTON, R., GERSTMAYER, B., BOURCIER, K., SHARIF, A., KRAJEWSKA, M.,

LORD, G. M., ROBERTS, I., GOLDMAN, M., WOOD, K. J., NEWELL, K., SEYFERT-MARGOLIS, V., WARRENS, A. N., JANSSEN, U., VOLK, H. D., SOULILLOU, J. P., HERNANDEZ-FUENTES, M. P. & LECHLER, R. I. 2010. Development of a cross-platform biomarker signature to detect renal transplant tolerance in humans. *J Clin Invest,* 120**,** 1848-61.

SAGOO, P., RATNASOTHY, K., TSANG, Y., BARBER, L. D., NOBLE, A., LECHLER, R. I. & LOMBARDI, G. 2012. Alloantigen specific regulatory T cells prevent experimental chronic graft-versus-host disease by simultaneous control of allo- and autoreactivity. *Eur J Immunol*.

SALAMA, A. D., DELIKOURAS, A., PUSEY, C. D., COOK, H. T., BHANGAL, G., LECHLER, R. I. & DORLING, A. 2001. Transplant Accommodation in Highly Sensitized Patients: A Potential Role for Bcl-xL and Alloantibody. *American Journal of Transplantation,* 1**,** 260-269.

SALAZAR-CAMARENA, D. C., ORTIZ-LAZARENO, P. C., CRUZ, A., OREGON-ROMERO, E., MACHADO-CONTRERAS, J. R., MUÑOZ-VALLE, J. F., OROZCO-LÓPEZ, M., MARÍN-ROSALES, M. & PALAFOX-SÁNCHEZ, C. A. 2015. Association of BAFF, APRIL serum levels, BAFF-R, TACI and BCMA expression on peripheral B-cell subsets with clinical manifestations in systemic lupus erythematosus. *Lupus*.

SALCIDO-OCHOA, F., TSANG, J., TAM, P., FALK, K. & ROTZSCHKE, O. 2010. Regulatory T cells in transplantation: does extracellular adenosine triphosphate metabolism through CD39 play a crucial role? *Transplantation Reviews,* 24**,** 52-66.

SANCHEZ-FREIRE, V., EBERT, A. D., KALISKY, T., QUAKE, S. R. & WU, J. C. 2012. Microfluidic single-cell real-time PCR for comparative analysis of gene expression patterns. *Nature Protocols,* 7**,** 829-838.

SCHMITTEL, A., KEILHOLZ, U., BAUER, S., KUHNE, U., STEVANOVIC, S., THIEL, E. & SCHEIBENBOGEN, C. 2001. Application of the IFN-γ ELISPOT assay to quantify T cell responses against proteins. *Journal of Immunological Methods,* 247**,** 17-24.

SCHOENBERGER, S. P., TOES, R. E. M., VAN DER VOORT, E. I. H., OFFRINGA, R. & MELIEF, C. J. M. 1998. T-cell help for cytotoxic T lymphocytes is mediated by CD40-CD40L interactions. *Nature,* 393**,** 480-483.

SCOTT-BROWNE, J., CRAWFORD, F., YOUNG, M., KAPPLER, J., MARRACK, P. & GAPIN, L. 2011. Evolutionarily Conserved Features Contribute to αβ T Cell Receptor Specificity. *Immunity,* 35**,** 526-535.

SEIFERT, M. & KÜPPERS, R. 2009. Molecular footprints of a germinal center derivation of human IgM +(IgD+)CD27 + B cells and the dynamics of memory B cell generation. *Journal of Experimental Medicine,* 206**,** 2659-2669.

SEIFERT, M., PRZEKOPOWITZ, M., TAUDIEN, S., LOLLIES, A., RONGE, V., DREES, B., LINDEMANN, M., HILLEN, U., ENGLER, H., SINGER, B. B. & KÜPPERS, R. 2015. Functional capacities of human IgM memory B cells in early inflammatory responses and secondary germinal center reactions. *Proceedings of the National Academy of Sciences,* 112**,** E546-E555.

SENTÍS, A., KERS, J., YAPICI, U., CLAESSEN, N., ROELOFS, J. J. T. H., BEMELMAN, F. J., TEN BERGE, I. J. M. & FLORQUIN, S. 2015. The prognostic significance of glomerular infiltrating leukocytes during acute renal allograft rejection. *Transplant Immunology,* 33**,** 168-175.

SERREZE, D. V., FLEMING, S. A., CHAPMAN, H. D., RICHARD, S. D., LEITER, E. H. & TISCH, R. M. 1998. B Lymphocytes Are Critical Antigen-Presenting Cells for the Initiation of T Cell-Mediated Autoimmune Diabetes in Nonobese Diabetic Mice. *The Journal of Immunology,* 161**,** 3912-3918.

SHABIR, S., GIRDLESTONE, J., BRIGGS, D., KAUL, B., SMITH, H., DAGA, S., CHAND, S., JHAM, S., NAVARRETE, C., HARPER, L., BALL, S. & BORROWS, R. 2015. Transitional B Lymphocytes Are Associated With Protection From Kidney Allograft Rejection: A Prospective Study. *American Journal of Transplantation,* 15**,** 1384-1391.

SHIU, K. Y., MCLAUGHLIN, L., REBOLLO-MESA, I., ZHAO, J., SEMIK, V., COOK, H. T., ROUFOSSE, C., BROOKES, P., BOWERS, R. W., GALLIFORD, J., TAUBE, D., LECHLER, R. I., HERNANDEZ-FUENTES, M. P. & DORLING, A. 2015. B-lymphocytes support and regulate indirect T-cell alloreactivity in individual patients with chronic antibody-mediated rejection. *Kidney Int,* 88**,** 560-568.

SHLOMCHIK, M. J., MADAIO, M. P., NI, D., TROUNSTEIN, M. & HUSZAR, D. 1994. The role of B cells in lpr/lpr-induced autoimmunity. *The Journal of Experimental Medicine,* 180**,** 1295-1306.

SIDNER, R. A., BOOK, B. K., AGARWAL, A., BEARDEN, C. M., VIEIRA, C. A. & PESCOVITZ, M. D. 2004. In vivo human B-cell subset recovery after in vivo depletion with rituximab, anti-human CD20 monoclonal antibody. *Human Antibodies,* 13**,** 55-62.

SILVA, H. M., TAKENAKA, M. C. S., MORAES-VIEIRA, P. M. M., MONTEIRO, S. M., HERNANDEZ, M. O., CHAARA, W., SIX, A., AGENA, F., SESTERHEIM, P., BARBÉ-TUANA, F. M., SAITOVITCH, D., LEMOS, F., KALIL, J. & COELHO, V. 2012.

Preserving the B-Cell Compartment Favors Operational Tolerance in Human Renal Transplantation. *Molecular Medicine,* 18**,** 733-743.

SIMS, G. P., ETTINGER, R., SHIROTA, Y., YARBORO, C. H., ILLEI, G. G. & LIPSKY, P. E. 2005. Identification and characterization of circulating human transitional B cells. *Blood,* 105**,** 4390-4398.

SIS, B., JHANGRI, G. S., BUNNAG, S., ALLANACH, K., KAPLAN, B. & HALLORAN, P. F. 2009. Endothelial gene expression in kidney transplants with alloantibody indicates Antibody-mediated damage despite lack of C4d staining. *American Journal of Transplantation,* 9**,** 2312-2323.

SIVAGANESH, S., HARPER, S. J., CONLON, T. M., CALLAGHAN, C. J., SAEB-PARSY, K., NEGUS, M. C., MOTALLEBZADEH, R., BOLTON, E. M., BRADLEY, J. A. & PETTIGREW, G. J. 2013. Copresentation of Intact and Processed MHC Alloantigen by Recipient Dendritic Cells Enables Delivery of Linked Help to Alloreactive CD8 T Cells by Indirect-Pathway CD4 T Cells. *The Journal of Immunology,* 190**,** 5829-5838.

SIVASAI, K. S. R., SMITH, M. A., POINDEXTER, N. J., SUNDARESAN, S. R., TRULOCK, E. P., LYNCH, J. P., COOPER, J. D., PATTERSON, G. A. & MOHANAKUMAR, T. 1999. Indirect recognition of donor HLA class I peptides in lung transplant recipients with bronchiolitis obliterans syndrome. *Transplantation,* 67**,** 1094-1098.

SMITH, H. J., HANVESAKUL, R., BENTALL, A., SHABIR, S., MORGAN, M. D., BRIGGS, D., COCKWELL, P., BORROWS, R., LARCHÉ, M. & BALL, S. 2011. T Lymphocyte Responses to Nonpolymorphic HLA-Derived Peptides Are Associated With Chronic Renal Allograft Dysfunction. *Transplantation,* 91**,** 279-286.

SMITH, J. G., LIU, X., KAUFHOLD, R. M., CLAIR, J. & CAULFIELD, M. J. 2001. Development and Validation of a Gamma Interferon ELISPOT Assay for Quantitation of Cellular Immune Responses to Varicella-Zoster Virus. *Clinical and Diagnostic Laboratory Immunology,* 8**,** 871-879.

SMITH, P. A., BRUNMARK, A., JACKSON, M. R. & POTTER, T. A. 1997. Peptide-independent Recognition by Alloreactive Cytotoxic T Lymphocytes (CTL). *J Exp Med,* 185**,** 1023-1034.

SMITH, R. N., KAWAI, T., BOSKOVIC, S., NADAZDIN, O., SACHS, D. H., COSIMI, A. B. & COLVIN, R. B. 2008. Four Stages and Lack of Stable Accommodation in Chronic Alloantibody-Mediated Renal Allograft Rejection in Cynomolgus Monkeys. *American Journal of Transplantation,* 8**,** 1662-1672.

SMYTH, L. A., HERVOUET, C., HAYDAY, T., BECKER, P. D., ELLIS, R., LECHLER, R. I., LOMBARDI, G. & KLAVINSKIS, L. S. 2012. Acquisition of MHC:Peptide Complexes by Dendritic Cells Contributes to the Generation of Antiviral CD8+ T Cell Immunity In Vivo. *The Journal of Immunology,* 189**,** 2274-2282.

SNANOUDJ, R., CLAAS, F. H. J., HEIDT, S., LEGENDRE, C., CHATENOUD, L. & CANDON, S. 2015. Restricted specificity of peripheral alloreactive memory B cells in HLA-sensitized patients awaiting a kidney transplant. *Kidney International,* 87**,** 1230-1240.

SNAPPER, C. M. 2012. Mechanisms underlying in vivo polysaccharide-specific immunoglobulin responses to intact extracellular bacteria. *Ann N Y Acad Sci,* 1253**,** 92-101.

SOROCEANU, L., AKHAVAN, A. & COBBS, C. S. 2008. Platelet-derived growth factor-[agr] receptor activation is required for human cytomegalovirus infection. *Nature,* 455**,** 391-395.

SPURGIN, L. G. & RICHARDSON, D. S. 2010. How pathogens drive genetic diversity: MHC, mechanisms and misunderstandings. *Proceedings of the Royal Society of London B: Biological Sciences,* 277**,** 979-988.

STEELE, D. J., LAUFER, T. M., SMILEY, S. T., ANDO, Y., GRUSBY, M. J., GLIMCHER, L. H. & AUCHINCLOSS, H. 1996. Two levels of help for B cell alloantibody production. *The Journal of Experimental Medicine,* 183**,** 699-703.

SUCHIN, E. J., LANGMUIR, P. B., PALMER, E., SAYEGH, M. H., WELLS, A. D. & TURKA, L. A. 2001. Quantifying the Frequency of Alloreactive T Cells In Vivo: New Answers to an Old Question. *The Journal of Immunology,* 166**,** 973-981.

SUCIU-FOCA, N., CIUBOTARIU, R., ITESCU, S., ROSE, E. A. & CORTESINI, R. 1998a. Indirect allorecognition of donor HLA-DR peptides in chronic rejection of heart allografts. *Transplantation Proceedings,* 30**,** 3999-4000.

SUCIU-FOCA, N., CIUBOTARIU, R., LIU, Z., HO, E., ROSE, E. A. & CORTESINI, R. 1998b. Persistent allopeptide reactivity and epitope spreading in chronic rejection. *Transplantation Proceedings,* 30**,** 2136-2137.

SYLWESTER, A. W., MITCHELL, B. L., EDGAR, J. B., TAORMINA, C., PELTE, C., RUCHTI, F., SLEATH, P. R., GRABSTEIN, K. H., HOSKEN, N. A., KERN, F., NELSON, J. A. & PICKER, L. J. 2005. Broadly targeted human cytomegalovirus-specific CD4(+) and CD8(+) T cells dominate the memory compartments of exposed subjects. *The Journal of Experimental Medicine,* 202**,** 673-685.

SÜSAL, C., WETTSTEIN, DANIEL, DÖHLER, BERND, MORATH, CHRISTIAN, RUHENSTROTH, ANDREA1, SCHERER, SABINE, TRAN, THUONG H., GOMBOS, PETRA, SCHEMMER, PETER WAGNER, ERIC, FEHR, THOMAS, ZIVCIC-COSIC, STELA, BALEN, SANJA, WEIMER, ROLF, SLAVCEV, ANTONIJ, BÖSMÜLLER, CLAUDIA, NORMAN, DOUGLAS J., ZEIER, MARTIN, OPELZ, GERHARD 2015. Association of Kidney Graft Loss With De Novo Produced Donor-Specific and Non-Donor-Specific HLA Antibodies Detected by Single Antigen Testing. *Transplantation,* 99**,** 1976-1980.

TAYLOR, A. L., NEGUS, S. L., NEGUS, M., BOLTON, E. M., BRADLEY, J. A. & PETTIGREW, G. J. 2007. Pathways of helper CD4 T cell allorecognition in generating alloantibody and CD8 T cell alloimmunity. *Transplantation,* 83**,** 931-937.

TAYLOR, J. J., PAPE, K. A. & JENKINS, M. K. 2012. A germinal center-independent pathway generates unswitched memory B cells early in the primary response. *Journal of Experimental Medicine,* 209**,** 597-606.

TERASAKI, P. I. 2003. Humoral Theory of Transplantation. *American Journal of Transplantation,* 3**,** 665-673.

TRETTER, T., VENIGALLA, R. K. C., ECKSTEIN, V., SAFFRICH, R., SERTEL, S., HO, A. D. & LORENZ, H. M. 2008. Induction of CD4+ T-cell anergy and apoptosis by activated human B cells. *Blood,* 112**,** 4555-4564.

TSE, G. H., JOHNSTON, C. J. C., KLUTH, D., GRAY, M., GRAY, D., HUGHES, J. & MARSON, L. P. 2015. Intrarenal B Cell Cytokines Promote Transplant Fibrosis and Tubular Atrophy. *American Journal of Transplantation,* 15**,** 3067-3080.

TUNYAPLIN, C., SHAFFER, A. L., ANGELIN-DUCLOS, C. D., YU, X., STAUDT, L. M. & CALAME, K. L. 2004. Direct Repression of prdm1 by Bcl-6 Inhibits Plasmacytic Differentiation. *The Journal of Immunology,* 173**,** 1158-1165.

VALUJSKIKH, A., MATESIC, D., GILLIAM, A., ANTHONY, D., HAQQI, T. M. & HEEGER, P. S. 1998. T cells reactive to a single immunodominant self-restricted allopeptide induce skin graft rejection in mice. *Journal of Clinical Investigation,* 101**,** 1398-1407.

VAN DE VEEN, W., STANIC, B., YAMAN, G., WAWRZYNIAK, M., SÖLLNER, S., AKDIS, D. G., RÜCKERT, B., AKDIS, C. A. & AKDIS, M. 2013. IgG4 production is confined to human IL-10–producing regulatory B cells that suppress antigen-specific immune responses. *Journal of Allergy and Clinical Immunology,* 131**,** 1204-1212.

VAN VOLLENHOVEN, R. F., KINNMAN, N., VINCENT, E., WAX, S. & BATHON, J. 2011. Atacicept in patients with rheumatoid arthritis and an inadequate response to methotrexate: Results of a phase II, randomized, placebo-controlled trial. *Arthritis & Rheumatism,* 63**,** 1782-1792.

VANARSDALL, A. L., WISNER, T. W., LEI, H., KAZLAUSKAS, A. & JOHNSON, D. C. 2012. PDGF Receptor-α Does Not Promote HCMV Entry into Epithelial and Endothelial Cells but Increased Quantities Stimulate Entry by an Abnormal Pathway. *PLoS Pathog,* 8**,** e1002905.

VELLA, J. P., SPADAFORA-FERREIRA, M., MURPHY, B., ALEXANDER, S. I., HARMON, W., CARPENTER, C. B. & SAYEGH, M. H. 1997a. Indirect allorecognition of major histocompatibility complex allopeptides in human renal transplant recipients with chronic graft dysfunction. *Transplantation,* 64**,** 795-800.

VELLA, J. P., VOS, L., CARPENTER, C. B. & SAYEGH, M. H. 1997b. Role of indirect allorecognition in experimental late acute rejection. *Transplantation,* 64**,** 1823-1828.

VICTORA, G. D., SCHWICKERT, T. A., FOOKSMAN, D. R., KAMPHORST, A. O., MEYER-HERMANN, M., DUSTIN, M. L. & NUSSENZWEIG, M. C. 2010. Germinal Center Dynamics Revealed by Multiphoton Microscopy with a Photoactivatable Fluorescent Reporter. *Cell,* 143**,** 592-605.

VYSE, A. J., HESKETH, L. M. & PEBODY, R. G. 2009. The burden of infection with cytomegalovirus in England and Wales: how many women are infected in pregnancy? *Epidemiology & Infection,* 137**,** 526-533.

WANG, H., LIU, C., LI, Y. & HUANG, Y. 2015. Efficacy of Rituximab for Pemphigus: A systematic review and Meta-analysis of different regimens. *Acta Dermato-Venereologica,* 95**,** 928-932.

WANG, X., HUONG, S.-M., CHIU, M. L., RAAB-TRAUB, N. & HUANG, E.-S. 2003. Epidermal growth factor receptor is a cellular receptor for human cytomegalovirus. *Nature,* 424**,** 456-461.

WATANABE, R., ISHIURA, N., NAKASHIMA, H., KUWANO, Y., OKOCHI, H., TAMAKI, K., SATO, S., TEDDER, T. F. & FUJIMOTO, M. 2010. Regulatory B cells (B10 cells) have a suppressive role in murine lupus: CD19 and B10 cell deficiency exacerbates systemic autoimmunity. *J Immunol,* 184**,** 4801-9.

WEISEL, FLORIAN J., ZUCCARINO-CATANIA, GRISELDA V., CHIKINA, M. & SHLOMCHIK, MARK J. 2016. A Temporal Switch in the Germinal Center Determines Differential Output of Memory B and Plasma Cells. *Immunity,* 44**,** 116-130.

WELLER, S., BONNET, M., DELAGREVERIE, H., ISRAEL, L., CHRABIEH, M., MARÓDI, L., RODRIGUEZ-GALLEGO, C., GARTY, B.-Z., ROIFMAN, C., ISSEKUTZ, A. C., ZITNIK, S. E., HOARAU, C., CAMCIOGLU, Y., VASCONCELOS, J., RODRIGO, C., ARKWRIGHT, P. D., CERUTTI, A., MEFFRE, E., ZHANG, S.-Y., ALCAIS, A., PUEL, A., CASANOVA, J.-L., PICARD, C., WEILL, J.-C. & REYNAUD, C.-A. 2012. *IgM+IgD+CD27+ B cells are markedly reduced in IRAK-4–, MyD88-, and TIRAP- but not UNC-93B–deficient patients*.

WELLER, S., BRAUN, M. C., TAN, B. K., ROSENWALD, A., CORDIER, C., CONLEY, M. E., PLEBANI, A., KUMARARATNE, D. S., BONNET, D., TOURNILHAC, O., TCHERNIA, G., STEINIGER, B., STAUDT, L. M., CASANOVA, J.-L., REYNAUD, C.-A. & WEILL, J.-C. 2004. Human blood IgM "memory" B cells are circulating splenic marginal zone B cells harboring a prediversified immunoglobulin repertoire. *Blood,* 104**,** 3647-3654.

WELLER, S., FAILI, A., GARCIA, C., BRAUN, M. C., LE DEIST, F., DE SAINT BASILE, G., HERMINE, O., FISCHER, A., REYNAUD, C.-A. & WEILL, J.-C. 2001. CD40-CD40L independent Ig gene hypermutation suggests a second B cell diversification pathway in humans. *Proceedings of the National Academy of Sciences,* 98**,** 1166-1170.

WELLER, S., MAMANI-MATSUDA, M., PICARD, C., CORDIER, C., LECOEUCHE, D., GAUTHIER, F., WEILL, J.-C. & REYNAUD, C.-A. 2008. Somatic diversification in the absence of antigen-driven responses is the hallmark of the IgM(+)IgD(+)CD27(+) B cell repertoire in infants. *J Exp Med,* 205**,** 1331-1342.

WIEBE, C., GIBSON, I. W., BLYDT-HANSEN, T. D., KARPINSKI, M., HO, J., STORSLEY, L. J., GOLDBERG, A., BIRK, P. E., RUSH, D. N. & NICKERSON, P. W. 2012. Evolution and Clinical Pathologic Correlations of De Novo Donor-Specific HLA Antibody Post Kidney Transplant. *American Journal of Transplantation,* 12**,** 1157-1167.

WILLE, P. T., WISNER, T. W., RYCKMAN, B. & JOHNSON, D. C. 2013. Human Cytomegalovirus (HCMV) Glycoprotein gB Promotes Virus Entry In Trans Acting as the Viral Fusion Protein Rather than as a Receptor-Binding Protein. *mBio,* 4**,** e00332-13.

WILSON, C. L., HINE, D. W., PRADIPTA, A., PEARSON, J. P., VAN EDEN, W., ROBINSON, J. H. & KNIGHT, A. M. 2012. Presentation of the candidate rheumatoid arthritis autoantigen aggrecan by antigen-specific B cells induces enhanced CD4+ T helper type 1 subset differentiation. *Immunology,* 135**,** 344-354.

WIRTHS, S. & LANZAVECCHIA, A. 2005. ABCB1 transporter discriminates human resting naive B cells from cycling transitional and memory B cells. *Eur J Immunol,* 35**,** 3433-3441.

WORTHINGTON, J. E., MARTIN, S., AL-HUSSEINI, D. M., DYER, P. A. & JOHNSON, R. W. G. 2003. Posttransplantation production of donor HLA-specific antibodies as a predictor of renal transplant outcome. *Transplantation,* 75**,** 1034-1040.

YANABA, K., BOUAZIZ, J.-D., HAAS, K. M., POE, J. C., FUJIMOTO, M. & TEDDER, T. F. 2008. A Regulatory B Cell Subset with a Unique CD1dhiCD5+ Phenotype Controls T Cell-Dependent Inflammatory Responses. *Immunity,* 28**,** 639-650.

YANABA, K., BOUAZIZ, J. D., MATSUSHITA, T., TSUBATA, T. & TEDDER, T. F. 2009. The development and function of regulatory B cells expressing IL-10 (B10 cells) requires antigen receptor diversity and TLR signals. *J Immunol,* 182**,** 7459-72.

ZACHARY, A. A., KOPCHALIISKA, D., MONTGOMERY, R. A. & LEFFELL, M. S. 2007a. HLA-specific B cells: I. A method for their detection, quantification, and isolation using HLA tetramers. *Transplantation,* 83**,** 982-8.

ZACHARY, A. A., KOPCHALIISKA, D., MONTGOMERY, R. A., MELANCON, J. K. & LEFFELL, M. S. 2007b. HLA-specific B cells: II. Application to transplantation. *Transplantation,* 83**,** 989-994.

ZENG, Q., NG, Y.-H., SINGH, T., JIANG, K., SHERIFF, K. A., IPPOLITO, R., ZAHALKA, S., LI, Q., RANDHAWA, P., HOFFMAN, R. A., RAMASWAMI, B., LUND, F. E. & CHALASANI, G. 2014. B cells mediate chronic allograft rejection independently of antibody production. *The Journal of Clinical Investigation,* 124**,** 1052-1056.

ZERRAHN, J., HELD, W. & RAULET, D. H. 1997. The MHC reactivity of the T cell repertoire prior to positive and negative selection. *Cell,* 88**,** 627-636.

ZOTOS, D., COQUET, J. M., ZHANG, Y., LIGHT, A., D'COSTA, K., KALLIES, A., CORCORAN, L. M., GODFREY, D. I., TOELLNER, K.-M., SMYTH, M. J., NUTT, S. L. & TARLINTON, D. M. 2010. IL-21 regulates germinal center B cell differentiation and proliferation through a B cell–intrinsic mechanism. *J Exp Med,* 207**,** 365-378.

ZUCCARINO-CATANIA, G. V., SADANAND, S., WEISEL, F. J., TOMAYKO, M. M., MENG, H., KLEINSTEIN, S. H., GOOD-JACOBSON, K. L. & SHLOMCHIK, M. J. 2014. CD80 and PD-L2 define functionally distinct memory B cell subsets that are independent of antibody isotype. *Nat Immunol,* 15**,** 631-637.